UNIVERSIDADE FEDERAL DO RIO GRANDE DO SUL

INSTITUTO DE GEOCIÊNCIAS

PROGRAMA DE PÓS-GRADUAÇÃO EM GEOCIÊNCIAS

CARACTERIZAÇÃO ARQUITETURAL E DISTRIBUIÇÃO DE FÁCIES DE LOBOS TURBIDÍTICOS NO MIOCENO DA BACIA DE ADANA, TURQUIA

DANIEL BAYER DA SILVA

ORIENTADORES – Prof. Dr. Eduardo Guimarães Barboza
Prof. Dr. Bryan T. Cronin
Prof. Dr. Hasan Çelik
Prof. Dr. Benjamin Kneller

CO-ORIENTADORA – Profª. Drª. Karin Goldberg

Volume I

Porto Alegre – 2018

UNIVERSIDADE FEDERAL DO RIO GRANDE DO SUL
INSTITUTO DE GEOCIÊNCIAS
PROGRAMA DE PÓS-GRADUAÇÃO EM GEOCIÊNCIAS

CARACTERIZAÇÃO ARQUITETURAL E DISTRIBUIÇÃO DE FÁCIES DE LOBOS TURBIDÍTICOS NO MIOCENO DA BACIA DE ADANA, TURQUIA

DANIEL BAYER DA SILVA

ORIENTADORES – Prof. Dr. Eduardo Guimarães Barboza
Prof. Dr. Bryan T. Cronin
Prof. Dr. Hasan Çelik
Prof. Dr. Benjamin Kneller

CO-ORIENTADORA – Profª. Drª. Karin Goldberg

BANCA EXAMINADORA
    Prof. Dr. Juliano Kuchle – Instituto de Geociências, Universidade Federal do Rio Grande do Sul (UFRGS)
    Prof. Dr. Michael Holz – Departamento de Geofísica do Instituto de Geociências, Universidade Federal da Bahia (UFBA)
    Dr. Adriano R. Viana – EXP/GEOF/MNS-Exploração/Geofísica/Métodos Não-Sísmicos - Petrobras

> Tese de Doutorado apresentada como requisito parcial para a obtenção do Título de Doutor em Ciências (Dupla Titulação e co-tutela com a University of Aberdeen).

Porto Alegre – 2018

AGRADECIMENTOS

Após mais de quatro anos de superação de várias questões emocionais, físicas e de saúde, gostaria de expressar toda a minha gratidão a uma infinidade de pessoas e instituições que me permitiram completar essa parte recompensadora e difícil da minha vida.

O autor reconhece com gratidão o apoio da Shell Brasil através do projeto na UFRGS "BG05: UoA-UFRGS-SWB Sistemas Sedimentares" e a importância estratégica do apoio dado pela ANP através do regulamento de coleta de R&D. Também, obrigado ao CNPq pela bolsa de doutorado sanduíche concedida. O programa de dupla diplomação foi um grande esforço que envolveu muitas pessoas. Eu gostaria de agradecer a todos os envolvidos.

Uma parte essencial deste PhD foi meus supervisores. Todos eles são os melhores em suas áreas de pesquisa e, por essa razão, extremamente ocupados, mas sempre encontram tempo para minhas perguntas "estranhas". Em primeiro lugar, minha orientadora brasileira, Prof^a. Dr^a. Karin Goldberg, que teve um papel essencial no começo e no fim. Quando ela se mudou para outro país, ela sempre tentou manter contato. Obrigado pelo seu entusiasmo e dedicação em rever minha redação. Agradeço também ao meu orientador Prof. Dr. Eduardo Guimarães Barboza, por aceitar me orientar ao final desta trajetória. Meus agradecimentos ao Prof. Dr. Hasan Çelik, da Turquia, que me permitiu perseguir meus objetivos e sempre se preocupou com minha situação em seu país, com uma cultura, idioma e principalmente devido aos últimos acontecimentos nos países vizinhos. Teşekkür ederim.

Minha imensa gratidão à um de meus orientadores no Reino Unido, o Prof. Dr. Bryan T. Cronin, que me chamou de herói por aceitei trabalhar nos turbiditos da grande Bacia de Adana. Tenho orgulho de fazer parte disto e agradeço que você compartilhe seu grande conhecimento comigo, mesmo vivendo longe um do outro. Por último, mas não menos importante, gostaria de agradecer ao meu outro orientador no Reino Unido, Prof. Dr. Benjamin Kneller (Ben), que apesar de seus problemas de saúde estava sempre disponível para se reunir e discutir geologia, e por seu esforço para manter a programa de bolsa de estudos de dupla diplomação funcionando para o bem de todos os alunos envolvidos. Obrigado por se importar com isso.

RESUMO

A crescente demanda por novas fronteiras exploratórias na geologia do petróleo e a melhoria do conhecimento dos reservatórios atuais, nos leva à necessidade de estudos detalhados sobre as rochas reservatórios e sua capacidade de acumulação de hidrocarbonetos. A análise de afloramentos ao longo de um perfil longitudinal contínuo, da borda da plataforma até a fundo da bacia onde os depósitos da Formação Cingöz (Mioceno Inferior ao Médio), Bacia de Adana, Turquia, teve como objetivo caracterizar mudanças na arquitetura de lobos turbidíticos ao longo do perfil deposicional, a partir da análise de associações de fácies, hierarquia e geometria dos lobos. Dois leques submarinos foram estudados, o Leque Oriental e o Ocidental. Dez associações de fácies foram identificadas com base na razão N:G, grau de amalgamação, distribuição de fácies, tamanho de grão modal, porcentagem de arenitos espessos, presença de laminações de ondulações de correntes e camadas gradadas, revelando padrões de distribuição espacial das associações de fácies. Quatro níveis hierárquicos dentro da arquitetura foram reconhecidos. O elemento básico, uma camada (*bed*) (espessura máxima de 1,9 m), representa sedimentos depositados em um único evento, o próximo nível hierárquico, elemento de espraiamento (*splay element*) (espessura máxima de 7,8 m) é empilhado para formar o lobo (*lobe*) (espessura entre 9,5 a 22 m); lobos empilhados formam o complexo de lobos (*lobe complex*) (espessura máxima de 40 m). Um total de 13 lobos (A a M) foi identificado. As dimensões estimadas do lobo (comprimento e largura), baseadas na taxa de afinamento obtida pela correlação entre os perfis colunares sedimentares, indicam uma espessura média de cerca de 15 m (máximo de 22 m), o comprimento varia de 5 a 12 km e a largura de 3 a 10 km. A razão comprimento/largura (L/W) (1,1 a 1,8) indica lobos sub-radiais à alongados. Os blocos construtores representados pelos níveis hierárquicos demonstram a importância da topografia do assoalho oceânico no controle do grau de confinamento e das trajetórias das correntes de turbidez. A análise das tendências verticais das camadas mostrou que a tendência geral é controlada por elemento de espraiamento empilhados. Em ambientes proximais (alto N: G) a sucessão é simétrica, tornando-se mais assimétrica à medida que a relação N: G diminui distalmente. Essa "assimetria distal" é interpretada como resultante do deslocamento lateral do elemento de espraiamento. Assim, o padrão de empilhamento dos lobos no Leque Oriental foi interpretado como agradacional, com algum empilhamento por

compensação. Os lobos estratigraficamente inferiores são mais confinados e menores devido à ocorrência do talude ao norte e depósitos antigos ao sul. Os lobos superiores foram desenvolvidos em um sistema menos confinado, com direção preferencial da paleocorrent para NE, como todos os lobos da região. Em geral, os lobos foram construídos em um ambiente semi-confinado. A Formação Cingöz registra uma história evolutiva complexa. A interpretação da arquitetura dos lobos aponta para uma mudança sutil no grau de confinamento e nas direções de paleocorrente, que sugerem uma sobreposição de parte do Leque Oriental sob o Leque Ocidental contemporâneo.

ABSTRACT

The increasing demand for new exploratory frontiers in Petroleum Geology and the improvement in knowledge of the current ones has prompted detailed studies on reservoir rocks and their potential for hydrocarbon accumulation. The analysis of outcrops along a continuous longitudinal profile, from the shelf edge to the bottom of the basin where deep-water deposits of the Cingöz Formation (Lower to Middle Miocene), Adana Basin, Turkey, purposed to characterize changes in the architecture of turbidite lobes along the depositional profile, based on the analysis of facies associations, lobe hierarchy and geometry. Two submarine fans were studied, the Eastern and the Western Fans, with the main lobes described in the eastern part of the Eastern Fan. Ten facies associations were identified on the basis of N-G ratio, degree of amalgamation, facies distribution, modal grain size, percentage of thick sandstones, presence of current ripple laminations and graded beds, revealing patterns of spatial distribution of the facies associations. Four hierarchical levels within lobe architecture were recognized. The basic element, a bed (maximum thickness of 1.9 m) represents sediments deposited in a single event; the next hierarchical level, splay element (maximum thickness of 7.8 m) are stacked to form a lobe (thickness between 9.5 and 22 m); stacked lobes form a lobe complex (maximum thickness of 40 m). A total of 13 lobes (A to M) was identified. Estimated of lobe dimensions (length and width), based on the thinning rate obtained from correlation of sedimentary logs, indicate average thickness of about 15 m (maximum 22 m), length varying from 5 to 12 km and width, 3 to 10 km. The L/W (1.1 to 1.8) indicates sub-radial to elongate lobes. Lobe building blocks represented by the hierarchical levels demonstrate the importance of basin-floor topography in controlling the degree of confinement and paths for turbidity currents. Analysis of vertical bed trends showed that the overall tendencies controlled by stacked splay elements. In proximal environments (high N:G), successions are symmetrical, becoming more asymmetrical as the N:G ratio decreases distally. This "distal asymmetry" is interpreted as resulting from the shift of splay elements. Hence, the stacking pattern of lobes in the Eastern Fan was interpreted as aggradational, with some compensational stacking. Stratigraphically lower lobes are more confined and smaller due to the occurrence of the slope to the north and ancient deposits to the south. Upper lobes were developed in a less confined system, with preferential palaeocurrent direction towards NE, like all lobes in that region. Overall, the lobes

were built in a semi-confined setting. The Cingöz Formation records a complex evolutionary history. Interpretation of lobe architecture points to a subtle change in the degree of confinement and palaeocurrent directions that suggest an overlapping of part of the Eastern Fan onto the coeval Western Fan.

LISTA DE FIGURAS

LISTA DE TABELAS

SUMÁRIO

1. INTRODUÇÃO

1.1. Apresentação

A demanda atual na busca de novas descobertas exploratórias visando expandir a produção de recursos como o petróleo e o gás direciona a pesquisa em depósitos turbidíticos, constantemente referenciados como um dos melhores reservatórios de hidrocarbonetos. Esta condição é aplicada aos lobos turbidíticos mais especificamente, pois trata-se de um depósito onde a presença de areia "limpa", bom grau de seleção de sedimentos, grande extensão lateral e boas condições de conectividade vertical, além da frequente presença de depósitos lamosos, isolando os corpos arenosos (trapa), justificam a busca por maior entendimento deste depósito.

Os afloramentos dos depósitos marinhos na região da Bacia de Adana (Turquia) oferecem uma oportunidade única para a análise da continuidade das camadas de arenitos e de folhelhos associados aos lobos turbidíticos, auxiliando na compreensão da conectividade dos corpos reservatórios, através do mapeamento da distribuição das fácies e das geometrias dos corpos. Esta região possui um grande potencial científico para a geologia marinha profunda, pois, além de conter boa parte dos sistemas encontrados neste ambiente, foi pouco estudada até o momento, quando comparada à outras regiões similares no mundo. Um dos aspectos a serem avaliados é a diferenciação dos chamados "*thin-bedded turbidites*" (TBTs), ou turbiditos finamente acamados, muito frequentes em sistemas turbidíticos, porém de difícil interpretação em relação à sua distribuição dentro dos sistemas de lobos associados. A distribuição de fácies em subambientes formados pelo espraiamento de lobos e a hierarquia dos corpos também são focos importantes, pois ainda há divergências quanto à essas características na literatura. Porém, a principal ênfase é a arquitetura dos lobos. Com o auxílio da correlação dos perfis colunares e o dimensionamento e geometria dos lobos é possível compreender a evolução, não só dos corpos arenosos individualmente, mas também de todo o sistema turbidítico envolvido.

Por tratar-se de uma bacia de *foreland*, onde a atividade tectônica controla a topografia e a geometria dos sistemas turbidíticos, há necessidade de melhor compreensão da potencialidade deste tipo de bacia, já que a formação e a migração de hidrocarbonetos estão condicionadas à evolução da bacia ou de estruturas

relacionadas. Por sua complexidade, o entendimento da evolução deste tipo de bacia é ainda bastante controverso.

1.2.   Área de Estudo

A Formação Cingöz é um sistema clástico de águas profundas, interpretado como contendo dois leques submarinos contemporâneos na Bacia de Adana (Gürbüz, 1993; Gürbüz and Kelling, 1993; Satur, 1999). É uma das várias bacias *foreland* no sul da Turquia, marcando o fechamento do Oceano Neotétis, no início do Mioceno Médio. Pouco foi publicado sobre a área de interesse desta tese, nas partes orientais da Formação Cingöz, mas recentemente novas exposições de corte de estrada nos permitiram estudar outros afloramentos na área.

A Formação Cingöz cobre uma área de aproximadamente 900 km^2, da cidade de Karaisalı (oeste) à Kozan (leste), uma distância de aproximadamente 65 km. No norte, limitada pela aldeia Meydan Yayla, localizada numa encosta, perto do canyon alimentador (interpretado) da Formação Cingöz (Leque Oriental, ou *Eastern Fan* (EF), em inglês), enquanto 25 km ao sul, o limite das exposições é o lago Çatalan (Figura 1).
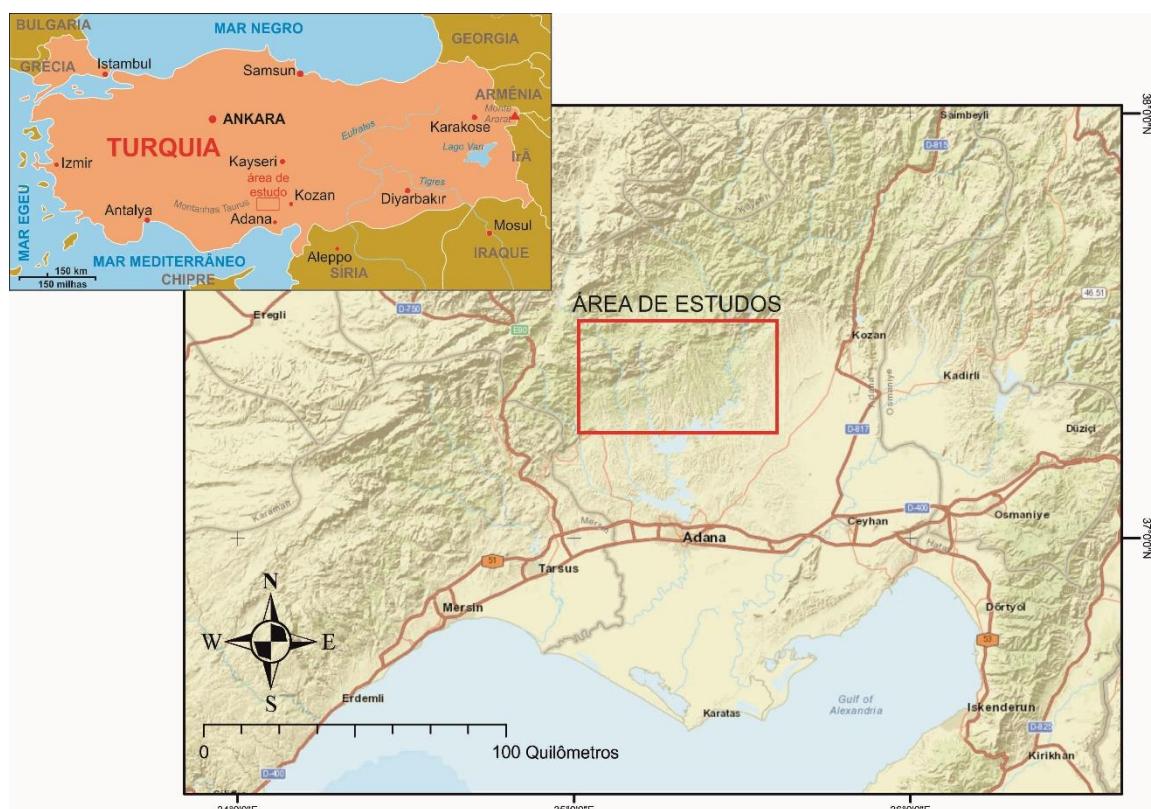
Figura 1: Mapa da área estudada (quadrado vermelho) na Bacia Adana. Anatólia, com as principais cidades e estradas em destaque.

A Formação Cingöz é um sistema clástico arenoso de águas profundas, formado em lâmina de água de mais de 200 m (Nazik and Gürbüz, 1992; Demircan and Toker, 2003) e alimentado por canyons submarinos que cortam uma plataforma estreita (Gürbüz, 1993). Ambos os ambientes da plataforma continental e do assoalho oceânico estão bem preservados e em seus locais originais.

A principal área de estudo está localizada ao longo da estrada Aladağ-Imamoğlu, entre a aldeia Çarkıpare e o sul da represa Sanibey (*Sanibey Baraj*), onde as melhores exposições dos lobos do *Eastern Fan* (EF) podem ser encontradas. Cortes de estrada recentes proporcionaram afloramentos extensos e espessos para a descrição de perfis colunares sedimentares. Vários outros locais (menores e mais intemperizados) também foram descritos, principalmente no EF.

A logística e o apoio ao trabalho de campo e desenvolvimento do projeto envolveu uma colaboração entre o Departamento de Geologia da Universidade Çukurova, em Adana, e a Universidade Firat, em Elazig, representada pelos Profs. Kemal Gürbüz e Hasan Çelik, respectivamente.

Foram realizadas cinco campanhas de campo, totalizando quase cinco meses de dados coletados na área de estudo. As campanhas ocorreram principalmente em maio ou outubro/novembro de 2016 e 2017.

1.3. Objetivos

Este projeto de doutorado teve como objetivo a caracterização das assinaturas de blocos de construção típicos de lobos turbidíticos de águas profundas, principalmente através da construção de uma classificação de associação de fácies, e estabelecimento de um esquema hierárquico e das dimensões dos lobos. A compreensão desses aspectos visou demonstrar como os depósitos em águas profundas se desenvolveram e quais foram os elementos responsáveis por sua construção, revelando o surgimento e a evolução de um sistema turbidítico.

Os principais estudos foram realizados através de uma análise detalhada da continuidade horizontal dos lobos e de seus arranjos verticais, combinados com uma revisão abrangente da literatura. Foi possível avaliar as diferenças entre os esquemas atuais publicados e sugerir novas possibilidades, testando a validade de

conceitos bem estabelecidos, como os esquemas hierárquicos prévios, as tendências da espessura de camadas, as alterações granulométricas e as características de terminações estratais em encostas de águas profundas.

1.4. Estrutura e organização da Tese

Esta tese segue o modelo de integração de artigos científicos, como estabelecido pelo Programa de Pós-graduação em Geociências do Instituto de Geociências da Universidade do Rio Grande do Sul (UFRGS), sendo estruturado em capítulos de introdutção e de apresentação, outros de revisões de literaturas, principais resultados, seguidos dos artigos científicos submetidos.

O capítulo 1 apresenta o tema de pesquisa da tese, detalhando os objetivos e a área de estudo, além de destacar os principais resultados obtidos.

Os capítulos 2 e 3 detalham a geologia da área, sendo que o primeiro tem o foco maior no contexto geotectônico da áre ade estudos e o capítulo seguinte procura abranger todos os detalhes de estratigrafia e geologia geral da área, utilizando a revisão da literatura.

A revisão da literatura está presente também no capítulo 4, onde há uma breve explicação dos principais elementos trabalhados no tema de lobos turbidíticos.

Os capítulos seguintes detalham a metodologia utilizada (capítulo 5) e as referências (capítulo 6).

Finalmente, o capítulo 7 contém os três artigos científicos submetidos à periódicos com corpo editorial permanente e revisores independentes. Todos o conteúdo de cada artigo foi elaborado e escrito pelo autor desta tese, referenciando toda a informação de terceiros.

1.5. Principais resultados

Os dados coletados nos afloramentos da Formação Cingöz e interpretados durante o desenvolvimento do projeto de doutorado tiveram resultados em diferentes escalas, desde a escala de fácies, até de evolução da bacia. A seguir serão destacados os resultados considerados mais relevantes contidos neste trabalho:

Padrões e classificação de associações de fácies

A classificação das associações de fácies (*facies association*, em inglês, F.A.) sugeridas neste trabalho (Figura 2) baseou-se no reconhecimento de dez fácies distintas, das quais as principais são: heterolitos, camadas híbridas e depósitos de transporte de massa (Tabela 1). Além disso, outros parâmetros incluídos no esquema F.A. foram o grau de amalgamação e a razão areia:intervalo medido (*net-to-gross, N:G*). A conjunção dos parâmetros permitiu separar as F.A. em três grupos principais: alto, médio e baixo *net-to-gross* (T_H, T_M, T_L, respectivamente) (Figura 2). Subgrupos foram criados para fornecer um esquema detalhado, usando os parâmetros restantes para classificá-los.
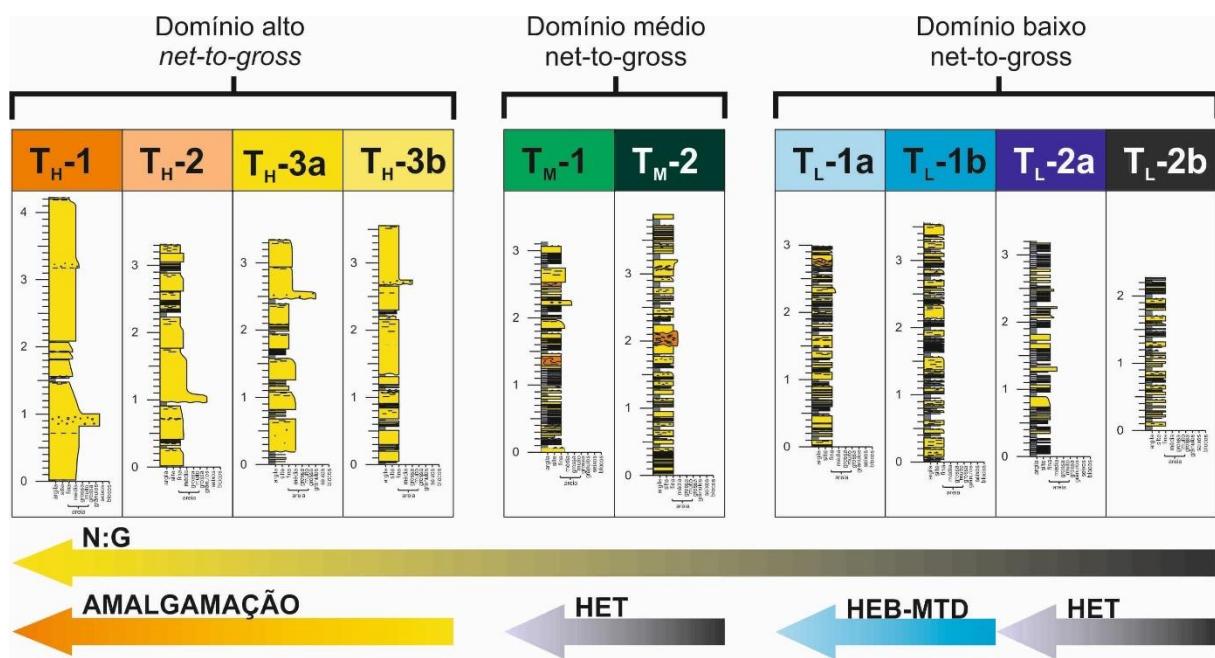
Figura 2: Perfis colunares esquemáticos representando padrões típicos que definem cada associação de fácies. As setas indicam direção crescente das características definidoras das associações de fácies. (HET = hetorolitos, HEB = Hybrid Beds, ou caamadas híbridas; MTD = Mass Transport Deposit, ou depósito de transporte de massa).

Tabela 1: Principais características das litofácies identificadas na Formação Cingöz.

Fácies	Litotipo	Descrição	Espessura da camada	Moda	Mecanismo de suporte de sedimentos	Processo deposicional	Tipo de fluxo	Referências
F1	Mistura de lamito e arenito contorcidos	Camadas de arenito finos e espessos e lamito contorcidos. Muitas das camadas contorcidas com a orientação aleatória. Localmente arenito granular	0,10 – 3,0 m	Areia fina à grânulos	Força matricial	Congelamento por fricção	Escorregamento/deslizamento/fluxo de detritos	Fácies 1 e 3 (Lowe, 1982); F1 (Mutti, 1992); MTD (Martinsen and Bakken, 1990)
F2	Linked debrite	Arenito maciço sobreposto por arenito lamoso com muitos clastos de lamito e arenito desorganizados e/ou injeção	0,10– 0,7 m	Areia fina à média	Força matricial /turbulênica fluida	Congelamento por fricção, tração e suspensão	Fluxo de detritos co-genético e corrente de turbidez	Linked debrite (Haughton et al., 2003); Hybrid flow (Haughton et al., 2009); debrito turbidito co-geneticos (Talling et al., 2004; Pyles and Jennette, 2009)
F3	Conglomerado suportado pela matriz	Conglomerado suport. pela matriz com clastos angulares à arredond. (90%) (plut., vulc., carbonato.) até 15 cm. Localmente lamitos (10 cm) marcam a orientação. Localmente clastos lamosos arredondados (até 25 cm)	0,30 – 2,3 m	Areia grossa à seixo	Turbulência fluída	Tração/carga de fundo	Corrente de turbidez de alta densidade	R3 (Lowe, 1982); F3 (Mutti, 1992)

F4	Arenito rico em clastos lamosos	Arenito espesso rico em clastos lamosos orientados, angulares (90%) à arredondados (até 60 cm)	0,10 – 1,4 m	Areia grossa à seixo	Turbulência fluída	Tração	Corrente de turbidez	R1 (Lowe, 1982); F2 (Mutti, 1992)
F5	Arenito maciço	Arenito maciço, de boa seleção à muito bem selecionado. Localmente rico em clastos lamosos e com estruturas flame, pipe e dish. Em geral, clastos orientados (até 60 cm), frequentemente em níveis	0,1 – 1,3 m	Areia fina à grânulo	Turbulência fluída	Tração e suspensão	Corrente de turbidez	Ta (Bouma, 1962); S3 (Lowe, 1982); F5 (Mutti, 1992)
F6	Arenito com laminação plano-paralela	Arenito com laminação plano-paralela (principalmente bem selecionado). Localmente lentes de grãos grossos definindo a laminação	0,01 – 0,3 m	Areia fina à fina-média	Turbulência fluída	Tração e suspensão	Corrente de turbidez	Tb (Bouma, 1962); S2 (Lowe, 1982); F8 (Mutti, 1992)
F7	Arenito com laminação cruzada	Arenito com laminação cruzada de pequeno porte (current ripple)	0,01 – 0,02 m	Areia muito fina à fina	Turbulência fluída	Tração e suspensão	Corrente de turbidez	Tc (Bouma, 1962 and Lowe, 1982); F6 (Mutti, 1992)
F8	Heterolito	Inter-acamamento centimétrico de lamito e arenito ou siltito e argilito	0,01 – 0,25 m	Argila à areia fina	Assentamento	Tração e suspensão	Corrente de turbidez	Ta-Te (Bouma, 1962); S3 (Lowe, 1982); F8, F9a, and F9b (Mutti, 1992)

F10	Folhelho	Argilito preto à cinza com pequenas lâminas de siltito	< 0,6 m	Argila	Assentamento	Suspensão	Corrente de turbidez/sedimentação hemipelágica	Te (Bouma, 1962; Lowe, 1982); F9a (Te) (Mutti, 1992)

A principal utilidade desta classificação é posicionar cada F.A em um lobo/espraiamento frontal. Através da integração da análise de correlação de perfis colunares e da classificação de F.A., foi elaborado um mapa de sub-ambientes, considerando um depósito ideal e simétrico (Figura 3). Este mapa permite a observação de como os principais parâmetros são distribuídos em um lobo/espraiamento, destacando a variação na concentração de cada parâmetro e possibilitando a comparação entre eles. A escala da F.A. é importante, mas não é necessária quando o objetivo é reconhecer a posição em um bloco de construção de lobo. No geral, a espessura máxima do F.A. mais espesso (T_H) é de 8 m, mas em partes distais do corpo de areia, mesmo F.A. finas, representando ciclos menores, pode ser interpretado como o mais espesso, já que a associação de fácies acima e abaixo provavelmente apresentarão as mesmas características. Em resumo, não é necessário reconhecer a hierarquia (escala) para determinar o grupo de associação de fácies, mas uma vez que um grupo é interpretado, as hierarquias envolvidas são muito provavelmente reconhecidas.
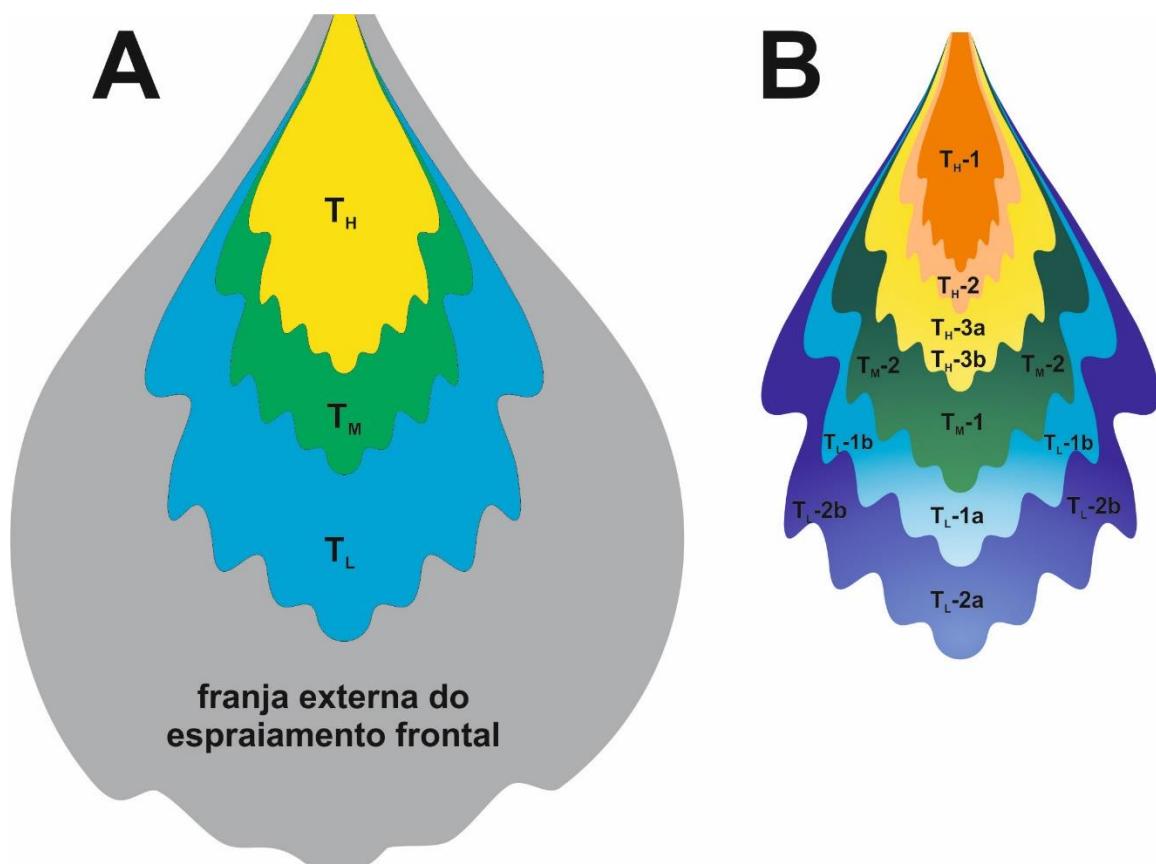
Figura 3: Modelo de um *frontal splay*, mostrando a distribuição das associações de fácies descritas neste trabalho (sem escala). A) As 3 divisões T_H, T_M e T_L, além da franja do espraiamaneto (*splay*), não incluídas no esquema F.A. devido a ausência de dados para estatística; B) Todas as 10 subdivisões das associações de fácies e as cores relacionadas.

Esquema de hierarquia em lobos

As exposições do EF forneceram evidências de quatro níveis hierárquicos de lobos turbidíticos (Tabela 2), reconhecidos através da análise da espessura das camadas em mais de 30 locais. Eles foram classificados de níveis mais baixos a mais altos, como *Bed* (Camada)*, Splay Element* (Elemento de espraiamento)*, Lobe* (Lobo)*, Lobe Complex* (Complexo de Lobos). A quantidade de dados coletados permitiu entender a relação entre os níveis e estabelecer alguns padrões úteis para comparação com outros locais, além de ajudar a esclarecer e prever as hierarquias dos lobos. Os dois primeiros níveis hierárquicos (*bed* e *splay element*) estão associados à eventos deposicionais individuais que formam a camada (evento único) e conjuntos de camadas (*splay element*). Este último relaciona-se diretamente com a classificação da associação de fácies. Como mencionado acima, os *splay element* e as associações de fácies exibem a mesma escala de espessura (um máximo de 8 m). Eles são responsáveis pela construção dos níveis acima.

Tabela 2: Espessuras típicas para cada nível hierárquico medido em 30 perfis colunares. Alguns ciclos estavam incompletos e, portanto, a espessura medida (em cinza) é menor que a espessura real. (N = número de ciclos).

Hierarquia	"N" completa	"N" incompleta	Total "N"	Espessura (m)			
				Min	Máx.	Média (incompleta)	Média real
Lobe complex	1	6	7	-	40	29.3	-
Lobe	13	11	24	9.5	22	14.8	14.5
Splay element	61	-	61	1.0	7.8	-	3.9
Bed	1141	-	30	0.01	1.9	-	0.36

Os próximos dois níveis (*lobe* e *lobe complex*) constituem o corpo principal do sistema de lobos e são fáceis de correlacionar com os dados sísmicos, diferentemente dos outros dois níveis mais baixos. A espessura do *lobe* pode atingir 22 m e a do *lobe complex* 40 m, mas a ausência de mais dados nesses níveis (principalmente o *lobe complex*) sugere espessuras ainda maiores.

Os limites dos níveis hierárquicos, onde os *thin-bedded turbidites* (TBT's) são considerados o "*interlobe*" entre *lobe complexes* (TBT's espessos) e lobos (TBTs

relativamente pouco espessos). As *beds* e os *splay elements* são separados por um lamito de espessura máxima de 10 centímetros, se não houver amalgamação. Para o *splay element*, o reconhecimento de uma sucessão ou ciclo completo é imperativo para separar dois *splay element*.

Arquitetura dos lobos

As tendências de espessura de camada (*bed thickness trends*) e correlação dos perfis colunares foram importantes para explicar a evolução do lobo e a arquitetura deposicional do EF. Em altas razões N:G, as tendências do ciclo na área de estudo mostram um padrão de sucessões simétricas em ambos os níveis hierárquicos (*lobe* e *splay element*). No médio N:G, as sucessões são predominantemente *thickening-then-thinning-upward (*espessamento seguido de afinamento ascendente*)*, principalmente com a parte do *thickening-upward* sendo mais espessa do que a parte de *thinning-upward.* A grande discrepância entre os tipos de ciclo nas escalas do *lobe* e do *splay element* é vista em intervalos estratigráficos de baixos N: G (Figura 4). Esse comportamento foi interpretado como um padrão de empilhamento compensatório.

A análise do tamanho e forma do lobo levou em conta as taxas de afinamento axiais e laterais obtidas a partir da correlação dos peris colunares. Na escala do lobo, a taxa de afinamento lateral (ao longo da seção transversal) na a região proximal é de cerca de 4 m.km^{-1}, enquanto que na medial é de 4,5 m.km^{-1}. A taxa de afinamento axial (ao longo da seção longitudinal) é menos clara, porque a seção de correlação principal é transversal, e, portanto, apenas a taxa de afinamento na a região proximal é dada, cerca de 2,4 m.km^{-1}. Assim, a largura estimada dos lobos está entre 3 e 10 km, enquanto o comprimento varia entre 5 e 12 km.

A interpretação e a integração dos resultados permitiram a compreensão de como os lobos se desenvolvem ao longo do tempo, em um empilhamento compensatório geral associado à agradação do sistema. A estimativa de comprimento e largura sugere construções de lobos ligeiramente radiais em um ambiente semi-confinado, refletindo a evolução de condições confinadas para condições não-confinadas.
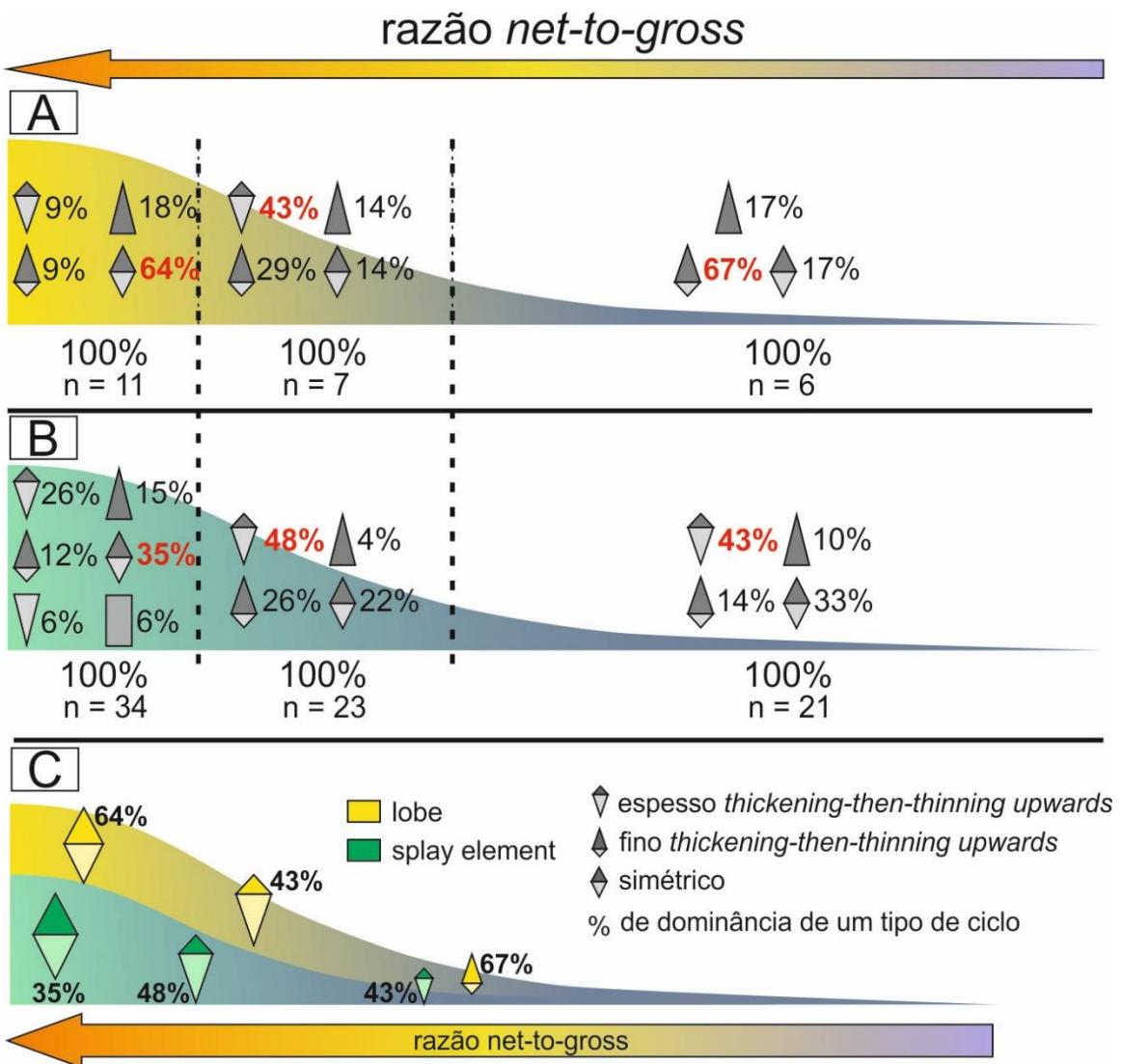
Figura 4: Esquema representando a porcentagem de tendências de ciclos nas hierarquias de *lobe* e *splay element* em alta, média e baixa razão N:G. Aumento de *net-to-gross* para a esquerda (representado pela forma da curva: espessura = alto N:G e fino = baixo N:G). A) Distribuição das porcentagens para os tipos de ciclo nas escalas de *lobes* (amarelo) e B (*splay element*) (verde). Observe que a porcentagem total está relacionada ao número de exemplos em uma região específica; C) Resumo da distribuição proximal a distal dos principais tipos de ciclo no *lobe* e no *splay element*, de acordo com as relações N:G. Para o *lobe*, os ciclos simétricos ocorrem sob ciclos de alto N:G, espessos *thickening-then-thinning-upwards* sob médio N:G, e finos *thickening-then-thinning-upwards*, sob baixo N:G. Para o *splay element*, os ciclos simétricos ocorrem sob altos níveis de N:G, e espessos *thickening-then-thinning-upwards* sob médio e baixo N:G.

Uma comparação entre o modelo para os lobos na Formação Cingöz e um sistema moderno (lobos da Córsega Oriental no Leque de Golo) mostra algumas semelhanças gerais com o EF. Além das semelhanças em relação às características dos leques e das bacias, as medidas no EF apontam para lobos com dimensões e taxas de afinamento intermediárias entre os lobos do Leque de Golo.

Evolução do sistema de leques (Formação Cingöz)

Padrões de paleocorrentes são fundamentais para entender a evolução do lobo em um sistema como o Cingöz, onde dois leques interagem. Duas direções principais de paleocorrente indicam a existência de um sistema alimentador do oeste e outro do noroeste (WF e EF, respectivamente). Uma análise detalhada, no entanto, mostra diferentes direções de paleocorrentes obtidas a partir de laminações de ondulação de corrente (para SE) e turboglifos (para NE), principalmente no EF (Figura 5), que aponta para uma evolução complexa ao longo do tempo.

A análise da espessura de camadas sugere que TBTs tendem a ter uma direção de paleocorrente para SE. A melhor explicação para isso no *Western Fan* (WF) é a associação com um alto topográfico que confinou o leque, resultando em uma tendência da parte superior do fluxo para depositar como depósito de *overbank* (Satur, 1999). No EF, foram consideradas duas explicações alternativas: 1) conforme mais distante da fonte, o particionamento de fluxo pode aumentar o ângulo entre os indicadores medidos e a parte com grãos finos do fluxo (superior) que escapa por cima dos altos topográficos; 2) a parte leste do EF é, na verdade, a parte distal da WF (Figura 6). Essa interpretação é diferente do que é sugerido na literatura.

A análise de afloramentos ao redor da vila de Cingöz sugere que a EF (ou pelo menos a última fase dele) foi depositada sob o WF. Isto significa que o WF atuou como um alto topográfico durante a última fase da construção do leque submarino, desviando o fluxo e depositando os lobos EF para o leste.

Com base na evolução dos lobos discutida, a alternativa 1 (acima) parece fornecer a melhor explicação para o desenvolvimento de lobos de EF para o NE, já que os blocos de construção dos lobos concordam com a interpretação de um depósito anterior ao sul (possivelmente o WF) agindo como um alto topográfico.

Figura 5: Análise de paleocorrentes na Formação Cingöz. A-B) Medidas de paleocorrentes em arenitos thin- e thick-bedded (CRL = laminações de ondulação de corrente); C) Medidas de paleocorrentes em CRL apenas; D) Medidas de paleocorrentes apenas em marcas de sola.
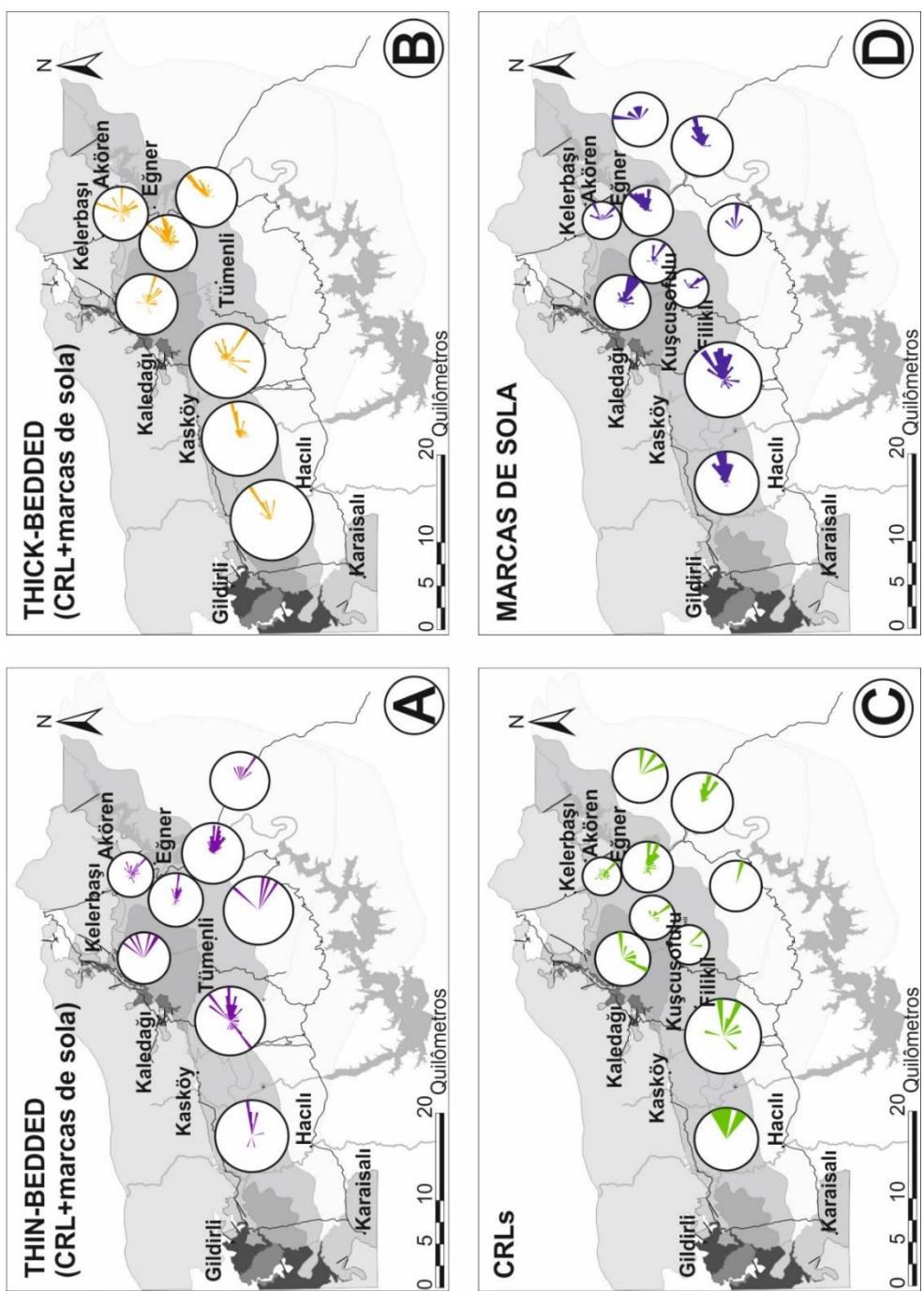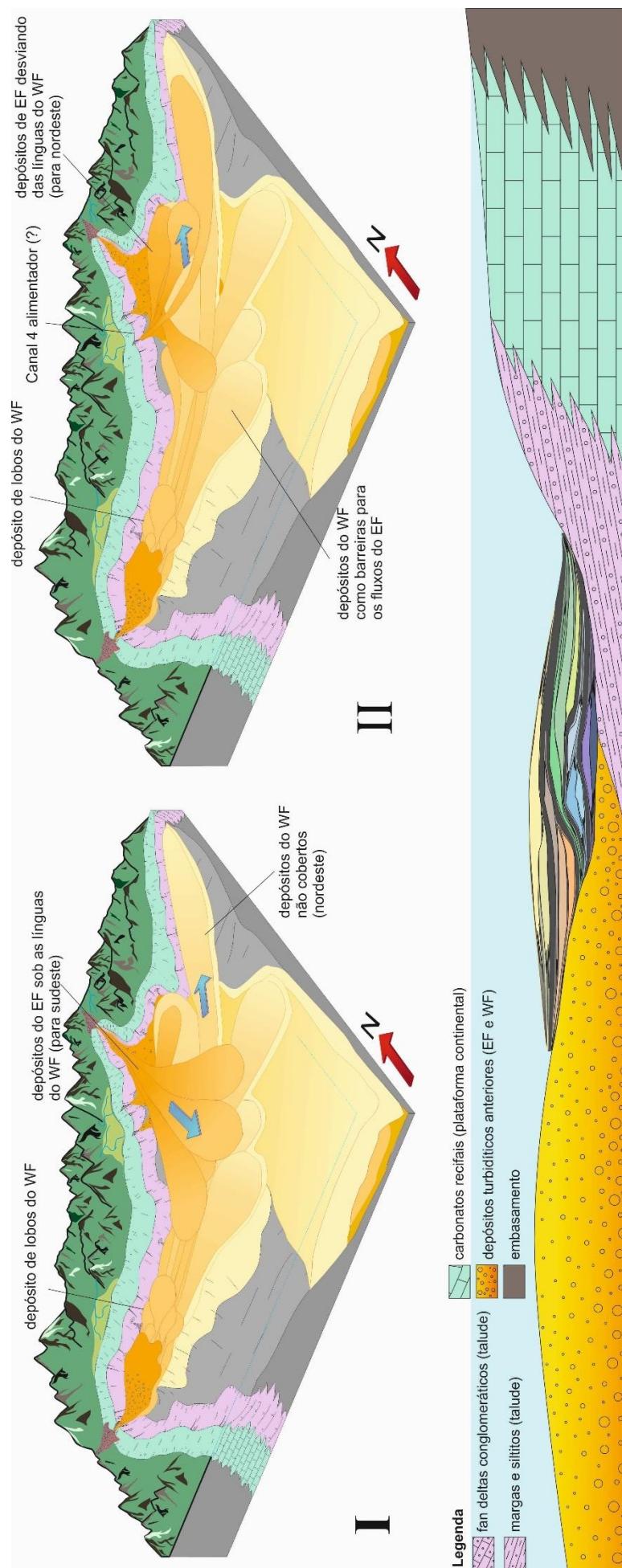
Figura 6: Evolução da Formação Cingöz - Estágio Serravaliano: retrogradação e etapas finais. O sistema começou a retrogradar, quando os lobos foram depositados nos estágios finais do WF (Satur *et al.*, 2007). O EF ainda está ativo, seguindo dois caminhos evolutivos alternativos: a alternativa I mostra o EF depositando sedimentos em direção ao sul/sudeste sobre as línguas do WF, principalmente através do Canal 1, enquanto na alternativa II os sedimentos eram transferidos principalmente através de canais 3 e 4 para leste/nordeste, desviando das línguas no sul, onde apenas sedimentos de grãos finos podiam passar. Abaixo dos bloco diagramas, a interpretação esquemática da análise da evolução dos lobos da Formação Cingöz, mostrando a relação entre os 13 lobos depositados e interpretados como sendo do EF em configurações semi-confinadas.

2. CONTEXTO GEOTECTÔNICO DA ÁREA

Este capítulo tem como objetivo revisar a literatura anterior sobre o cenário tectônico, paleogeografia e estratigrafia da Bacia Adana, e especificamente a Formação Cingöz, o foco principal desta tese.

2.1. Resumo da evolução tectônica da Turquia

A história geológica da Turquia é marcada por um grande número de eventos tectônicos nas Eras Mesozóica e Paleozóica. Ela faz parte do cinturão orogênico Alpino-Himalaia, marcando o extremo leste do setor alpino do Mediterrâneo, e provavelmente a melhor área para estudar os Oceanos Paleo e Neotétis (Şengör and Yilmaz, 1981). O Oceano Paleotétis, desenvolvido entre o Gondwana e a Laurásia a pelo menos 350 milhões de anos, no início do Carbonífero, era caracterizado por vias marítimas estreitas separadas por inúmeras ilhas, como o sudoeste do Pacífico hoje (Okay, 2008). Vários estudos propuseram a distinção entre Paleotétis (pré-Triássico) e Neotétis (pós-Triássico), provavelmente coexistindo durante este período (Tekeli, 1981; Şengör *et al.*, 1984; Okay, 2008). De acordo com a geologia da Anatólia, todos os ofiolitos (relíquias oceânicas) na Turquia são de idade Cretácea, enquanto os melanges ofiolíticos representam todos os períodos mesozóicos (Okay, 2008). O Oceano Tétis Paleozóico (Paleotétis) é reconhecido apenas na região de Pontides, interpretado como Paleozóico ao Triássico. Ambos, ofiolitos e o Complexo Karakaya são imbricados ao longo da sutura Izmir-Ankara-Erzincan (Tekeli, 1981; Okay e Göncüoğlu, 2004; Okay, 2008) (Figura 7), mas a relação entre o Paleo e Neotétis é desconhecida.

A Turquia é composta por três unidades tectônicas: os Pontides, os Anatolides-Taurides e a Plataforma Árabe (Figura 7). Eles eram micro-continentes cercados por oceanos e agora presos ao longo de linhas de sutura (Ketin, 1966; Okay, 2008). Os Pontides, na parte mais setentrional da Turquia, têm afinidades com a Laurasia (unidades tectônicas semelhantes na Europa central). A sutura Izmir-Ankara-Erzincan marca o fechamento da Neotétis e do limite com a unidade Anatolides-Taurides (Figura 7), que tem afinidade com o Gondwana (unidades similares na Arábia e na África) e está em contato com a Plataforma Árabe ao longo da sutura assíria (Okay, 2008).

Figura 7: Configuração tectônica dos principais fragmentos que constituem a Turquia: Pontides, Anatolides-Taurides e Plataforma Árabe. A área de estudo está localizada no retângulo vermelho. Adaptado de Ketin (1966).

O Paleotétis (Permiano/Triássico) foi estabelecido no norte da Turquia (região do Mar Negro), onde uma plataforma de carbonato foi formada (Figura 8A). A subducção levou ao fechamento deste mar, e durante este evento o Mediterrâneo oriental começou a se abrir para criar o Neotétis (Şengör, 1979a, b; Şengör and Yılmaz, 1981) e a massa de terra continental Ciméria (Şengör, 1979b) (Figura 8A).

Durante o Jurássico Médio, o Paleotétis fechou e a entrada de sedimentos clásticos aumentou em direção ao sul devido ao continente no norte que se aproximava. A ruptura do continente Cimério criou a unidade Anatolide-Tauride, enquanto o Neotétis continuou a crescer (Şengör and Yılmaz, 1981) (Figura 8B).

O Jurássico Superior e o Cretáceo Inferior foram marcados pela deposição generalizada em uma plataforma de carbonato e pelo tamanho máximo do Oceano Neotético, principalmente ao longo do braço norte. No final do período Cretáceo, a sedimentação pelágica ocorreu nos Pontides (Brinkmann, 1976; Biju-Duval *et al.*, 1978; Şengör and Yılmaz, 1981). Durante esse período, foram produzidos ofiolitos bem preservados (Dewey *et al.*, 1973).

No período Cretáceo Superior, a subducção entre placas africanas e euro-asiáticas, devido à abertura do Atlântico meridional e o braço norte do Neotétis

abaixo dos Pontides são indicativos da abertura do Oceano Atlântico Norte, do Mar Vermelho e do Golfo de Áden (Biju-Duval *et al.*, 1978; Şengör and Yılmaz, 1981; Satur, 1999), que foram ampliados nesse período, forçando os movimentos das placas (Figura 8C).

Acredita-se que a colisão entre as unidades Anatolides-Tauride e Pontides (micro-continentes) no Paleoceno Superior - Eoceno Inferior seja responsável pela formação dos Anatolides (Figura 8C e D), um maciço cristalino central da Anatólia (Ketin, 1966; Şengör and Yılmaz, 1981).

O Mioceno da Turquia é marcado pelo fechamento do Oceano Neotétis (Yilmaz, 1993) e pela colisão entre a Arábia e a Eurásia (Dewey *et al.*, 1973; Şengör and Yilmaz, 1981) (Figura 8D). Este evento é importante para o presente estudo, pois é responsável pelo soerguimento da área de origem dos turbiditos aqui estudados, conforme descrito na próxima seção.

Figura 8A: Evolução paleotectônica da Turquia (delineada em vermelho) do período Permiano ao Triássico. Adaptado de Şengör and Yılmaz (1981).
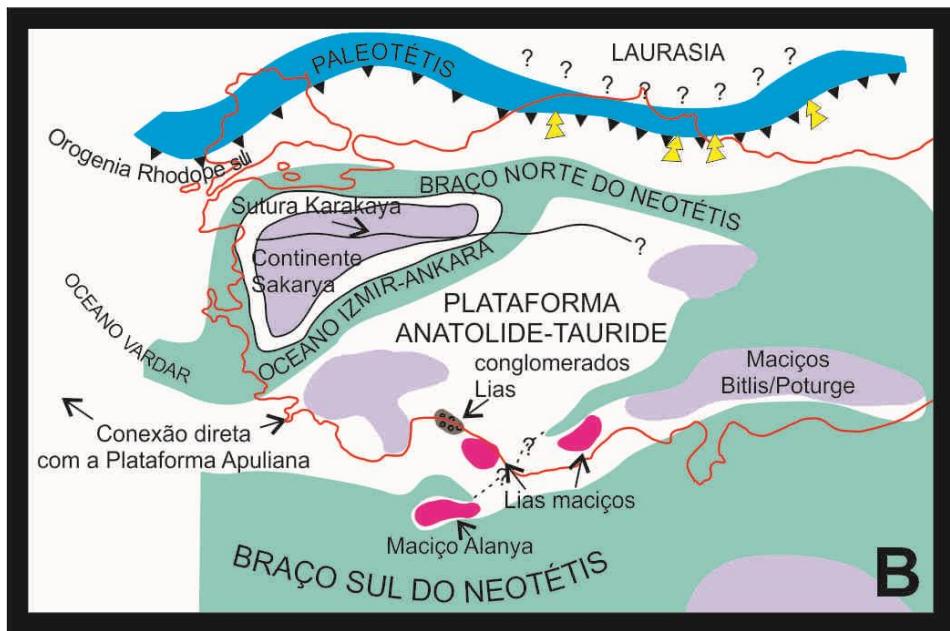
Jurássico inicial
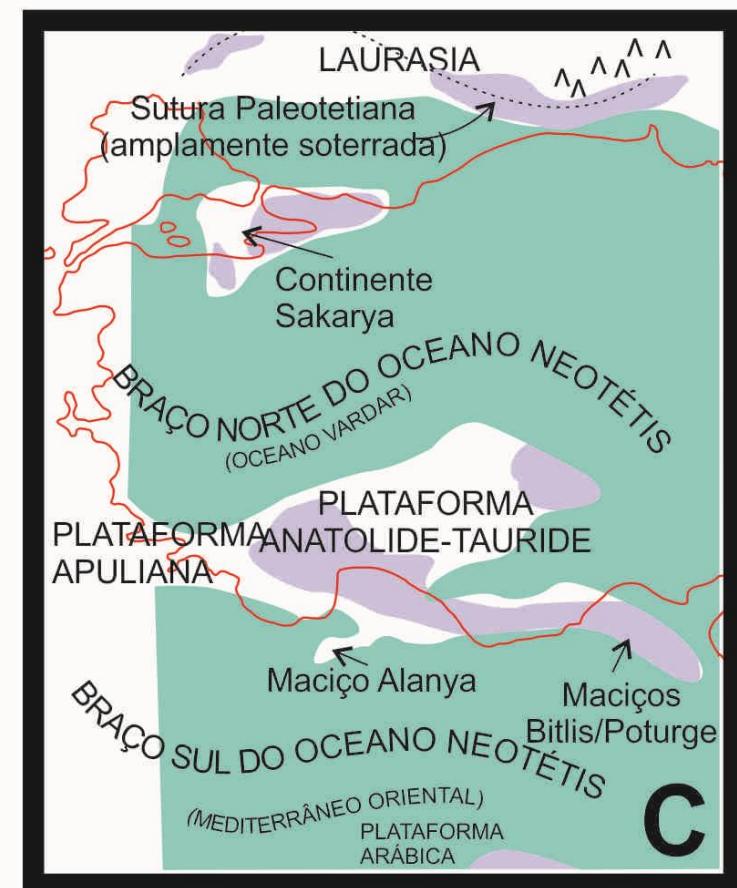
Jurássico tardio - Cretáceo inicial

Figura 8B: Evolução paleotectônica da Turquia (delineada em vermelho) dos tempos do início do período Jurássico ao início do Cretáceo. Adaptado de Şengör and Yılmaz (1981).
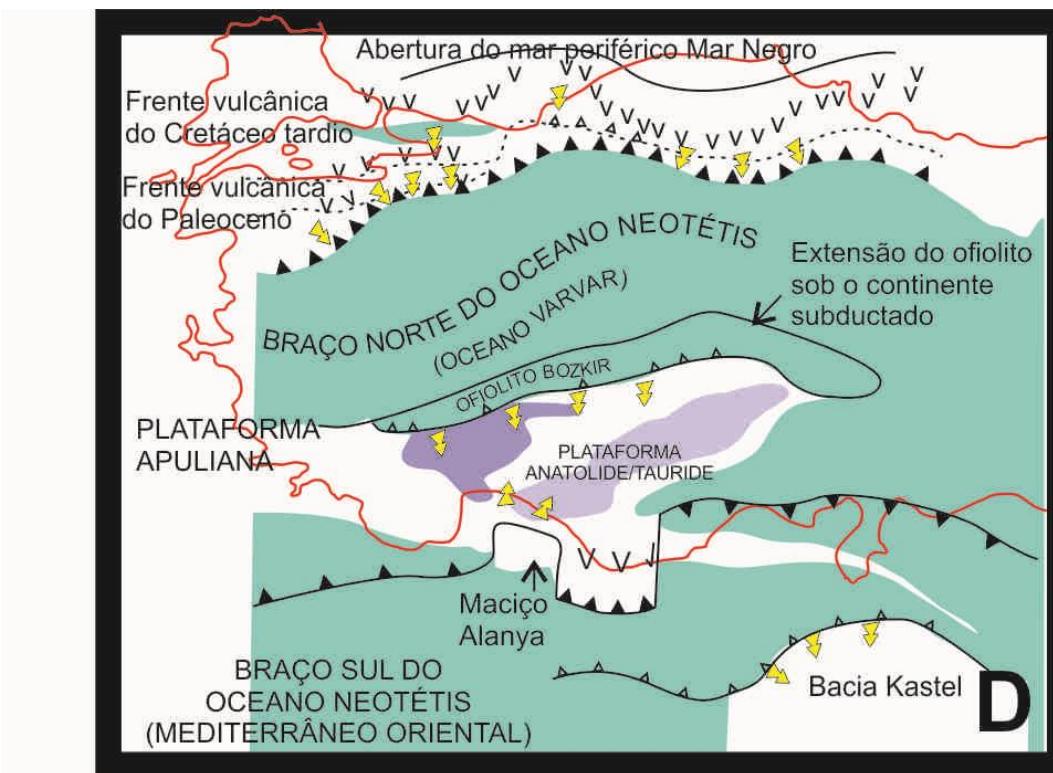
Cretáceo-Paleoceno
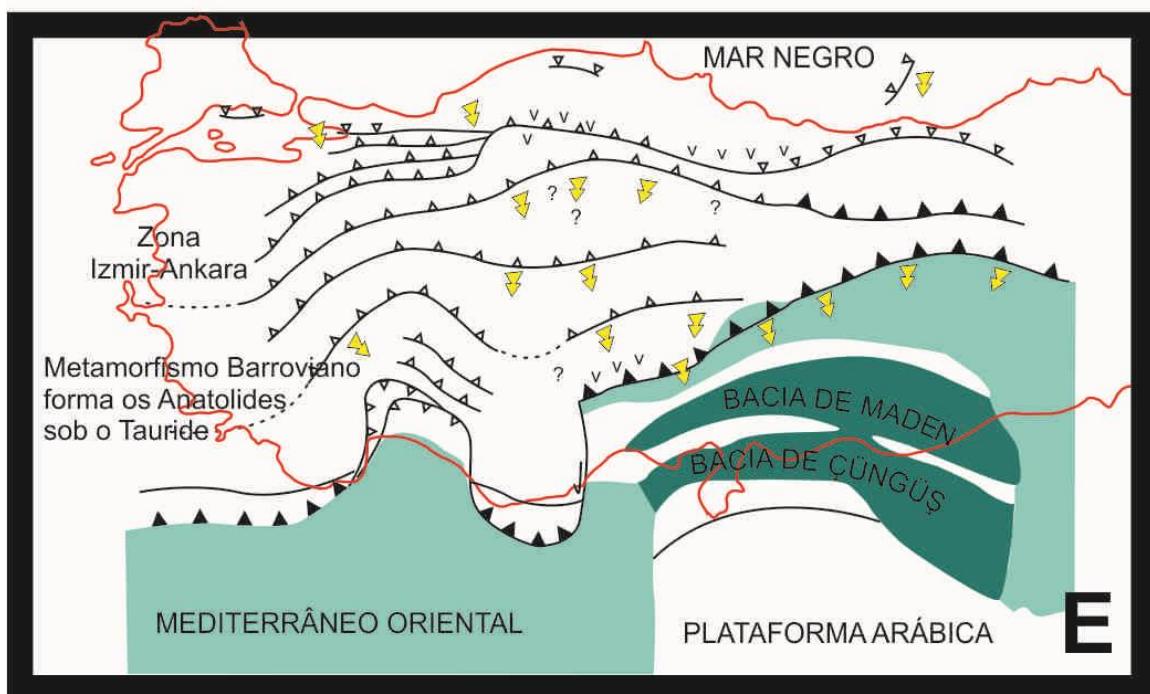
Eocene médio

Figura 8C: Evolução paleotectônica da Turquia (delineada em vermelho) dos tempos do Cretáceo ao Eoceno Médio. Adaptado de Şengör and Yılmaz (1981).
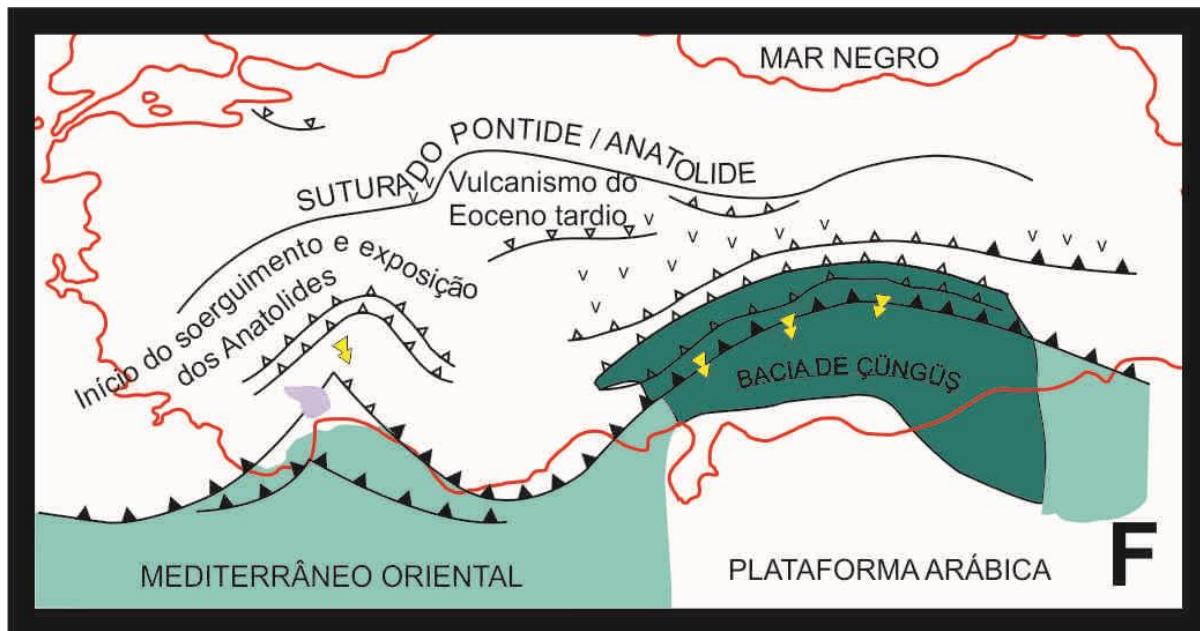
Eoceno tardio-Mioceno inicial
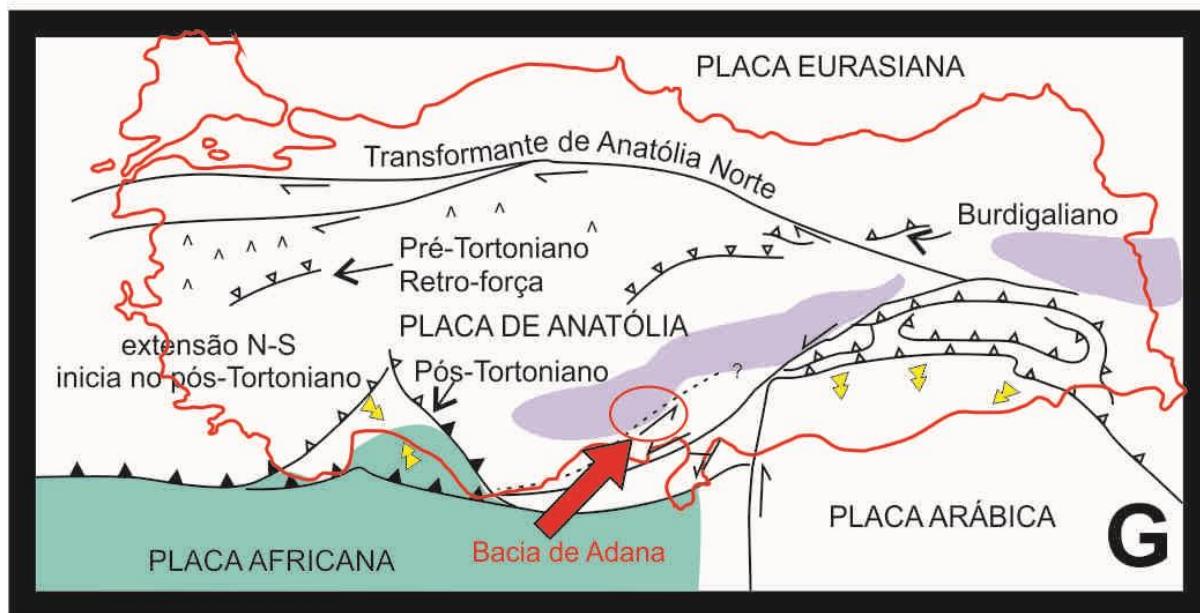
Mioceno médio-Plioceno

Figura 8D: Evolução paleotectônica da Turquia (delineada em vermelho) do final do Eoceno para os tempos Mioceno Médio/Plioceno. A seta vermelha indica a localização da Bacia de Adana. Adaptado de Şengör and Yılmaz (1981).

2.2.   Bacia de Adana e evolução das áreas adjacentes

A Bacia de Adana está localizada no sul da Turquia, muito próxima à junção tripla de microplacas (Árabe, Africana e Egéia-Anatólia) (Cipollari *et al.*, 2013; Radeff *et al.*, 2015). Ela é a parte terrestre da Bacia de Adana-Cilícia (Brinkmann, 1976; Kelling *et al.*, 1987), sendo a Bacia da Cilícia sua contrapartida marítima (*offshore*) (Figura 9).

A Bacia Adana-Cilícia é limitada ao N e ao NW pelo planalto da Anatólia Central, e ao S e SE pelas Montanhas de Kyrenia e Misis (lineamento de Kyrenia-Misis) (Figura 9). As Montanhas Misis foram erguidas durante o Mioceno Superior (Kelling *et al.*, 1987; Williams *et al.*, 1995). Há duas sugestões em relação ao seu início; Kelling *et al.* (1987) sugeriram que as Montanhas Misis são uma estrutura floral positiva relacionada à transpressão do Mioceno Superior (cinturão de dobra e empurrão). Robertson *et al.* (2004) defendem que as montanhas de Misis resultaram de uma história de deformação multifásica, não apenas do Impulso do Mioceno Superior, mas também da deformação deslizamento no Plio-Quaternário.

Segundo Cipollari *et al.* (2013), muitos modelos diferentes foram sugeridos para o início do complexo da Bacia de Adana-Cilícia, que incluem: 1) uma bacia de extração relacionada à zona de transformação da Falha da Anatólia Oriental (Şengör *et al.*, 1985); 2) uma bacia *backarc* (Kelling *et al.*, 1987); 3) juntamente com a Bacia de Iskenderun-Latakia, parte da transtensional cinemática lateral esquerda ao longo da zona de falha de Misis-Kyrenia (Karig and Kozlu, 1990); 4) uma bacia criada por extensão difusa (Kempler, 1994); 5) uma bacia de *foreland* subsidente, induzida pela carga orogênica dos Taurides (Ünlügenç, 1993; Williams *et al.*, 1995); 6) uma bacia extensional (Robertson, 1998, 2000); 7) uma bacia *foredeep*, criada por tectônica de compressão (Burton-Ferguson *et al.*, 2005; Aksu *et al.*, 2005).
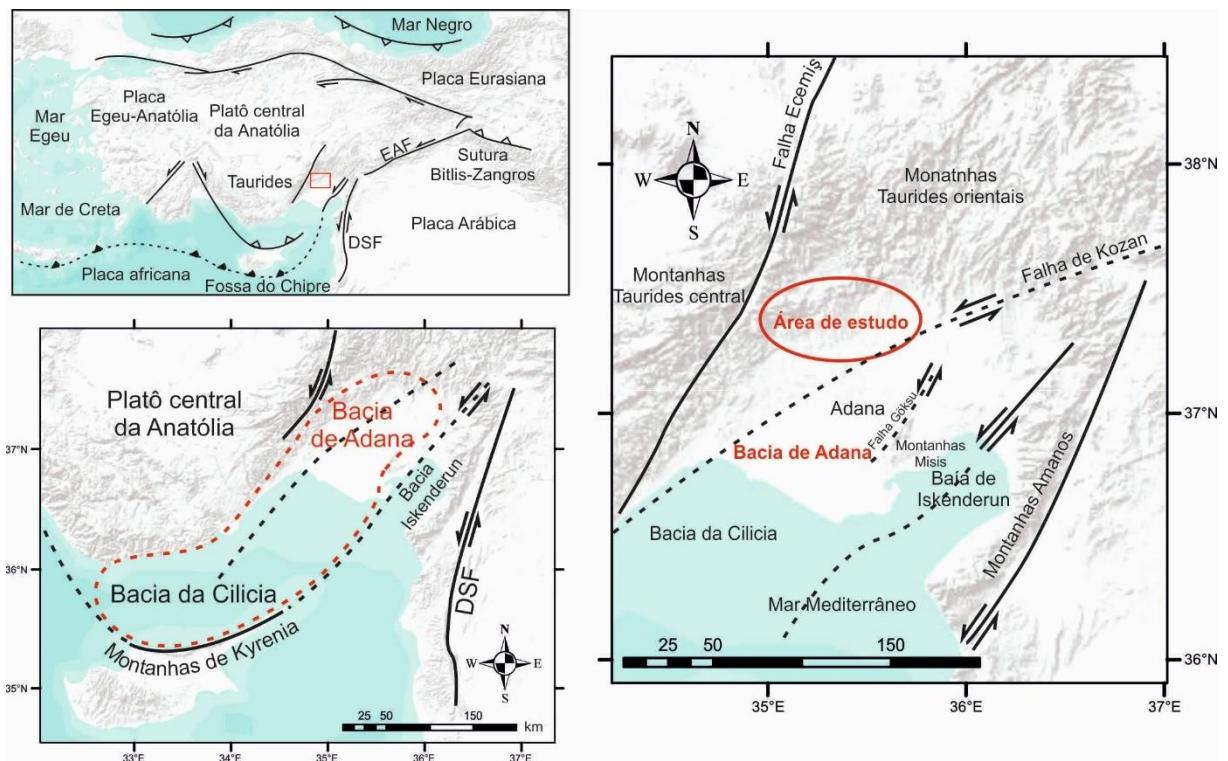
Figura 9: Mapa tectônico destacando a Bacia Adana e arredores. Em linhas tracejadas vermelhas, o Complexo da Bacia Adana-Cilícia. A área de estudo (círculo vermelho) está localizada ao norte da cidade de Adana, e limitada ao norte pelas Montanhas Tauride Centrais e ao sul pela Falha Kozan. Adaptado de Radeff *et al.* (2015).

3. GEOLOGIA DA ÁREA

3.1. Estratigrafia da Bacia de Adana

A Bacia de Adana é uma das maiores bacias de *foreland* do Mioceno no sul da Turquia (Ilgar *et al.*, 2013). Sua estratigrafia foi proposta pela primeira vez por Schmidt (1961). A sucessão sedimentar compreende até 6 km de depósitos siliciclásticos e carbonáticos do Mioceno e do Quaternário (Figura 10).

O embasamento da bacia é constituído por rochas paleozóicas, incluindo calcários coralíneos e arenitos devonianos, calcários permo-carboníferos, carbonatos plataformais mesozóicos e turbiditos (Ilgar *et al.*, 2013), juntamente com uma mistura ofiolítica da orogenia Tauride (Cipollari *et al.*, 2013).

O preenchimento do Neógeno na Bacia Adana é dividido em três megasesquências, com base no caráter sísmico interno e relações de contorno

(discordâncias) (Williams *et al.* 1995), ou em depósitos transgressivos e regressivos pré-transgressivos (Yetiş *et al.*, 1995; Satur, 1999) (Tabela 3).

Tabela 3: Comparação das proposições estratigráficas, baseada em megasseqüência (Williams *et al.*, 1995) e ciclos regressivos/transgressivos (Yetiş *et al.*, 1995). De Satur (1999).

Formação Terciária	Ambiente (profundidade relativa do mar)	Megasequência	Regressivo/transgressivo
Handere	Terrestre/águas rasas	Megasequência 3	Regressivo
Kuzgun			
Güvenç	Água profunda	Megasequência 2	Transgressivo
Cingöz			
Kaplankaya			
Karaisalı	Águas rasas	Megasequência 1 (embasamento sísmico)	Pré-transgressivo
Gildirli	Terrestre	Não resolvido pela sísmica	
Karsanti			
Mesozóico	-		Embasamento

De acordo com Gürbüz (1993, 1999), as mudanças relativas no nível do mar na Bacia de Adana se encaixam bem no esquema global de subida e descida do nível do mar de Mitchum *et al.* (1977) e Haq *et al.* (1987, 1988) para o Paleógeno - Neógeno Superior (Satur, 1999). Um ciclo transgressivo-regressivo de frequência mais baixa (aprox. 15 ma.) compreende todo o preenchimento da bacia do Neógeno, com altas frequências representando variações de fácies (Gürbüz, 1993; Ünlügenç, 1993; Satur, 1999).

Com base em estudos bioestratigráficos e interpretações litológicas (Gürbüz, 1993; Nazik, 2004), uma curva relativa do nível do mar para a Bacia de Adana revela uma transgressão principal durante o Burdigaliano Superior - Langhiano Inferior e uma regressão no Serravaliano Superior (Figura 11).
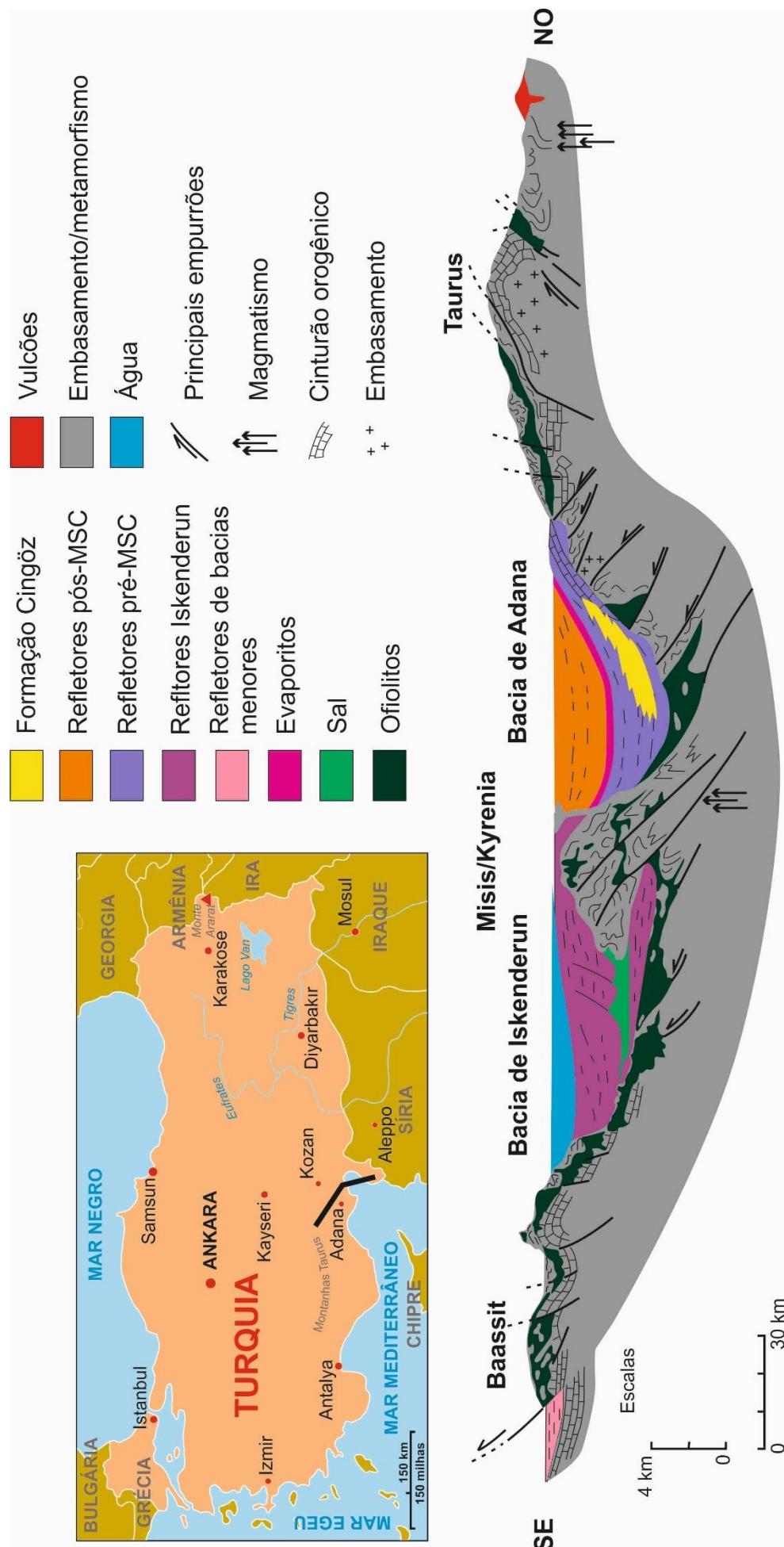
Figura 10: Seção transversal (NW-SE) através das Montanhas Tauride, com as Bacias de Adana e Iskenderun e algumas características relevantes destacadas. Adaptado de Biju-Duval *et al.* (1978). (MSC = Messinian Salt Crisis, ou crise salina do Messiniano).

Principais unidades geológicas

A primeira deposição na Bacia de Adana, sobreposta aos sedimentos Paleozóicos sobrejacentes, consiste em camadas vermelhas fluviais e lacustres do Oligoceno-Mioceno Inferior das Formações Karsantı e Gildirli (Schmidt, 1961; Yetiş, 1988; Ünlügenç *et al., 1991*; Gürbüz and Kelling , 1993) (Figura 11). A Formação Karsantı consiste em conglomerados avermelhados (leque aluvial e preenchimento de canais entrelaçados) e arenito cascalhoso na base, recoberto por margas e argilitos (origem lacustre e planície de inundação) (Yetiş *et al*. 1995; Radeff *et al*., 2015) depositados em uma bacia intramontanha, um precursor da Bacia de Adana (Ünlügenç, 1993). A Formação Gildirli é composta por conglomerados, arenitos e folhelhos dispostos numa série de sequências de 2 - 20 m em granodecresência ascendente, sobrepostas por 20 - 30 m de lamito (Yetiş, 1988; Görür, 1992).

A Formação Kaplankaya, que se sobrepõe à Fm. Gildirli, é o primeiro depósito transgressivo marinho na Bacia Adana, compreendendo arenitos, siltitos, margas e calcários arenosos (Burdigaliano-Serravalino). Esta formação é interpretada como depositada principalmente no ambiente de talude continental (Figura 12A-B), parcialmente contemporânea e topograficamente lateral e vertical às Formações Gildirli, Karaisalı e Cingöz (Gürbüz and Kelling, 1993).

A Formação Karaisalı (Figura 12A) consiste em calcários recifais que são subdivididos em seis subfacies: coral *packstone* e *boundstone*, pequenos *packstones* bentônicos de algas e foraminíferos, coral *wackestone* e *packstone*, grandes *packstones* bentônicos de algas e foraminíferos, *packstone* bioclástico composto por foraminíferos (globigerinóides) e algas e *wackestone* argiloso composto por foraminíferos (globigerinóides) (Görür, 1979; Nazik, 2004). A Formação, com uma idade variando de Burdigaliana a Langhiana, ou possivelmente Serravaliana (Görür, 1979), tem cerca de 20 - 350 m de espessura e está localizada em altos estruturais.
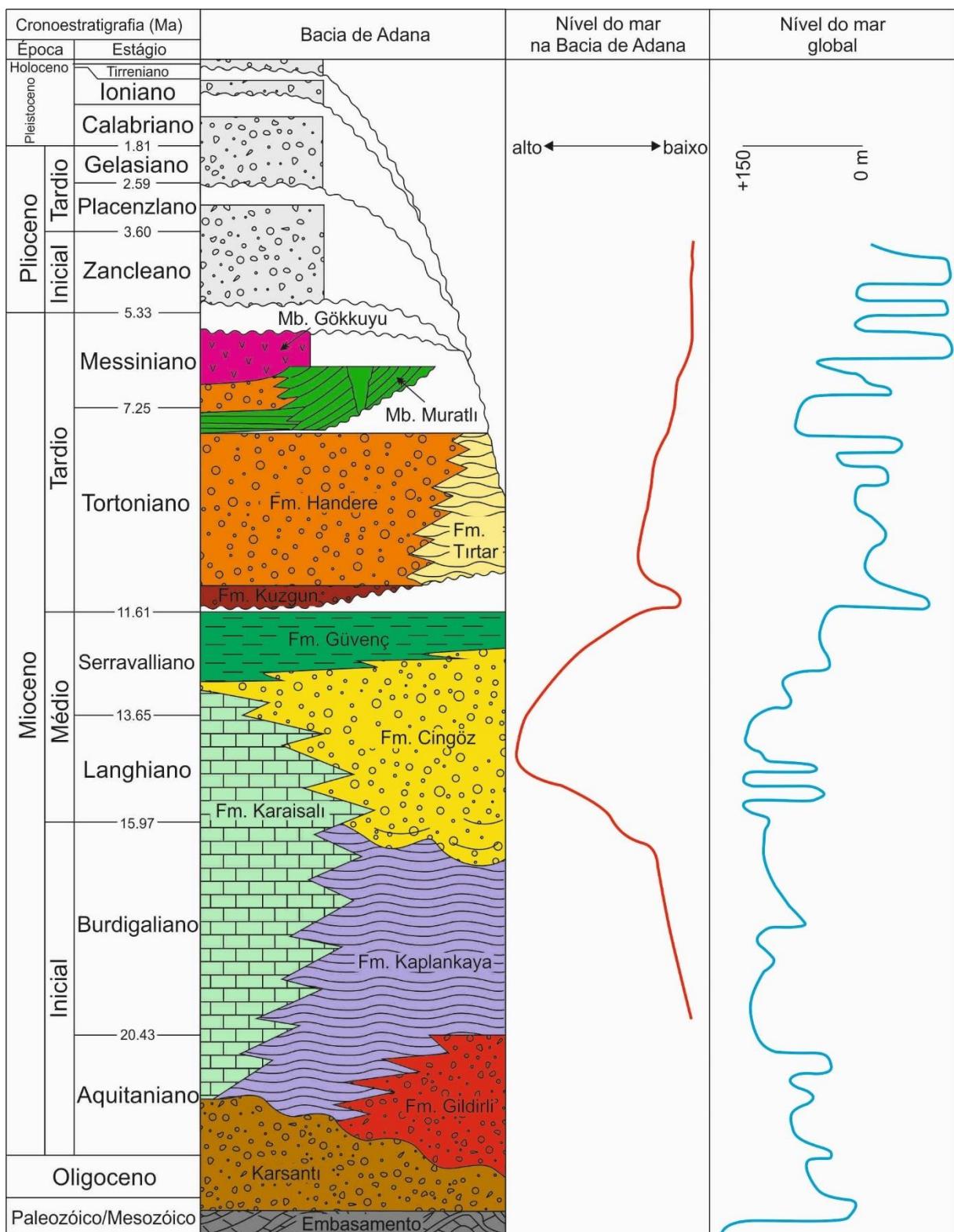
Figura 11: Diagrama estratigráfico da Bacia de Adana com os tratos de sistema da estratigrafia de seqüências, e as curvas de nível do mar da Bacia de Adana e global. De Haq *et al.* (1987); Nazik and Gürbüz (1992); Gürbüz, (1993); Yetiş *et al.* (1995); Ilgar *et al.* (2013).

A Formação Cingöz (Figura 12C) é composta por arenitos canalizados, em blocos e cascalhosos a arenitos turbidíticos tabulares (Gürbüz and Kelling, 1993) depositados durante o Burdigaliano Superior ao Serravaliano Inferior (Nazik and Gürbüz, 1992). Na parte ocidental da Formação Cingöz, um canal/canyon corta as Formações Gildirli, Karaisalı e Kaplankaya, criando o sistema turbidítico (Görür, 1979; Yetiş and Demirkol, 1986; Yetiş, 1988; Gürbüz and Kelling, 1993; Williams *et al.* 1995, Satur, 1999). De acordo com Gürbüz (1993), os depósitos da Formação Cingöz têm de 1000 a 3000 m de espessura e foram depositados em 5 milhões de anos (Satur, 1999).
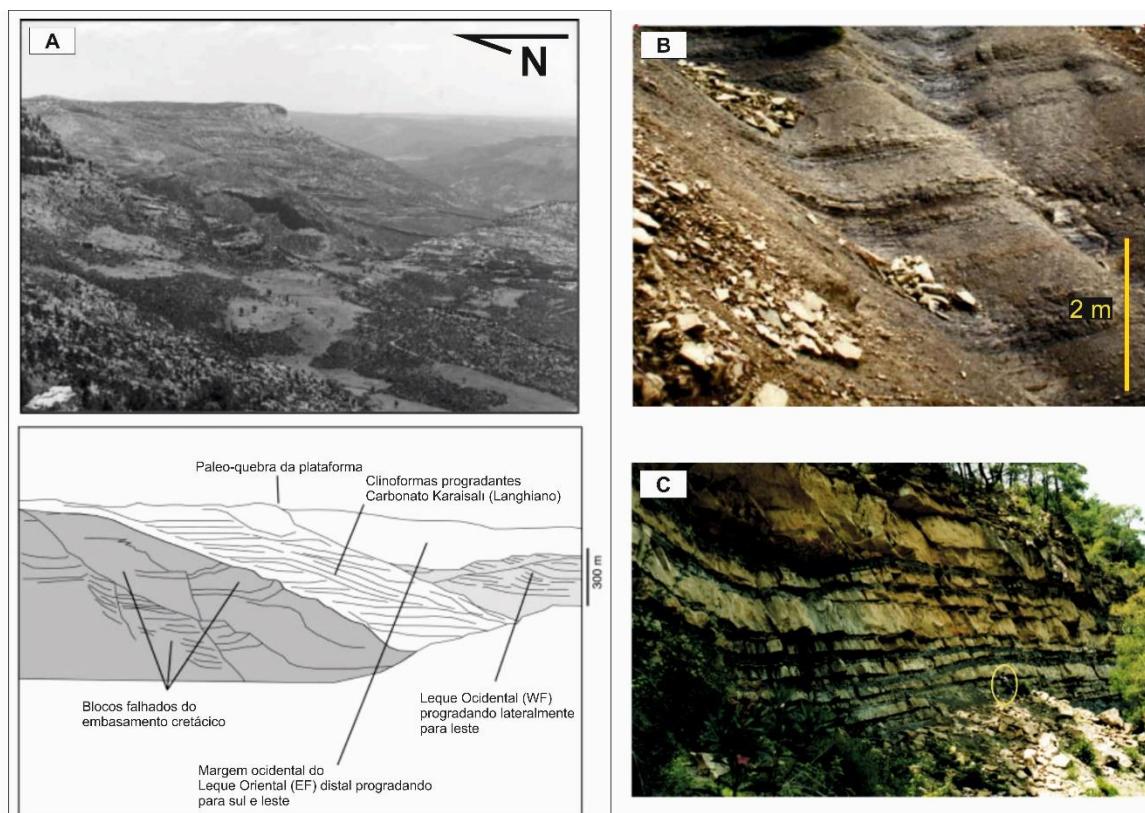
Figura 12: Visão geral das três principais formações, foco do presente estudo: A) vista do topo da Formação Karaisalı, mergulhando para o sul em direção às Formações Kaplankaya e Cingöz (foto e esquema adaptado de Cronin *et al.* (2000); B) depósitos de siltitos da Formação Kaplankaya (Satur, 1999); C) sucessão espessamento ascendente de arenitos em forma de língua da Formação Cingöz (Satur, 1999; Satur *et al.*, 2000).

Outra formação, parcialmente contemporânea à Cingöz, Karaisalı e Kaplankaya, é a Formação Güvenç, composta por até 2100 m de sedimentos de tamanho de grão fino (abaixo do tamanho areia) de fundo de bacia marinha profunda depositados no Serravaliano (Ünlügenç *et al.* 1991; Nazik and Gürbüz 1992; Gürbüz and Kelling 1993; Gürbüz, 1993; Ünlügenç 1993).

Uma discordância sobrepõe essa sequência, marcando o retorno da deposição continental durante a acumulação da Formação Kuzgun no Serravaliano–Tortonian Inferior (Ünlügenç 1993; Faranda *et al.*, 2013), após uma queda relativa no nível do mar no final de Serravaliano (Ilgar *et al.*, 2013). A formação foi subdividida em três membros: o Kuzgun, o Salbaş Tuffite e o Memisli (Yetiş and Demirkol, 1986). O Membro Kuzgun cobre diretamente a discordância, e consiste de aproximadamente 435 m de arenitos vermelhos e amarelos, conglomerados e folhelho depositados por um sistema fluvial (Yetiş *et al.*, 1995). Sobrepondo este membro está o membro relativamente fino de Salbaş Tuffite, composto por arenitos tufáceo depositados no Tortoniano. Finalmente, o Membro Memisli é um pacote de 443 m de sedimento deltáico, lagunar e marinho raso composto por arenitos e siltitos de idade Tortoniano-Messiniano (Tanar, 1985; Gürbüz and Gökçen 1985).

A última formação do Neógeno da Bacia de Adana é a Formação Handere de 450 m de espessura (Schmidt, 1961), depositada predominantemente no Mioceno Superior-Plioceno, e constituída por arenitos marinho raso e lagunar e lamito, e localmente conglomerados fluviais (Öğrünç *et al.*, 2000). Cosentino *et al.* (2010) e Cipollari *et al.* (2013) sugeriram que o limite Kuzgun/Handere está correlacionado com o MES (*Messinian Erosional Surface*), relacionado com a Crise Salina do Messiniano ou *Messinian Salinity Crisis* (MSC) da Bacia do Mediterrâneo (Hsü, 1973; Ryan, 2009), representado por uma sucessão cíclica de anidritos e folhelhos negros.

As formações mais importantes nesta tese são as Formações Cingöz e Kaplankaya, geneticamente ligadas para criar o Leque (submarino) Cingöz.

3.2.   Trabalhos anteriores na Formação Cingöz

Embora a Bacia de Adana tenha sido objeto de vários estudos, incluindo geologia estrutural, bioestratigrafia, paleoclima, etc., os estudos da Formação Cingöz, objeto desta tese, são menos frequentes. A área de estudo é composta por três formações contemporâneas: Cingöz, Karaisalı e Kaplankaya (Figura 13).

A fisiografia atual da Formação Karaisalı, formada por depósitos recifais, ainda reflete o fundo do mar do Mioceno. Por exemplo, a antiga quebra da plataforma é amplamente preservada em altitudes de até 1500 m (Cronin *et al.* 2000). Estas clinoformas mergulham para o sul e se interdigita com os depósitos de talude da

Formação Kaplankaya, sobrepostos pelos arenitos e conglomerados da Formação Cingöz (Figura 13). Esta distribuição permite o estudo das relações espaciais entre os três diferentes ambientes.

Os principais estudos da Formação Cingöz incluem Naz *et al.* (1991), que usaram dados sísmicos e de testemunho para comparar com a análise de afloramentos. A descrição sedimentológica dos afloramentos fornecidos por Gürbüz (1993) ainda é o trabalho mais completo sobre sedimentologia, seguido por outros como Gürbüz and Kelling (1993), que estudaram as áreas de proveniência.

Nazik and Gürbüz (1992) publicaram um estudo paleontológico completo, e Demircan and Toker (2003) descreveram traços fósseis. As influências tectônicas na formação foram discutidas por Ünlügenç (1993). Satur (1999) realizou um estudo completo dos dois leques, principalmente no sistema alimentador e no WF.

A maior parte da Formação Cingöz consiste em depósitos turbidíticos com geometria tabular (Yetiş, 1988; Ünlügenç and Demirkol, 1988), depositados durante o período tardio de Burdigaliano Tardio-Serravaliano Inicial, entre 13 e 17 Ma atrás (Nazik and Gürbüz, 1992).

Segundo Posamentier and Vail (1988) e Posamentier *et al.* (1991), um leque submarino é depositado principalmente durante rebaixamentos globais do nível do mar, como parte do trato de sistema de nível baixo (*low stand tract* (LST), em inglês). No entanto, Mutti (1992) destacou que, em bacias controladas tectonicamente, o nível do mar eustático é menos importante, e a atividade tectônica (por exemplo, elevação) será o principal controle na sedimentação.

As tentativas de criar uma curva do nível do mar para a Bacia de Adana (Figura 11) usaram análise de fácies e evidência fóssil (Yetiş, 1988; Yetiş and Demirkol, 1986) e mostram grande semelhança com a curva de Haq *et al.* (1987). A Formação Cingöz foi atribuída a um trecho de sistema de mar alto (Figura 11), sugerindo que outros fatores, além do nível do mar global (ou seja, tectônica) controlavam a sedimentação da Formação Cingöz.

Gürbüz (1993) sugeriu que o rebaixamento da plataforma carbonática preexistente no final de Burdigaliano forneceu o espaço de acomodação para a deposição dos sedimentos de Cingöz. O influxo de sedimentos de granulação muito

grossa na sucessão inferior de Cingöz sustenta isso, uma vez que a elevação tectônica da área da fonte pode causar queda relativa no nível do mar.
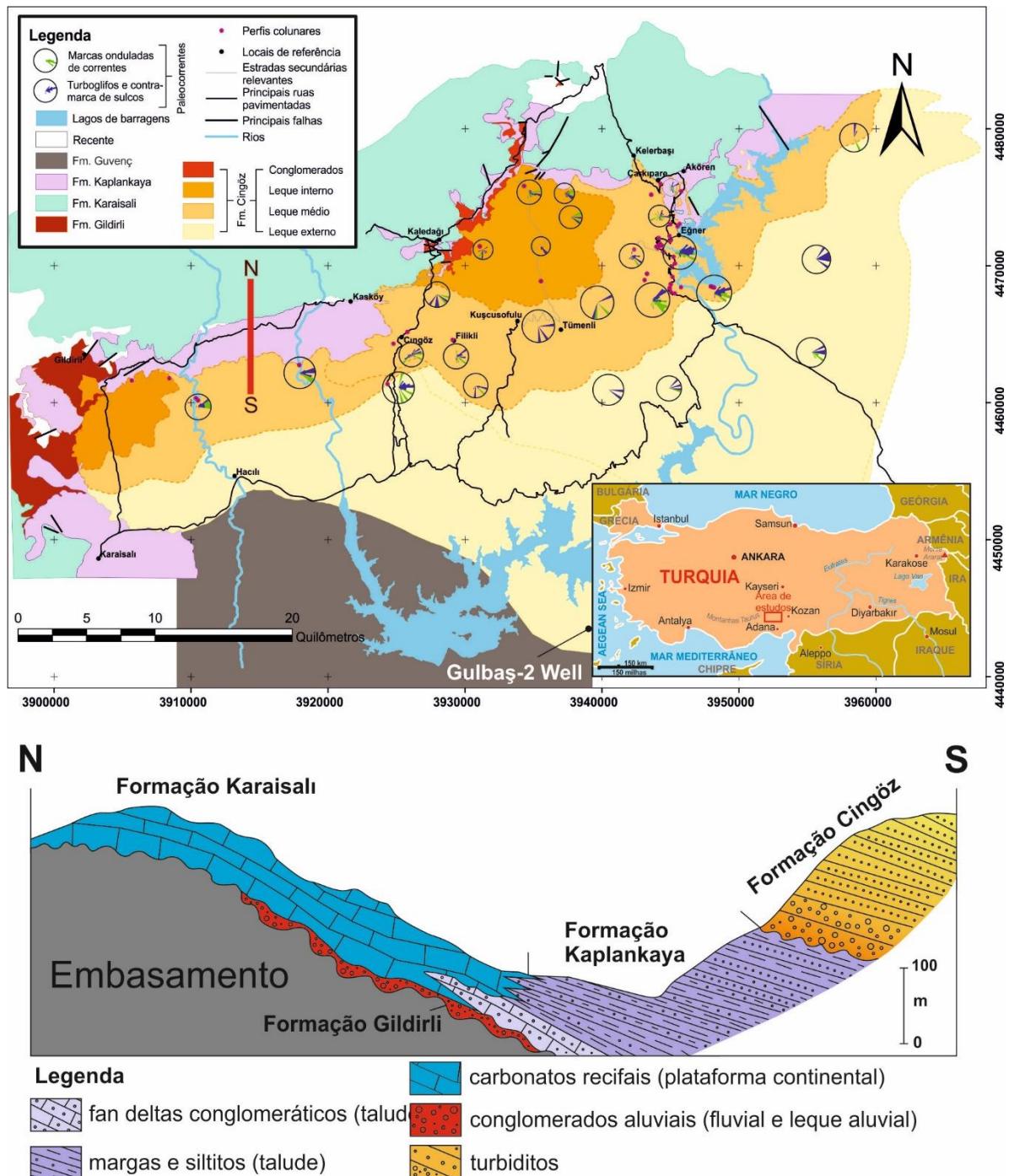
Figura 13: Mapa geológico da área de estudo (após Gürbüz and Kelling, 1993) e o corte transversal mostrando a relação de três formações principais (redesenhadas após Gürbüz, 1993). Observe a localização do Furo Gulbaş-2 no sul, que será descrita mais adiante.

3.2.1. Breve descrição do Leque Ocidental (WF)

Sistema alimentador do WF

Satur (1999) descreveu dois sistemas alimentadores diferentes para cada leque submarino: o WF, derivou de uma fonte pontual a oeste, enquanto o EF foi construído por vários canais ao norte. A denominação utilizada no presente estudo (EF e WF) foi sugerida por Gürbüz and Kelling (1993) e Gürbüz (1993).

O WF ultrapassa a plataforma carbonática contemporânea, distribuindo sedimentos predominantemente à leste (080 - 110 °) ao longo de um gradiente de 1,7 - 2,9 °. Segundo Satur (1999), as margens do canyon estão no norte e no sul, exibindo uma seção transversal assimétrica (Figura 14), com uma configuração íngreme no norte e suave no sul.
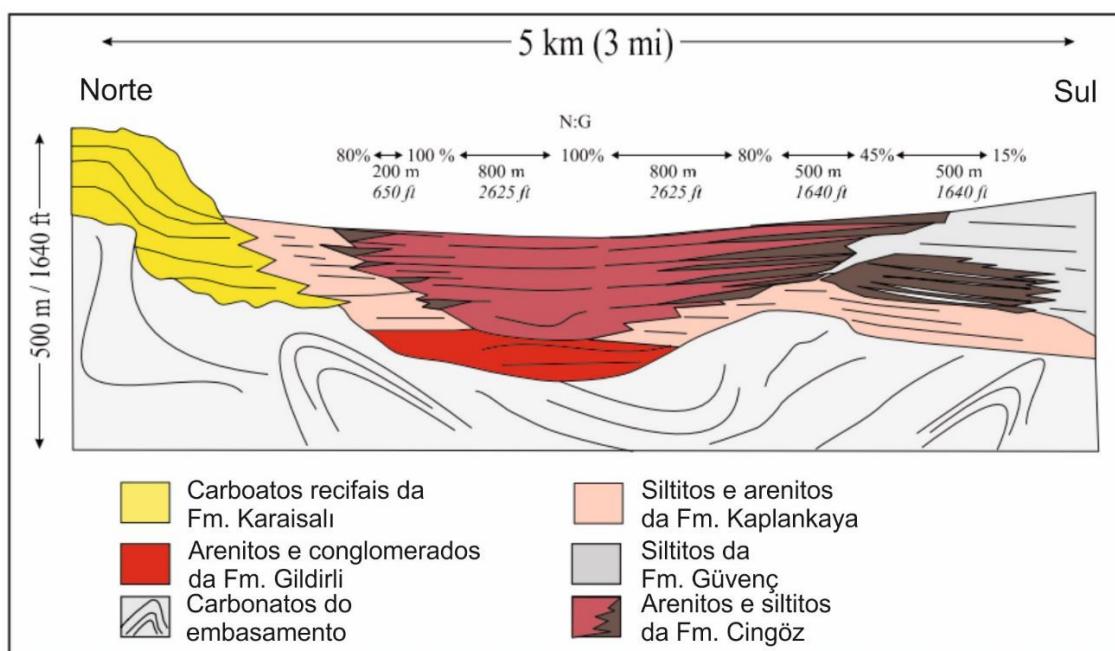
Figura 14: Seção transversal interpretada do canal no WF, corroendo os sedimentos de Kaplankaya e Gildirli (Satur *et al*., 2007). A seção transversal assimétrica mostra a variação N:G da margem norte para a margem sul e as distâncias em metros e em pés (*ft*).

Os TBTs ao longo da margem sul foram interpretados como depósitos de extravasamento, baseados nas paleocorrentes oblíquas (090 - 185 °) em relação às principais paleocorrentes oeste-leste do canal, e também a rápida mudança na relação *net-to-gross*. (Figura 14). Outra razão para considerá-los um depósito de extravasamento é que eles ocorrem apenas na margem sul, devido ao relativo alto relevo da margem norte. Além disso, no hemisfério norte, a ação de Coriolis forçaria

os sedimentos a serem derramados do canyon para a direita (ou seja, para o sul) (Satur, 1999).

Sistema deposicional do Leque Ocidental (WF)

O WF foi formado por um sistema turbidítico confinado (topograficamente e/ou estruturalmente) (Şengör and Yilmaz, 1981; Satur, 1999; Satur *et al.*, 2007). Satur (1999) distinguiu dois estilos deposicionais: os corpos em forma de língua (alongados) e os corpos em forma de lobos (radiais). Satur (1999) defende que essas línguas influenciaram as paleocorrentes do nordeste dos depósitos do EF para o nordeste, em vez de sul/sudeste.

Os corpos alongados são separados verticalmente e lateralmente por 50 a 100 m de TBT's. Os arenitos em forma de lobos foram depositados acima das línguas, cerca de 10 km da cabeça do canal (Figura 15), e provavelmente são estratigraficamente equivalentes à parte superior do WF (Satur, 1999).

A evolução do WF é mostrada na Figura 15. A deposição inicial de sedimentos preencheu o canal, seguida pelos depósitos em forma de língua que representam a progradação máxima, e recobertos por lobos com canais distributários, desenvolvidos durante a retrogradação do sistema (Satur, 1999).

Figura 15: A) Mapa geológico do WF, onde as linhas tracejadas exibem a margem do canal; B) Diferentes componentes da Formação Cingöz no WF; C) Corte transversal esquemático (I-I') ilustrando a relação espacial e temporal entre os componentes; D) Evolução do depósito para o WF em três etapas (I, II, III). Leques aluviais/fan deltas alimentam o sistema criando o canal (I), seguido pela progradação máxima do WF onde as línguas se estendem em direção à bacia (II), e finalmente os lobos aref níticos (III) desenvolvidos pela retrogradação do leque. De Satur *et al.* (2000).

I
Alluvial/
fan delta

Shelf
Slope
Basin floor
Feeder fairway

N

D

II

Sediment from
the Eastern Fan

Tongue-shaped
sandstone bodies

III

Lobe-shaped sandstone
bodies with distributary
channels

Eastern Fan

25 km

A

Stratigraphy
Recent.
Güvenc.
Cingöz deep-
water fan.
Kaplankaya
alluvium.
Kaplankaya
slope siltstone.
Karaisalı
Gildirli.
Mesozonic
Basement.
River
N

KARAİSALI

Eğlence River

Körkun River

Fairway margin

Fairway margin

B

FAIRWAY

LOBES-
DISTRIBUTARY
CHANNELS

TONGUES

Körkun River

Eğlence River

Scale
0   5 km

Outline of Cingöz Formation
Feeder alluvial fan / fan delta
Canyon
Lobes with distributary channels
Tongue-shaped sandstone bodies
Sand from the eastern area of the Cingöz Fan

I

I'

C

Alluvial fan/
fan delta
Canyon
Inter-lobes and lobes with distributary channels
Canyon to tongue transition zone
Tongues and inter-tongues

I'

Basin floor
Limestone
Basement

3.2.2. Breve descrição do Leque Oriental

Sistema alimentador do Leque Oriental (EF)

Em contraste com o WF, de acordo com Satur (1999), o EF tinha pelo menos quatro canais de alimentação (Figura 16). O canal principal foi denominado Canal 1 e os outros três foram interpretados como distributários (canais 2, 3 e 4).

A cabeceira do Canal 1 estava localizada ao sul da vila de Meydan Yayla. A margem oeste do Canal 1 é confinada por carbonatos da Formação Karaisalı, que alcançam até 100 m acima do topo do canal. A margem leste não é exposta, mas as descrições de campo inferem uma largura de canal de pelo menos 500 - 600 m (Satur *et al*., 2004).
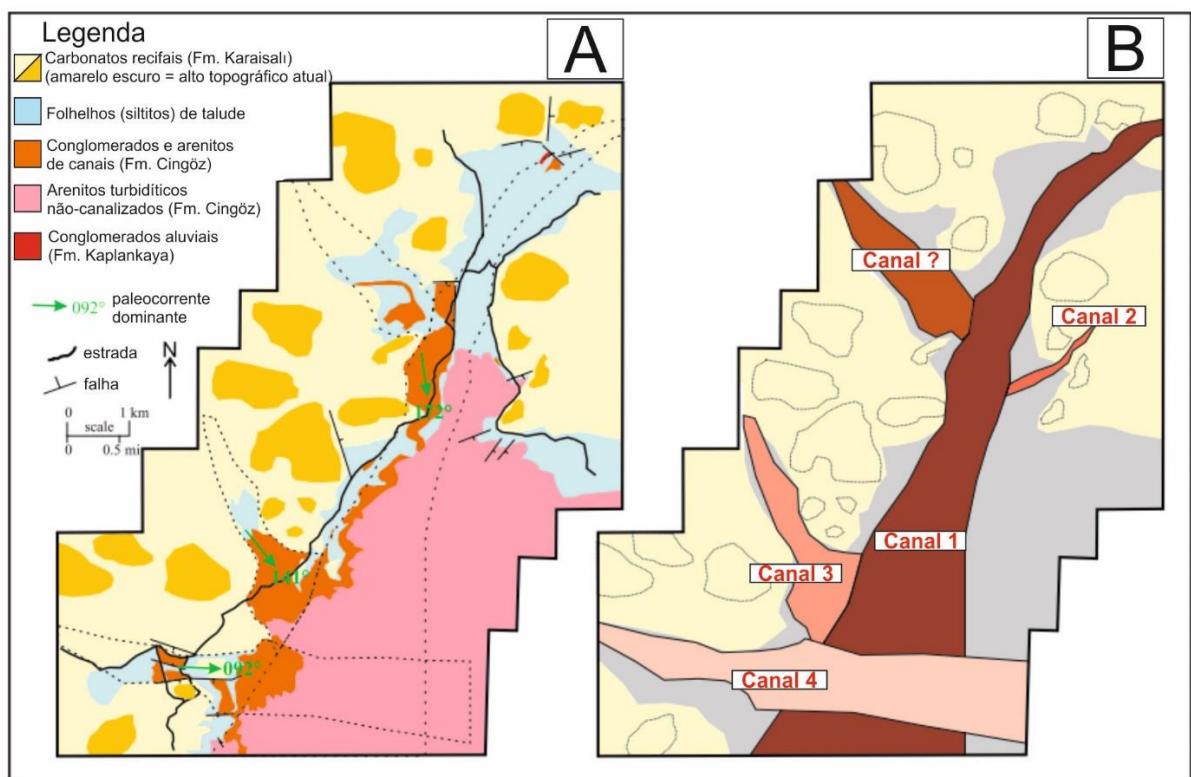
Figura 16: Mapa geológico (A) e interpretação dos canais (B) do sistema alimentador no *Eastern Fan*. As direções de paleocorrente baseiam-se principalmente em clastos imbricados (Satur *et al*., 2007).

Outros três canais foram condutores de sedimentos no EF. Os canais 2 e 3 eram distributários do Canal 1 e o Canal 4 é mais jovem (Satur *et al*., 2004). O canal 2 está localizado na margem leste do Canal 1 e na margem oposta, o Canal 3, que

possui 750 m de largura na desembocadura e é aparentemente controlado por falhas.

O canal 4 (400 m de largura) é interpretado como o mais recente, cortando os Canais 3 e 1 de oeste para leste, com direção de paleocorrente de 090°. Como o Canal 3, parece ser controlado por falhas. Nas partes distais do Canal 4 é possível observar arenitos depositados em sequências de lobos (Gürbüz, 1993).

Sistema deposicional do Leque Oriental (EF)

O EF (aproximadamente 750 km^2 de área exposta) foi descrito por Gürbüz and Kelling (1993) e Gürbüz (1993). Esses autores concluíram que o EF é um sistema de alta eficiência (rico em areia) com lobos não-canalizados, influenciado pela atividade tectônica, disponibilidade de sedimentos e flutuações relativas do nível do mar (Satur, 1999).

O EF foi dividido em leque interno, médio e externo (Figura 17) por Gürbüz and Kelling (1993). O leque interno consiste no sistema de alimentação e nos "canais distributários", representados por arenitos espessos e fortemente amalgamados e raros TBTs. Gürbüz (1993) descreveu lobos deposicionais não canalizados no leque médio. Os depósitos formam sucessões de espessamento e granocrescência ascendente, com espessuras que variam entre 5 e 100 m ("pacotes de arenito não canalizados" de Gürbüz, 1993). O leque externo, em geral, é constituído de TBTs, diminuindo a espessura dos arenitos distalmente.

Figura 17: A) Seção vertical esquemática baseada no furo Gulbaş-2 (ver localização na Figura 13) mostrando depósitos aluviais na base (Formação Gildirli), recobertos por depósitos de canais e leque interno (520 m), leque médio (155 m), depósitos de lobo de leque externo (1200 m), cobertos por sedimentos de assoalho oceânico (~ 1000 m) da Formação Güvenç. De Satur et al. (2007) com base em Naz et al. (1991); B) Desenvolvimento temporal e espacial do EF (redesenhado de Satur *et al.*, 2007); C) Interpretações de linhas sísmicas adquiridas entre 1986 e 1988 na Bacia de Adana exibindo a natureza agradacional dos refletores da megassequência 2 (sistema Cingöz). Adaptado de Gürbüz (1999), após Ünlügenç (1993) e Williams *et al.* (1995).
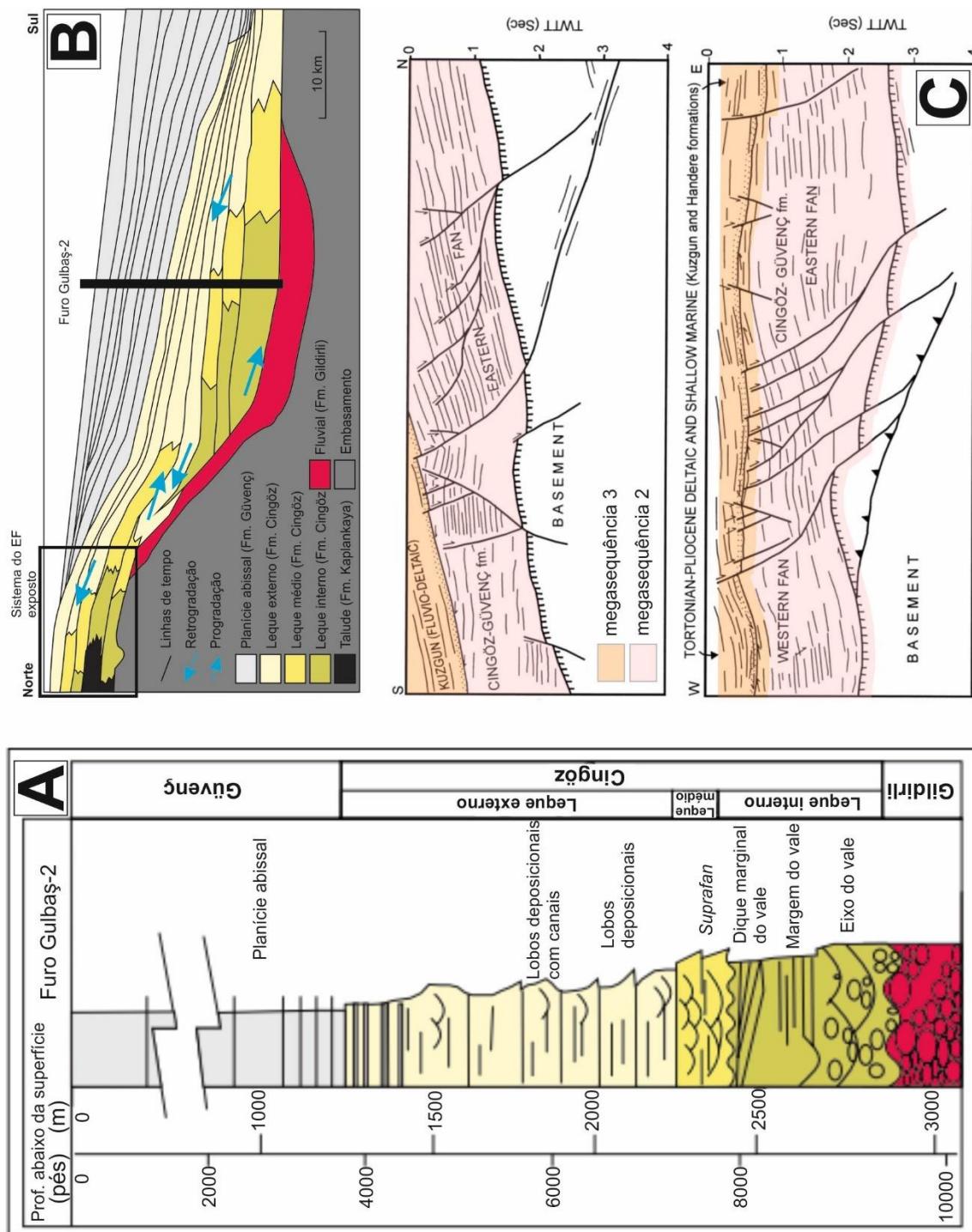
Os limites entre os leques interno, médio e externo são graduais e não são facilmente distinguíveis, uma vez que os lobos são lateral e verticalmente conectados ao sistema alimentador por canais (Gürbüz, 1993).

3.2.3.   Relações entre o WF e o EF

Para entender a Formação Cingöz, as relações entre os dois leques devem ser investigadas. Gürbüz (1993) desenvolveu uma seção composta generalizada para cada um dos leques (Figura 18). Ambas as sucessões mostram um afinamento ascendente, com depósitos grossos e cascalhosos na base, representando o leque interno, sucedidos pela alternância de camadas de arenitos e lamito, interpretados como depósitos de lobos que formam o leque médio. A sucessão mais acima, em ambos os leques, é composta por turbiditos muito finos, depositados no leque externo distal (Figura 18).
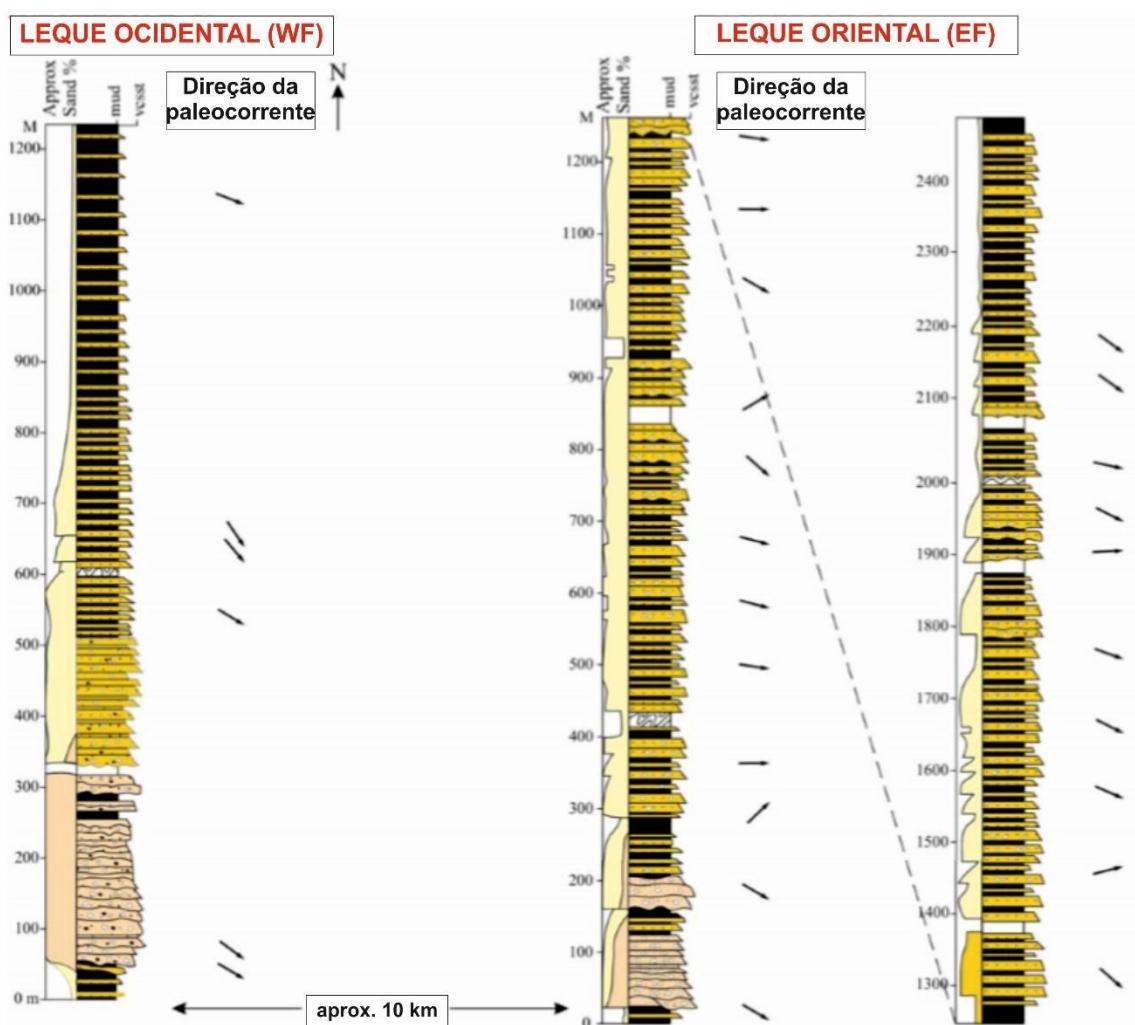
Figura 18: Seções compostas generalizadas do WF e EF. De Satur (1999) redesenhado de Gürbüz (1999).

Algumas feições são particulares de cada leque. Um resumo das principais características para ambos os leques é fornecido na Tabela 4.

Segundo Gürbüz (1993) e Satur (1999), o WF e o EF se interdigitaram em algum momento da evolução do sistema, embora evidências sejam raras. Gürbüz (1993) sugeriu a interdigitação em algum momento da deposição devido à idade baseada na bioestratigrafia (foraminíferos planctônicos e ostracodes) de todo o sistema. Três medidas de direção de paleocorrente em um único local (aldeia de Cingöz) por Satur (1999) indicam a paleocorrente para SO nos TBTs. No entanto, as direções da paleocorrente medida em arenitos espessos indicam uma paleocorrente em direção ao NE, sugerindo duas direções de origem opostas.

Tabela 4: Principais características no WF e EF. Baseado em Naz *et al.* (1991), Gürbüz (1993), Demircan and Toker (2003) e Satur (1999).

Características	Leque Ocidental *(WF)*	Leque Oriental *(EF)*
Extensão da área	~150 m^2 expostos	~750 m^2 expostos
Espessura	<1500 m	<3000 m
Sistema alimentador	1 canal rico em areia	1 canal principal e 3 distributários
Tamanho de grão dominante	Conglomerado/arenito grosso	Arenito fino
Fonte	NO	N, NO e O
Tempo de deposição	Burdigaliano Tardio – Serravallian	Burdigaliano Tardio – Serravallian
Controle estrutural	Confinamento de canal, confinamento de bacia no norte e sul	Confinamento de canal, confinamento de bacia no norte e nordeste
Assembleias icnofósseis	*Cruziana*	Misturado e *Nereites*
Condições ambientais	Eutrófica (alta produtividade orgânica)	Oligotrófica (baixa produtividade orgânica)
Batimetria	Sublitoral (profundidade de água de ~200 m)	Abissal (profundidade de água de 500 a ~2000 m)

4.   LOBOS TURBIDÍTICOS

4.1.   Introdução

O termo lobo tem sido usado desde Normark (1970) para descrever depósitos distais de um sistema turbidítico com morfologia lobada e baixa topografia positiva (convexa para cima). Os lobos são principalmente uma área deposicional (Mutti and Ricci-Lucchi, 1972). Diversos autores citaram algumas características clássicas do lobo (Mutti and Ricci-Lucchi, 1972; Mutti, 1977, 1985; Mutti and Normark, 1987; Shanmugam and Moiola, 1988; Macdonald *et al.*, 2011): 1) tabulares e camadas extensas lateralmente; 2) pacotes distintos delimitados por superfícies paralelas; 3) dominância de arenitos espessamente acamadados alternando com lamitos e (TBTs); 4) camadas de arenito amalgamados; 5) cicatriz; 6) pacotes de espessamento ascendente; 7) tamanho do grão varia de grosso a fino; 8) geometria tipo lençol; 9) espessura comum entre 3 e 15 m; 10) desenvolvido perto de bocas de desembocadura de canais submarinos.

Os lobos são amplamente estudados pois são excelentes reservatórios de hidrocarbonetos, um dos melhores em sistemas turbidíticos (Galloway, 1998). A informação dos lobos é baseada em ferramentas sísmicas e de sonar (Gervais *et al.*, 2006; Deptuck *et al.*, 2008) e também na análise de afloramentos. Estudos sísmicos e de sonar são essenciais para entender a geometria externa dos lobos, enquanto os afloramentos e testemunhos ajudam a entender sua geometria interna e litofácies. Por causa dessas diferentes escalas, uma gama de nomes é usada para o mesmo tipo de depósito, como espraiamento frontal, lençóis de arenito e lobos. Por exemplo, Posamentier and Kolla (2003) observaram que os canais podem alimentar os lobos diretamente ou não, mas sugeriram chamá-los de espraiamantos frontais, porque isso implica em um processo de "espraiamento" de um sistema confinado para um não confinado. Portanto, para esses autores, o termo complexo espraiamento frontal associa um processo deposicional a uma forma morfométrica.

4.2.   Formação e evolução dos lobos

Os mesmos controles alocíclicos que afetam todo o sistema turbidítico influenciarão, portanto, a criação dos lobos (isto é, a área de origem, clima, ambiente tectônico, fisiografia e tipo de sedimento). A diferença entre os sistemas ricos em cascalho e ricos em lama é que o último tende a criar lobos mais canalizados e

desanexados (Mutti and Ricci-Lucchi, 1972; Piper and Normark, 2001), porque a lama se torna uma barreira para o fluxo devido a sua baixa resistência ao cisalhamento, criando canais com diques (Figura 19).
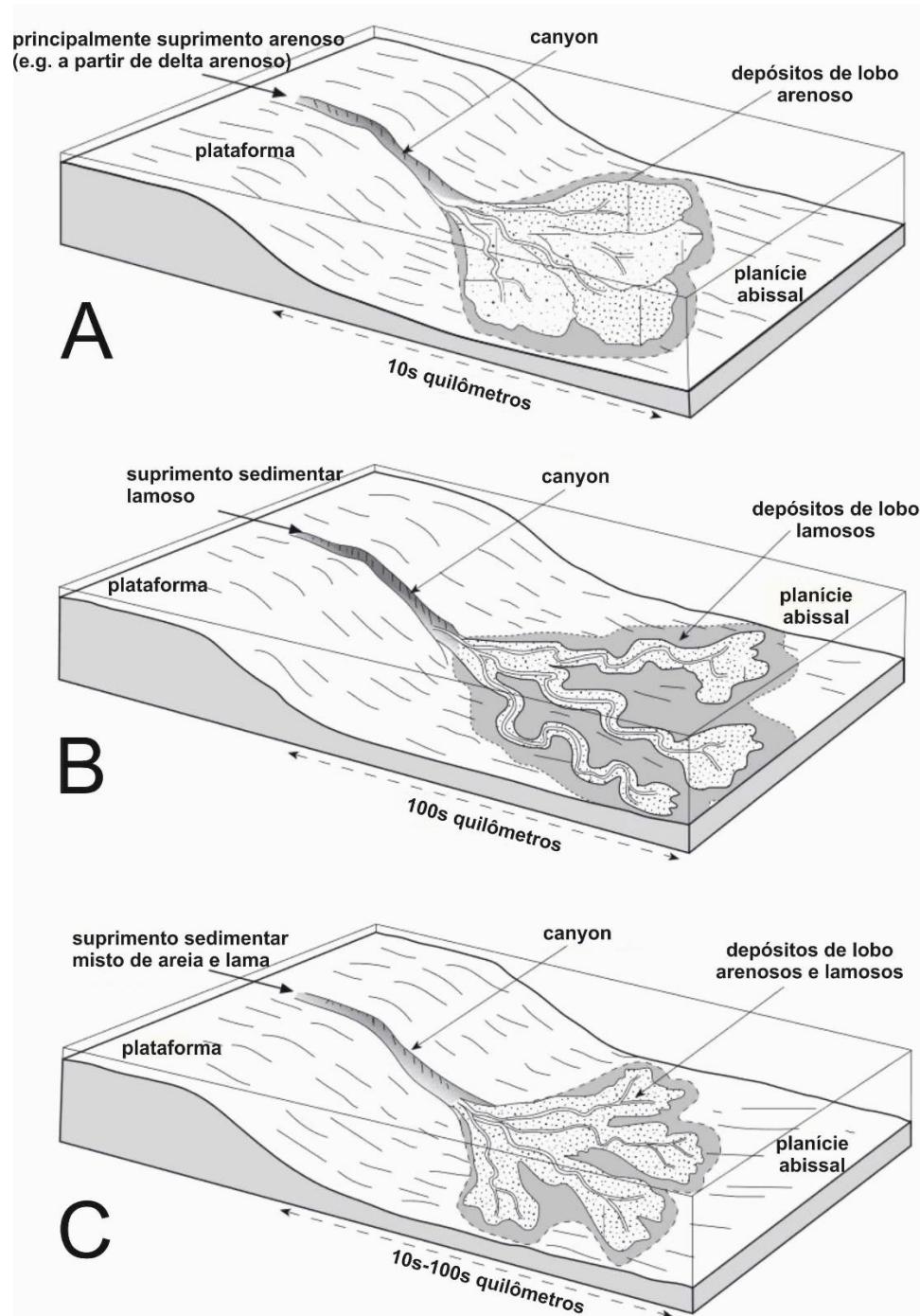
Figura 19: Variações da geometria do lobo em três tipos distintos de sistemas turbidíticos: A) ricos em areia, que formam lobos construídos na planície abissal, com empilhamento compensatório; B) ricos em lama, que formam lobos muito alongados e as areias são depositadas em torno dos canais; C) areia-lama mista, os lobos são construídos mais longe. Adaptado de Nichols (2009) depois de Mutti (1985).

Todos esses controles alocíclicos contribuem para moldar os lobos (Figura 20). A Amazônia e o Leque do Congo, por exemplo, têm lobos típicos de sistemas ricos em lama (Damuth *et al.*, 1983; Jegou *et al.*, 2008; Mulder and Etienne, 2010), com um sistema bem desenvolvido de canais com diques marginais, alcançando grandes distâncias na bacia (> 400 km de distância). Em contraste, o Leque Hueneme criou grandes lobos que emanavam diretamente do canyon, muito próximos à base do talude, típicos de sistemas ricos em areia (Piper and Normark, 2001).
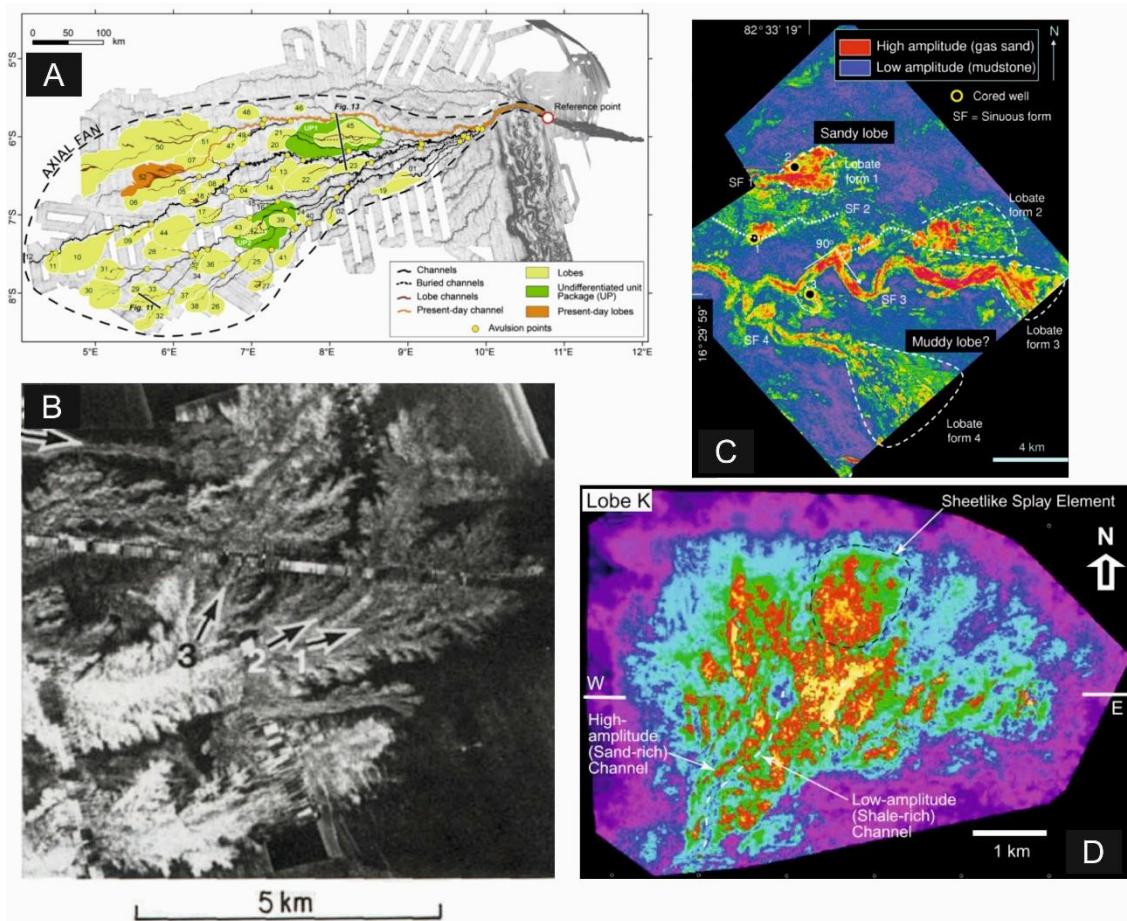
Figura 20: Formas diferentes do lobos: A) Leque do Congo com uma miríade de lobos arredondados conectados por canais de lobo (Picot *et al.*, 2016); B) Leque do Mississippi exibindo complexo de lobos em lobos de formato dendrítico e limites abruptos (Paskevitch *et al.*, 2001); C) Bacia de Krishna-Godavari com lobos em formato lobado ligados a canais únicos (Shanmugam *et al.*, 2009); D) Bacia de Kutai em um lobo de forma irregular (espraiamento). Uma espraiamento de alta amplitude ocorre na parte distal (Saller *et al.*, 2008).

A variação na geometria do lobo é bem documentada (Normark, 1970; Mutti e Normark, 1987; Prélat *et al.*, 2009; Bourget *et al.*, 2010; Groenenberg *et al.*, 2010;

Mulder *et al.*, 2010). Três zonas morfológicas de lobos são reconhecidas (Mulder and Etienne, 2010):

• O lobo canalizado é a continuação de um canal (principalmente o complexo canal-dique marginal). Comumente tem canais rasos distributários (correntes), dispersos e temporários, marcados por avulsões. Os diques são baixos devido à baixa relação lama/areia e à baixa resistência ao cisalhamento resultante das paredes do canal;

• O lobo não canalizado é criado principalmente por lençóis de areia resultantes da rápida deposição de fluxos concentrados;

• A franja do lobo é uma área constituída de sedimentos de grão fino e hemipelágicos, com relações de silte/argila diminuindo o fluxo abaixo.

A evolução de um lobo começa com um pequeno depósito não confinado, passando para um grande lobo não confinado que pode exibir uma variedade de geometrias e composições de sedimentos (Galloway, 1998). Esses grandes lobos não confinados são chamados de lençóis de lobos, compostos principalmente de arenitos finos, com baixa topografia e dezenas de quilômetros de dimensão.

Um lobo de avulsão (Flood *et al.*, 1991) é gerado após a formação de espraiamento crevasse (*crevasse splay*) formada devido à ruptura de diques tornando-se um caminho permanente ao longo do novo canal. Neste caso, o lobo pode evoluir de um lobo em *crevasse splay* para um lobo de avulsão e finalmente um lobo terminal, o membro final da evolução, que pode ser formado diretamente do canal.

As dimensões do lobo podem variar de acordo com a disponibilidade de sedimentos (área de origem) e o grau de confinamento na desembocadura do canal e na bacia (Mulder and Etienne, 2010).

A espessura típica dos lobos antigos (estudos de afloramentos) na literatura varia entre 2 a 15 m (Figura 21). Esses números podem ser diferentes quando comparados aos leques modernos. As medições nos lobos modernos mostram uma grande variação nas espessuras, de menos de 5 a 50 m. Mesmo em um único leque, essa variação pode ser bastante grande, como por exemplo, no leque do

Mississippi, onde a espessura dos lobos varia de 10 a 40 m (Twichell *et al.*, 1992; Mulder and Etienne, 2010).

Como mostra a Figura 21, existem diferenças entre as variações de espessura medidas em afloramentos e em subsuperfície, possivelmente devido à variação em cada esquema hierárquico, com o termo lobo sendo generalizado para todas as escalas, principalmente devido à dificuldade em ter descrições detalhadas dos elementos sub-sísmicos.
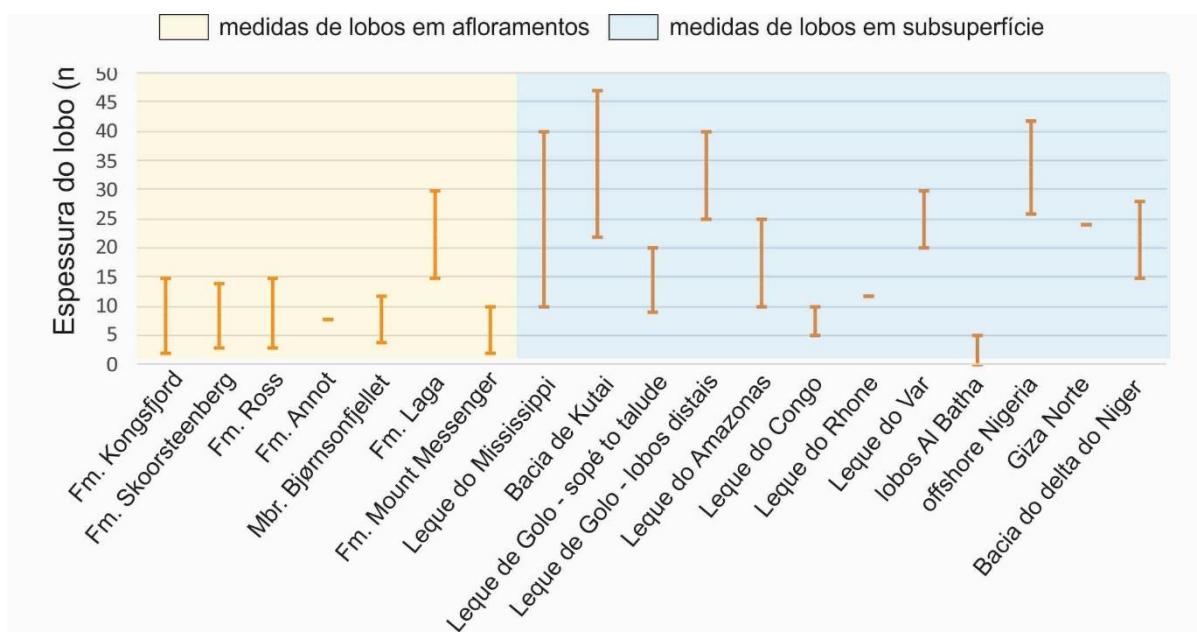
Figura 21: Compilação de medições do lobo em leques conhecidos em todo o mundo em afloramentos (laranja) e em subsuperfície (azul). Cada intervalo (linhas laranja) representa o intervalo de espessuras dos lobos para um leque específico. Dados compilados e agrupados de Pickering, (1981); Doust and Omatsola (1990); Twichell *et al.* (1992); Deptuck *et al.* (2008); Jegou *et al.* (2008); Saller *et al.* (2008); Prélat *et al.* (2009); Bourget *et al.* (2010); Prélat *et al.* (2010); Mulder and Etienne (2010); Etienne *et al.* (2012); Macdonald *et al.* (2011); Grundvåg *et al.* (2014); Morris *et al.* (2014); Marini *et al.* (2015); Masalimova *et al.* (2016); Zhang *et al.* (2016).

4.3. Padrões de empilhamento

Segundo Gervais *et al.* (2006), os lobos podem prograr, retrograr e migrar lateralmente, bem como agradar. Na natureza, os sedimentos tendem a preencher preferencialmente os baixos topográficos e suavizar o relevo, em um processo chamado de compensação (Mutti and Sonnino, 1981). Essa migração lateral dos lobos mostra uma gama de tendências de espessura, englobando tendências de espessamento e adelgaçamento ascendente em uma mesma unidade de lobo

(Marini *et al*., 2011). A identificação dessas tendências é imperativa para reconhecer o padrão de empilhamento dos lobos. Essa compensação topográfica (Figura 22 e Figura 23) provavelmente é o principal mecanismo de deposição no ambiente do lobo (Gervais *et al*., 2006).
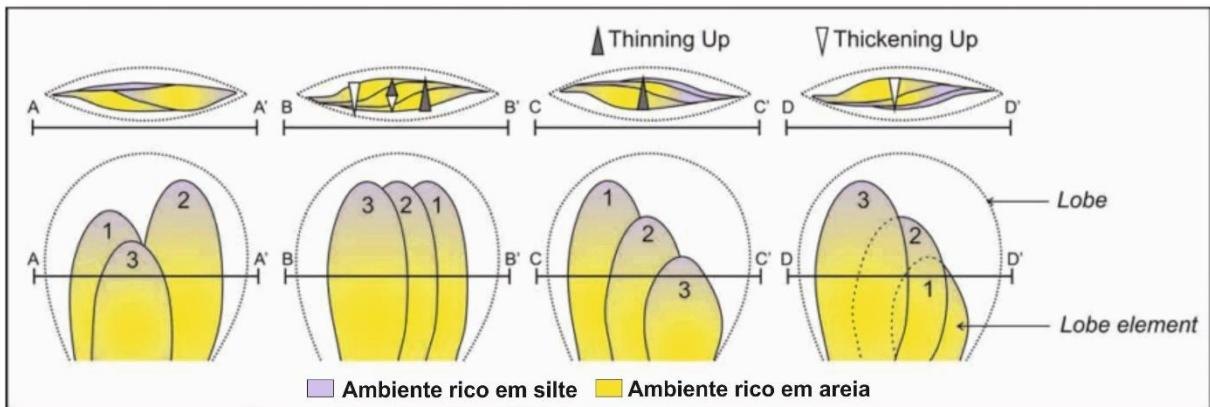
Figura 22: Modelo conceitual de Prelát and Hodgson (2013) relativo aos padrões de empilhamento em lobos. A migração lateral pode variar e portanto, as tendências de espessura das camadas também (representadas pelos triângulos).

Como apontado na Figura 22, na análise das tendências de espessura das camadas, a sucessão de espessamento-ascendente não se restringe a uma fase progradacional do lobo, mas também é encontrada em configurações de empilhamento compensatório e como resultado de migração lateral simples.

Um lobo é construído pela deposição de vários fluxos gravitacionais, caracterizados por volumes, concentrações e velocidades distintas. Chen and Hiscott (1999) argumentaram que cada fluxo tende a preencher a topografia baixa criada por corpos sedimentares adjacentes a partir do fluxo anterior, construindo um relevo deposicional, ou seja, um empilhamento compensatório. Em afloramento, o empilhamento compensatório em lobos é mais aparente em seções transversais, onde o espessamento de um lobo é comumente observado enquanto o lobo abaixo afina, indicando a existência de uma topografia antiga baixa durante a deposição do lobo acima (Prélat *et al*., 2009; Groenenberg *et al*., 2010; Straub and Pyles, 2012). A localização e o tipo de sistema alimentador, a altura do dique (se houver) e as correntes de contorno também são responsáveis pelo empilhamento compensatório (Mutti and Sonnino, 1981).
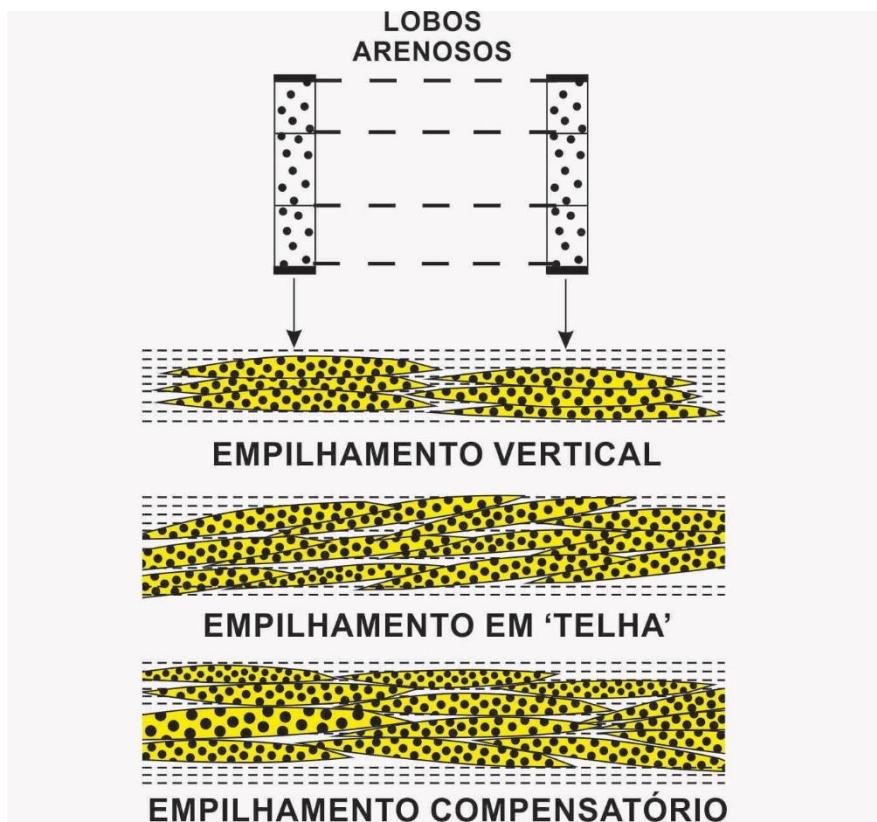
Figura 23: Alguns padrões de empilhamento nos lobos mostrando a dificuldade em reconhecer cada um através de testemunhos, por exemplo. Redesenhado de Bouma (2000).

Por exemplo, fluxos sucessivos, construindo um único lobo, mudarão a localização do depocentro (centro de massa no lobo) através do tempo (Pickering, 1981; Piper and Normark, 1983; Kirshner and Bouma, 2000; Gervais *et al.*, 2006; Deptuck *et al.*, 2008; Prélat *et al.*, 2009), também a localização e tamanho do sistema alimentador é determinante na geometria deposicional de um lobo. Ambas as características funcionarão juntas e implicarão que é improvável que a parte mais espessa de sucessivos elementos do lobo mantenham a mesma posição. Portanto, o padrão de espessura de camada preservado em um lobo terminal é, principalmente, o resultado de um padrão de empilhamento compensatório 3D em uma escala de elemento menor. Segundo Prélat *et al.* (2009) em qualquer seção 1D, um lobo consiste de 2 a 4 elementos de lobos empilhados. Uma consequência comum deste padrão de empilhamento é a amalgamação de camadas local (isto é, estas amalgamações não continuam durante todo o contato entre um elemento do lobo e outro) devido à erosão da lama hemipelágico e parte superior do arenito depositado antes do fluxo subsequente.

Mulder and Etienne (2010) sugeriram que os lobos tendem a ter um comportamento progradacional quando ainda ativo, diminuindo à medida que se

aproxima do abandono. Isso está relacionado à conexão com o canal alimentador, que se torna preenchido, causando migração do fluxo e consequentemente do lobo (Piper and Normark, 1983; Kirshner and Bouma, 2000). Mulder and Etienne (2010) argumentam que, em ambientes proximais, um lobo tende a progradar devido ao alto suprimento sedimentar. Em contraste, Jegou *et al*. (2008) observaram, no Leque da Amazônia, que a progradação e a retrogradação podem alternar-se nos lobos distais. De acordo com essas observações, nenhuma relação geral comum a todos os sistemas está bem estabelecida, uma vez que a distância relativa da fonte parece ser insuficiente para demonstrar um padrão de progradação e/ou retrogradação para todos os sistemas.

Apesar dos lobos serem amplamente estudados, o conceito de progradação do lobo ainda é controverso. Por exemplo, sequências assimétricas, especialmente pacotes de espessamento ascendente, têm sido interpretados como progradação (Mutti, 1984; Pickering *et al*., 1989; Macdonald *et al*., 2011), e estudos como Hiscott (1981) ilustram a ausência de ciclos assimétricos e a importância da agradação do lobo. Diferentemente dos sistemas fluviais, os depósitos marinhos profundos são independentes do nível do mar para causar agradação (já que o espaço de acomodação está sempre disponível), reduzindo a importância da progradação (Macdonald *et al*., 2011; Chen and Hiscott, 1999), mesmo se a entrada de areia for muito fortemente controlada pela mudança do nível do mar.

4.4. Hierarquia do lobo

Como parte da evolução do lobo, o conhecimento da hierarquia deposicional (Figura 24) é imperativo para entender a relação entre as escalas e o espaço envolvido.

O elemento hierárquico básico é amplamente chamado de "*bed*", ou camada, que é formado por um único evento de fluxo. Uma única camada pode ter centenas de milhares de metros de largura e uma espessura média de 1 m (Nof, 1996). Um conjunto de camadas gera um "*lobe element*", ou elemento de lobo (Gervais *et al*., 2006; Deptuck *et al*., 2008; Prélat *et al*., 2009), que ocorre em uma escala de tempo inferior a 5 mil anos e pode atingir 5 km de comprimento, 3,5 km de largura e 1 a 2 m de espessura (Prélat *et al*., 2009; Mulder *et al*., 2010).

Um grupo de elementos de lobo forma o "*lobe*", ou lobo (Figura 24), o elemento arquitetural mais conhecido e descrito. As dimensões do lobo podem variar, dependendo da localização e interpretação do autor, mas geralmente é aceito como tendo cerca de 10 km de comprimento por 30 km de largura e 5 a 20 de espessura (Pickering, 1981; Gervais *et al.*, 2006; Deptuck *et al.*, 2008; Prélat *et al.*, 2009; Grundvåg *et al.*, 2014; Marini *et al.*, 2015). O tempo estimado envolvido na construção do lobo na Amazônia, por exemplo, é de 600 anos, enquanto no complexo de lobos do Zaire, a duração de um lobo é estimada em 1450 anos (Jegou *et al.*, 2008 cita Bonnel, 2005). Isso mostra que a escala de tempo de um lobo é dependente da atividade da corrente de turbidez, maior e contínua em um sistema tão grande, como o Leque da Amazônia.
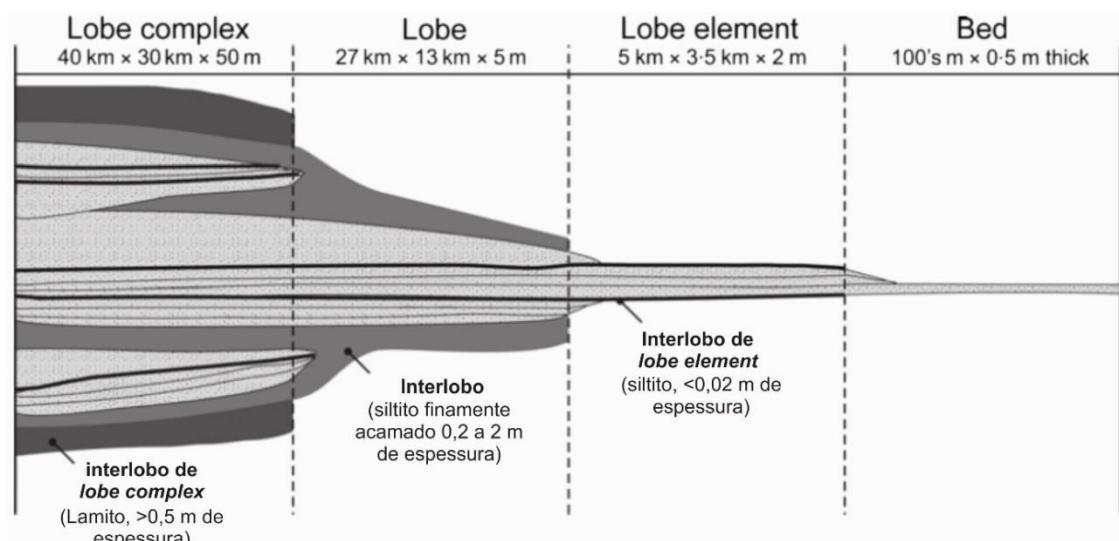
Figura 24: Esquema hierárquico desenvolvido por Prélat *et al.* (2009). Os lobos são separados por unidades de grãos finos (interlobes), enquanto o complexo do lobo é separado por lama hemipelágica.

O próximo elemento na escala hierárquica é o "*lobe complex*", ou complexo de lobos, um aglomerado de lobos com dimensões de 30 a 40 km de largura e 50 m de espessura, de acordo com Prélat *et al.* (2009), depositado durante 50 a 100 mil anos (Deptuck *et al.*, 2008).

No entanto, a terminologia ambígua do lobo pode ser encontrada também nos níveis hierárquicos. Mulder and Etienne (2010) sugeriram o termo *lobe system*, em vez de *lobe complex*. Eles argumentaram que o *lobe complex* é um nível acima na hierarquia (um grupo de *lobe system*), com mais de um canal alimentador, enquanto o *lobe system* seria construído por um único canal.

Mais estudos são necessários para reconhecer as diferentes hierarquias nos loboss porque esses modelos não se encaixam em todos os casos, devido à variabilidade de sistemas e ambientes em diferentes escalas.

4.5.   Reservatórios de lobos turbidíticos

Os reservatórios de hidrocarbonetos nos sistemas turbidíticos estão entre os melhores do mundo, não só pela sua qualidade, mas também pela abundância nas regiões marinho profundas (Weimer and Link 1991; Stow, 1992; Stelting *et al.*, 2000; McCaffrey and Kneller 2001; Zhang *et al.*, 2009).

Diversos elementos arquiteturais em sistemas turbidíticos têm sido reconhecidos como reservatórios de boa qualidade (Mutti, 1974; Chapin *et al.*, 1994; Mchargue, 2014). Lawrence and Bosmin-Smits (2000) estimaram que cerca de 60% da produção do Golfo do Norte do México em águas profundas vem de lençóis de areia (ou lobos), 25% de depósitos de canal e 15% de TBTs e diques marginais.

Os lobos areníticos são considerados um dos melhores reservatórios, também em termos de taxa de recuperação de óleo em reservatórios de águas profundas (Figura 25). Isso se deve à sua geometria simples e boa continuidade lateral, bom potencial de conectividade vertical, pequena variação de tamanho de grão e amalgamação (Chapin *et al.*, 1994; Mahaffie, 1994; Dudley *et al.*, 1997; Piper and Normark, 2001; Gervais *et al.*, 2006; Deptuck *et al.*, 2008).
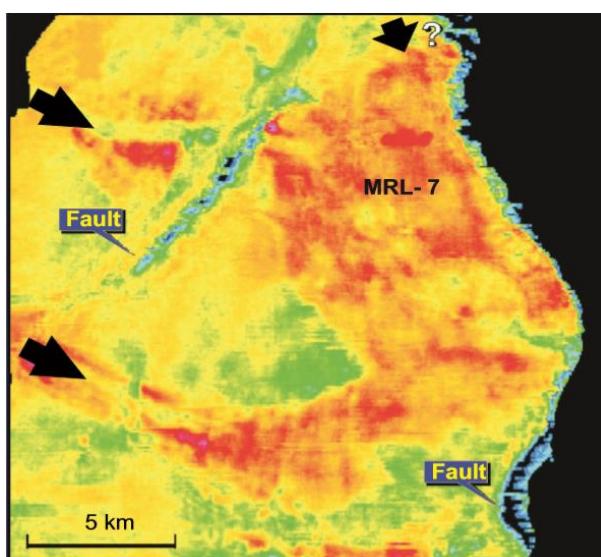
Figura 25: Mapa de amplitude do topo do campo de Marlim e Marlim Sul, na Bacia de Campos, Brasil (MRL-7). As três setas pretas indicam canais alimentadores de um lobo. De Abreu *et al.* (1998).

Algumas características relevantes para a qualidade do reservatório em lobos turbidíticos incluem:

• Camadas amalgamadas e estratificadas

Os lençóis de arenito podem se acumular como camadas amalgamadas, ou intercaladas com um lamito hemipelágico, sem conexão entre as camas, formando lençóis em camadas. Esta definição é baseada em estudos de afloramento da Formação Ross, Carbonífero Superior, Irlanda (Figura 26) por Chapin *et al.* (1994). O grau de amalgamação entre as camadas de arenito controlará a qualidade do reservatório, pois os lençóis amalgamados terão uma melhor permeabilidade vertical do que os lençóis estratificados, apresentando maior conectividade vertical entre os corpos de areia.
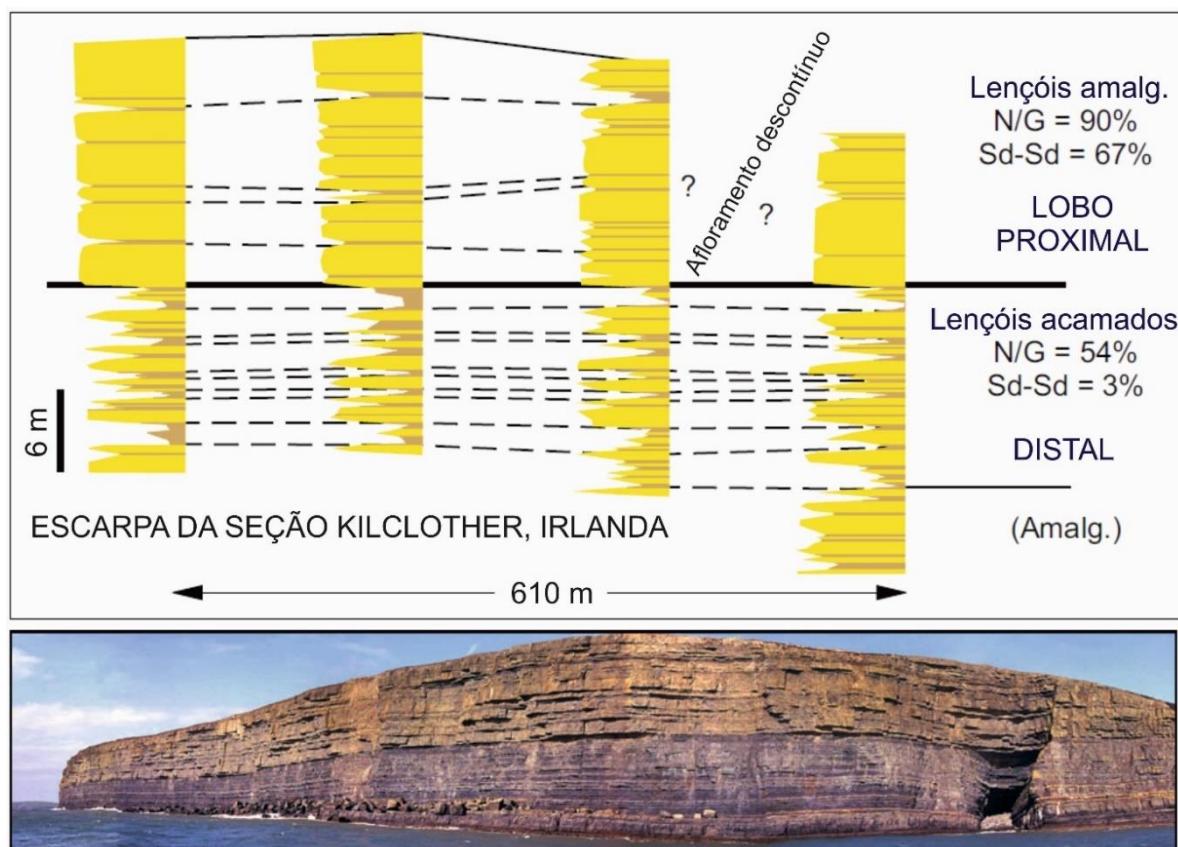
Figura 26: Seção transversal baseada em perfis de raios gama, no penhasco Kilclother (Formação Ross, Oeste da Irlanda). A seção inferior é composta por lençóis estratificados, com porcentagem de areia de 54% e cerca de 3% de contato entre as camadas de arenito. A seção superior é composta por lençóis amalgamados, com porcentagem de areia volumétrica de 90% e 67% de contato arenito-arenito. Abaixo, uma foto da seção de afloramento é mostrada. Observe a rápida mudança lateral na espessura dos arenitos

amalgamados, o que influenciará a conectividade da camada. Após de Chapin *et al.* (1994) e Sullivan *et al.* (2000).

Nota-se que nos lençóis amalgamados predominam os arenitos sem estrutura e a fácies Ta de Bouma (Bouma, 1962), enquanto nas camadas estratificadas (TBTs) as fácies Tb, Tc e Td de Bouma são muito comuns (Chapin *et al.*, 1994).

• Conectividade lateral e vertical

A espessura individual da camada e as mudanças laterais são parâmetros críticos na análise do desempenho do reservatório e na recuperação de óleo. A amalgamação da camada de arenito pode melhorar significativamente a conectividade vertical e, assim, aumentar a chance de recuperação de hidrocarbonetos (Stephen *et al.*, 2001; Hofstra *et al.*, 2017).

Frequentemente, as medidas de continuidade de camada no afloramento não permitem observar toda a extensão da camada de arenito (Slatt, 2000). No entanto, a taxa de mudança da espessura da camada é mensurável no campo e pode fornecer uma estimativa da extensão original das camadas. Medindo a espessura e a porcentagem volumétrica da areia, a taxa de afinamento lateral pode ser calculada.

A geometria *pinch-out* em lençóis pode ser variável. Hurst *et al.* (1999) diferenciaram o *pinch-out* gradacional, representando a falta de confinamento, de *pinch-out* abrupto, quando o fluxo é confinado, destacando que outros fatores também são importantes, como suprimento de areia, densidade e reologia do fluxo, geometria da bacia e topografia e tamanho de grão (Figura 27). Perfis colunares podem não permitir prever a geometria lateral, embora a geometria *pinch-out* possa ser significativa no cálculo volumétrico do desempenho do reservatório (Cobain *et al.*, 2017).
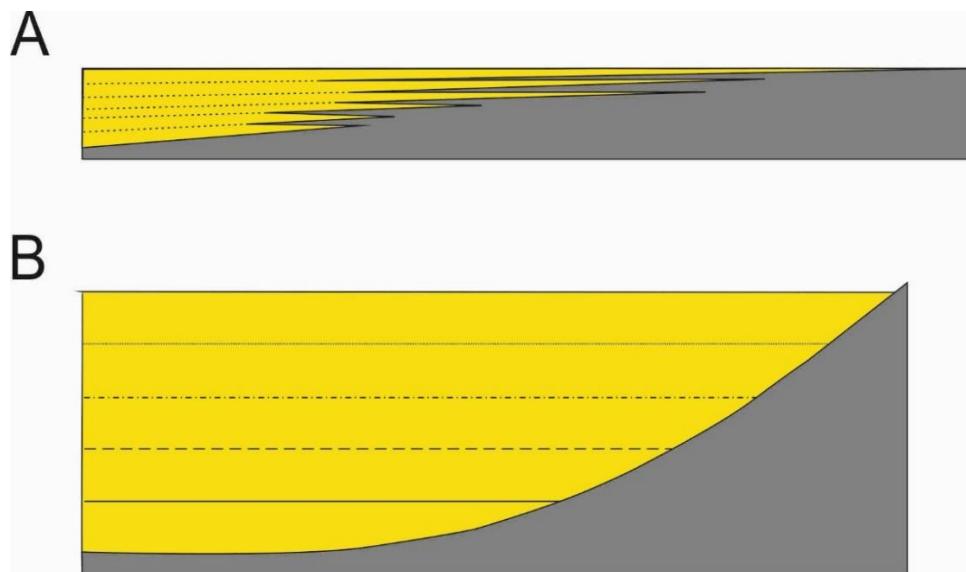
Figura 27: Seção transversal esquemática mostrando dois tipos de limites de deposição para lençóis de arenito (amarelo): A) pinch-out gradacional em uma superfície horizontal; B) onlap sob a um relevo significativo. De Hurst *et al.* (1999).

Um fator importante no desempenho do reservatório é a presença de folhelhos, principalmente porque eles podem bloquear o fluxo vertical em um lençol de arenito individual, como visto em lençóis estratificados (Lomas *et al.*, 2000; Stephen *et al.*, 2001). Em depósitos não confinados, os folhelhos tendem a ser lateralmente extensos, como os arenitos associados. Quanto maior a extensão lateral de um folhelho, menor a chance de uma conexão vertical entre as camadas de arenito (Schuppers, 1993).

A conectividade vertical é a medida do empilhamento vertical das camadas de arenito, com ou sem a interposição de outras camadas, como o folhelho. A conectividade é relativamente alta em lençóis amalgamadas e baixa em lençóis estratificados (Hofstra *et al.*, 2017). Quanto maior a relação net-to-gross (relação volumétrica de areia no depósito), maior a porcentagem de camadas amalgamadas em contato.

5. MATERIAIS E MÉTODOS

Este estudo consistiu em coleta de dados de afloramentos, principalmente em cortes de estrada, criando perfis colunares. Estes foram medidos em escala 1:20 e descritos camada por camada. A coleta de dados incluiu a descrição de coloração,

textura (tamanho de grão, seleção, grau de arredondamento, fábrica), composição, estruturas sedimentares e grau de bioturbação.

No total, cerca de 44 afloramentos foram detalhadamente descritos, incluindo seus perfis colunares. Muitos outros de dimensões menores ou inacessíveis foram descritos, sendo cerca de mais que 50 exposições descritas em toda a área de estudos. Os 44 perfis colunares equivalem a mais de 1060 m, sendo 8 destes no WF.

Medidas sistemáticas de paleocorrentes e construção de diagramas de roseta para determinação das paleocorrentes dominantes foram amplamente utilizados. No total, 952 indicadores foram medidos em toda área de estudo, sendo 335 em laminações de ondulação de correntes (*current ripple lamination*), 406 em turboglifos (*flute casts*) e contramarcas de sulcos (*groove casts*). Muitas destas medidas também consideravam a espessura da camada para o auxíliio na interpretação posterior.

Outro método amplamente utilizado foi a construção de seções laterais a partir de fotomosaicos nos afloramentos mais representativos, visando reconstruir a arquitetura deposicional dos diferentes intervalos estratigráficos. Estes painéis destinaram-se a documentar: (i) as relações laterais e verticais de fácies em detalhe dentro dos sistemas deposicionais e (ii) mudanças verticais no estilo de sedimentação, que podem refletir a evolução temporal dos sistemas deposicionais.

Todos os dados foram integrados para obtenção dos resultados e interrpretações.

6. REFERENCES

Abreu, C.E.B.S., Johann, P.R.S., Freitas, L.C.S., Bruhn, C.H.L., Beer, R., Sarzenski, D.J. and Camoleze, Z. (1998) '3-D Seismic Stratigraphic Inversion: a Lithotoly-Based Approach for Seismic Reservoir Characterization in the Deep-Water Campos Basin', AAPG International Conference & Exhibition, Rio de Janeiro, Brazil, Extended Abstracts Book.

Aksu, A.E., Calon, T.J., Hall, J., Mansfield, S. and Yaşar, D. (2005) 'The Cilicia-Adana basin complex, Eastern Mediterranean: Neogene evolution of an active fore-arc basin in an obliquely convergent margin', *Marine Geology*, 221(1–4), pp. 121 – 159.

Biju-Duval, B., Letouzey, J. and Montadert, L. (1978) 'Structure and evolution of the Mediterranean basins', *Initial Reports of the Deep-Sea Drilling Project*, 42(1), pp. 951

– 984.

Bonnel, C. (2005) *Mise en place des lobes distaux dans les systèmes turbiditiques actuels: analyse comparée des systèmes du Zaïre, Var, et Rhone.* PhD thesis. Université Bordeaux I, p. 293. (In French).

Bouma, A. (1962) 'Sedimentology of some flysch deposits: A graphical approach to facies interpretation', *Amsterdam, Elsevier*, 168 pp.

Bouma, A.H. (2000) 'Coarse-grained and fine-grained turbidite systems as end member models: Applicability and dangers', *Marine and Petroleum Geology*, 17(2), pp. 137 – 143.

Bourget, J., Zaragosi, S., Mulder, T., Schneider, J.L., Garlan, T., Van Toer, A., Mas, V. and Ellouz-Zimmermann, N. (2010) 'Hyperpycnal-fed turbidite lobe architecture and recent sedimentary processes: A case study from the Al Batha turbidite system, Oman margin', *Sedimentary Geology.* Elsevier B.V., 229(3), pp. 144 – 159.

Brinkmann, R. (1976) 'Geology of Turkey', pp. 158. *Elsevier Scientific Publishing Company*, Amsterdam, the Netherlands.

Burton-Ferguson, R., Aksu, A.E., Calon, T.J. and Hall, J. (2005) 'Seismic stratigraphy and structural evolution of the Adana Basin, eastern Mediterranean', *Marine Geology*, 221(1–4), pp. 189 – 222.

Chapin, M.A., Davies, P., Gibson, J.L. and Pettingill, H.S. (1994) 'Reservoir architecture of turbidite sheet sandstones in laterally extensive outcrops, Ross Formation, Western Ireland', *in Weimer, P., Bouma, A.H. and Perkins, B.F. (eds.), Submarine fans and turbidite systems: sequence stratigraphy, reservoir architecture, and production characteristics: Gulf Coast Section SEPM Foundation 15th Annual Research Conference Proceedings*, Houston, p. 53 – 68.

Chen, C. and Hiscott, R.N. (1999) 'Statistical analysis of turbidite cycles in submarine fan successions: tests for short-term persistence', *Journal of Sedimentary Research*, v. B69, p. 486 – 504.

Cipollari, P., Cosentino, D., Radeff, G., Schildgen, T.F., Faranda, C., Grossi, F., Gliozzi, E., Smedile, A., Gennari, R., Darbaş, G., Dudas, F.Ö., Gürbüz, K., Nazik, A. and Echtler, H. (2013) 'Easternmost Mediterranean evidence of the Zanclean flooding event and subsequent surface uplift: Adana Basin, southern Turkey', *Geological Society, London, Special Publications*, 372(1), pp. 473 – 494.

Cobain, S.L., Hodgson, D.M., Peakall, J. and Shiers, M.N. (2017) 'An integrated model of clastic injectites and basin floor lobe complexes: implications for stratigraphic trap plays', *Basin Research*, pp. 1 – 20.

Cosentino, D., Darbaş, G. and Gürbüz, K. (2010) 'The Messinian salinity crisis in the marginal basins of the peri-Mediterranean orogenic systems: examples from the central Apennines (Italy) and the Adana Basin (Turkey)', *Geophysical Research Abstracts Vol. 12. EGU General Assembly* 2010., 12, pp. 2010 – 2462.

Cronin, B.T., Gürbüz, K., Hurst, A. and Satur, N. (2000) 'Vertical and lateral organization of a carbonate deep-water slope marginal to a submarine fan system, Miocene, southern Turkey', *Sedimentology*, 47(4), pp. 801 – 824.

Damuth, J.E., Kowsmann, R.O., Flood, R.D., Belderson, R.H. and Gorini, M.A. (1983) 'Age relationships of distributary channels on Amazon deep-sea fan: implications for

fan growth pattern', *Geology*, v. 11, p. 470 – 473.

Dermican, H. and Toker, V. (2003) 'Trace fossils in the Western Fan of the Cingöz Formation in the northern Adana Basin (Southern Turkey)', *Fossils*, 1862, pp. 15 – 32.

Deptuck, M.E., Piper, D.J.W., Savoye, B. and Gervais, A. (2008) 'Dimensions and architecture of late Pleistocene submarine lobes off the northern margin of East Corsica', *Sedimentology*, 55(4), pp. 869 – 898.

Dewey, J.F., Pitman, W., Ryan, W.B.F. and Bonnin, J. (1973) 'Plate Tectonics and the Evolution of the Alpine System Plate Tectonics and the Evolution of the Alpine System', *Geological Society of America Bulletin*, 84(October), pp. 3137 – 3180.

Doust, H., Omatsola, E. (1990) 'Niger Delta', in Edwards, J.D., Santagrosse, P.A. (eds.), Divergent/Passive margin basins: *AAPG Memoir*, 45, pp. 201 – 238.

Dudley, P.R.C., Rehmer, D.E. and Bouma, A.H. (1997) 'Reservoir scale characteristics of fine-grained sheet sandstone, Tanqua Karoo Subbasin, South Africa', *GCSSEPM Foundation 20th Annual Research Conference Deep-Water Reservoirs of the World*, December 3 – 6, 2000

Etienne, S., Mulder, T., Bez, M., Desaubliaux, G., Kwasniewski, A., Parize, O., Dujoncquoy, E. and Salles, T. (2012) 'Multiple scale characterization of sand-rich distal lobe deposit variability: Examples from the Annot Sandstones Formation, Eocene-Oligocene, SE France', *Sedimentary Geology*. Elsevier B.V., 273–274, pp. 1 – 18.

Faranda, C., Gliozzi, E., Cipollari, P., Grossi, F., Darbaş, G., Gürbüz, K., Nazik, A., Gennari, R. and Cosentino, D. (2013) 'Messinian paleoenvironmental changes in the easternmost Mediterranean Basin: Adana Basin, southern Turkey', *Turkish Journal of Earth Sciences*, 22(5), pp. 839 – 863.

Flood, R.D., Manley, P.L., Kowsmann, R.O., Appi, C.J. and Pirmez, C. (1991) 'Seismic facies and late Quaternary growth of Amazon submarine fan', *in Weimer, P. and Links, M.H. (eds.), Seismic facies and sedimentary processes of submarine fans and turbidite systems: New York, Springer-Verlag*, p. 415 – 433.

Galloway, W.E. (1998) 'Siliciclastic slope and base-of-slope depositional systems: Component facies, stratigraphic architecture and classification', *AAPG Bulletin* 82, p. 569 – 595.

Gervais, A., Savoye, B., Mulder, T. and Gonthier, E. (2006) 'Sandy modern turbidite lobes: A new insight from high resolution seismic data', *Marine and Petroleum Geology*, 23(4), pp. 485 – 502.

Görür, N. (1979) 'Karaisalı Kireçtaşı'nın (Miyosen) Sedimantolojisi', *Türkiye Jeologi Kurumu Bülteni*, 22, pp. 227 – 232 (in Turkish).

Görür, N. (1992) 'A tectonically controlled alluvial fan which developed into a marine fan-delta at a complex triple junction: Miocene Gildirli Formation of the Adana Basin, Turkey', *Sedimentary Geology*, 81(3 – 4), pp. 243 – 252.

Groenenberg, R.M., Hodgson, D.M., Prélat, a., Luthi, S.M. and Flint, S.S. (2010) 'Flow-Deposit Interaction in Submarine Lobes: Insights from Outcrop Observations and Realizations of a Process-Based Numerical Model', *Journal of Sedimentary Research*, 80(3), pp. 252 – 267.

Grundvåg, S.A., Johannessen, E.P., Helland-Hansen, W. and Plink-Björklund, P. (2014) 'Depositional architecture and evolution of progradationally stacked lobe complexes in the Eocene Central Basin of Spitsbergen', *Sedimentology*, 61(2), pp. 535 – 569.

Gürbüz, K. (1993) *Identification and evolution of Miocene submarine fans in the Adana Basin, Turkey*. Unpublished PhD Thesis. University of Keele, Keele, 327 pp.

Gürbüz, K. (1999) 'Regional implications of structural and eustatic controls in the evolution of submarine fans; an example from the Miocene Adana Basin, southern Turkey', *Geological Magazine*, 136(3), pp. 311 – 319.

Gürbüz, K. and Gökçen, S.L. (1985) 'Provenance and sedimentology of the Late Tertiary foreland deposits of the Northern Adana Basin, Turkey', *International symposium on foreland basins*. Fribourg, Switzerland, p. 66.

Gürbüz, K. and Kelling, G. (1993) 'Provenance of Miocene submarine fans in the northern Adana Basin, southern Turkey: A test of discriminant function analysis', *Geological Journal*, 28(3–4), pp. 277 – 293.

Haq, B.U., Hardenbol, J. and Vail, P. R. (1987) 'Chronology of Fluctuating Sea Levels Since the Triassic', *Science*, 235(4793), pp. 1156 – 1167.

Haq, B.U., Hardenbol, J. and Vail, P.R. (1988) 'Mesozoic and Cenozoic chronostratigraphy and cycles of sea-level change', *in Wilgus, C.K., Hastins, B.S., Kendall, C.G., Posamentier, H.W., Ross, C.A. and Van Wagoner, J.C. (eds.), Sea-Level Changes: An Integrated Approach. C.K. Wilgus, B.S. Hastins, C.G.St.C. Kendall, H.W. Posamentier, C.A. Ross and J.C. Van Wagoner, SEPM Special Publication*, p. 72 – 108.

Haughton, P.D.W., Barker, S.P., and McCaffrey, W.D. (2003) "Linked" debrites in sandrich turbidite systems—origin and significance", *Sedimentology*, v. 50, p. 459-482.

Haughton, P., Davis, C., McCaffrey, W. and Barker, S. (2009) 'Hybrid sediment gravity flow deposits - Classification, origin and significance', *Marine and Petroleum Geology*. Elsevier Ltd, 26(10), pp. 1900 – 1918.

Hiscott, R.N. (1981) 'Deep-sea fan deposits in the Macigno Formation (middle upper Oligocene) of the Gordanna Valley, northern Apenines, Italy - Discussion', *Journal of Sedimentary Petrology*, 51:1015 – 10(3).

Hofstra, M., Pontén, A.S. M., Peakall, J., Flint, S.S., Nair, K.N. and Hodgson, D.M. (2017) 'The impact of fine-scale reservoir geometries on streamline flow patterns in submarine lobe deposits using outcrop analogues from the Karoo Basin', *Petroleum Geoscience*, 23(2), pp. 159 – 176.

Hsü, K.J., Ryan, W.B.F. and Cita, M.B. (1973) 'Late Miocene desiccation of the Mediterranean', *Nature*, 242, 240 – 244.

Hurst, A., Verstralen, I., Cronin, B. and Hartley, A. (1999) 'Sand-Rich Fairways in Deep-Water Clastic Reservoirs: Genetic Units, Capturing Uncertainty, and a New Approach to Reservoir Modeling', *AAPG Bulletin*, 83(7), pp. 1096 – 1118.

Ilgar, A., Nemec, W., Hakyemez, A. and Karakuş, E. (2013) 'Messinian forced regressions in the Adana Basin: A near-coincidence of tectonic and eustatic forcing', *Turkish Journal of Earth Sciences*, 22(5), pp. 864 – 889.

Jegou, I., Savoye, B., Pirmez, C. and Droz, L. (2008) 'Channel-mouth lobe complex of the recent Amazon Fan: The missing piece', *Marine Geology*, 252(1–2), pp. 62 – 77.

Karig, D.E. and Kozlu, H. (1990) 'Late Palaeogene-Neogene evolution of the triple junction region near Maras, south-central Turkey', *Journal of the Geological Society*, 147(6), pp. 1023 – 1034.

Kelling, G., Gökçen, S.L., Floyd, P.A. and Gökçen, N. (1987) 'Neogene tectonics and plate convergence in the eastern Mediterranean: New data from southern Turkey', *Geology*, v. 15, p. 425 – 429.

Kempler, D. (1994) 'An outline of northeastern Mediterranean tectonics in view of Cruise 5 of the Akademik Nikolaj Strakhov', *in Krasheninnikov, V.A. and Hall, J.K. (eds.), Geological Structure of the Northeastern Mediterranean (Cruise 5 of the research vessel 'Akademik Nikolaj Strakhov'), Historical Production Hall*, Jerusalem, 396.

Ketin, I. (1966) 'Tectonic units of anatolia (asia minor)', *Bulletin of the Mineral Research and Exploration Institute of Turkey*, (66), pp. 24 – 37.

Kirschner, R.H., and Bouma, A.H. (2000) 'Characteristics of a distributary channel-levee-overbank system, Tanqua Karoo', *in Bouma, A.H. and Stone, C.G. (eds.), Fine-grained turbidite systems, AAPG Memoir 72/SEPM Special Publication* 68, p. 233 – 244.

Lawrence, D.T. and Bosman-Smits, D.F. (2000) 'Exploring deep water technical challenges in the Gulf of Mexico', *in Weimer, P., Slatt, R.M., Coleman, J.L., Rosen, N., Nelson, C.H., Bouma, A.H., Styzen, M. and Lawrence, D.T. (eds.), Global Deepwater Reservoirs: Gulf Coast Section–SEPM Bob F. Perkins 20th Annual Research Conference*, p. 473 – 477.

Lomas, S.A., Cronin, B.T., Hartley, A.J., Duranti, D., Hurst, A., Mackay, E., Clark, S.J., Palumbo, B. and Kelly, S. (2000) 'Characterization of lateral heterogeneities in an exceptionally exposed turbidite sand body, Grès d'Annot (Eocene-Oligocene), SE France', *GCSSEPM Foundation 20th Annual Research Conference Deep-Water Reservoirs of the World*, December 3 – 6.

Lowe, D. (1982). 'Sediment gravity flows: II. Depositional models with special reference to the deposits of high-density turbidity currents', *Journal of Sedimentary Petrology*, v. 52, p. 279-297.

Macdonald, H. a., Peakall, J., Wignall, P.B. and Best, J. (2011) 'Sedimentation in deep-sea lobe-elements: implications for the origin of thickening-upward sequences', *Journal of the Geological Society*, 168(2), pp. 319 – 332.

Mahaffie, M.J. (1994) 'Reservoir classification for turbidite intervals at the Mars discovery, Mississippi Canyon 807, Gulf of Mexico', *in Weimer, P., Bouma, A.H. and Perkins, B.F. (eds.), Submarine fans and turbidite systems—sequence stratigraphy, reservoir architecture, and production characteristics: Gulf Coast Section SEPM Foundation 15th Annual Research Conference*, p. 233 – 244.

Marini, M., Milli, S. and Moscatelli, M. (2011) 'Facies and architecture of the Lower Messinian turbidite lobe complexes from the Laga Basin (central Apennines, Italy)', *Journal of Mediterranean Earth Sciences*, 3, pp. 45 – 72.

Marini, M., Milli, S., Ravnås, R. and Moscatelli, M. (2015) 'A comparative study of

confined vs. semi-confined turbidite lobes from the Lower Messinian Laga Basin (Central Apennines, Italy): Implications for assessment of reservoir architecture', *Marine and Petroleum Geology*. Elsevier Ltd, 63, pp. 142 – 165.

Martinsen, O.J., and Bakken, B. (1990) 'Extensional and compressional zones in slumps and slides in the Namurian of County Clare, Ireland', *Journal of the Geological Society*, London, v. 147, p. 153-164.

Masalimova, L.U., Lowe, D.R., Sharman, G.R., King, P.R. and Arnot, M.J. (2016) 'Outcrop characterization of a submarine channel-lobe complex: The Lower Mount Messenger Formation, Taranaki Basin, New Zealand', *Marine and Petroleum Geology*. Elsevier Ltd, 71, pp. 360 – 390.

McCaffrey, W. and Kneller, B. (2001) 'Process controls on the development of stratigraphic trap potential on the margins of confined turbidite systems and aids to reservoir evaluation', *AAPG Bulletin*, v. 85, (6), pp. 971 – 988.

Mchargue, T. (2014) 'The Reservoir Architecture of Turbidite Channels: Models and Mysteries*', *AAPG Foundation Distinguished Lecture*.

Mitchum, R.M., Vail, P.R. and Thompson, S. (1977) 'Seismic Stratigraphy and Global Changes of Sea Level, Part 2: The Depositional Sequence as a Basic Unit for Stratigraphic Analysis: Section 2. Application of Seismic Reflection Configuration to Stratigraphic Interpretation', *Seismic Stratigraphy: Applications to Hydrocarbon Exploration AAPG Memoir 26*, pp. 53 – 62.

Morris, E.A., Hodgson, D.M., Flint, S.S., Brunt, R. L., Butterworth, P.J. and Verhaeghe, J. (2014) 'Sedimentology, Stratigraphic Architecture, and Depositional Context of Submarine Frontal-Lobe Complexes', *Journal of Sedimentary Research*, 84(9), pp. 763 – 780.

Morris, W.R., and Normark, W.R. (2000) 'Sedimentologic and geo-metric criteria for comparing modern and ancient sandy turbidite elements', in Weimer, P., Slatt, R.M., Coleman, J.L., Rosen, N., Nelson, C.H., Bouma, A.H., Styzen, M. and Lawrence, D.T. (eds.) *Deep-water reservoirs of the world (CD-ROM): Gulf Coast Section SEPM*, p. 606 – 623

Mulder, T., Callec, Y., Parize, O., Joseph, P., Schneider, J.L., Robin, C., Dujoncquoy, E., Salles, T., Allard, J., Bonnel, C., Ducassou, E., Etienne, S., Ferger, B., Gaudin, M., Hanquiez, V., Linares, F., Marchès, E., Toucanne, S. and Zaragosi, S. (2010) 'High-resolution analysis of submarine lobes deposits: Seismic-scale outcrops of the Lauzanier area (SE Alps, France)', *Sedimentary Geology*. Elsevier B.V., 229(3), pp. 160 – 191.

Mulder, T. and Etienne, S. (2010) 'Lobes in deep-sea turbidite systems: State of the art', *Sedimentary Geology*, 229(3), pp. 75 – 80.

Mutti, E. (1974) 'Turbiditas de suprafan em el Eoceno de los alrededores de Ainsa (Huesca)', *VII Congreso del Grupo Español de Sedimentologia*, Bellaterra-Tremp, Resumenes, Sesion 7a, 23-28 Settembre, p. 68 – 72. (In Spanish).

Mutti, E. (1977) 'Distinctive thin-bedded turbidite facies and related depositional environments in the Eocene Hecho Group (South-central Pyrenees, Spain)', *Sedimentology*, 24, 107 – 131.

Mutti, E. (1984) 'The Hecho Eocene submarine fan system, south-central Pyrenees, Spain', *Geo-Marine Letters*, 3(2–4), pp. 199 – 202.

Mutti, E. (1985). 'Turbidite systems and their relations to depositional sequences', *in Zuffa, G.G. (eds.), Provenance of Arenites, D. Reidel Publishing Company.*, p. 65 – 93.

Mutti, E. (1992) 'Turbidite sandstones' *AGIP-Istituto di Geologia dell'Università di Parma*, Milano, San Donato Milanese, 275 p.

Mutti, E. and Normark, W.R. (1987) 'Comparing examples of modern and ancient turbidite systems: problems and concepts', *in Leggett, J.R. and Zuffa, G.G. (eds.), Marine clastic sedimentology: concepts and case studies, London: G. Graham and Trotman*, pp. 1 – 37.

Mutti, E. and Ricci-Lucchi, F. (1972) 'Le Torbiditi dell'Appennino settentrionale: introduzione all'analisi di facies', *Memorie della Società Geologica Italiana*, 11, 161 – 199 (In Itallian).

Mutti, E. and Sonnino, M. (1981) 'Compensation cycles; a diagnostic feature of turbidite sandstone lobes', *International Association of Sedimentologists abstracts; 2nd European regional meeting.*, (October), pp. 120 – 123.

Naz, H., Cuhadar, O. and Yehiay, G. (1991) 'Middle Miocene Cingöz deep-sea fan deposits of the Adana Basin, Southern Turkey', in Sungurlu, O. (eds.), *Tectonics and hydrocarbon potential of Anatolia and surrounding regions*, Ankara, Turkey.

Nazik, A. (2004) 'Planktonic foraminiferal biostratigraphy of the Neogene sequence in the Adana Basin, Turkey, and its correlation with standard biozones', *Geological Magazine*, 141(3), pp. 379 – 387.

Nazik, A. and Gürbüz, K. (1992) 'Yöresi (Kb Adana) Alt-Orta Miyosen Yaşli Denizalt Yelpazelerinin Planktoni Foramini Biyostratigrafisi', *Türkiye Jeoloji Bülteni*, 32(February), pp. 67 – 80 (in Turkish).

Nichols, G. (2009) 'Deep Marine Environments - Submarine Fans', *in Nichols, G. (eds.), Sedimentology and Stratigraphy, second edition*, pp. 247 – 262.

Nof, D. (1996) 'Rotational turbidity flows and the 1929 grand banks earthquake', Deep-Sea Research Part I: *Oceanographic Research Papers*, 43(8), pp. 1143 – 1163.

Normark, W.R. (1970) 'Growth patterns of deep-sea fans', *American Association of Petroleum Geologists, Bulletin*, v. 54, p. 2170 – 2195.

Öğrünç, G., Gürbüz, K. and Nazik, A. (2000) 'Adana Baseni Üst Miyosen-Pliyosen istifinde "Messiniyen tuzluluk Krizine" ait bulgular', *Yerbilimleri, Hacettepe Üniversitesi Yerbilimleri Uygulama ve Araştırma Merkezi Bülteni* 22, 183 – 92.

Okay, A.I. (2008) 'Geology of Turkey: A synopsis', *Anschnitt*, 21(November), pp. 19 – 42.

Okay, A.I. and Göncüoğlu, C. (2004) 'The Karakaya Complex: A review of data and concepts', *Turkish Journal of Earth Sciences*, 13(2), pp. 77 – 95.

Paskevich, V., Twichell, D.C. and Schwab, W.C. (2001) 'SeaMARC 1A sidescan sonar mosaic, cores and depositional interpretation of the Mississippi Fan—ArcView GIS data release', *U.S. Geological Survey, Open-File Report 00-352, CD-ROM*.

Pickering, K.T. (1981) 'Two types of outer fan lobe sequence, from the late Precambrian Kongsfjord Formation submarine fan, Finnmark, North Norway', *Journal*

of Sedimentary Research, 51(4), pp. 1277 – 1286.

Pickering, K.T., Hiscott, R.N. and Hein, F.J. (1989) 'Deep marine environments: clastic sedimentation and tectonics', *London, Unwin Hyman*, 416 p.

Picot, M., Droz, L., Marsset, T., Dennielou, B. and Bez, M. (2016) 'Controls on turbidite sedimentation: Insights from a quantitative approach of submarine channel and lobe architecture (Late Quaternary Congo Fan)', *Marine and Petroleum Geology*. Elsevier Ltd, 72, pp. 423 – 446.

Piper, D.J.W. and Normark, W.R. (1983) 'Turbidite deposition patterns and flow characteristics, Navy Submarine Fan, Californian Borderland', *Sedimentology*, 30(5), pp. 681 – 694.

Piper, D.J.W. and Normark, W.R. (2001) 'Sandy fans - from Amazon to Hueneme and beyond', *AAPG Bulletin*, v. 85, no. 8 (August 2001), pp. 1407 – 1438.

Posamentier, H.W., Erskine, R.D. and Mitchum, Jr., R.M. (1991) 'Models for submarine-fan deposition within a sequence-stratigraphic framework', *Seismic facies and sedimentary processes of submarine fans and turbidite systems.*, pp. 127 – 136.

Posamentier, H.W. and Kolla, V. (2003) 'Seismic geomorphology and stratigraphy of depositional deep-water deposits 383', *Journal of Sedimentary Research*, 73(3), pp. 367 – 388.

Posamentier, H.W. and Vail, P.R. (1988) 'Eustatic controls on clastic deposition II - sequence and systems tract models', Sea-level Changes – An Integrated Approach, *SEPM Special Publication* n. 42.

Prélat, A., Covault, J.A., Hodgson, D.M., Fildani, A. and Flint, S.S. (2010) 'Intrinsic controls on the range of volumes, morphologies, and dimensions of submarine lobes', *Sedimentary Geology*. Elsevier B.V., 232(1–2), pp. 66 – 76.

Prélat, A. and Hodgson, D.M. (2013) 'The full range of turbidite bed thickness patterns in submarine lobes: controls and implications', *Journal of the Geological Society*, 170(1), pp. 209 – 214.

Prélat, A., Hodgson, D.M. and Flint, S.S. (2009) 'Evolution, architecture and hierarchy of distributary deep-water deposits: a high-resolution outcrop investigation from the Permian Karoo Basin, South Africa', *Sedimentology*, 56(7), pp. 2132 – 2154.

Pyles, D.R. and Jennette, D.C. (2009) 'Geometry and architectural associations of co-genetic debrite-turbidite beds in basin-margin strata, Carboniferous Ross Sandstone (Ireland): Applications to reservoirs located on the margins of structurally confined submarine fans', *Marine and Petroleum Geology*. Elsevier Ltd, 26(10), pp. 1974–1996.

Radeff, G., Schildgen, T. F., Cosentino, D., Strecker, M. R., Cipollari, P., Darbaş, G. and Gürbüz, K. (2015) 'Sedimentary evidence for late Messinian uplift of the SE margin of the Central Anatolian Plateau: Adana Basin, southern Turkey', *Basin Research*, 29, pp. 488 – 514.

Robertson, A.H.F. (1998) 'Mesozoic-Tertiary tectonic evolution of the easternmost Mediterranean area: integration of marine and land evidence', *Proceedings of the Ocean Drilling Program, 160 Scientific Results*, 160.

Robertson, A.H.F. (2000) 'Mesozoic-Tertiary Tectonic-Sedimentary Evolution of a South Tethyan Oceanic Basin and its Margins in Southern Turkey', in Bozkurt, E.,

Winchester, J.A. and Piper, J.D. (eds.), Tectonics and Magmatism in Turkey and the Surrounding Area. *Geological Society, London, Special Publications*, 173, 97 – 138.

Robertson, A., Unlügenç, Ü.C., Inan, N. and Taşli, K. (2004) 'The Misis-Andırın Complex: A Mid-Tertiary melange related to late-stage subduction of the Southern Neotethys in S Turkey', *Journal of Asian Earth Sciences*, 22(5), pp. 413 – 453.

Ryan, W.B.F. (2009) 'Decoding the mediterranean salinity crisis', *Sedimentology*, 56(1), pp. 95 – 136.

Saller, A., Werner, K., Sugiaman, F., Cebastiant, A., May, R., Glenn, D. and Barker, C. (2008) 'Characteristics of Pleistocene deep-water fan lobes and their application to an upper Miocene reservoir model, offshore East Kalimantan, Indonesia', *AAPG Bulletin*, 92(7), pp. 919 – 949.

Satur, N. (1999) *Internal architecture, facies distribution and reservoir modelling of the Cingöz deepwater clastic system in southern Turkey*. PhD Thesis. University of Aberdeen, Aberdeen, UK, 520 p.

Satur, N., Cronin, B.T., Hurst, A., Kelling, G. and Gürbüz, K. (2004) 'Down-channel variations in stratal patterns within a conglomeratic, deepwater fan feeder system (Miocene, Adana Basin, Southern Turkey)', in *Lomas S. and Joseph, P. (eds.), Confined turbidite systems: Geological Society (London) Special Publication 222*, p. 241 – 260.

Satur, N., Hurst, A., Cronin, B.T., Kelling, G. and Gürbüz, K. (2000) 'Sand body geometry in a sand-rich deepwater clastic system, Miocene Cingöz Formation of southern Turkey', *Marine and Petroleum Geology*, pp. 128 – 141.

Satur, N., Hurst, A., Kelling, G., Cronin, B.T. and Gürbüz, K. (2007) 'Controlling Factors on the Character of Feeder Systems to a Deep-water Fan, Cingöz Formation, Turkey', *Atlas of Deep-Water Outcrops, CD-ROM*, pp. 1 – 28.

Schmidt, G. (1961) 'Stratigraphic nomenclature for the Adana region petroleum district VII'. *Petroleum Administration, Bulletin*, v. 6, p. 47 – 63.

Schuppers, J.D. (1993) 'Quantification of turbidite facies in a reservoir-analogous submarine-fan channel sand body, south-central Pyrenees, Spain', *Special Publications of the International Association of Sedimentologists* 15, 99 – 112.

Şengör, A.M.C. (1979a) 'The North Anatolian transform fault: its age, offset and tectonic sirmificance', *Journal of Geological Society of London*, v. 136, pp. 269 – 282.

Şengör, A.M.C. (1979b) 'Mid-Mesozoic closure of Permo-Triassic Tethys and its implications', *Nature*, v. 279, p. 590 – 593.

Şengör, A.M.C. and Yılmaz, Y. (1981) 'Tethyan evolution of Turkey: A plate tectonic approach', *Tectonophysics*, 75(3 – 4).

Şengör, A.M.C., Yılmaz, Y. and Sungurlu, O. (1984) 'Tectonics of the Mediterranean Cimmerides: nature and evolution of the western termination of Palaeo-Tethys', *Geological Society, London, Special Publications*, 17(1), pp. 77 – 112.

Şengör, A.M.C., Gorür, N. and Saroğlu, F. (1985) 'Strike-Slip Faulting and Related Basin Formation in Zones of Tectonic Escape: Turkey as a Case Study', in: *Biddle, K. and Christie-Blick, N., (eds.), Strike-Slip Deformation, Basin Formation and Sedimentation, Special Publications, SEPM Society for Sedimentary Geology*, Tulsa, vol. 37, 227 – 264.

Shanmugam, G. and Moiola, R.J. (1988) 'Submarine Fans: Characteristics, Models, Classification, and Reservoir Potential', *Earth-Science Reviews*, 24, pp. 383 – 428.

Shanmugam, G., Shrivastava, S.K. and Das, B. (2009) 'Sandy Debrites and Tidalites of Pliocene Reservoir Sands in Upper-Slope Canyon Environments, Offshore Krishna-Godavari Basin (India): Implications', *Journal of Sedimentary Research*, 79(9), pp. 736–756.

Slatt, R.M. (2000) 'Why outcrop characterization of turbidite systems', in Bouma, A.H. and Stone, C.G. (eds.), Fine-grained turbidite systems, *AAPG Memoir 72 /SEPM Special Publication* 68, p. 181 – 186.

Stelting, C.E., Bouma, A.H., Stone, C.G. (2000) 'Fine-grained turbidite systems: overview', in Bouma, A.H., Stone, C.G. (eds.), Fine-grained Turbidite Systems, AAPG Memoir 72/SEPMSpecial Publication, no. 68. *American Association of Petroleum Geologists*, pp. 1 – 8.

Stephen, K.D., Clark, J.D. and Gardiner, A.R. (2001) 'Outcrop-based stochastic modelling of turbidite amalgamation and its effects on hydrocarbon recovery', *Petroleum Geoscience*, 7(2), pp. 163 – 172.

Stow, D.A.V. (1992) 'Deep-water Turbidite Systems', *Blackwell Scientific Publications*, Oxford. 473 pp.

Straub, K.M. and Pyles, D.R. (2012) 'Quantifying the Hierarchical Organization of Compensation in Submarine Fans Using Surface Statistics', *Journal of Sedimentary Research*, 82(11), pp. 889 – 898.

Sullivan, M., Jensen, G., Goulding, F., Jennette, D., Foreman, L. and Stern, D. (2000) 'Architectural analysis of deep-water outcrops: implications for exploration and production of the Diana sub-basin, western Gulf of Mexico', *in Weimer, P., Slatt, R.M., Coleman, J.L., Rosen, N., Nelson, C.H., Bouma, A.H., Styzen, M. and Lawrence, D.T. (eds.), Global Deep-Water Reservoirs: Gulf Coast Section-SEPM Foundation 20th Annual Bob F. Perkins Research Conference*, p. 1010 – 1031.

Talling, P.J., Amy, L.A., Wynn, R.B., Peakall, J. and Robinson, M. (2004) 'Beds comprising debrite sandwiched within co-genetic turbidite: Origin and widespread occurrence in distal depositional environments', *Sedimentology*, 51(1), pp. 163–194.

Tanar, Ü. (1985) 'Körlü (Tarsus-Mersin) Bölgesi Karaisalı, Kuzgun, Memişli Formasyonlarının Molluska Faunası', *Jeoloji Mühendisliği* 24, 17 – 24 (in Turkish).

Tekeli, O. (1981) 'Subduction complex of pre-Jurassic age, northern Anatolia, Turkey', *Geology*, 9(2), pp. 68 – 72.

Twichell, D.C., Schwab, W.C., Nelson, C.H., Kenyon, N.H. and Lee, H.J. (1992) 'Characteristics of a sandy depositional lobe on the outer Mississippi fan from SEAMARC 1A sidescan sonar images', *Geology*, 20 (November), pp. 689 – 692.

Ünlügenç, U.C. (1993) *Controls on Cenozoic sedimentation, Adana Basin, Southern Turkey*. PhD. Thesis. University of Keele, Keele, UK.

Ünlügenç, U.C. and Demirkol, C. (1988) 'Stratigraphy of Kızıldağ Yayla (Adana region)', *Geological Engineering* 32 – 33, 17 – 25 (in Turkish).

Ünlügenç, U.C., Kelling, G. and Demirkol, C. (1991) 'Aspects of basin evolution in the Neogene Adana Basin, SE Turkey', *International Earth Scientific Congress on Aegean Regions, Proceedings*, 1, 357 – 370.

Weimer, P., and Link, M.H. (1991) 'Global petroleum occurrences in submarine fans and turbidite systems', in *Weimer, P., and Link, M.H., (eds.), Seismic facies and sedimentary processes of submarine fans and turbidite systems*: New York, Springer-Verlag, p. 9 - 67.

Williams, G.D., Ünlügenç, U.C., Kelling, G. and Demirkol, C. (1995) 'Tectonic controls on stratigraphic evolution of the Adana Basin, Turkey', *Journal of the Geological Society*, 152, pp. 873 – 882.

Yetiş, C. (1988) 'Reorganization of the Tertiary stratigraphy in the Adana Basin, Southern Turkey', *Newsletters on Stratigraphy*, 20(1), pp. 43 – 58.

Yetiş, C. and Demirkol, C. (1986) 'Adana baseni batı kesiminin detay jeoloji etüdü', MTA *Enstitüsü, Derleme*, 8037, (in Turkish).

Yetiş, C., Kelling, G., Gökçen, S.L. and Baroz, F. (1995) 'A revised stratigraphic framework for Late Cenozoic sequences in the northeastern Mediterranean region', *Geol Rundsch*, 84, pp. 794 – 812.

Yılmaz, Y. (1993) 'New evidence and model on the evolution of the southeast Anatolian orogen New evidence and model on the evolution of the southeast Anatolian orogen', *Geological Society of America Bullet*in, (2), pp. 251 – 271.

Zhang, X., Pyrcz, M.J. and Deutsch, C.V. (2009) 'Stochastic surface modeling of deepwater depositional systems for improved reservoir models', *Journal of Petroleum Science and Engineering.* Elsevier B.V., 68(1–2), pp. 118 – 134.

Zhang, J.J., Wu, S.H., Fan, T.E., Fan, H.J., Jiang, L., Chen, C., Wu, Q.Y. and Lin, P. (2016) 'Research on the architecture of submarine-fan lobes in the Niger Delta Basin, offshore West Africa', *Journal of Palaeogeography.* Elsevier Ltd, 5(3), pp. 185 – 204.

7. ARTIGOS SUBMETIDOS

7.1. Artigo 1

Submetido à *Journal of Sedimentary Research*

Facies association and distribution in submarine frontal splays: an example from the Cingöz formation, Turkey

DANIEL BAYER DA SILVA - Department of Stratigraphy, Federal University of Rio Grande do Sul, Av. Bento Gonçalves, 9500, CEP 91501-970, Porto Alegre, Brazil.

BRYAN T. CRONIN - Tullow Ghana Ltd, Plot 70, George Walker Bush Highway, North Dworzulu, Accra, Ghana

HASAN ÇELIK - Department of Geological Engineering, Engineering Faculty, Fırat University, 23119, Elazığ, Turkey.

KARIN GOLDBERG ˉ Department of Geological Engineering, Engineering Faculty, Fırat University, 23119, Elazığ, Turkey.

ONLINE MANUSCRIPT SUBMISSION AND PEER REVIEW

The Journal of Sedimentary Research

SEPM Society for Sedimentary Geology

Journal of Sedimentary   Contact Us   Tips & Tricks   Requirements
Research Home

Home

Detailed Status Information

Manuscript #	2018-123
Current Revision #	0
Submission Date	22nd Aug 18
Current Stage ..	Initial QC Started
Title	FACIES ASSOCIATION AND DISTRIBUTION IN SUBMARINE FRONTAL SPLAYS: AN EXAMPLE FROM THE CINGÖZ FORMATION, TURKEY
Suggested Running Title	FACIES ASSOCIATION IN FRONTAL SPLAYS: AN EXAMPLE FROM THE CINGÖZ FM., TURKEY
Manuscript Type	Research Articles
Corresponding Author	Mr. Daniel Bayer da Silva (Universidade Federal do Rio Grande do Sul)
Contributing Authors	Dr. Bryan Cronin , Prof. Hasan Çelik , Prof. Karin Goldberg
Associate Editor	Not Assigned
Keywords	facies distribution, frontal splay, Cingöz Formation, turbidite, Adana Basin
Conflict of Interest	**No**, there is no conflict of interest that I should disclose, having read the above statement.
Ethics statement agreement	Yes

Stage	Start Date
Initial QC Failed	23rd Aug 18
Initial QC Started	22nd Aug 18
Author Approved Converted Files	22nd Aug 18
Preliminary Manuscript Data Submitted	22nd Aug 18

FACIES ASSOCIATION AND DISTRIBUTION IN SUBMARINE FRONTAL SPLAYS: AN EXAMPLE FROM THE CINGÖZ FORMATION, TURKEY

DANIEL BAYER DA SILVA[1], BRYAN T. CRONIN[2], HASAN ÇELIK[3], KARIN GOLDBERG[4]

[1] Department of Stratigraphy, Federal University of Rio Grande do Sul, Av. Bento Gonçalves, 9500, CEP 91501-970, Porto Alegre, Brazil.

[2] Tullow Ghana Ltd, Plot 70, George Walker Bush Highway, North Dworzulu, Accra, Ghana

[3] Department of Geological Engineering, Engineering Faculty, Fırat University, 23119, Elazığ, Turkey.

[4] Department of Geology, Kansas State University, 207 Thompson Hall, Manhattan, KS 66506, United States.

Corresponding author: daniel.bayer.silva@gmail.com

ABSTRACT

Facies associations in submarine frontal splays are essential to understanding the development of the deposits, the hierarchy and the complexity of the fundamental blocks in frontal splays. Th facies associations, based on detailed sedimentary description of well-exposed outcrops from the Middle Miocene Cingöz Formation in the Adana Basin, southern Turkey, has shown frontal splays formed by channelled, cobbly and pebbly sandstones to turbiditic tabular sandstones, also fine-grained facies and MTDs. Three main groups of facies associations, based on the net-to-gross (low, middle and high), were identified. These groups comprise ten facies associations recognized on the basis of degree of amalgamation, presence of specific facies (mainly heterolithics, hybrid beds and mass transport deposits), modal grain size, percentage of thick sandstones in the succession, and presence of current ripple laminations and graded beds. Identification and comparison of facies association allowed the definition of a distribution pattern for each parameter in a frontal splay, helpful to identify sub-environment and to recognize the hierarchies and building blocks of frontal splay.

INTRODUCTION

Facies in turbidite deposits are widely studied since Bouma (1962), through the first outcrop analysis, and since his work, the classification became even more detailed. Authors such as Mutti and Ricci Lucchi (1972), Lowe (1982), Mutti (1992), Ghibaudo (1992), Haughton et al. (2003), Talling et al. (2004) and Cronin (2018), also contributed to improving the understanding of turbidite deposits. In frontal splays the facies association identification facilitates the interpretation of the distribution of the sheets, sub-environment locations and hierarchy identification (Hofstra et al., 2017). Detailed sedimentological description of laterally continuous exposures through frontal splays is required to undertake facies and facies association analysis to achieve this. For that reason, the Cingöz Formation, of the Miocene in Adana Basin, southern Turkey is used as an example of facies association studies. Good exposures, through different parts of the frontal splays, allows the recognition of the various facies associations that define the frontal splay sub-environments, and to recognize the patterns of deposition.

Some authors (Hodgson, 2009; Spychala et al., 2017) have also contributed to the advance in the understanding of facies distribution in splays, showing, for example, the differences between the lateral versus distal margins of the frontal splay, the latter interpreted by their preponderance of hybrid beds.

The present study intends to create a facies association classification scheme that will allow workers to predict location on a frontal splay from vertical sedimentological profiles using the Cingöz Formation as an example to contribute to the similar lobe deposits worldwide (Tanqua Karoo, Grès d`Annot, Ross Formation, Golo Fan, Laga Basin, etc). Most of the characteristics used to distinguish the groups are easy to observe, but to get a better resolution, to separate even more the groups, a bed analysis is needed.

Geological Setting of the Cingöz Formation

The Adana Basin is located in southern Turkey (Fig 1A), very close to the triple junction (Arabian, African and Aegean-Anatolian plates) (Ketin, 1966; Şengör, 1979; Kelling et al., 1987; Robertson et al., 2004; Cipollari et al., 2013; Radeff et al., 2015), and it is the onshore part of Adana-Cilicia Basin (Brinkmann, 1976; Kelling et al., 1987), the Cilicia Basin being its offshore counterpart (Fig. 1B-C). The Adana-Cilicia

Basin is bounded to the N and NW by the Central Anatolian plateau, and to the S and SE by the Kyrenia and Misis Mountains (a structural feature known as the Kyrenia – Misis lineament) (Fig. 1B). The Misis Mountains were uplifted during the Late Miocene (Kelling et al., 1987; Williams et al., 1995).

Stratigraphy of Adana Basin.---The Adana Basin is one of the largest Miocene foreland basins in southern Turkey (Ilgar et al., 2013). Its stratigraphy was first proposed by Schmidt (1961). The sedimentary succession comprises up to 6 km of Miocene and Quaternary siliciclastic and carbonate deposits.

According to Gürbüz (1993, 1999), the relative sea-level changes in the Adana Basin fit with the global sea-level rise and fall scheme of Mitchum et al. (1977) and Haq et al. (1987, 1988) for the upper Palaeogene – Neogene (Satur, 1999). One lower-frequency transgressive-regressive cycle (approx. 15 my) comprises the entire Neogene basin fill, with high frequencies representing facies variations (Gürbüz, 1993, Ünlügenç, 1993, Satur, 1999).
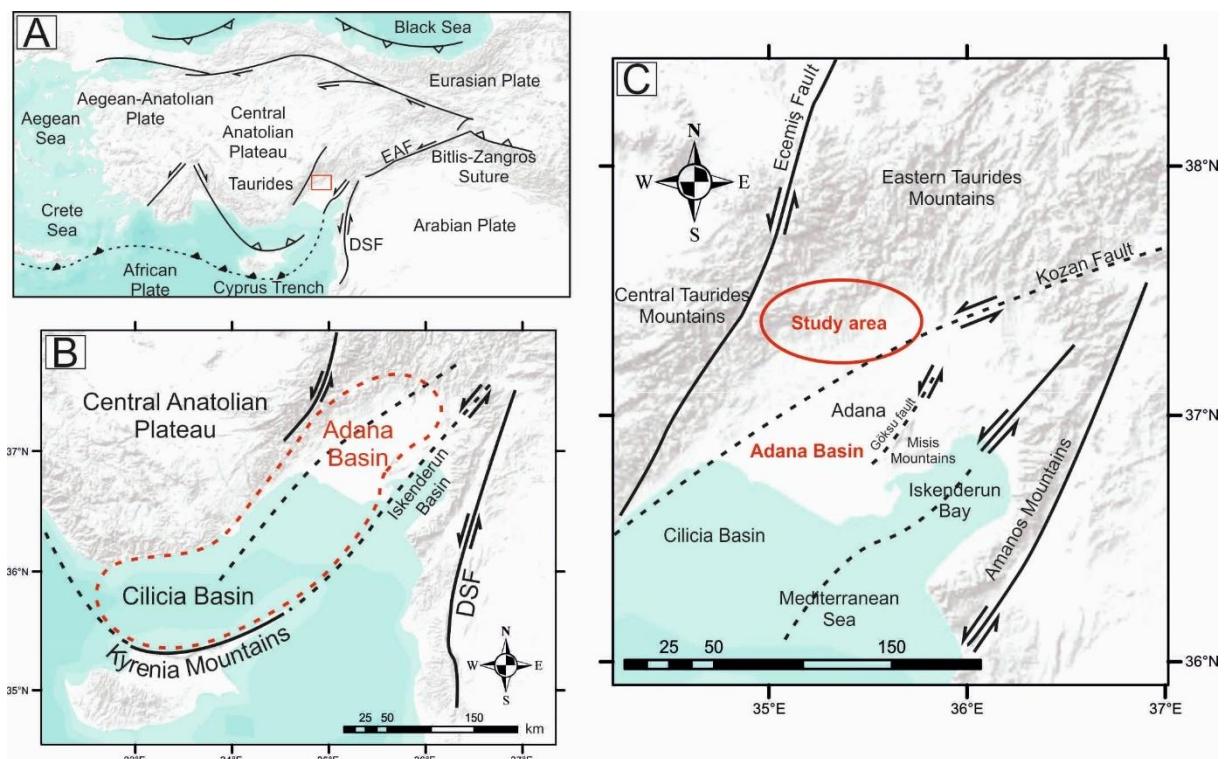
Fig. 1: Tectonic maps highlighting the Adana Basin and surroundings. In red dashed lines, the Adana-Cilicia Basin. The study area (red circle) is located to the north of Adana city, and limited to the north by the Central Tauride Mountains and to the south by the Kozan Fault. Adapted from Radeff et al. (2015).

Based on biostratigraphic studies and lithological interpretations (Gürbüz, 1993, Nazik, 2004), a relative sea-level curve for the Adana Basin reveals a main transgression during the Upper Burdigalian – Lower Langhian and a regression in the Upper Serravallian (Fig. 2).
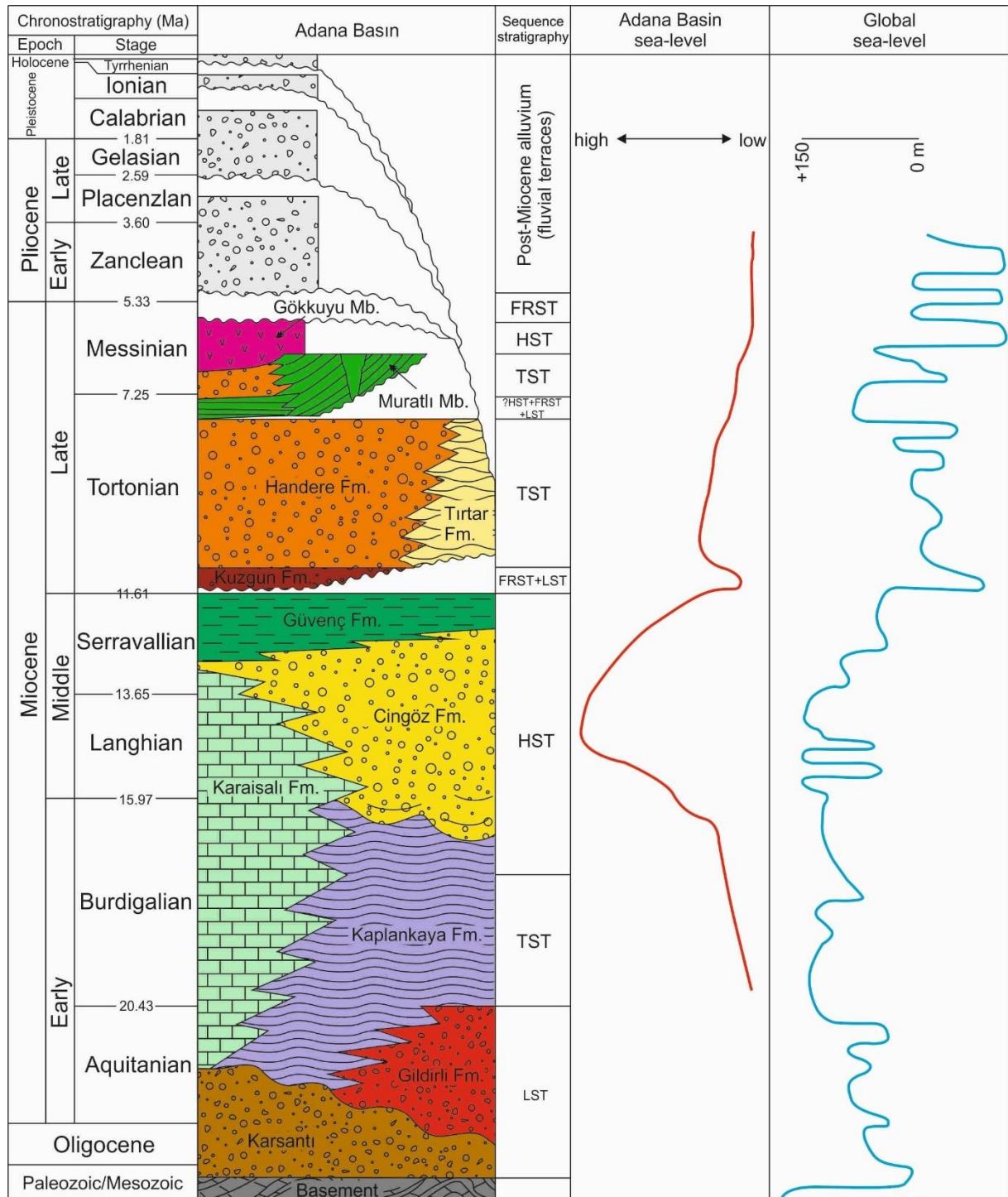
Fig. 2: Stratigraphic chart of the Adana Basin with the sequence stratigraphic system tracts, and Adana Basin with Global sea-level curves. From Haq et al. (1987); Nazik and Gürbüz (1992); Gürbüz, (1993); Yetiş et al. (1995); Ilgar et al. (2013).

The Cingöz Formation (Fig. 3) is composed of channelled, cobbly and pebbly sandstones (mainly related to the feeder system), turbiditic tabular sandstones (Fig. 3), fine-grained deposits and MTDs (Gürbüz and Kelling, 1993), deposited during the Upper Burdigalian to Lower Serravallian (Nazik and Gürbüz, 1992). According to Gürbüz (1993), the Cingöz Formation deposits are 1000 – 3000 m thick and were deposited in 5 million years (Satur, 1999).

Satur (1999) described two different feeder systems for each submarine fan: the Western Fan (WF) derived from a single point source to the west, whereas the Eastern Fan (EF) was built by multiple channels to the north.

Fig. 3: Overview of the main elements described in the frontal splays from the Cingöz Formation. The photo shows thin-, medium- and thick-sandstones.

The main focus of this study, the Eastern Fan (EF) (approximately 750 km^2 of exposed area) was described by Gürbüz and Kelling (1993) and Gürbüz (1993). These authors concluded that the EF is a high-efficiency (sand-rich) system with unchannelized lobes, influenced by tectonic activity (seafloor topography controlled by active faulting), sediment supply and relative sea-level fluctuations (Satur, 1999). Most of the sand was deposited in the splays, but the feeder system to the exposed

splays is not exposed. Instead the sediments (probably gravelly, from what we know about the channel and canyon fills of earlier parts of the fan) from the exposed feeder system are older and are covered by the current system (Satur, 1999).

The EF was divided into inner, middle and outer fan by Gürbüz and Kelling (1993) (Fig. 4). The inner fan consists of the shallow channels, represented by strongly amalgamated, thick sandstone beds and rare thin-bedded sandstones. Gürbüz (1993) described un-channelized depositional lobes in the middle fan, forming thickening- and thinning-upward successions. The outer fan is mainly composed of TBTs with occasional isolated thicker sandstone beds (up to 1 m thick).
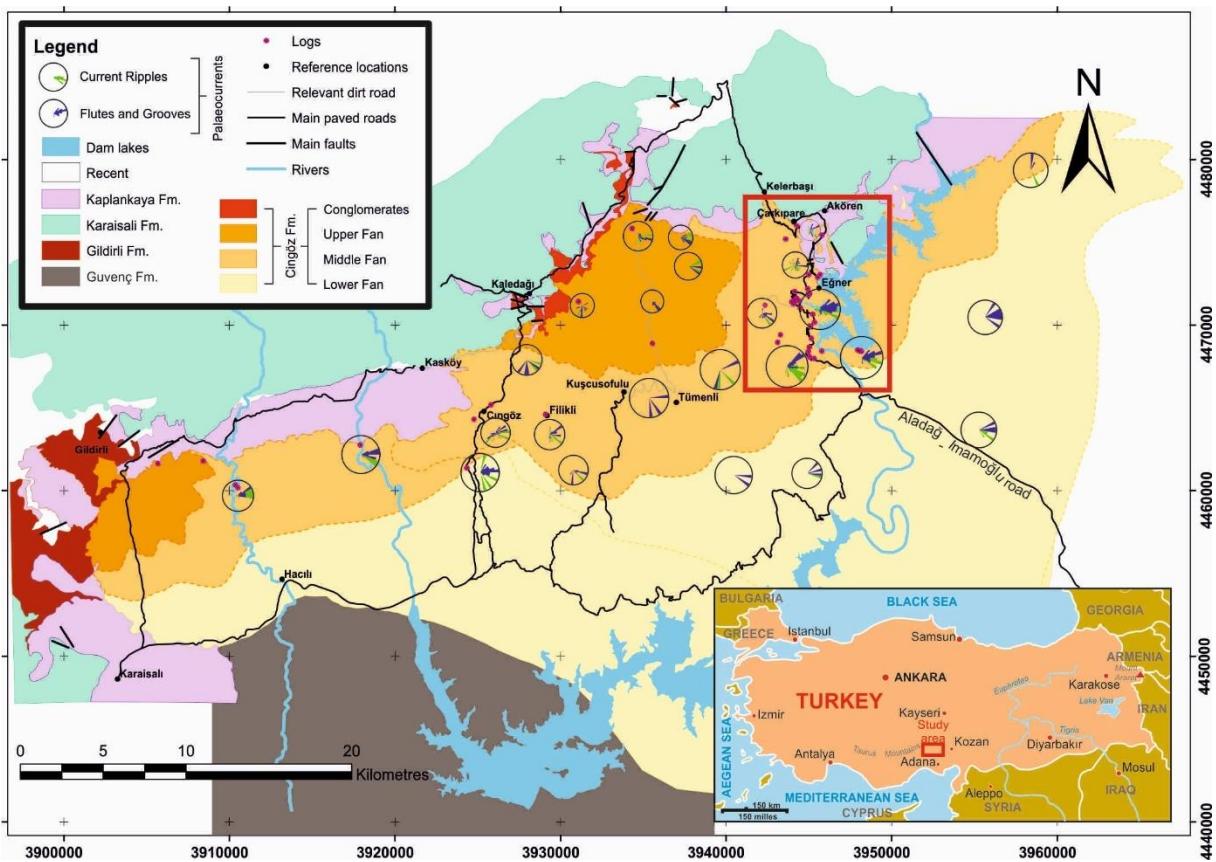
Fig. 4: Geological map based on the data acquired (re-interpreted from Gürbüz, 1993). The red box highlights the main study location.

METHODOLOGY

The basic methodology used was the detailed description of selected outcrops in the area, to identify and describe the distinct lithofacies, facies associations and bounding surfaces, through the construction of lithological logs for each studied outcrop. The vertical sections were measured and recorded layer by layer. The data

collected include colour, texture (grain size, sorting, roundness, fabric), composition, sedimentary structures and degree of bioturbation.

The definition of facies associations in this study took into consideration not only the overall facies attributes and vertical facies succession, but also some characteristics relevant to reservoir properties, such as net-to-gross, degree of amalgamation, and the relative proportion of specific facies such as mass-transport deposits (MTD), hybrid beds (HEB) and heterolithics (HET) (Table 1). Facies associations here represent intervals of section that have broadly the same ranges of these parameters and sedimentary features and are defined top and base by a marked change to another facies association. Thus, there are particular packages of lithofabrics that can be interpreted to reflect a particular part of a sedimentary body, such as a splay margin or axis for example. See Cronin (2018) and Cronin and Jones (2018) for broader application of facies association in deep-water systems.

The main parameter for classification of the facies associations was the net-to-gross (N:G), or percentage of sand to mud fraction. Three groups were recognised, based on net-to-gross ranges (Table 1): low (T_L, 0.29-0.60), medium (T_M, 0.61-0.75) and high (T_H, 0.76-1.00). The N:G also relates to the degree of amalgamation and the proportion of thick sandstones in the succession (i.e. high N:G also have higher degree of amalgamation and a larger proportion of thick sandstones). Thick sandstones refer to those with thickness greater than 10 cm (Ingram, 1954; Campbell, 1967).

All the proportions referred here were calculated as a ratio between the analysed parameter (e.g. thick sandstones or heterolithics facies) and total thickness of the vertical section. Twenty-six vertical successions (sedimentary logs) were analysed to define the parameters listed in Table 1. Total thickness in individual sections ranged from 8 to 72 m, summing up to 690 m of analysed vertical successions. Although the calculated percentages showed in Table 1 cannot be taken as absolute values, they provide a good approximation of the overall characteristics in each facies association. Following the identification of groupings based on N:G, further differentiation took into account the degree of amalgamation (for T_H), the proportion of heterolithics (HET for T_M) and of mass-transport deposit and hybrid beds (HEB-MTD for T_L).

Table 1: Defining characteristics of the 10 facies associations, with the main characteristics shaded grey and the most common lithofacies marked in red. (N:G = net-to-gross; HET = heterolithics; HEB = hybrid beds; MTD = mass-transport deposits).

Facies assoc.	N:G	Modal grain size	% HET	% HEB-MTD	Degree of amalgamation	% Thick sandstones	%grain size larger than modal	Presence of current ripples	Presence of graded beds	Common lithofacies	Average thickness (m)
T_H-1	>0.90	lower medium sand	<5%	-	>71%	>46%	>38%	rare to common	very common	F5-6-7	3.81
T_H-2	0.80-0.97	lower medium sand	<7%	<7%	30-71%	16-86%	13-75%	rare to common	very common	F4-5-6-7	3.53
T_H-3a	0.81-0.96	fine to medium sand	<9%	-	<29%	>32%	20-64%	rare to common	very common	F5-6-8-10	3.76
T_H-3b	0.76-0.92	Fine sand	<5%	<13%	<29%	23-75%	3-27%	common	common	F1-5-6-7-10	3.8
T_M-1	0.61-0.75	Fine sand	7-37%	<18%	-	<30%	<40%	rare to very common	common	F1-2-5-6-8-10	2.63
T_M-2		Fine sand	<6%	<25%	-	<29%	<16%	rare to very common	common	F1-2-5-6-7-10	3.11
T_L-1a	0.50-0.60	Fine sand	4-37%	4-23%	-	<25%	<40%	rare to very common	uncommon	F1-2-5-6-7-8-10	2.55
T_L-1b		Fine sand	<60%	-	-	<16%	<21%	rare to very common	common	F5-6-7-8-10	2.31
T_L-2a	0.29-0.49	Fine sand	15-50%	<23%	-	<15%	<20%	rare to common	uncommon	F1-5-6-7-8-10	1.76
T_L-2b	0.33-0.47	Fine sand	<10%	-	-	<10%	<20%	common to very common	rare	6-7-9-10	2.07

The degree of amalgamation used here to distinguish the facies association in T_H is the ratio between the number of amalgamated beds and the total number of thick sandstones (> 10 cm) in the facies association. For example, if a facies association has 10 beds more than 10-cm thick and two of them are amalgamated, the degree of amalgamation will be 2/10, or 20%.

Heterolithics, identified mainly in thin-bedded turbidites, are characterized by a low percentage of very fine or fine sand fraction at the base, abruptly overlain by silt and/or clay. The proportion of heterolithics (HET) was used to differentiate two facies associations in T_M. It was calculated as the ratio between the cumulative thickness of HET and the total thickness of the facies association.

A similar systematic was used to calculate the proportion of hybrid beds and mass-transport deposits (HEB-MTD) in the facies associations forming T_L (Table 1). The HB-MTD is the ratio between the number of HEB and/or MTD beds and the total beds of the facies association. HEB and MTD were put together as the same characteristic due to the similar behavior (related to viscosity) in the flow (or part of the flow, in hybrid beds). Furthermore, the facies associations in this group (T_L) very often have one or other, suggesting that they are found in similar positions in frontal splays.

As the modal grain size in the study location is fine sand, the grain size larger than modal parameter was used to determine the ratio between beds that contain this parameter and the total beds of the facies association, which mostly represent fine sand.

In each logged section, N:G-based groupings of facies were visually recognized first (T_H, T_M or T_L), followed by a more detailed analysis of the other defining characteristics to assign these packages to one of the 10 facies associations in Table 1.

RESULTS

Lithofacies Analysis

The lithofacies classification for the Cingöz Formation, adopted in this paper, was based on the classification schemes developed by Mutti and Ricci Lucchi (1972),

Walker (1978), Lowe (1982), Ghibaudo (1992) and Cronin (2018) adapted to include the peculiarities of the study area.

A total of 10 facies was identified, based on the texture, clast content and organization, internal structure and mud content (Table 2 and Fig. 5). Since this work was focused on frontal splays, the facies from the feeder systems were not included here.

In general, the sandstones are clay-free and very well to well sorted. They may be normally-graded or ungraded. The basal contact of the beds is frequently flat, mainly in fine or medium grained sandstones. The complete Bouma sequence (Bouma, 1962) is rare in individual beds. The T_{abc} sequence is widely present in beds in most of the splay areas, in medium to fine-grained sandstones (T_a and $T_{b)}$ and fine to very fine sandstones (T_c). Bioturbation is quite common in most of the sandstones and mudstone facies (weak or moderate), resulting in mostly horizontal (Palaeodictyon, Planolites, Chondrites and Thalassinoides ichnofacies) rather than vertical (Scolicia and Ophiomorpha ichnofacies) burrows.

Table 2: Main characteristics of the lithofacies identified in the Cingöz Formation.

Lithofacies code	Lithotype name	Description	Bed thickness	Modal grain size	Interpreted sediment support	Interpreted depositional process	Interpreted flow type	Reference
F1	Mixed, contorted mudstone and sandstone	Thin- and thick-bedded sandstone and mudstone contorted. Most of the folded beds with random orientation. Locally granule sandstone	0.10 – 3.0 m	Fine to granules	Matrix strength	Frictional freezing	Slump/slide /debris flow	Facies 1 and 3 (Lowe, 1982); F1 (Mutti, 1992); MTD (Martinsen and Bakken, 1990); L26 (Conin, 2018)
F2	Linked debrite	Structureless sandstone overlain by muddy sandstone with mostly disorganized mudstone and sandstone clasts and/or injection	0.10– 0.7 m	Fine to medium	Matrix strength/fluid turbulence	Frictional freezing, tractive and suspension	Co-genetic debris flow and turbidity current	Linked debrite (Haughton et al., 2003); Hybrid flow (Haughton et al., 2009); Co-genetic debrite turbidite (Talling et al., 2004; Pyles and Jennette, 2009); L22 (Cronin, 2018)
F3	Matrix-supported conglomerate	Matrix-supported conglomerate with angular to rounded (90%) clasts (plutonic, volcanic, carbonate sources) up to 15 cm. Locally some orientation marked by mud chips (10 cm). Locally rounded mudclasts (up to 25 cm)	0.30 – 2.3 m	Coarse to pebble	Dispersive pressure	Traction/bedload	High-density turbidity current	R3 (Lowe, 1982); F3 (Mutti, 1992)
F4	Shale-clast, gravelly sandstone	Thick-bedded sandstone rich in oriented, angular (90%) to rounded mudclasts up to 60 cm.	0.10 – 1.4 m	Coarse to pebble	Fluid turbulence	Traction	Turbidity current	R1 (Lowe, 1982); F2 (Mutti, 1992)

Lithofacies code	Lithotype name	Description	Bed thickness	Modal grain size	Interpreted sediment support	Interpreted depositional process	Interpreted flow type	Reference
F5	Structureless sandstone	Structureless sandstone, mostly well to very well sorted. Locally rich in mudclasts and with flame, pipe and dish structures. In general, oriented mudclasts (up to 60 cm), often in levels.	0.1 – 1.3 m	Fine to granules	Fluid turbulence	Traction and suspension	Turbidity current	Ta (Bouma, 1962); S3 (Lowe, 1982); F5 (Mutti, 1992); L17 (Cronin, 2018)
F6	Parallel-laminated sandstone	Sandstone with parallel lamination (mainly well sorted). Locally, lenses of coarse grains defining the lamination	0.01 – 0.3 m	Very fine to fine-to-medium	Fluid turbulence	Traction and suspension	Turbidity current	Tb (Bouma, 1962); S2 (Lowe, 1982); F8 (Mutti, 1992)
F7	Cross-laminated sandstone	Sandstone with cross lamination (ripples)	0.01 – 0.02 m	Very fine to fine	Fluid turbulence	Traction and suspension	Turbidity current	Tc (Bouma, 1962 and Lowe, 1982); F6 (Mutti, 1992); L15 (Cronin, 2018)
F8	Heterolithics	Centimetric inter-bedding of sandstone and mudstone or siltstone and claystone	0.01 – 0.25 m	Clay to fine sandstone	Hindered settling	Traction and suspension	Turbidity current	Ta-Te (Bouma, 1962); S3 (Lowe, 1982); F8, F9a, and F9b (Mutti, 1992)
F9	Siltstone	Grayish laminated siltstone, commonly rich in plant debris	0.1 – 0.25 m	Silt	Fluid turbulence	Traction	Turbidity current	Td (Bouma, 1962); F9a (Mutti, 1992)
F10	Shale	Grayish to black claystone with minor siltstone laminations	< 0.6 m	Clay	Hindered settling	Suspension	Turbidity current/ hemipelagic fallout	Te (Bouma, 1962; Lowe, 1982); F9a (Te) (Mutti, 1992)
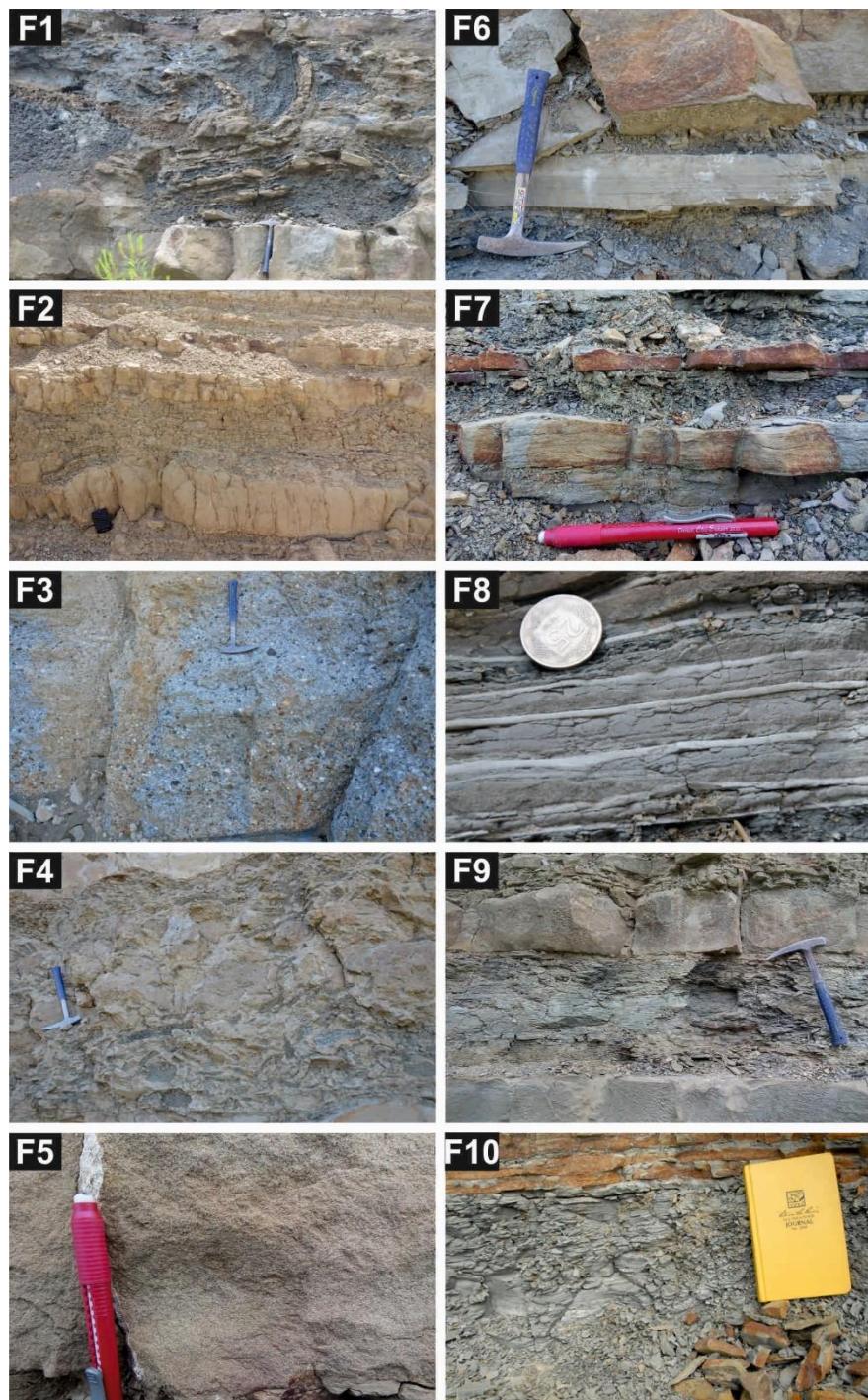
Fig. 5: Representative photos of the lithofacies recognized in the frontal splays, from the highest to the lowest hydrodynamic energy during deposition (F1 – F10).

Descriptions of the Facies Association

The characteristics of each facies association (Table 1 and Fig. 6), from the lowest to the highest net-to-gross, is described below.

- $\underline{T_L\ (0.29 - 0.60)}$ – This group of facies associations has the lowest proportion of thick sandstone beds and the lowest average thickness (2.17 m).

T_L-1 has net-to-gross ranging from 0.50 to 0.60. It is subdivided in 1a and 1b based on the presence/absence of MTD facies (F1). MTD facies (F1) occurs only in T_L-1a (Fig. 7).

T_L-2 has net-to-gross ranging from 0.29 to 0.49. It is subdivided in 2a and 2b based on the proportion of HET facies (F8) (Fig. 7). The proportion of HET facies (F8) in T_L-2a is high (>15%) in relation to T_L-2b (<10%).

- $\underline{T_M\ (0.61 - 0.75)}$ – This facies associations has intermediary characteristics between T_H and T_L and it was subdivided into two facies associations, based on the proportion of HET (F8). It displays higher N:G and thick sandstones than T_L.

T_M-1 has a high proportion of HET (>7%) in relation to T_M-2 (<6%).

- $\underline{T_H\ (> 0.76)}$ – This facies associations comprises the largest proportion of thick sandstones, and hence it contains the highest average mean thickness (3.74 m). Based on the degree of amalgamation, it was divided into 3 facies associations.

T_H-1 is characterized by net-to-gross greater than 90% and high degree of amalgamation (> 71%). T_H-2 display degrees of amalgamation between 30 and 71%. T_H-3 display the lowest degree of amalgamation (<29%). It is subdivided in 3a and 3b based on grain size. T_H-3a is dominated by medium-sand fraction or coarser, whereas in T_H-3b fine sand is dominant.
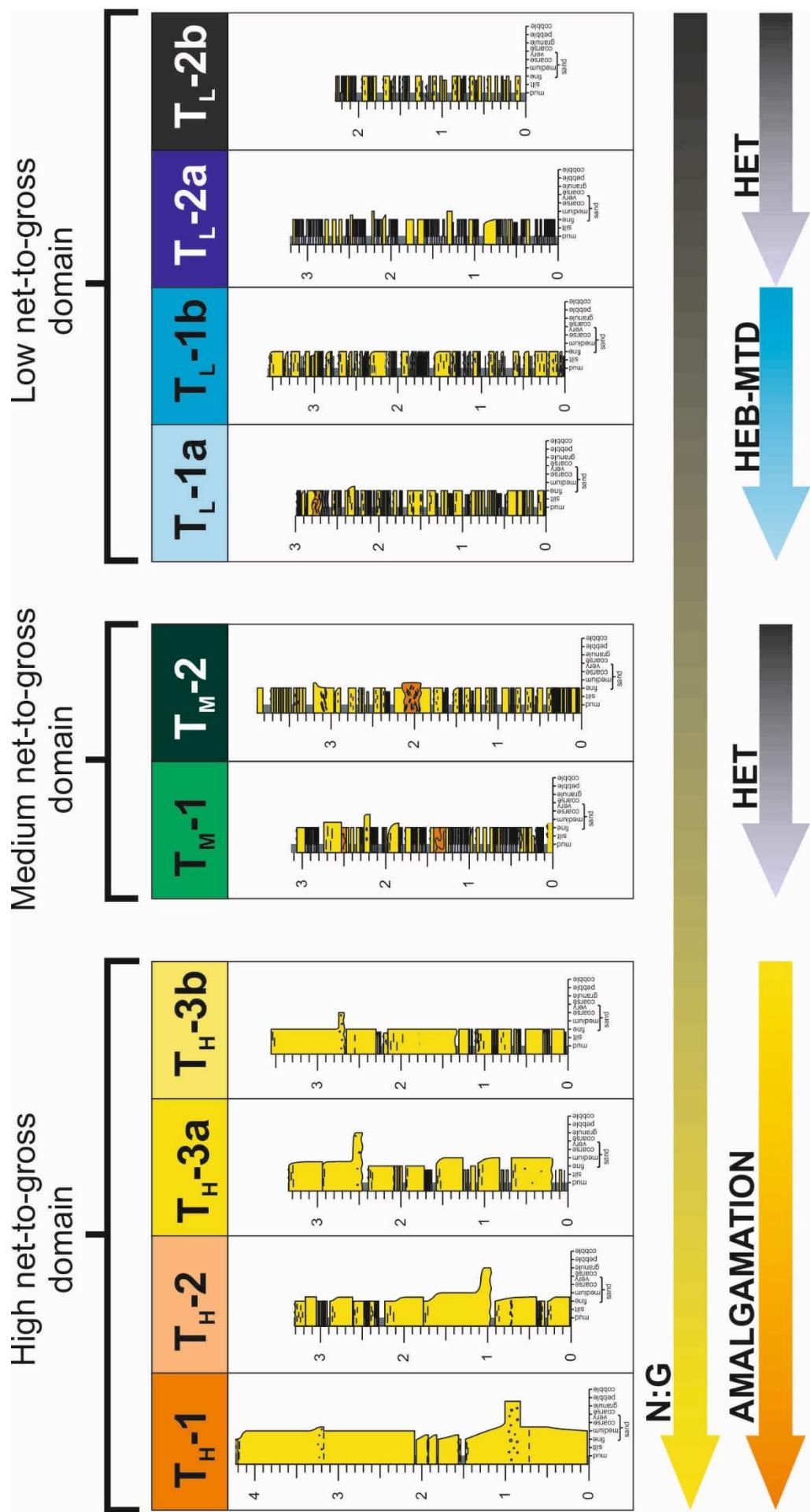
Fig. 6: Schematic logs representing typical patterns that define each facies association. Arrows indicate increasing direction of the defining characteristics of the facies associations (Table 1).
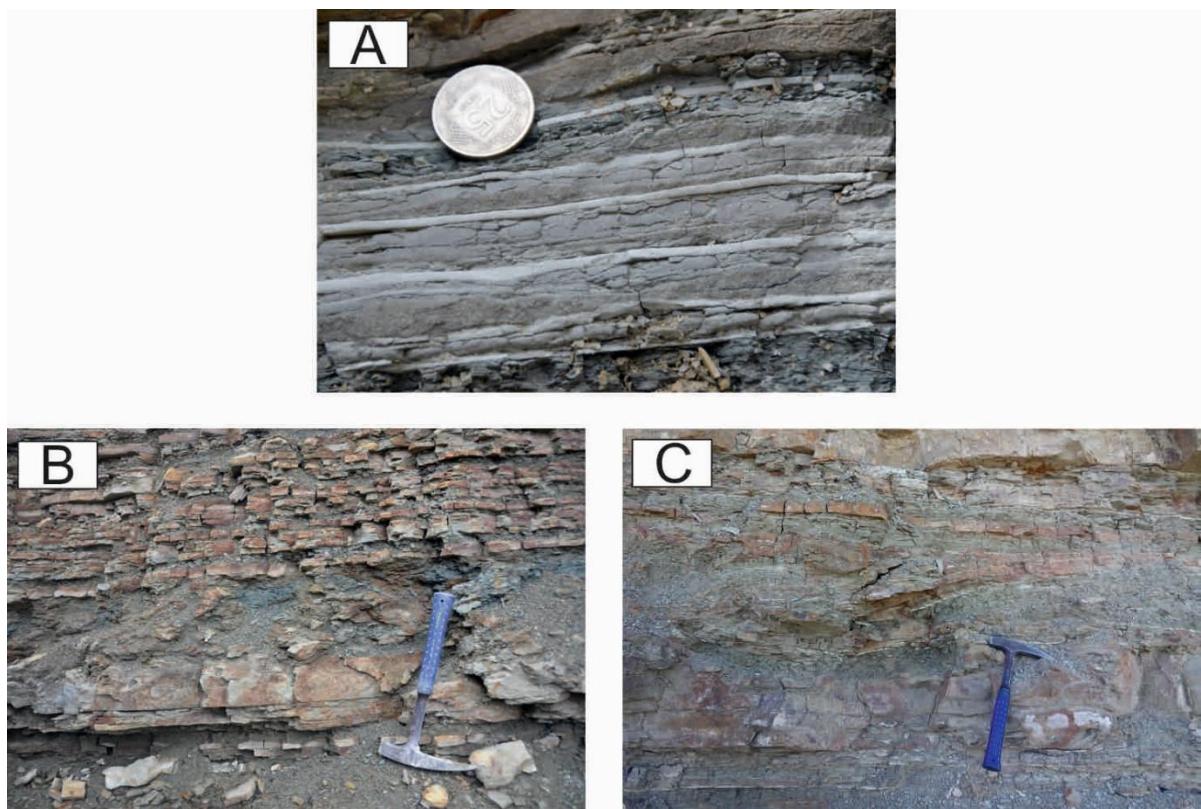
Fig. 7: Photos representative of lithofacies F8/HET (A), F2/HEB (B) and F1/MTD (C).

DISCUSSION

Environmental Interpretation

The identification of facies associations and their environmental interpretation across frontal splays may be used as a guide to assign the location of a given succession within the splay.

Despite heterogeneities in the sandstone bodies, caused by deposition in cycles of different hierarchies, data from the facies associations provide enough information for an approximate positioning in a splay, independent of the scale. The parameters used for that purpose were the average and maximum thicknesses of each facies association, the net-to-gross, degree of amalgamation and predominant lithofacies.

Table 3 summarizes the minimum, maximum and average thicknesses for each facies association. These values were calculated from the twenty-six vertical successions analysed.

Table 3: Minimum, maximum and average thicknesses (in metres) for the 10 facies associations. N refers to the number of times the facies association was identified in the 26 vertical successions analysed.

FAs	N	Min.	Max.	Average	Average for subgroups	Average for N:G group
T_H-1	22	1.90	7.30	3.82	3.82	
T_H-2	21	1.80	5.80	3.58	3.58	3.74
T_H-3a	10	2.25	5.90	3.76	3.78	
T_H-3b	10	2.00	7.30	3.80		
T_M-1	13	1.10	4.90	2.63	2.63	2.87
T_M-2	18	0.85	7.15	3.11	3.11	
T_L-1a	11	0.85	6.30	2.55	2.43	
T_L-1b	20	0.65	5.80	2.31		2.17
T_L-2a	14	0.65	4.00	1.76	1.92	
T_L-2b	7	1.30	3.35	2.07		
Total average		**1.34**	**5.78**	**2.94**	**2.98**	**2.98**

From Table 3 it is evident that a high net-to-gross means high average thickness of the sandstone beds. The average thickness values do not exceed about 4 m (3.82 m) in any of the facies associations. The maximum thickness values, however, are quite variable, reaching up to 7.30 m in T_H, but not exceeding 8 m in the study area.

One caveat is that it may be difficult to determine the limits between facies associations in a vertical succession, especially in T_H (as a result of the high degree of amalgamation). Therefore, maximum and average thickness values may be overestimated.

Since net-to-gross (N:G) is the relationship between sand and the thickness of the interval the sand is in, it is safe to assume that facies associations with greater net-to-gross ratios tend to be more proximal within a frontal splay deposit, due to the low amount of fine-grained facies and high amalgamation degree, while the N:G decreasing radially towards the margins, for the opposite reason.

Likewise, the degree of amalgamation tends to be greater in proximal regions of the frontal splays, where coarser-grained sandstones with erosive bases tend to be more abundant, hence forming amalgamated sandstone beds. The individual lithofacies are not a good parameter to determine position of the facies associations in the splay. However, the presence and/or frequency and thickness of certain lithofacies may be related to their position in the frontal splays. For instance, heterolithic facies (HET) are usually not common in proximal and medial positions along the frontal splay axis, occurring commonly in distal and/or lateral settings.

The facies associations described above can be distributed in a frontal-splay, as shown in Figure 8.
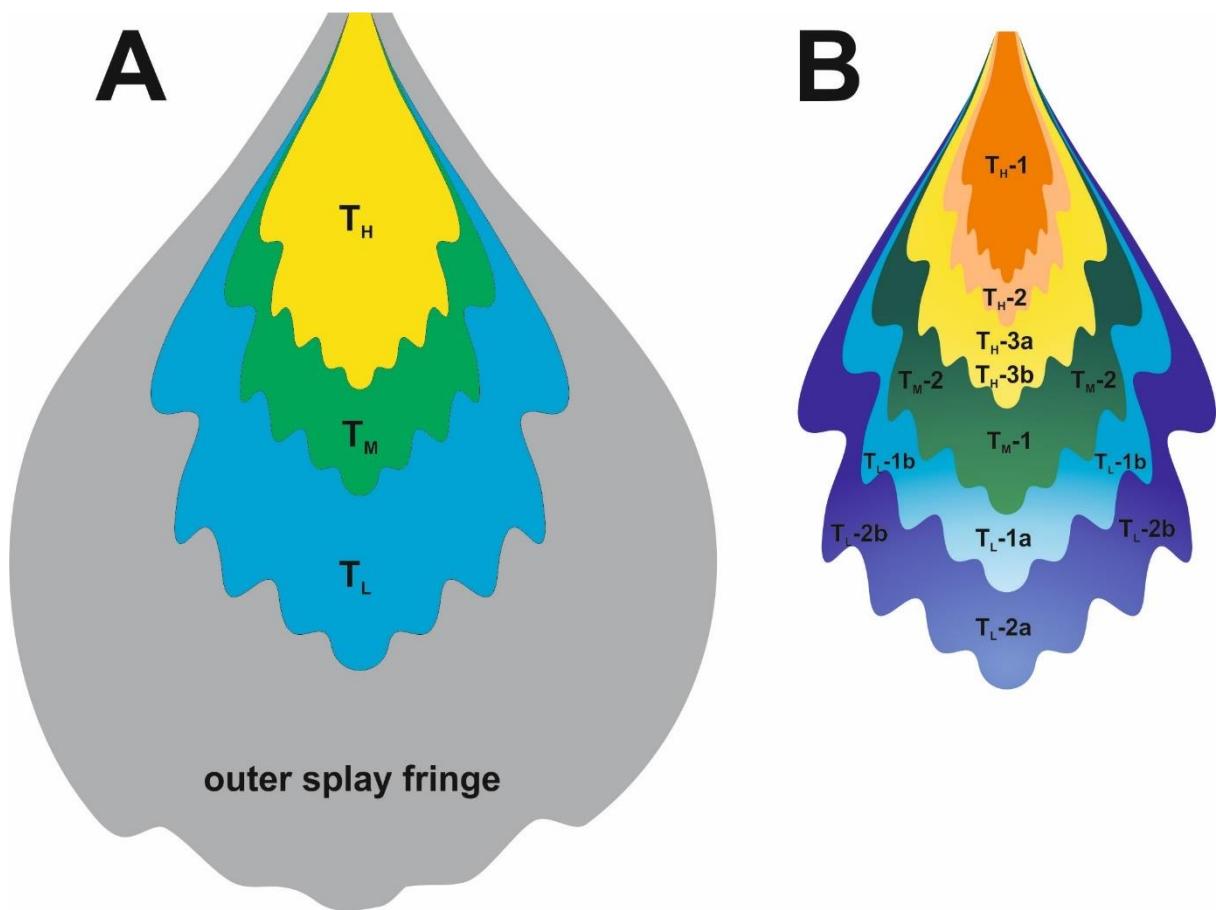
Fig. 8: Model of a frontal-splay, showing the distribution of the facies associations described in this work (not in scale). A) The 3 division TH, TM and TL added to splay fringe, not included in the FA scheme due the absent of data for statistic; B) All 10 subdivisions of the facies associations and the related colours are showed in Table 1.

Figure 8 represents the location of the facies associations described in Table 1, taking into consideration the comparative analysis between the facies associations identified, correlation of sedimentary logs and depositional models from the literature.

The limited data on outer splay fringe deposits in this study prevented the inclusion of those in the facies association scheme. Although the exposure of fringe is quite common, the absence of sedimentary logs in these regions prevents a better and sufficient statistical analysis, as the classification scheme was made based on logs. Nonetheless, all the described outcrops that included these deposits suggest a net-to-gross ratio less than 0.29, with abundant very thin-bedded turbidites and abruptly interbedded with rare thick sandstones (< 1 m thick), commonly occurring as linked debrites, or mud clast-rich horizons at the top and in the middle of the bed in axial regions. Net-to-gross decreases distally, while thin-bedded turbidites become ever more vertically spaced.

In order to show the method used for interpretation, Figure 9 displays a correlation between facies associations in different logs (EF#14, 14B, 15 and 26). Four logs were used in this example, in which one, slump structures (MTD) deposit was used for correlation along a maximum horizontal distance of about 1 km. In this situation, only some facies associations were correlated, due to the lack of description in part of the logs.

Firstly, after correlation based on sedimentologic features, the FA scheme was applied to each log. Seven FAs were chosen for the most complete log, which were used to correlate with other FA present in the other three logs. Applying this interpretation to other logs, the sub-environment maps for the FA classification were established   (Fig.   10).
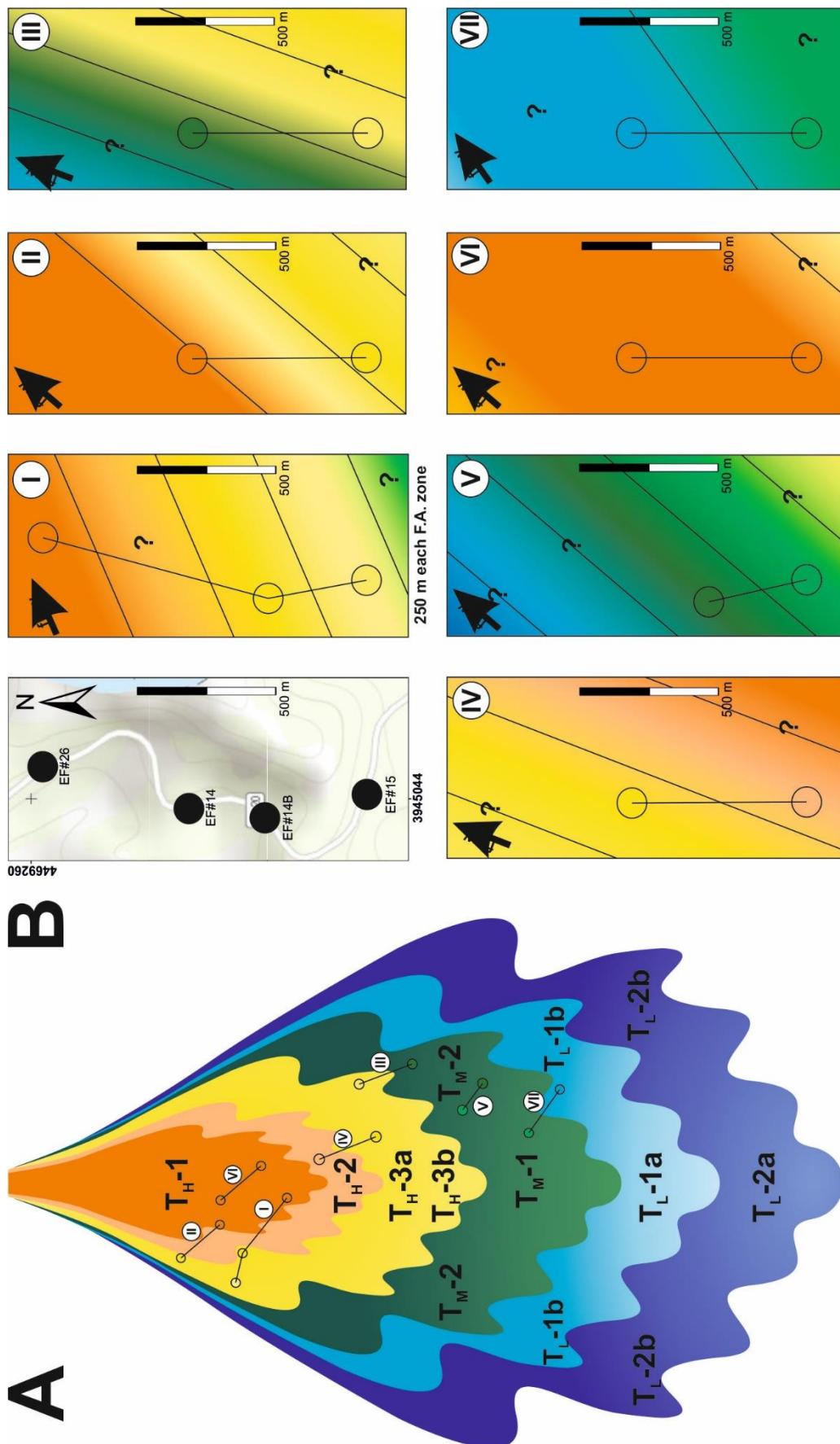
Fig. 9: Interpretation scheme of facies association sub-environments in a frontal splay: A) interpretation scheme from Figure 8, with the interpreted sections in B. Location of each section is based on palaeocurrent directions and correlation of FA; B) FA (I to VII) correlated between the four logs (see map). The coloured circles represent each FA group, and the surrounding colours are based on palaeocurrent direction (for each FA group) and the neighboring group location.

Distribution of the Main Characteristics

Based on the data collected in this study, it is possible to predict the distribution of the different characteristics defining the facies associations in Table 1. The distribution of eight relevant parameters is shown in Figure 10.
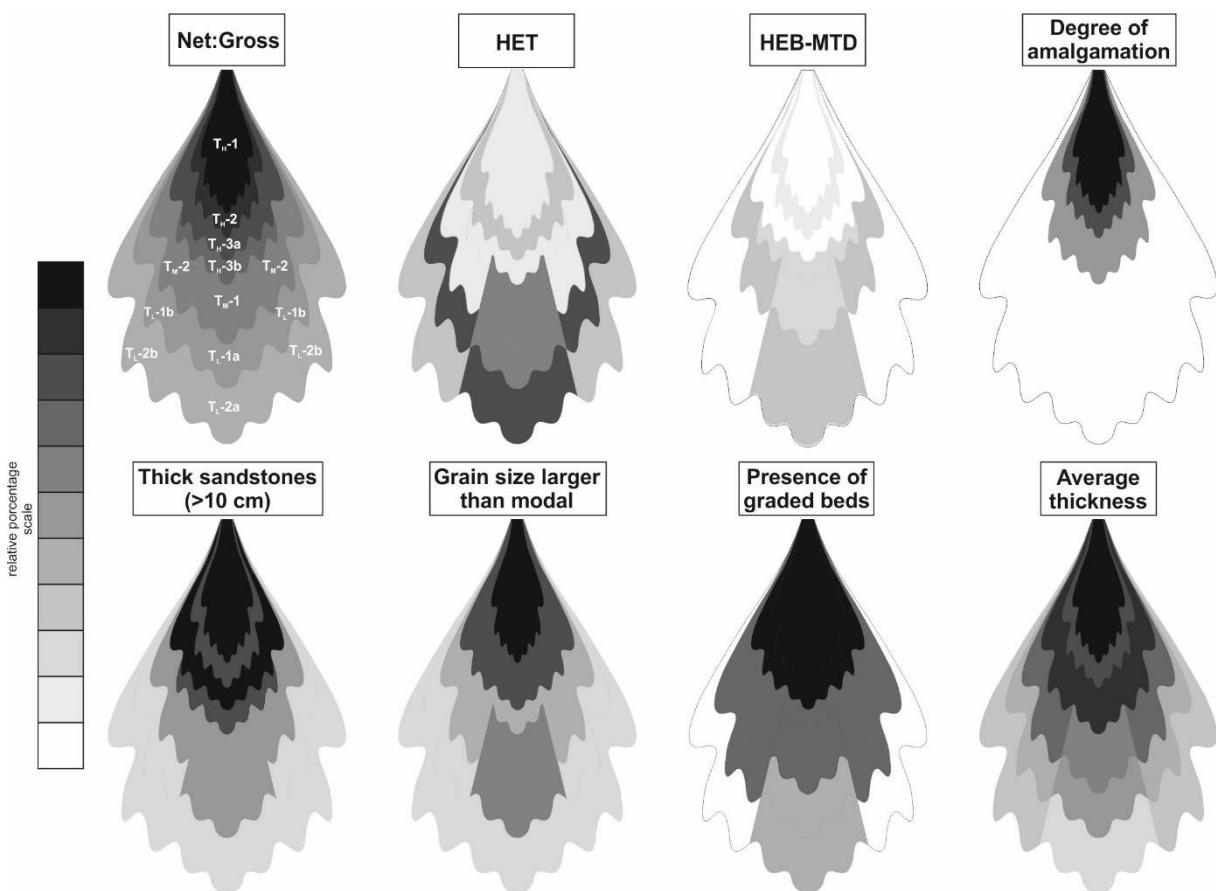
Fig. 10: Distribution of eight relevant parameters for the classification of the facies associations. The grey scale is proportional to the relative percentage (black being the most abundant region).

Overall, the net-to-gross decreases from proximal to distal settings, whereas the abundance of HET and HEB/MTD increases along this axis (Fig. 10). Both HET and HEB-MTD are most abundant in the medial and distal portions of the main frontal splay body.

An important factor in frontal splay deposits, the degree of amalgamation is highest in the proximal portions (T_H) (Fig. 10). The T_H facies associations are characterized by the presence of thick sandstone and graded beds, abundant coarse sediments, and high average thicknesses.

Graded beds are concentrated along the central axial, in more proximal positions of the splay. This distribution probably reflects the behaviour of the stratified flow that generated the gradational deposits, as well as the presence of thick beds that allow the identification of gradation possible and evident.

Although the distribution of facies associations in a depositional model is important for the interpretation of frontal splays, another key element is the recognition of the hierarchical control on splay construction.

Application of Facies Association Analysis

Despite the difficulties in identifying and separate each FA in distal portions of a frontal splay, thick TBTs can display useful for identification of facies associations, since they can be easily recognized when compared to rocks below and above. Unlike the proximal and medial portions of the frontal splay, in distal environments it is not uncommon to have similar FA, stacked vertically, interpreted as a single thick FA. The interpretation of TBTs in detail may lead to two different interpretations of hierarchy, but it is not always possible to distinguish these.

Average thickness of FA is about 4 m, and the maximum is 8 m, but these are based on measurements from all groups. In distal portions, FAs thin and pinchout, about up to 2 m. For this reason, thicknesses above which it would probably be another hierarchy level, interpreted as only one. These details are important in the interpretation of FA, because a TBT succession more than 2 m thick could be interpreted as a single FA and still be correct.

Figure 11 shows a similar situation, representing the interpretation of a log description (EF#19B) according to the FA classification. The outcrop photo highlights the subtle differences in the TBT. The exposed TBT is more than 11 m thick, with at least two distinct packages. The first package (about 5 m) is marked by frequent thick-bedded sandstones, while the second, above, is composed of only thin-bedded sandstones. This detail is the main characteristic to distinguish both packages and assign different classification, because, in this case, the N:G, degree of amalgamation, HET content and presence of HEB-MTD are not alone adequate.
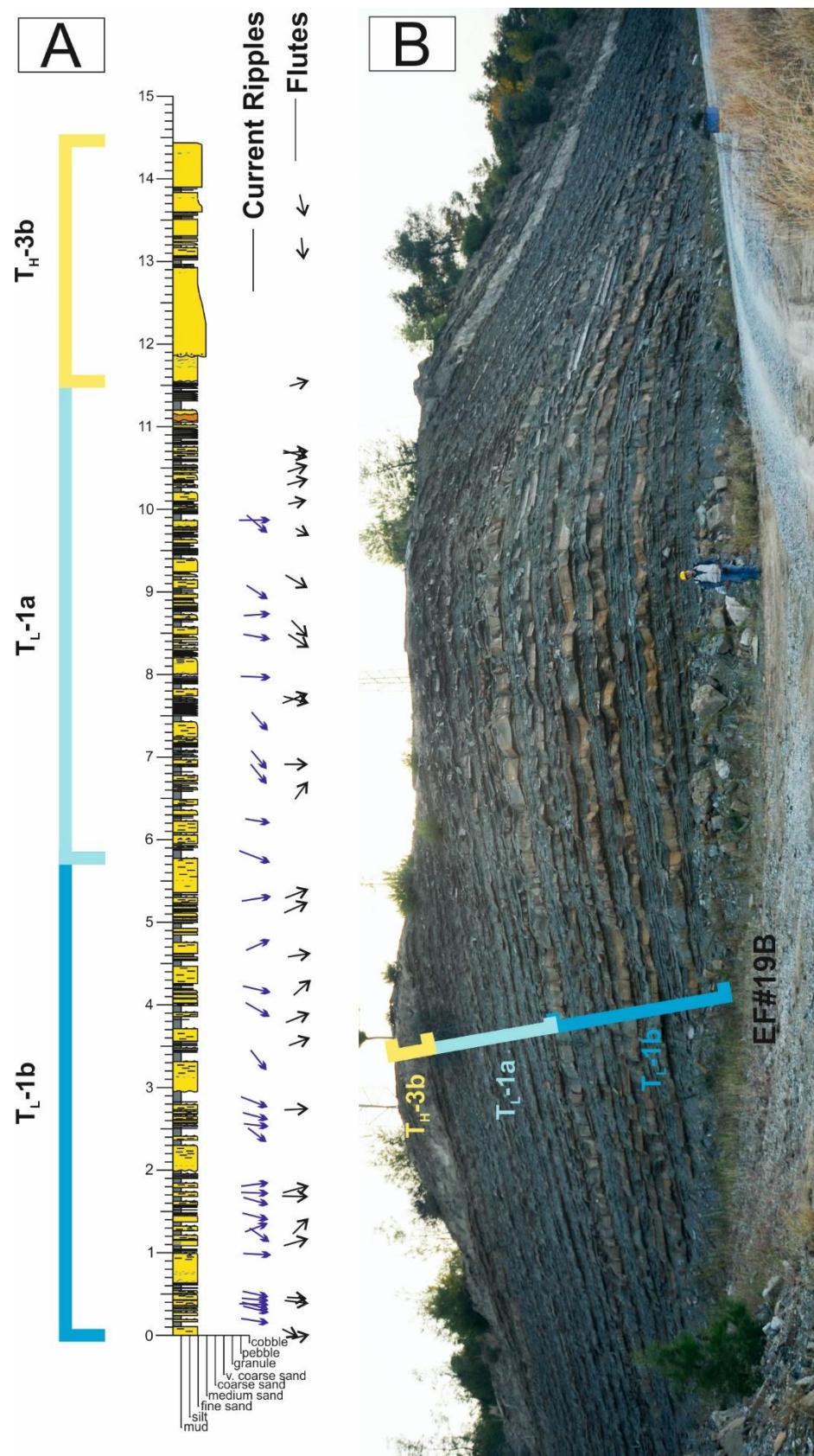
Fig. 11: Application of the facies association scheme in a distal area of a frontal splay building block: A) log EF#19B with palaeocurrent directions (obtained from current ripple laminations and flute casts) and the interpreted FA; B) EF#19B outcrop displaying the log location.

Overall, three FAs were interpreted in this location, the low-N:G T_L-1b, T_L-1a and the high-N:G T_H-3b. Based on palaeocurrent measurements obtained from current ripple laminations and flute casts, these three FAs represent different frontal splay architectural elements (not considering the scale here). The T_L-1b is dominated by a NE direction, while the T_L-1a is variable, but with more indicators towards SE than the previous package. The main difference appears in the T_H-3b, showing a SSE direction, and representing the deposition of a new frontal splay from a distinct direction, and the establishment of a new architectural element (Fig. 11).

CONCLUSIONS

The classification of facies associations suggested in this work was based on the recognition of ten distinct facies, of which the main ones are the sandstones, heterolithics, hybrid beds and mass transport deposits. Besides that, other parameters included in the FA scheme were the degree of amalgamation and net-to-gross. All parameters together enable to separate FA into three main groups, high, medium and low net-to-gross (T_H, T_M, T_L respectively). Subgroups, or the FAs, were created to provide a detailed scheme, using the remaining parameters to classify them.

The classification scheme is based on numbers (percentage) and not only in visual interpretation. The main utility of this classification is to position each FA in a frontal splay. Through the integration of log correlation analysis and FA classification, a sub-environment map was designed, considering an ideal and symmetric deposit. This map allows the observation of how the main parameters are distributed in a frontal splay, highlighting the variation in the concentration of each parameter and thus enabling the comparison between them. It was demonstrated, for example, that the HEBs are distributed in the axial zone of the splay, also tends to increase the thickness distally, which agrees with some of the recent HEBs studies (Hodgson, 2009; Spychala et al., 2017).

The FAs distribution map is based on a symmetric shape, where the location of each FA is mirrored sideway. Any confinement or relief will change the geometry of the deposit and hence the FA distribution needs to be used with caution to not interpret both sides of the splay as the same FA distribution.

Overall, the maximum thickness of the thickest FA (T_H) is 8 m, and the average about 4 m. From a hierarchical level recognized, the splay element level (next level up the bed) relates directly to the facies association classification displaying the same scale of thickness (a maximum of 8 m). In summary, it is not necessary to recognize the hierarchy (scale) to determine the facies association group, but once a group is interpreted, the hierarchies involved are very likely recognized.

Commonly works involving facies association in frontal splay (or lobes) tend to focus on a specific parameter or some generic facies (Bourget et al., 2010; So et al., 2013; Morris et al., 2014; Masalimova et al., 2016; Spychala et al., 2017), disregarding the minimum differences, but essentials to differentiate and positioning them. Most of these works show a detail description but without a deep interpretation.

The scheme presented here is ideal to be used in poor laterally exposed locations, where a good analysis of a vertical succession is sufficient to identify each FAs and interpret the location into a frontal splay. For the reason, the Eastern Fan, in Adana Basin, is a great analog to analyse the facies association in frontal splays.

ACKNOWLEDGMENTS

REFERENCES

Bouma, A. (1962) 'Sedimentology of some flysch deposits: A graphical approach to facies interpretation', Amsterdam, Elsevier, 168 pp.

Bourget, J., Zaragosi, S., Mulder, T., Schneider, J.L., Garlan, T., Van Toer, A., Mas, V. and Ellouz-Zimmermann, N. (2010) 'Hyperpycnal-fed turbidite lobe architecture

and recent sedimentary processes: A case study from the Al Batha turbidite system, Oman margin', *Sedimentary Geology.* Elsevier B.V., 229(3), pp. 144–159.

Brinkmann, R. (1976) 'Geology of Turkey', pp. 158. *Elsevier Scientific Publishing Company*, Amsterdam, the Netherlands.

Campbell, C. (1967) 'Lamina, lamina set, bed and bedset', *Sedimentology*, 8, pp. 7–26.

Cipollari, P., Cosentino, D., Radeff, G., Schildgen, T.F., Faranda, C., Grossi, F., Gliozzi, E., Smedile, A., Gennari, R., Darbaş, G., Dudas, F.Ö., Gürbüz, K., Nazik, A. and Echtler, H. (2013) 'Easternmost Mediterranean evidence of the Zanclean flooding event and subsequent surface uplift: Adana Basin, southern Turkey', *Geological Society, London, Special Publications*, 372(1), pp. 473–494.

Cronin, B.T. (2018) 'Lithofabric classification and distribution of coarse-grained deep-water clastic depositional systems', In: Turner, C.C. and Cronin, B.T. (eds), Rift-related coarse-grained submarine fan reservoirs; the Brae Play, South Viking Graben, North Sea, *AAPG Memoir 115*, Tulsa, Oklahoma.

Cronin, B. T., and M. A. Jones (2018) 'Facies classification and facies association of deep-water depositional systems: Application to the prediction of slope and fan architecture in the Upper Jurassic Thelma field area, South Viking Graben, North Sea', in C. C. Turner and B. T. Cronin, eds., Rift-related coarse-grained submarine fan reservoirs; the Brae Play, South Viking Graben, North Sea: *AAPG Memoir 115*, p. 339–384.

Ghibaudo, G. (1992) 'Subaqueous sediment gravity flow deposits: practical criteria for their field description and classification', *Sedimentology*, 39(3), pp. 423–454.

Gürbüz, K. (1993) *Identification and evolution of Miocene submarine fans in the Adana Basin, Turkey.* Unpublished PhD Thesis. University of Keele, Keele, 327 pp.

Gürbüz, K. (1999) 'Regional implications of structural and eustatic controls in the evolution of submarine fans; an example from the Miocene Adana Basin, southern Turkey', *Geological Magazine*, 136(3), pp. 311–319.

Gürbüz, K. and Kelling, G. (1993) 'Provenance of Miocene submarine fans in the northern Adana Basin, southern Turkey: A test of discriminant function analysis',

Geological Journal, 28(3–4), pp. 277–293.

Haq, B.U., Hardenbol, J. and Vail, P. R. (1987) 'Chronology of Fluctuating Sea Levels Since the Triassic', *Science*, 235(4793), pp. 1156–1167.

Haq, B.U., Hardenbol, J. and Vail, P.R. (1988) 'Mesozoic and Cenozoic chronostratigraphy and cycles of sea-level change', in Wilgus, C.K., Hastins, B.S., Kendall, C.G., Posamentier, H.W., Ross, C.A. and Van Wagoner, J.C. (eds.), *Sea-Level Changes: An Integrated Approach.* C.K. Wilgus, B.S. Hastins, C.G.St.C. Kendall, H.W. Posamentier, C.A. Ross and J.C. Van Wagoner, SEPM Special Publication, p. 72-108.

Haughton, P.D.W., Barker, S.P., and McCaffrey, W.D. (2003) "Linked" debrites in sandrich turbidite systems—origin and significance", *Sedimentology*, v. 50, p. 459-482.

Haughton, P., Davis, C., McCaffrey, W. and Barker, S. (2009) 'Hybrid sediment gravity flow deposits - Classification, origin and significance', *Marine and Petroleum Geology*. Elsevier Ltd, 26(10), pp. 1900–1918.

Hodgson, D.M., 2009, Distribution and origin of hybrids beds in sand-rich submarine fans of the Tanqua depocentre, Karoo Basin, South Africa: *Marine and Petroleum Geology*, v. 26, p. 1940-1956.

Hofstra, M., Pontén, A.S. M., Peakall, J., Flint, S.S., Nair, K.N. and Hodgson, D.M. (2017) 'The impact of fine-scale reservoir geometries on streamline flow patterns in submarine lobe deposits using outcrop analogues from the Karoo Basin', *Petroleum Geoscience*, 23(2), pp. 159–176.

Ilgar, A., Nemec, W., Hakyemez, A. and Karakuş, E. (2013) 'Messinian forced regressions in the Adana Basin: A near-coincidence of tectonic and eustatic forcing', *Turkish Journal of Earth Sciences*, 22(5), pp. 864–889.

Ingram, R.L. (1954) 'Terminology for the thickness of stratification and parting units in sedimentary rocks', *Bulletin of the Geological Society of America*, 65(9), pp. 937–938.

Kelling, G., Gökçen, S.L., Floyd, P.A. and Gökçen, N. (1987) 'Neogene tectonics and plate convergence in the eastern Mediterranean : New data from southern Turkey',

Geology, v. 15, p. 425–429.

Ketin, I. (1966) 'Tectonic units of anatolia (asia minor)', *Bulletin of the Mineral Research and Exploration Institute of Turkey*, (66), pp. 24–37.

Lowe, D. (1982). 'Sediment gravity flows: II. Depositional models with special reference to the deposits of high-density turbidity currents', *Journal of Sedimentary Petrology*, v. 52, p. 279-297.

Martinsen, O.J., and Bakken, B. (1990) 'Extensional and compressional zones in slumps and slides in the Namurian of County Clare, Ireland', *Journal of the Geological Society*, London, v. 147, p. 153-164.

Masalimova, L.U., Lowe, D.R., Sharman, G.R., King, P.R. and Arnot, M.J. (2016) 'Outcrop characterization of a submarine channel-lobe complex: The Lower Mount Messenger Formation, Taranaki Basin, New Zealand', *Marine and Petroleum Geology*. Elsevier Ltd, 71, pp. 360–390.

Mitchum, R.M., Vail, P.R. and Thompson, S. (1977) 'Seismic Stratigraphy and Global Changes of Sea Level, Part 2: The Depositional Sequence as a Basic Unit for Stratigraphic Analysis: Section 2. Application of Seismic Reflection Configuration to Stratigraphic Interpretation', *Seismic Stratigraphy: Applications to Hydrocarbon Exploration AAPG Memoir 26*, pp. 53–62.

Morris, E.A., Hodgson, D.M., Flint, S.S., Brunt, R. L., Butterworth, P.J. and Verhaeghe, J. (2014) 'Sedimentology, Stratigraphic Architecture, and Depositional Context of Submarine Frontal-Lobe Complexes', *Journal of Sedimentary Research*, 84(9), pp. 763–780.

Mutti, E. (1992) 'Turbidite sandstones' *AGIP-Istituto di Geologia dell'Università di Parma, Milano, San Donato Milanese,* 275 p*.*

Mutti, E. and Ricci-Lucchi, F. (1972) 'Le Torbiditi dell'Appennino settentrionale: introduzione all'analisi di facies', *Memorie della Società Geologica Italiana*, 11, 161–199.

Nazik, A. (2004) 'Planktonic foraminiferal biostratigraphy of the Neogene sequence in the Adana Basin, Turkey, and its correlation with standard biozones', *Geological Magazine*, 141(3), pp. 379–387.

Nazik, A. and Gürbüz, K. (1992) 'Yöresi (Kb Adana) Alt-Orta Miyosen Yaşli Denizalt Yelpazelerinin Planktoni Foramini Biyostratigrafisi', *Türkiye Jeoloji Bülteni*, 32(February), pp. 67–80 (in Turkish).

Pyles, D.R. and Jennette, D.C. (2009) 'Geometry and architectural associations of co-genetic debrite-turbidite beds in basin-margin strata, Carboniferous Ross Sandstone (Ireland): Applications to reservoirs located on the margins of structurally confined submarine fans', *Marine and Petroleum Geology*. Elsevier Ltd, 26(10), pp. 1974–1996.

Radeff, G., Schildgen, T. F., Cosentino, D., Strecker, M. R., Cipollari, P., Darbaş, G. and Gürbüz, K. (2015) 'Sedimentary evidence for late Messinian uplift of the SE margin of the Central Anatolian Plateau: Adana Basin, southern Turkey', *Basin Research*, 29, pp. 488–514.

Robertson, A., Unlügenç, Ü.C., Inan, N. and Taşli, K. (2004) 'The Misis-Andırın Complex: A Mid-Tertiary melange related to late-stage subduction of the Southern Neotethys in S Turkey', *Journal of Asian Earth Sciences*, 22(5), pp. 413–453.

Satur, N. (1999) *Internal architecture, facies distribution and reservoir modelling of the Cingöz deepwater clastic system in southern Turkey*. PhD Thesis. University of Aberdeen, Aberdeen, UK, 520 p.

Schmidt, G. (1961) 'Stratigraphic nomenclature for the Adana region petroleum district VII'. *Petroleum Administration, Bulletin*, v. 6, p. 47-63.

Şengör, A.M.C. (1979) 'The North Anatolian transform fault: its age, offset and tectonic significance', *Journal of Geological Society of London*, v. 136, pp. 269–282.

So, Y.S., Rhee, C.W., Choi, P.Y., Kee, W.S., Seo, J.Y. and Lee, E.J. (2013) 'Distal turbidite fan/lobe succession of The Late Paleozoic Taean Formation, Western Korea', *Geosciences Journal*, 17(1), pp. 9–25.

Spychala, Y.T., Hodgson, D.M. and Lee, D.R. (2017) 'Autogenic controls on hybrid bed distribution in submarine lobe complexes', *Marine and Petroleum Geology*. Elsevier Ltd, 88, pp. 1078–1093.

Talling, P.J., Amy, L.A., Wynn, R.B., Peakall, J. and Robinson, M. (2004) 'Beds comprising debrite sandwiched within co-genetic turbidite: Origin and widespread occurrence in distal depositional environments', *Sedimentology*, 51(1), pp. 163–194.

Ünlügenç̧, U.C. (1993) *Controls on Cenozoic sedimentation, Adana Basin, Southern Turkey*. PhD. Thesis. University of Keele, Keele, UK.

Walker, R.G. (1978) 'Deep-water sandstone facies and ancient submarine fans: models for exploration for stratigraphic traps', *AAPG Bulletin*, v. 62, p. 932-966.

Williams, G.D., Ünlügenç, U.C., Kelling, G. and Demirkol, C. (1995) 'Tectonic controls on stratigraphic evolution of the Adana Basin, Turkey', *Journal of the Geological Society*, 152, pp. 873–882.

Yetiş, C., Kelling, G., Gökçen, S.L. and Baroz, F. (1995) 'A revised stratigraphic framework for Late Cenozoic sequences in the northeastern Mediterranean region', *Geol Rundsch*, 84, pp. 794–812.

7.2. Artigo 2

Submetido à *Sedimentology*

Hierarchy and architecture of turbidite lobes in the Cingöz Formation, southern Turkey

DANIEL BAYER DA SILVA - Department of Stratigraphy, Federal University of Rio Grande do Sul, Av. Bento Gonçalves, 9500, CEP 91501-970, Porto Alegre, Brazil.

BRYAN T. CRONIN - Tullow Ghana Ltd, Plot 70, George Walker Bush Highway, North Dworzulu, Accra, Ghana

HASAN ÇELIK - Department of Geological Engineering, Engineering Faculty, Fırat University, 23119, Elazığ, Turkey.

KARIN GOLDBERG ˉ Department of Geological Engineering, Engineering Faculty, Fırat University, 23119, Elazığ, Turkey.

Assunto	**Sedimentology – Manuscript ID SED-2018-OM-222**
Remetente	Elaine Richardson <onbehalfof@manuscriptcentral.com>
Para	<daniel.bayer@ufrgs.br>
Responder para	<E.A.Richardson@leeds.ac.uk>
Data	2018-08-23 14:55

CHASQUE WEBMAIL

Universidade Federal do Rio Grande do Sul

23-Aug-2018

Dear Mr. Bayer da Silva:

Your manuscript entitled "Hierarchy and architecture of turbidite lobes in the Cingöz Formation, southern Turkey" has been successfully submitted online and is presently being given full consideration for publication in Sedimentology.

Your manuscript ID is SED-2018-OM-222.

Please quote the above manuscript ID in all future correspondence. If you have an existing user account for Sedimentology and there have been any changes to your contact details since you last used the website, please log in to Manuscript Central at https://mc.manuscriptcentral.com/sed and edit your user information as appropriate.

You can also view the status of your manuscript at any time by checking your Author Center after logging in to https://mc.manuscriptcentral.com/sed.

Thank you for submitting your manuscript to Sedimentology.

Yours sincerely
Elaine Richardson
Editorial Office Manager
Sedimentology

Hierarchy and architecture of turbidite lobes in the Cingöz Formation, southern Turkey

DANIEL BAYER DA SILVA[1], BRYAN T. CRONIN[2], HASAN ÇELIK[3], KARIN GOLDBERG[4]

[1] Department of Stratigraphy, Federal University of Rio Grande do Sul, Av. Bento Gonçalves, 9500, CEP 91501-970, Porto Alegre, Brazil (e-mail: daniel.bayer@ufrgs.br)

[2] Tullow Ghana Ltd, Plot 70, George Walker Bush Highway, North Fzorwulu, Accra, Ghana

[3] Department of Geological Engineering, Engineering Faculty, Fırat University, 23119, Elazığ, Turkey.

[4] Department of Geology, Kansas State University, 207 Thompson Hall, Manhattan, KS 66506, United States.

ABSTRACT

This study explores outcrops of a deep-water depositional system from the shelf to the basin floor, focusing on depositional architecture along depositional dip through a series of channel-fed depositional lobe complexes. The studied exposures, in southern Turkey, are on the north margin of the Adana Basin (Lower to Middle Miocene), one of several foreland basins in southern Anatolia, which marked the closure of Neotethys Ocean. The purpose of this work is to characterize the changes in the architecture of turbidite lobes, through the hierarchy, stacking patterns and dimension analysis. Four hierarchical levels within lobe architecture were recognized. The basic element, a bed (maximum thickness of 1.9 m) represents sediments deposited in a single event; the next hierarchical level, splay element (maximum thickness of 7.8 m) are stacked to form a lobe (thickness between 9.5 and 22 m); stacked lobes form a lobe complex (maximum thickness of 40 m). A total of thirteen lobes were identified. Estimated lobe dimensions, based on the thinning rate obtained from the correlation of sedimentary logs, indicate average thickness of

about 15 m (maximum 22 m), the length (L) varying from 5 to 12 km and width (W), 3 to 10 km. The L/W (1.1 to 1.8) indicates sub-radial to elongate lobes. Analysis of vertical bed trends showed that the overall trends are controlled by stacked splay elements. In proximal environments (high N:G), the bed thickness trend successions are symmetrical, becoming more asymmetrical as the N:G ratio decreases distally. Hence, the stacking pattern of lobes was interpreted as aggradational, with some compensational stacking. Stratigraphically lower lobes are more confined and smaller due to the occurrence of the precursive seafloor topography. Upper lobes were developed in a less confined system, like all lobes in that region. Overall, the lobes were built in a semi-confined setting.

INTRODUCTION

Depositional lobes are one of the most important reservoirs in deep-water and for that reason they became an important role of the petroleum geology, once it represents an excellent oil and gas reservoirs (Mutti *et al.*, 2009; Covault & Romans, 2009). Submarine lobes are less well known and undersampled from the modern sea on the depositional floor. The internal complexity of lobes, analysed in well-exposed outcrops has been the subject of important works in the area in order to better understand the heterogeneities of these deposits (Deptuck *et al.*, 2008; Prélat *et al.*, 2009; 2010).

The Adana Basin provides a good analogue for detailed studies of a deep-marine succession characterised by significant thickness of well-exposed depositional lobes. On the north margin of the basin, exposures of a rare and continuous longitudinal profile of a deep-water depositional system from the shelf edge to the basin floor (Gürbüz & Kelling 1993), relatively rare globally, represents a great opportunity to analyse the architectural elements of different environments. The main siliciclastic unit, the Cingöz Formation, covers an area of approx. 900 km^2, composed by two submarine fans (Western and Eastern Fans, WF and EF). While the WF is fed by a single slope channel complex, the EF has multiple feeder canyons and channels. This study focuses on the lobes from the EF, more specifically the eastern part of it, in recent exposures through sedimentary logs to characterize the depositional architecture of submarine lobes.

According to Gervais *et al.* (2006), lobes can prograde, retrograde and migrate laterally, as well as aggrade. In nature the sediments tend to preferentially fill topographic lows and to smooth the topographic relief, in a process called compensation (Mutti & Sonnino, 1981). This lateral migration of lobes shows a range of thickness trends, encompassing thickening and thinning upward trends in the same lobe unit (Marini *et al.*, 2011). The identification of these trends is imperative to recognize the stacking pattern of lobes. This topographic compensation probably is the key mechanism for deposition in the lobe environment (Gervais *et al.*, 2006).

Some lobe characteristics still poorly understood, as the stacking patterns and its inception, the controls of it and the variation in different basin styles. The classical thickening-upwards sequences related to lobes are now in a long debate, as the last discoveries identified not only thinning-upwards, but symmetric sequences as well (Hiscott, 1981; Anderton, 1995; Prélat & Hodgson, 2013). The real influence of the seafloor topography in the building blocks of lobes is also a great focus in the last decades. Despite the hierarchy scheme receive less debate, the relationship between the levels still need a better approach as new discoveries challenges the standard models constantly.

This paper aims to establish a scheme on lobe hierarchy as an alternative to others and establish certain principles about stacking patterns. These analyses allowed a detailed architecture evolution of well-exposed turbidites in Cingöz Formation, providing new interpretations for the area and for future works on the same themes.

GEOLOGICAL SETTING

The Adana Basin, southern Turkey, is the onshore part of Adana-Cilicia Basin (Brinkmann, 1976; Kelling *et al.*, 1987), the Cilicia Basin being its offshore counterpart (Fig. 1). The Adana-Cilicia Basin is bound by: the Central Anatolian plateau to the N and NW, and to the S and SE by the Kyrenia and Misis Mountains (Kyrenia – Misis lineament) (Fig. 1).

The origin of Adana-Cilicia Basin has many models, including, for example, a pull-apart basin related to the transform zone of the East Anatolian Fault (Şengör *et al.*, 1985), a back-arc basin (Kelling *et al.*, 1987), a subsiding foreland basin, induced by the orogenic load of the Taurides (Ünlügenç,1993; Williams *et al.*, 1995), an extensional basin (Robertson, 1998, 2000); and a foredeep basin, created by

compressional tectonics (Aksu *et al.*, 2005; Burton-Ferguson *et al.*, 2005), between others Cipollari *et al.* (2013).
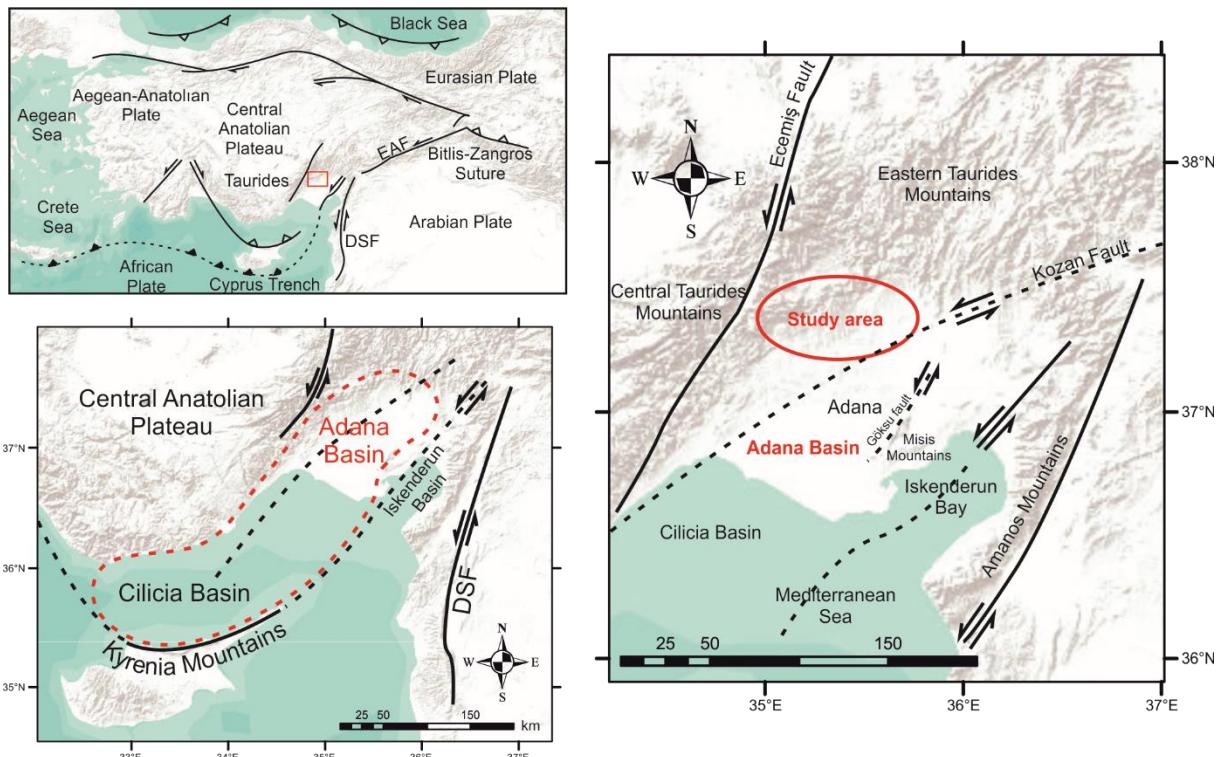
Fig. 1. Tectonic map highlighting the Adana Basin and surroundings. In red dashed lines, the Adana-Cilicia Basin Complex. The study area (red circle) is located to the north of Adana city, and limited at the north by the Central Tauride Mountains and at the south by the Kozan Fault. Adapted from Radeff et al. (2015).

The Adana Basin is one of the largest Miocene foreland basins in southern Turkey (Ilgar *et al.*, 2013). Its sedimentary succession comprises up to 6 km of Miocene and Quaternary siliciclastic and carbonate deposits.

According to Gürbüz (1993, 1999), the relative sea-level changes in the Adana Basin fit well the global sea-level rise and fall scheme of Mitchum *et al.* (1977) and Haq *et al.* (1987, 1988) for the upper Palaeogene – Neogene (Satur, 1999). This relative sea-level curve for the Adana Basin reveals a main transgression during the upper Burdigalian – Lower Langhian and a regression in the upper Serravallian (Fig. 2). The Cingöz Formation was deposited during a global sea-level high (Fig. 2), suggesting that local tectonics controlled the sedimentation of the Cingöz Formation.

Gürbüz (1993) suggested that downwarping of the pre-existing carbonate platform in the late Burdigalian provided the accommodation space for the deposition of the

Cingöz sediments. The influx of very coarse-grained sediments in the lower Cingöz succession supports this, since tectonic uplift of the source area may cause relative sea-level fall.
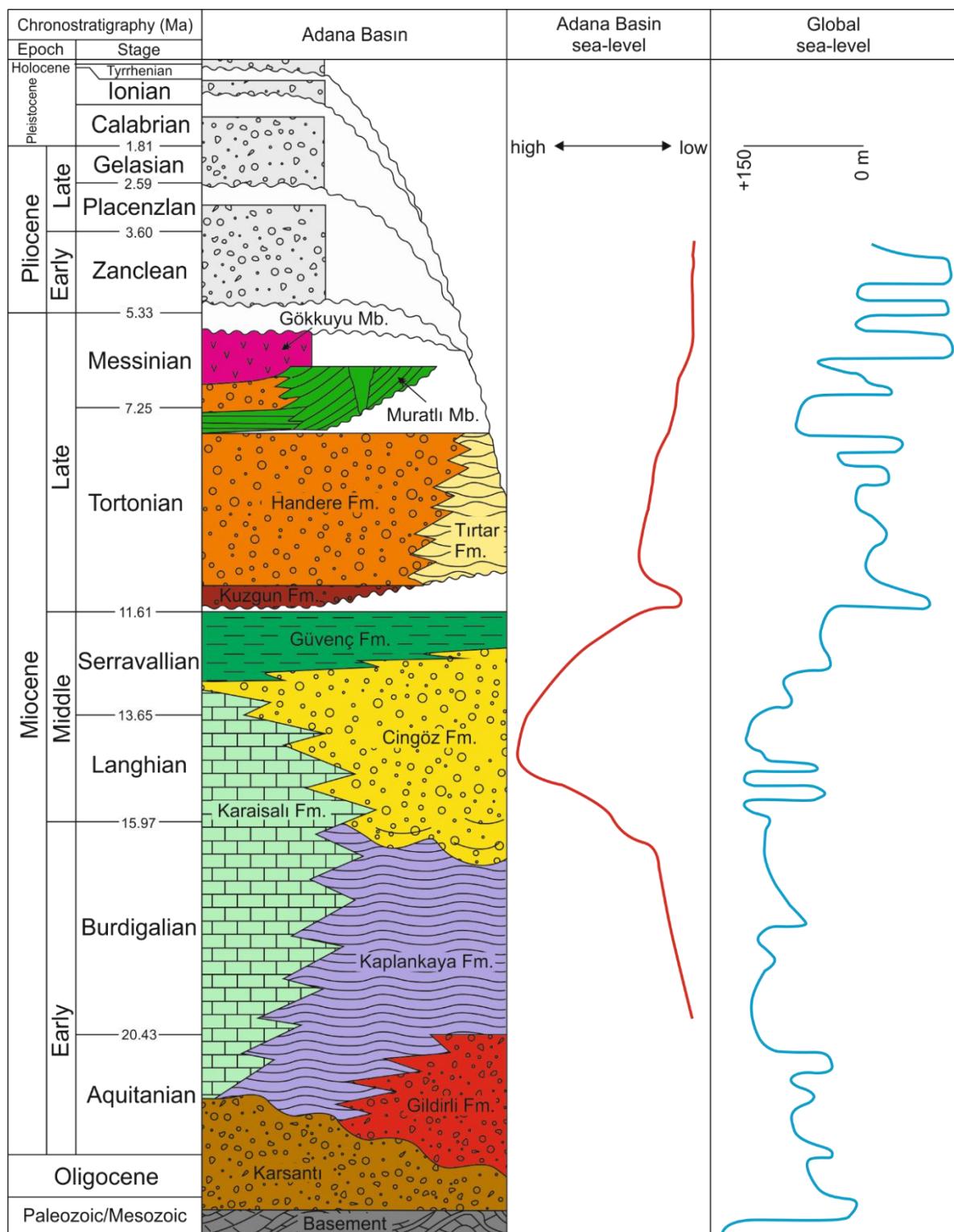
Fig. 2. Stratigraphic chart of the Adana Basin with the sequence stratigraphic system tracts, and Adana Basin and Global sea-level curves. From Haq et al. (1987); Nazik & Gürbüz (1992); Gürbüz, (1993); Yetiş et al. (1995); Ilgar et al. (2013).

The main unit studied in this work is the Cingöz Formation, composed of channelled, cobbly and pebbly sandstones to turbiditic tabular sandstones (Gürbüz & Kelling, 1993), also fine-grained clastic sediments and MTDs, deposited during the upper Burdigalian to Lower Serravallian (Nazik & Gürbüz, 1992). The Cingöz Formation deposits are 1000 – 3000 m thick and were deposited over a period of approximately five million years (Gürbüz, 1993) and it is composed of two coeval fans, the EF and WF (Gürbüz & Kelling, 1993; Gürbüz 1993). This paper will focus on the architecture of lobes of the Eastern Fan. The geological map shows the relationship between both fans and the surrounding formations (Fig. 3).
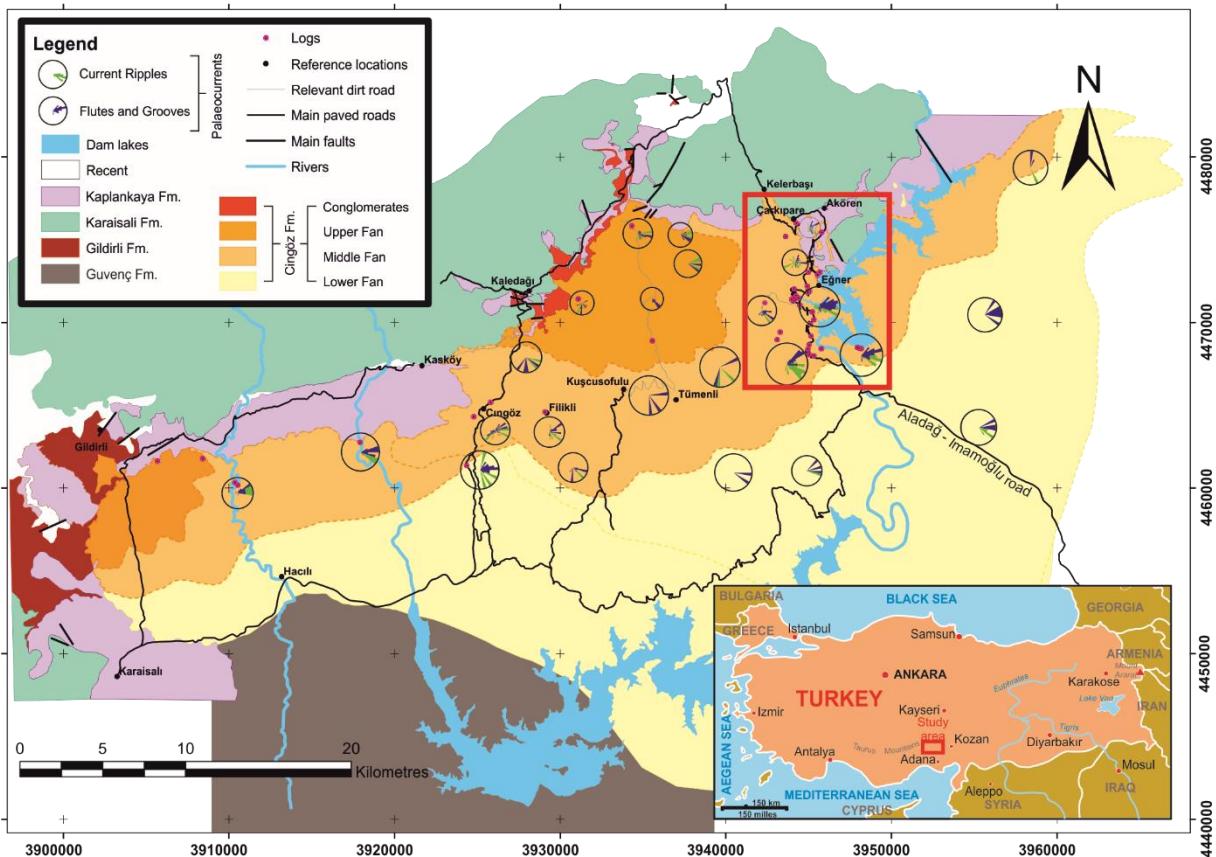
Fig. 3. Geological map based on the data acquired (re-interpreted from Gürbüz, 1993). The red square highlights the main study location along the main road.

Satur (1999) described at least four feeder channels to the EF (Fig. 4). The main channel was named Channel 1, and the other three were interpreted as secondary (Channels 2, 3 and 4).

Channels 2 and 3 were secondaries of Channel 1, and Channel 4 is younger (Satur *et al.*, 2004). Channels 2 and 3 display similar facies to those described in the Channel 1, but without the vertical organization in lower, middle and upper units

(Satur *et al.*, 2007), while the Channel 4 has more chaotic conglomeratic facies and more slumps than the others. Channel 2 is located on the eastern margin of Channel 1 and the Channel 3 on the opposite margin. It is 750 m wide at its mouth and apparently controlled by faults. Channel 4 (400 m wide) is interpreted as the youngest one, cutting Channels 3 and 1 from west to east, with palaeocurrent direction of 090°. Like Channel 3, it seems to be controlled by faults. In the distal parts of Channel 4 it is possible to observe sandstones deposited in lobe sequences (Gürbüz, 1993).
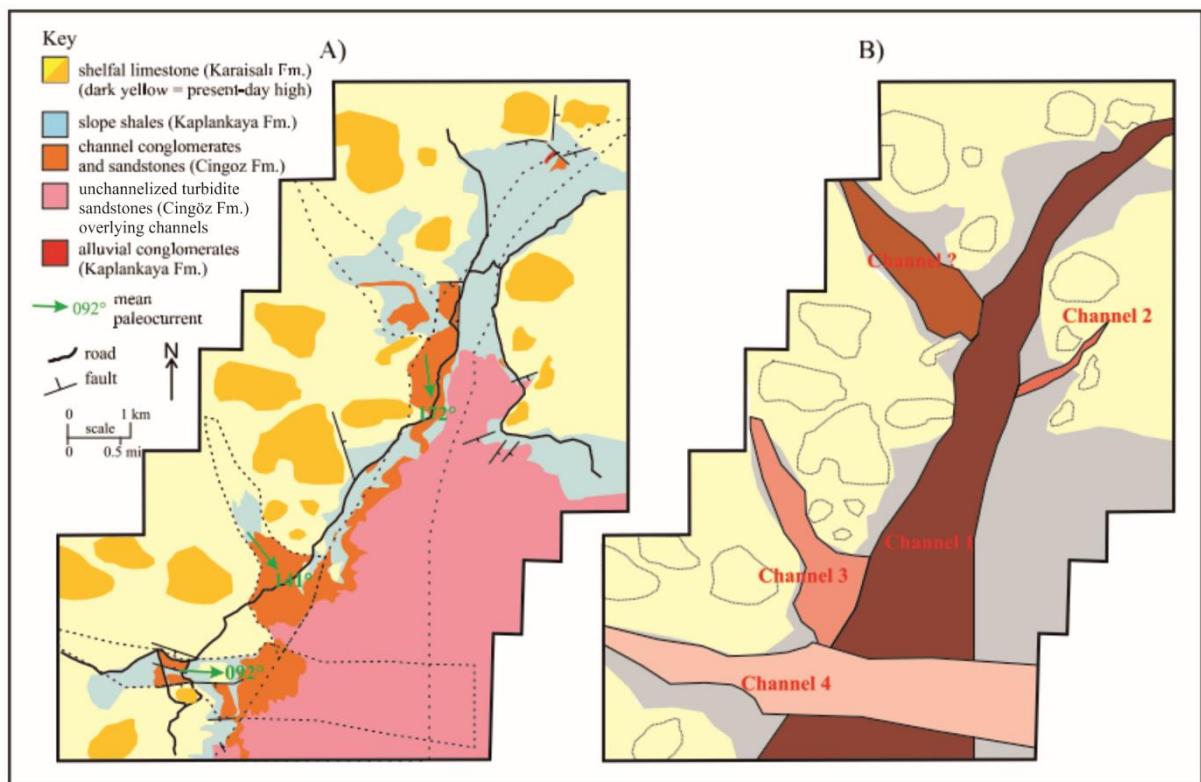
Fig. 4. Geological map (A) and channels interpretation (B) of the feeder system in the Eastern Fan. Palaeocurrent directions are mainly based on clast imbrication (Satur et al., 2007).

Channel 4 indicates a gradual increase in water depth due to the facies interpretations from the base as a fan delta setting, indicating a shallower-water (abundance of shell and coral fragments), and from the upwards units, becoming more recognizable as turbidites.

The EF is a low-efficiency (sand-rich) system with un-channelized lobes, influenced by tectonic activity, sediment supply and relative sea-level fluctuations (Gürbüz 1993; Gürbüz & Kelling 1993; Satur, 1999).

The EF was divided into inner, middle and outer fan by Gürbüz & Kelling (1993) (Fig. 3). The inner fan consists of the feeder system and the "secondary channels", represented by strongly amalgamated, thick sandstone beds and rare thin-bedded sandstones. Gürbüz (1993) identified levee deposits related to these channels. The middle fan is composed by unchannelized depositional lobes in the middle fan, while the outer fan shows a predominant presence of thin-bedded turbidites related to these lobes.

METHODOLOGY

The study was based on detailed sedimentary description (1:20) of 30 outcrops on lobes of the Eastern Fan (Fig. 5). The collected data included bed-by-bed attributes such as colour, grain size, sorting, sedimentary structures, composition, paleocurrent measurements and degree of bioturbation, described in sedimentary logs.
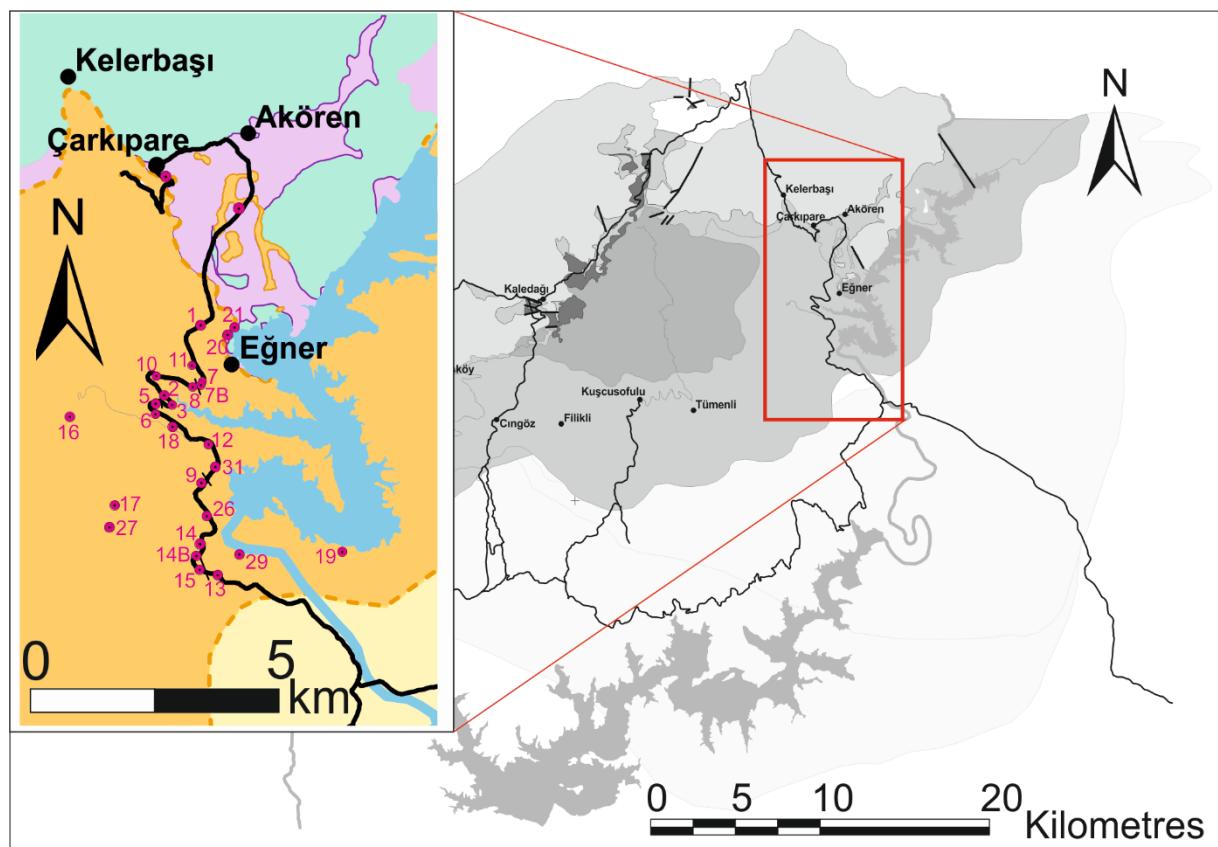
Fig. 5. Main log locations in the Eastern Fan, Cingöz Formation. Geological details in Figure 3.

Bed thickness analysis (Anderton, 1995; Murray *et al.*, 1996; Straub *et al.*, 2009) can be carried out by identifying each sandstone bed in relation to the bed number along

the vertical succession, counting from the base. Recognition of architectural patterns organised at different scales levels allowed to the establishment of an hierarchical scheme, which was defined through a two-step approach. First, the identification of thick intervals composed of thin-bedded turbidites (TBTs) was used to separate the largest scale cycles. Next, bed thicknesses in the vertical successions were used to separate hierarchical levels. Hierarchical analysis was mostly based on sedimentary log 19 analysis, the thickest and most complete vertical succession in the EF, complemented by bed thickness analysis in the other representative logs.

Bed thickness analysis followed the moving average method (Heller & Dickinson, 1985), in which thickness is considered in intervals of 5, 10, 15 and 20 beds. For example, the average for the 5-bed interval is calculated for beds #1 through the first 5, then for beds # 2 through the second to the six and so on, until the average thickness for all beds in the succession are calculated. The same procedure is done for the 10-bed interval, 15-bed interval and finally 20-beds interval.

Four hierarchical levels were considered in the present study: the first hierarchical level, representing a single event, is the bed. The level above is the splay element, which is composed of a bed set. The next level up is the lobe, considered the main hierarchical element, as it is in the seismic scale (Prather, *et al.*, 2000). Lobes stacked to form the last hierarchical level, the lobe complex.

In the bed thickness analysis, it was observed that the thinning- and thickening-upwards successions may form asymmetrical (Mutti, 1977; Hodgson *et al.*, 2006; Macdonald *et al.*, 2011) or symmetrical (Hiscott, 1981; Anderton, 1995; Prélat & Hodgson, 2013) cycles. The definition of symmetry adopted here refers to the number of beds in each cycle; for example, a thickening-upwards succession with five beds followed by a thinning-upwards succession also with five beds comprises a symmetrical cycle. Different numbers of beds in any part of the cycle are then defined as being asymmetrical.

The splay element scale is essential to determine the degree of symmetry of the entire complex. The type of trend (thickening-upwards vs. thinning-upwards) that is dominant in the splay element scale will define the type of succession in the upper level (the lobe scale), and consequently, the lobe complex level.

Bed-thickness trend analysis in the Eastern Fan also allowed the understanding of the trend distribution on lobe and splay element scales (Fig. 6). This analysis considered the N:G ratio (high, medium and low), and the facies association classification. A total of twenty-four cycles were recognised for this analysis in lobes, and seventy-eight in splay elements. The analysed cycles were separated into: 1) thickening-then-thinning-upwards, further subdivided into relatively thick and thin thickening succession; 2) thickening-upwards succession; 3) thinning-upwards succession; 4) symmetric thickening- and thinning-upwards succession; 5) No trend succession. Thinning-then-thickening-upwards successions were not recognised.
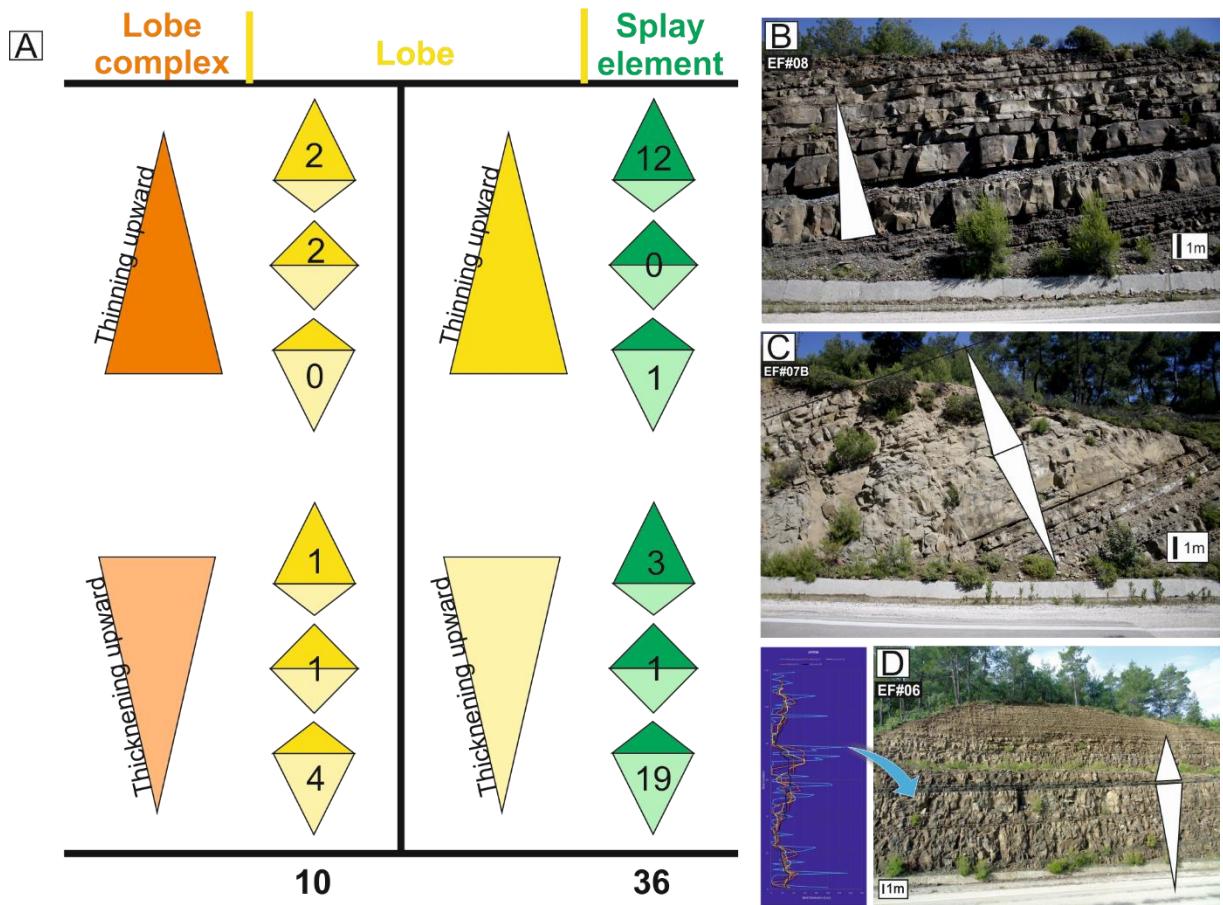
Fig. 6. (A) Schematic representation of how the main trends (large triangles) are controlled by the trends in the lower hierarchical elements (numbered diamonds representing thickening-upward/thinning-upward cycles). The numbers indicate how many cycles were asymmetrical-towards-thickening (bottom), symmetrical (centre) and asymmetrical-towards-thinning (top); Representative photos of (B) a thinning-upward succession (log 08); (C) a symmetric cycle (log 7B); and D) an asymmetric-towards-thickening cycle (log 06).

Correlation of twenty sedimentary logs was carried out to establish the hierarchical scheme. Since no regional marker was identified in the study area, when sections couldn't be walked out, correlation was carried out along bed sets with different vertical and horizontal depositional patterns (So *et al.*, 2013; Masalimova *et al.*, 2016).

Laterally persistent abandonment surfaces, characterised by thick shales, are rare. One true flooding surface was recognised, was 60cm thick, darker in colour and organic rich. Other, thinner, shales are seen but are interpreted as lower order flooding surfaces. Due to the depositional patterns (below and above the thick mudstone), this facies was used for log correlation (Fig. 7). Some logs (01, 08, 12, 18) have these shale beds varying between 20 and 60 cm. In these logs, the shale is preceded by 7 to 8 m of thin-bedded turbidites with two thick sandstones at the top of this TBT sequence (in log 01 and 08, the sandstone beds are amalgamated).
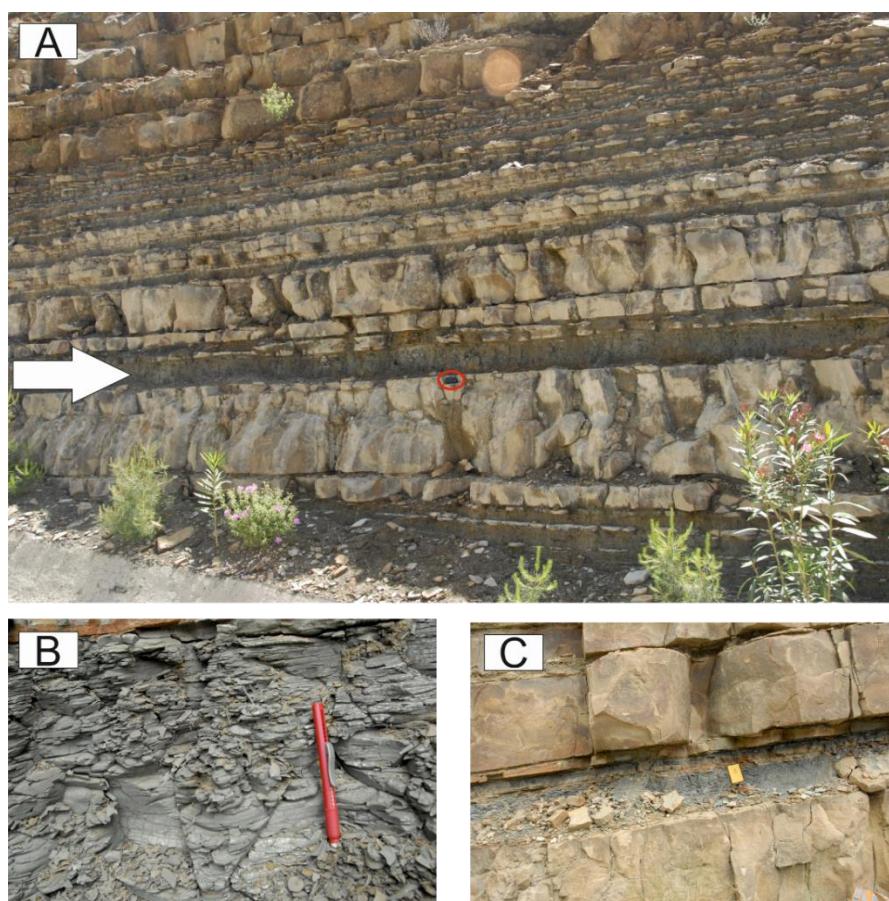
Fig. 7. Shale bed used for correlation in the northern study area: (A) outcrop log 01 with the shale bed within the cycle (white arrow). Compass for scale (10 cm); (B) Close-up of shale in the log 08. Scale = 13 cm; (C) View of the same bed in log 08. Scale = 19 cm.

This shale bed allowed correlation between the logs in the northern part of study area. In the south, the marker bed used for correlation was a relatively thick slump deposit (about 3 m thick), in comparison with others of less than 1 m in the region. This unusual bed occurs across the area, and it was described in 14B, 15 and 26 (Fig. 8). It is composed of predominantly medium to coarse-sand matrix with dispersed granules and pebbles, with several shale and sand clasts up to 5 m (shale) across, as well as many contorted clasts. The vertical successions below and above the slump deposit, in the three logs, are also similar. It is underlain by medium- and thick-bedded sandstones, and a thick shale. It is overlain by a thick (about 10 m thick) succession of thin-bedded sandstones (not observed in log 26 due to erosion of the exposure at its far end).
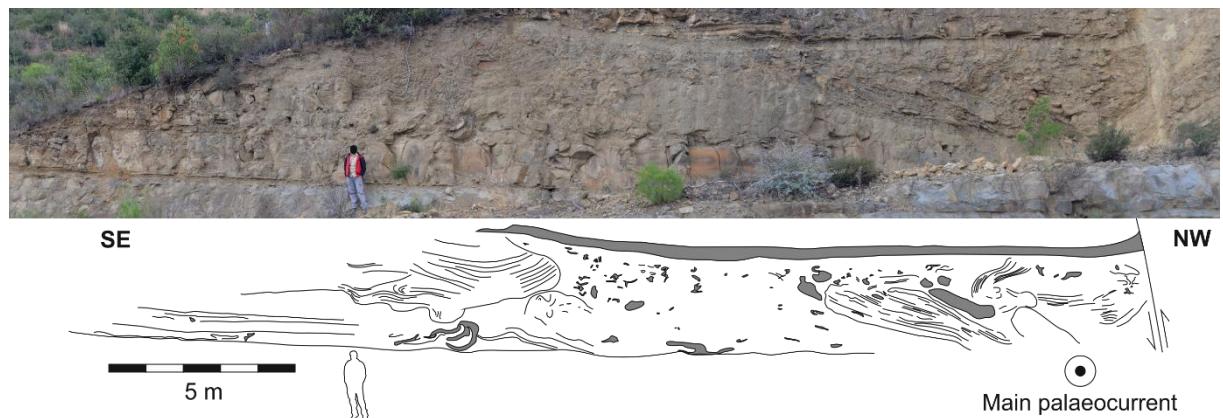
Fig. 8. Slump deposit in log 26, up to 3 m thick, containing mainly contorted clasts, mud clasts and coarse to very coarse sandstones.

Log correlation was also carried out using TBT intervals (Hodgson *et al.*, 2006; Prélat *et al.*, 2009; Kane *et al.*, 2016), because the lateral continuity is greater than the thick beds of sandstone. In addition, the thicker the TBT sequence, the greater the reliability of few changes over short distances (100's of metres). TBTs were also used with the marker beds to adjust the log comparison and to indicate a change of a specific hierarchy (*i.e.*, lobe complex).

RESULTS

Hierarchy

Four hierarchy levels were recognized. Table 1 shows the measurements from all sedimentary logs where it was possible to identify and separate the cycles. Total N is the sum of complete and incomplete cycles measured in all studied sections.

Table 1. Typical thicknesses for each hierarchical level measured in 30 sedimentary logs. Some cycles were incomplete, and therefore the thickness measured (in grey) is less than the real thickness. (N = number of cycles).

Hierarchy	Complete N	Incomplete N	Total N	Thickness (m)			
				Min	Max	Average (incomplete)	Average (complete)
Lobe complex	1	6	7	-	40	29.3	-
Lobe	13	11	24	9.5	22	14.8	14.5
Splay element	61	-	61	1.0	7.8	-	3.9
Bed	1141	-	30	0.01	1.9	-	0.36

Complete lobe complex levels were identified only in two sedimentary logs (15 and 19), and hence there is an uncertainty about the maximum thickness of a lobe this level.

Figure 9 shows the bed thickness analysis of the log 19 in relation to bed number. The two thick TBT intervals (8 and 13 metres thick, from base to top) were interpreted as separating lobe complexes. This is the thickest cycle (level) identified in the Eastern Fan (40 metres thick). Some TBT intervals have a gradational pattern (thickening and thinning-upward successions), mainly in the top and base of the interval, included in part of the hierarchy scheme (Fig. 9).

Fig. 9. Criteria used for hierarchical classification. Lobe complex are separated by thick TBT intervals and thinner hierarchical levels are defined based on bed thickness analysis, illustrated in sedimentary log 19. From left to right, the five graphs display the moving average of intervals with 5, 10, 15 and 20 beds, respectively. The coloured triangles represent thickening- and thinning-upward successions.
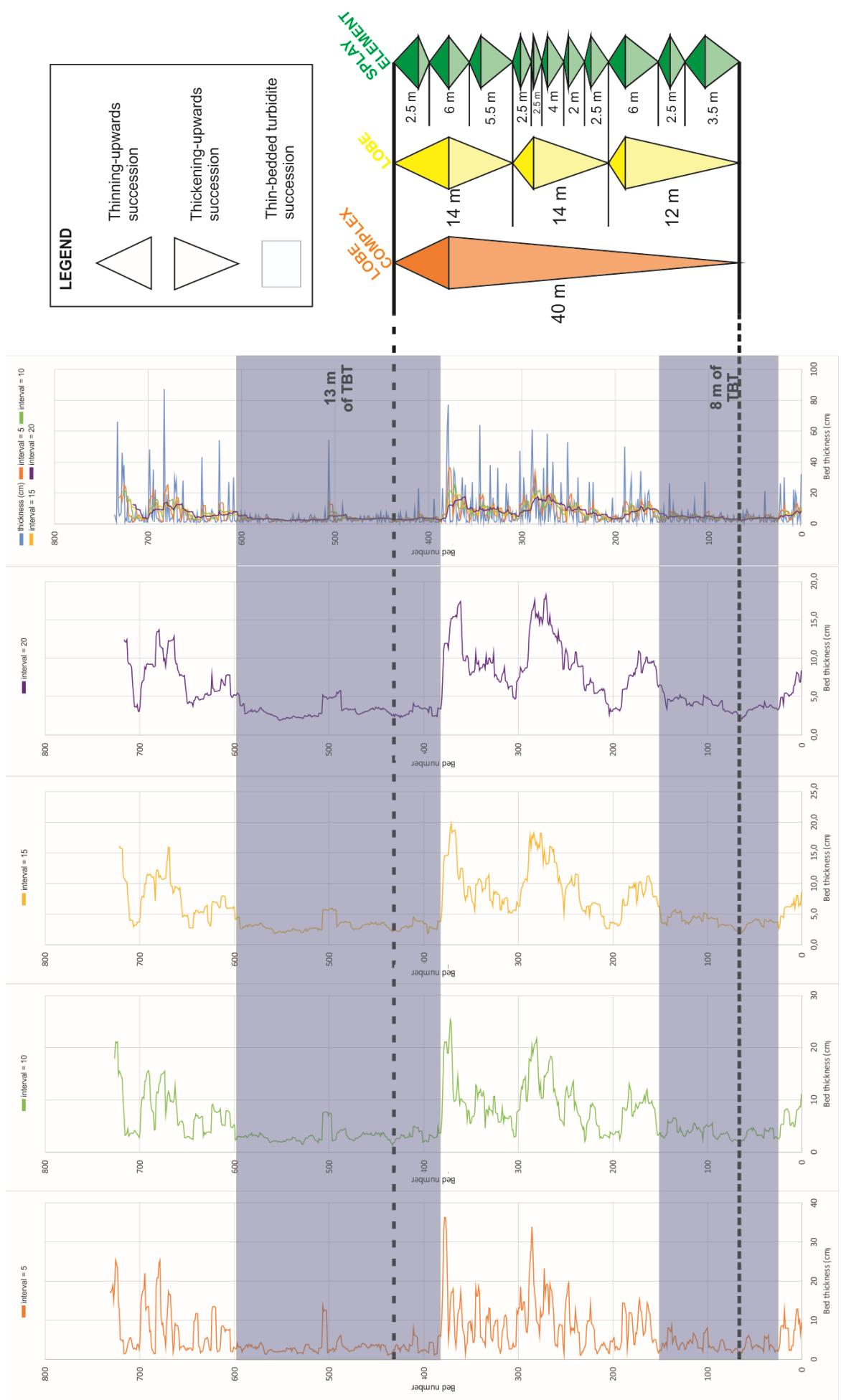
Lobe complex is bounded by TBTs (orange) and is composed of three smaller cycles (yellow) that represent the hierarchical level of a lobe, no more than 14 m thick each one. The lobe is easy to identify in the 20-bed moving average interval (purple line) in Figure 9. An upper hierarchical level is observed within these cycles, forming packages that vary between 2 and 6 m thick (splay elements). Splay element levels are mainly seen in the 10-bed moving average interval (green line), where eleven cycles are recognized in log 19 (Fig. 9).

The analysis of bed thickness in all logs showed important results regarding to the symmetry of the trends and the splay element scale should represent the best results, as the number of cycles identified is more than three times that of lobe scale. In high N:G ratios, both on lobe and splay element scales, the dominant bed trend is symmetrical cycles (Fig. 10), while in medium N:G the successions are dominantly thickening-then-thinning-upward, mainly with the thickening-upward portion of the cycle thicker than the thinning-upward one. The large discrepancy between cycle types on lobe and splay element scales are seen in low N:G stratigraphic intervals. Although in both scales the dominant bed trend is thickening-then-thinning-upward cycles, the thickening-upward succession of the cycle is thin in lobe scale, and thick in splay element scale (Fig. 10).
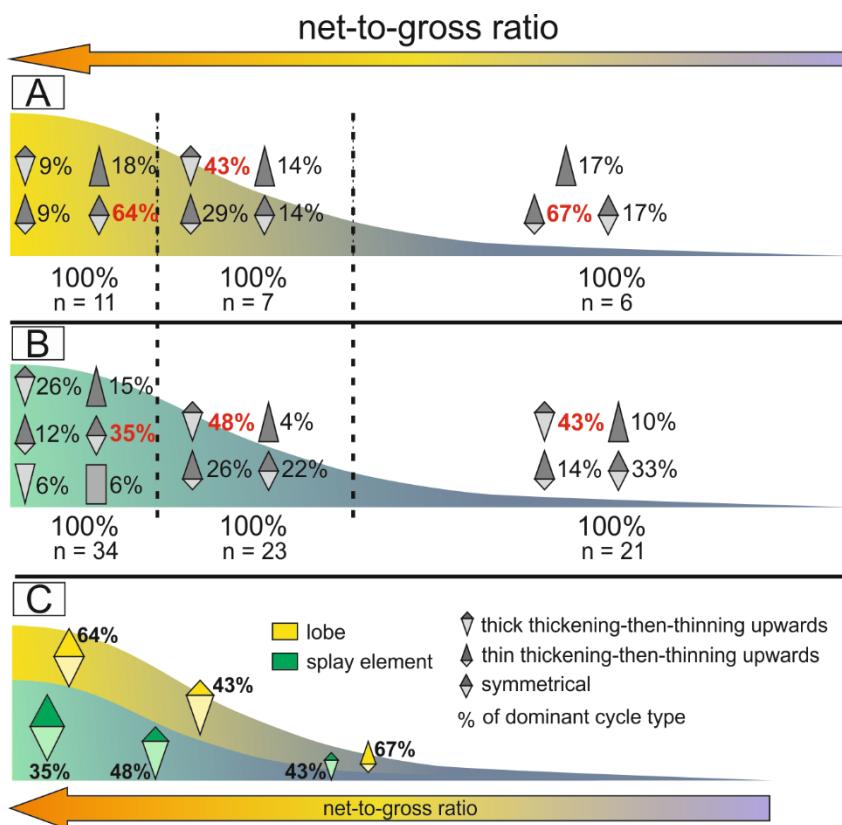
Fig. 10. Scheme representing the percentage of cycle trends in lobe and splay element hierarchies in high, medium and low N:G ratio. Net-to-gross increasing to the left (represented by the curve shape: thick = high N:G and thin = low N:G). (A) Distribution of percentages for cycle types in lobe (yellow) and (B) splay element (green) scales. Note that the total percentage is related to the number of examples in a specific location; (C) Summary of proximal to distal distribution of main cycle types in lobe and splay element, according to N:G ratios. For lobe, symmetric cycles occur under high N:G, thick thickening-then-thinning-upward cycles under medium N:G, and thin thickening-then-thinning-upward under low N:G. For splay element, symmetric cycles occur under high N:G, and thick thickening-then-thinning-upward under medium and low N:G.

Following recognition of different-level cycles, the next step was to understand the relationship between the hierarchical levels. Within lobe complex levels, the maximum number of the lobes is three, and five is the maximum number of splay elements within the lobes (Fig. 11). The comparison is only related to the thickness and number of levels based on the Figure 5.
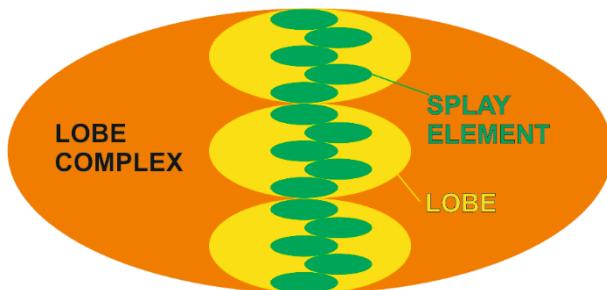
Fig. 11. Thickness relationship between lobe complex, lobe and splay element hierarchical levels (maximum number of each level).

Relationships between the different levels can be observed in Figure 12, considering maximum and average thicknesses (Fig. 12A and B, respectively). The same relationship can be shown in different ways: the number of times that one hierarchical level is within the level above, the typical thickness in the different-level cycles, or the percentage of each level in relation to lobe complex thicknesses (100%) (Fig. 12). One practical outcome of this graphic representation is the order of magnitude which one cycle is thinner than the one immediately above. For example, considering average thickness, bed levels are about 10 times thinner than splay element level (1 to 13%).
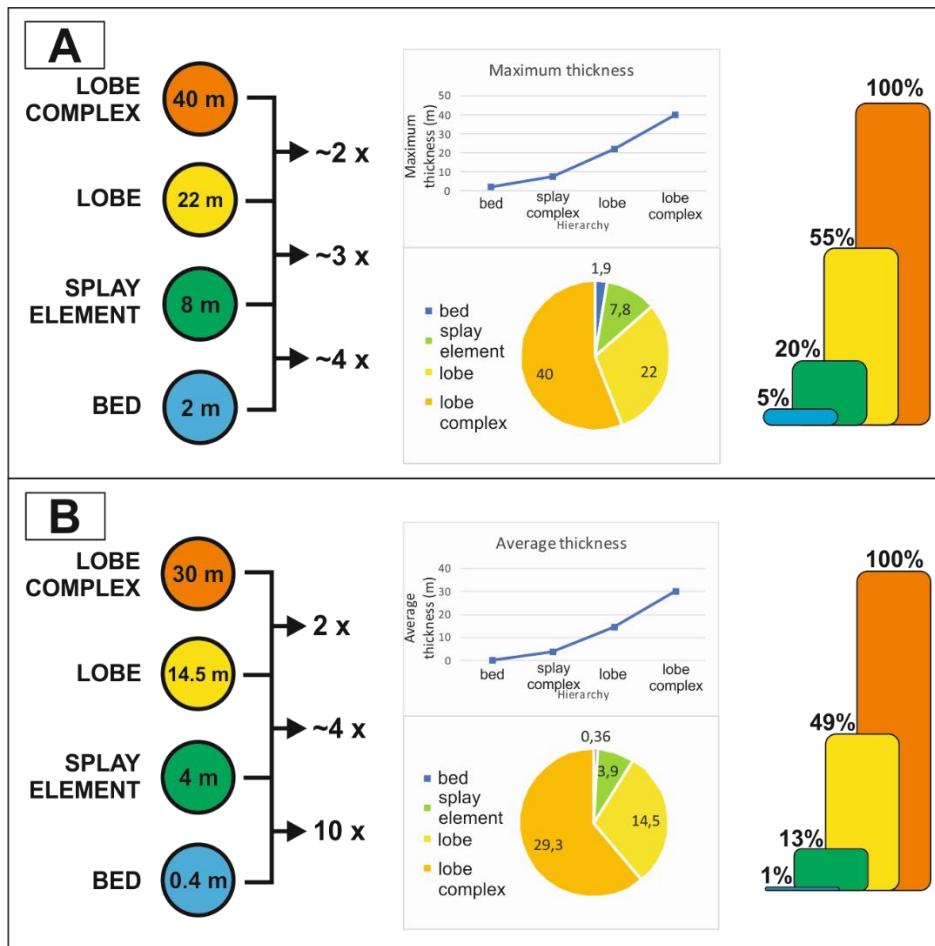
Fig. 12. Relationships between the hierarchical levels reflected in maximum (A) and average (B) thicknesses. The scheme on the left shows how many times typically one hierarchical level is within the order above. The pie charts and dispersion graphs in the middle show thicknesses in the different-level cycles. The bars on the right displays the percentage of each level in relation to the lobe complex thickness.

Log correlation

A cross section with the correlation panel (Fig. 13) displays thirteen sandstone-dominated packages (A to M). These packages are separated by TBT intervals with thicknesses that vary between 1 and 5 m. Sandstone packages, representing the lobes, reaching a maximum thickness of 19 m (in this correlation). Packages B to G (and probably H) are visible in the main outcrop in the correlation panel (02) (Fig. 14). The lobe complexes are TBT-bound units form 5 larger cycles, numbered 1 to 5. This hierarchical level is composed of two or three lobes, reaching a maximum thickness of about 50 m. Bed thicknesses and stacking patterns were used for the interpretation of cycles and the evolutionary history of the lobe hierarchical levels.
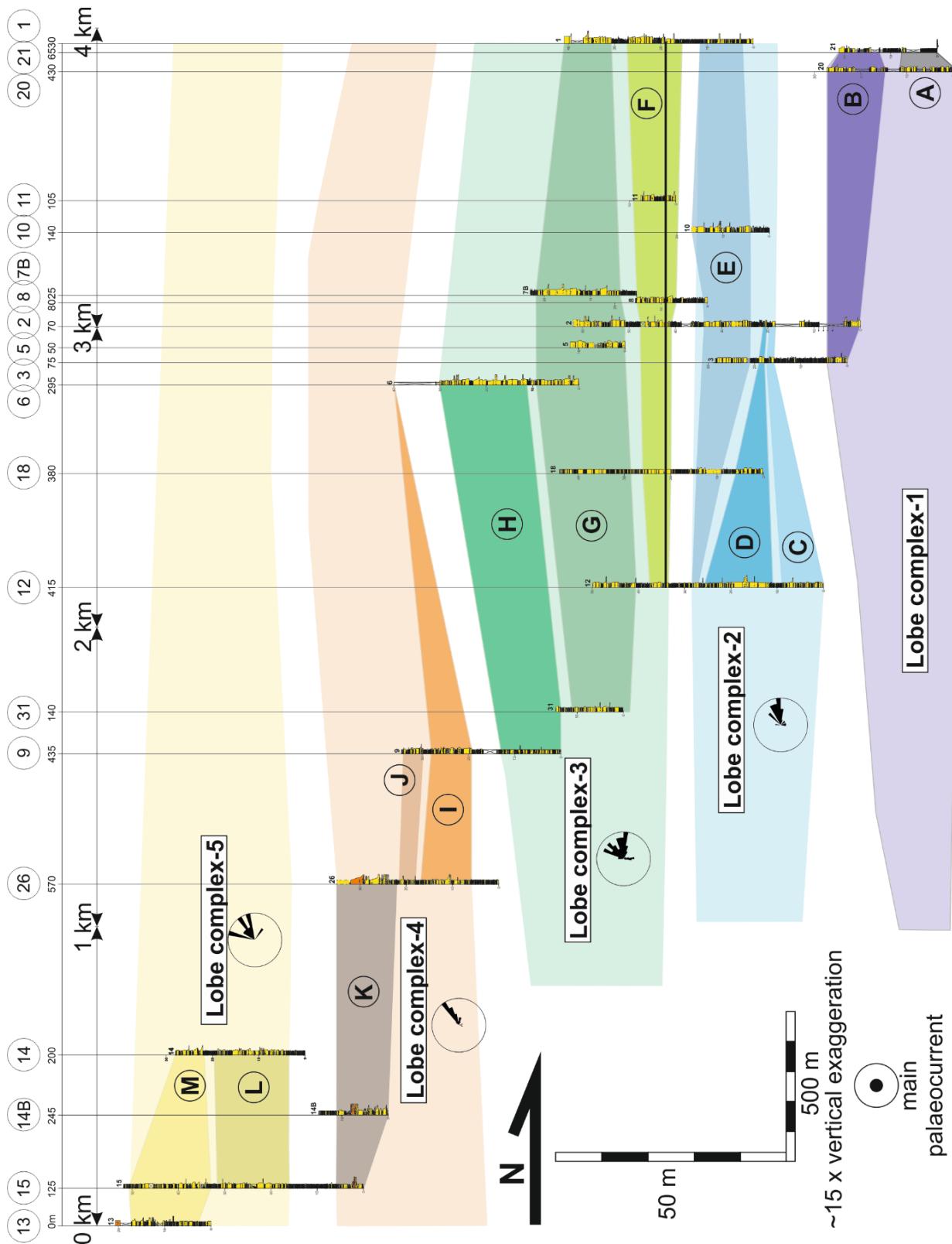
Fig.13. Cross section showing the correlation of twenty logs along the Aladağ-Imamoğlu road, with the interpreted lobes (A to N) and lobe complexes (Units 1 to 5) hierarchies. Palaeocurrent directions for each lobe complex shows palaeocurrent to NE. Numbers in circles indicate the log number; small numbers below them refer to the distance between log.

Correlation of the Aladağ-Imamoğlu road profiles considered twenty logs along a N-S transect of about 4 km (Fig. 5). The thick shale bed was used as a marker to correlate the logs in the northern half of the transect (01, 20, 21, 11, 10, 7B, 08, 02, 05, 03, 06, 18, 12), and the slump deposit as a marker for the southern half (31, 09, 26, 14, 15, 13). The distance between the logs varied from 70 to 570 m, and the total vertical thickness in the correlation was 182 m.

Axial and lateral thinning rate

Through integration of log correlation data, photomosaic and bed thickness analyses, it was possible to estimate lateral/axial continuity patterns and consequently contribute to the knowledge of the architecture of lobes in Eastern Fan. These data can be used to estimate the axial and lateral thinning rate (Fig. 15 and Table 2), determined based on the relationship between the maximum thickness of the element in two different locations (at least) and the distance between them. The thinning rate can be lateral, when the variation is derived from strike section, or axial, from proximal to distal regions (in dip section).

In a lobe, the thinning rate varies along dip and strike sections. Therefore, low rates mean small lateral variation of thickness, which is commonly associated with significant downdip extension of the lobes, but low thinning rates are described in proximal regions as well, with relatively short spatial extension. In general, thinning rate is relatively higher in strike than dip sections (Deptuck *et al.*, 2008). With increasing distance from the axis, thinning rates decrease considerably, resulting in elements of lobe that extend laterally for kilometres (Prélat & Hodgson, 2013; Cobain *et al.*, 2017; Spychala, *et al.*, 2017).
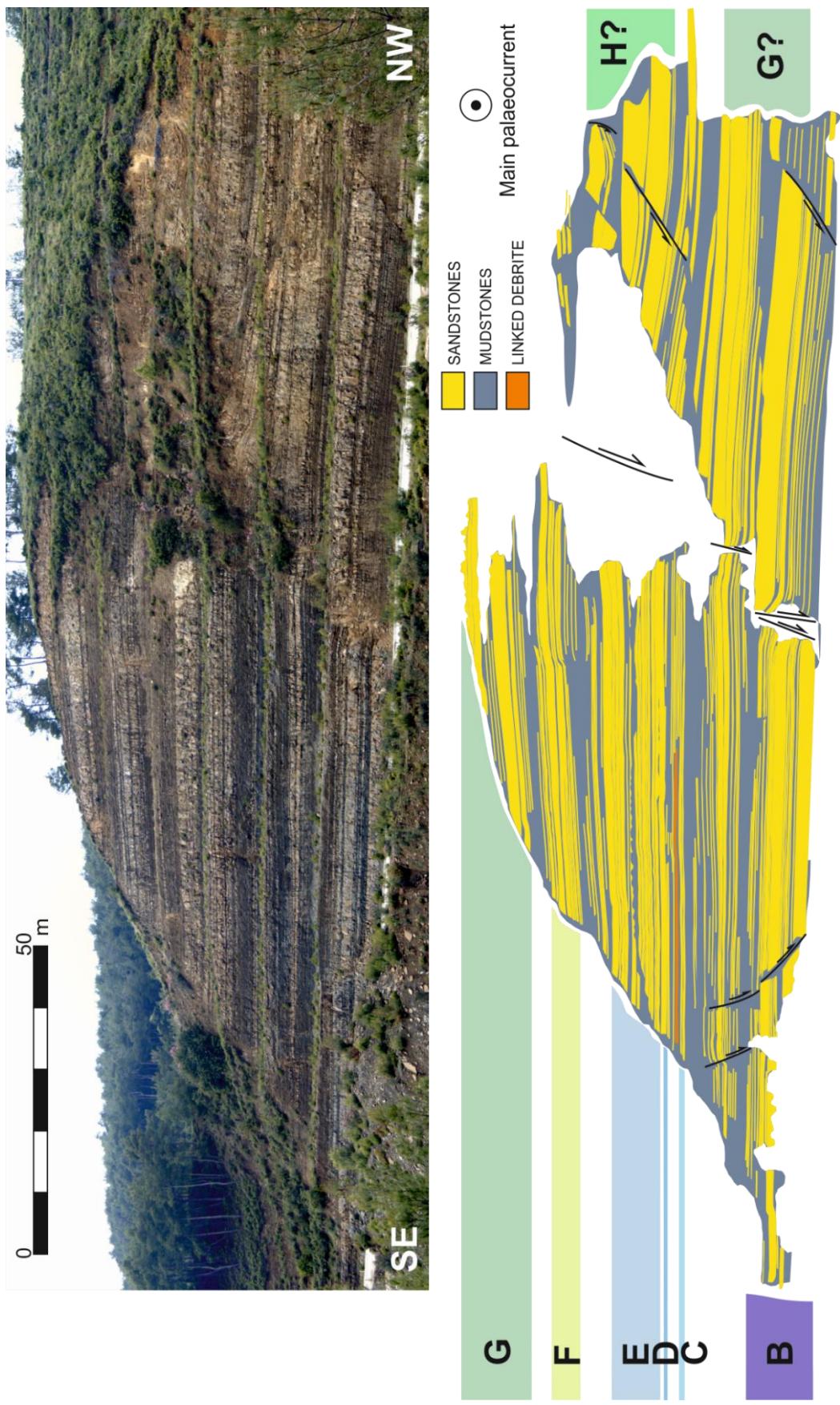
Fig. 14. Largest outcrop logged in the Aladağ-Imamoğlu road (log 02). Interpretation of lobe packages is indicated with the same colours as the correlation panel (Fig. 13).
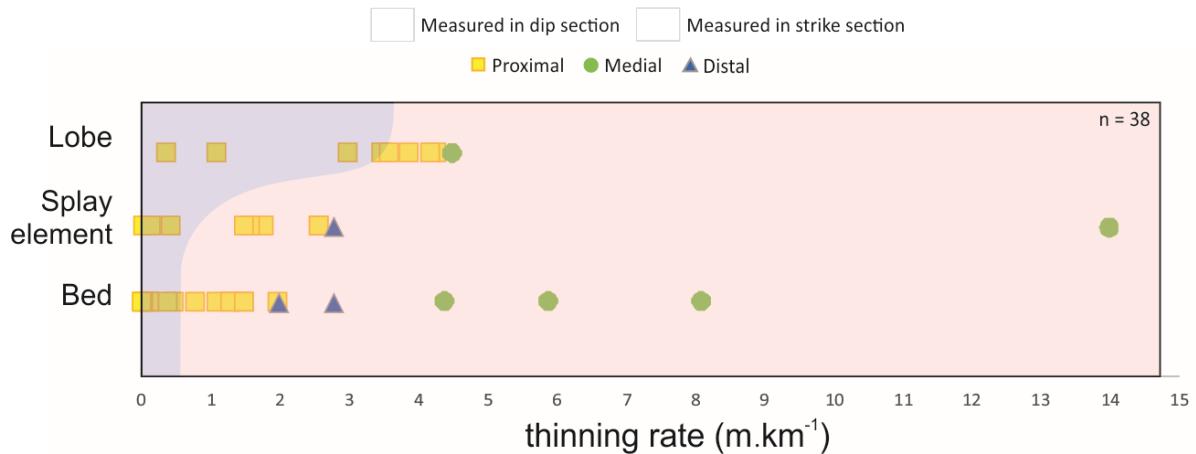
Fig. 15. Graphic representation of the lateral (along strike) and axial (along dip) thinning rate for the different hierarchy levels, based on the palaeo-environmental position in the lobe (proximal, medial and distal).

Table 2. Thinning rate (in m.km^{-1}) for three hierarchical levels in the Cingöz Fm. lobes along strike (lateral) and dip (proximal to distal). (N = number of measurements in sedimentary logs).

Hierarchy	Environment	N		Average		Minimum		Maximum	
		strike	dip	strike	dip	strike	dip	strike	dip
Bed	proximal	7	6	1.3	0.13	0.5	0.02	2	0.4
	medial	3	-	6.1	-	4.4	-	8.1	-
	distal	3	-	1.8	-	0.8	-	2.8	-
	Total	**13**	**6**	***2.5**	***0.13**				
Splay element	proximal	5	3	2.02	0.21	1.5	0.06		0.44
	medial	1	-	14	-	14	-	14	-
	distal	1	-	2.8	-	2.8	-	2.8	-
	Total	**7**	**3**	***3.8**	***0.21**				
Lobe	proximal	3	5	4.03	2.4	3.6	0.39	4.3	3.9
	medial	1	-	4.5	-	4.5	-	4.5	-
	distal	-	-	-	-	-	-	-	-
	Total	**4**	**5**	***4.15**	***2.4**				

*average based on all sampling for the specific element.

Figure 15 shows a comparison between thinning rates along strike and dip at different hierarchical levels, comparing proximal, medial and distal lobe regions, based on the facies association classification, T_H, T_M and T_L respectively (*i.e.*, net-to-gross ratio). Corresponding data is reported in Table 2. It is observed that, at all hierarchical levels, relatively lower thinning rates (overall less than 4.3 m.km^{-1}) are mainly concentrated in the proximal region, characterized by amalgamated sandstones. Thinning rates tend to accompany the hierarchical level; in other words, thinning rates are higher in upper hierarchical levels. On a bed scale, the maximum rate is 2 m.km^{-1} in strike section, while in lobes it can reach 4.3 m.km^{-1}.

Thinning rates for beds and splay elements in distal regions are also relatively low; only a slightly over the proximal region, with 2.8 m.km^{-1} in both levels, while in the proximal the maximum is about 2.0 m.km^{-1} (Fig. 15 blue triangles). The present study was unable to do this analysis on a lobe scale.

On all hierarchical levels, the medial region is where the higher thinning rates are concentrated, reaching up to 14 m.km^{-1} in strike section for splay elements (although this measurement is from only one section). Values for lobes and beds do not exceed 4.5 m and 8.1 m.km^{-1} respectively. The proximal region represents only high N:G, in T_H facies association, where the maximum thickness is located, also occupying a relatively short distance. Hence, the thinning rate (lateral or axial) is quite similar to distal locations. Despite the amalgamated beds pinch out relatively quickly, when this change occurs, this study interprets that a change in the facies association took place, becoming medial regions (T_M).

In summary, the average thinning rates along strike is 2.5 m.km^{-1} for beds, 3.8 m.km^{-1} for splay elements, and 4.15 m.km^{-1} for lobes. Thinning rates are lower in dip sections, about 0.13 m.km^{-1} (bed), 0.21 m.km^{-1} (splay element) and 2.4 m.km^{-1} (lobe), all these values based on the proximal region.

DISCUSSION

Scale relationships and interlobes

Despite similarities between different published schemes regarding lobe architecture hierarchical, thicknesses for the hierarchical components in the Cingöz Formation are different, possibly due to the accumulation in a different type of basin, in which the

sediment input is different. For example, lobe complex thicknesses in this work, exceeding 40 m, are compatible with lobe thicknesses in the literature, reaching 47 m or greater in confined systems (Milliman & Syvitski, 1992; Saller *et al.*, 2008).

Figure 16 shows a comparison between the Cingöz Formation and the Tanqua Karoo (South Africa), which has a similar amount of hierarchical levels (Prélat *et al.*, 2009, 2010). Despite the similarities, the graphs in Figure 16 suggest some differences, mainly related to the relationship between these hierarchical levels. In the Cingöz Fm., there is a linear relationship between the thickness from bed to lobe complex (considering both average and maximum thicknesses), meaning, a constant increase in thickness between adjacent orders. In the Tanqua Karoo, however, there is a significant difference in thickness between lobe complex and lobe, but not so much between adjacent lower levels. That could be important in the interpretation of the type and shape of lobes, for example, also for the confinement degree.

Different factors could be responsible for the distinct character of hierarchical elements in the Adana Basin and the Tanqua Karoo. One possibility is related to the type and size of the basin. The smaller size of the Adana Basin may not allow for the widespread development of a complex set of lobes, therefore concentrating them in a relatively small portion of the basin (*i.e.*, a confined or semi-confined setting), resulting in the linear (constant) relationship between the levels (Marini *et al.*, 2015). The Tanqua Karoo, on the other hand, may represent independent lobe scale (*i.e.*, unconfined setting), allowing each lobe to develop individually, branching out more, in an oak-leaf-shaped pattern, for example, or indistinct shape (Sprague *et al.*, 2005).

Another possibility is the source area influence. A clastic sedimentation relatively constant through time (seasonal) would result in the linear relation between the hierarchical levels, as seen in Cingöz Fm., whereas inconstant or variable, even multiple sources in the sedimentary input would favour a more random behaviour, with no evident trend. Perhaps even the stacking pattern could influence the thickness relations between hierarchical levels, with the "aggradational behaviour" of the Cingöz Fm. related to a linear pattern, and the asymptotic curve of the Tanqua Karoo representing more stacked lobes.
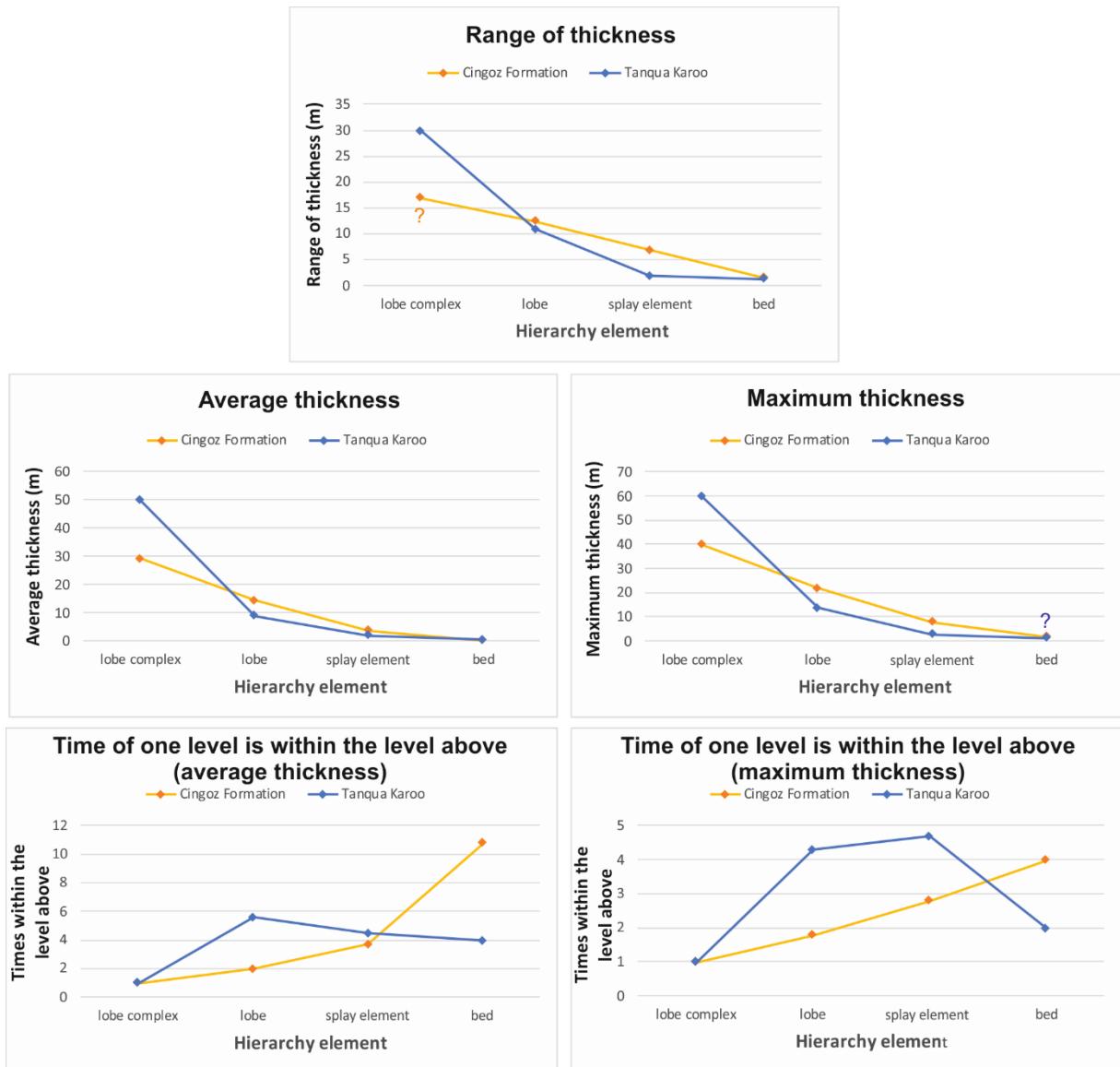
Fig. 16. Relationships between the hierarchical levels in the Cingöz Formation and the Tanqua Karoo (South Africa), represented by thickness range (difference between minimum and maximum thickness), average and maximum thickness, and the relationship between the hierarchical levels, showing how many times one level is within the level above (for average and maximum thickness), as seen in the Figure 12. The question mark means doubtful or insufficient information. Data on the Tanqua Karoo from Prélat et al. (2009, 2010).

The linear relation between hierarchical levels depicted in the graphs in Figure 15 can be expressed as a linear equation. The linear equation can be used to estimate the thickness of all hierarchical levels, given the thickness of one of the hierarchical elements, if we consider how many times one hierarchical level is within the level up (Fig. 12 and Fig. 16). A total of three equations can be derived for average thickness,

and three for the maximum thickness, where the elements are represented by lobe complex (LC), lobe (L), splay element (SE) and bed (B), adding (*max)* for maximum and (*avg)* for average.

The three basic equations for average thickness are:

SE(avg) = 10.8×B(avg)

L(avg) = 3.7×SE(avg)

LC(avg) = 2×L(avg)

For the maximum thickness:

SE(max) = 4×B(max)

L(max) = 2.8×SE(max)

LC(max) = 1.8×L(max)

The equations allow the prediction of the thickness of adjacent hierarchical levels in the Cingöz Fm. lobes, from the measured thickness of any given element. Prélat *et al.* (2009) and Spychala *et al.* (2017) described lobes as 5 metre-thick packages. Nevertheless, in this study, this thickness is considered as splay-element level, which varies between 0.65 and 7.8 m (average of 4 m) (Table 3). Actually, the thickness of 2 m reported for splay element by the same authors is included in the same hierarchical level here.

Table 3. Comparison between this study and other sand-rich systems from the literature, regarding thicknesses of hierarchical levels.

Hierarchical level	Present sdudy (Adana Basin)		Prélat *et al.,* 2010 (Tanqua Karoo)		Deptuck *et al.,* 2008 (Golo Basin)		Grundvåg *et al.,* 2014 (Spitsbergen Basin)	
	Avg.	Max.	Avg.	Max.	Avg.	Max.	Avg.	Max.
Lobe complex	29.3 m	40 m	50 m	-	-	-	-	60 m
Lobe	14.5 m	22 m	9 m	14 m	24 m	38 m	-	12 m
Splay element	3.9 m	7.8 m	2 m	-	-	-	-	5 m
Bed	0.36 m	1.9 m	0.5 m	-	-	-	0.1 - 1 m	4 m

Table 3 shows the variation in thickness for hierarchical levels in different basins. All of them are sand-rich systems, but only the Golo Fan and Spitsbergen Basins were interpreted as confined (frontal or lateral). Thickness data is not available for all levels, but a comparison is possible at lobe scale. At lobe and splay element (with partial data from Prélat *et al.*, 2009 and Grundvåg *et al.*, 2014), thicknesses in the Adana Basin (present study) are relatively higher, if both average and maximum thicknesses are considered.

Hierarchical significance of facies associations

The facies associations (Bayer da Silva *et al.*, in press) and hierarchical classification described can be integrated to provide a framework for interpretation of lobe deposits. Our goal here is to demonstrate that facies associations are tied to splay elements in the hierarchical classification, not to lower or higher levels. As such, the recognition of facies associations in a succession can be used to identify the hierarchy (*i.e.* splay element), allowing the detection of different-level cycles. Conversely, the identification of a splay element is helpful for the recognition of facies associations.

Comparing the average and maximum thicknesses in the facies associations and hierarchical classification, the similarity between facies association and the hierarchical level of splay element is clear. Average thicknesses in the facies associations do not exceed 4 m, and maximum values reach 8 m. Average and maximum thicknesses for splay elements (Table 3) are similar (average 3.9 m and maximum 7.8 m thick). That means they work in the same scale (<8 m) (Fig. 17).

Most splay elements are made of at least two facies associations, the first coinciding with thickening- and the second with the thinning-upward successions (when present), but only one facies association can make a single splay element, but this situation is mainly restricted to the proximal portions, or T_H (F.A.). Which facies association will be present (and how thick it will be) depends on the position within the splay element. The facies association classification in Cingöz Formation is based on the high (T_H), medium (T_M) and low (T_L) net-to-gross, beyond other parameters such as amalgamation degree, lithofacies, thick sandstones, heterolithics, modal grain size and grading beds (Bayer da Silva *et al.*, in press).
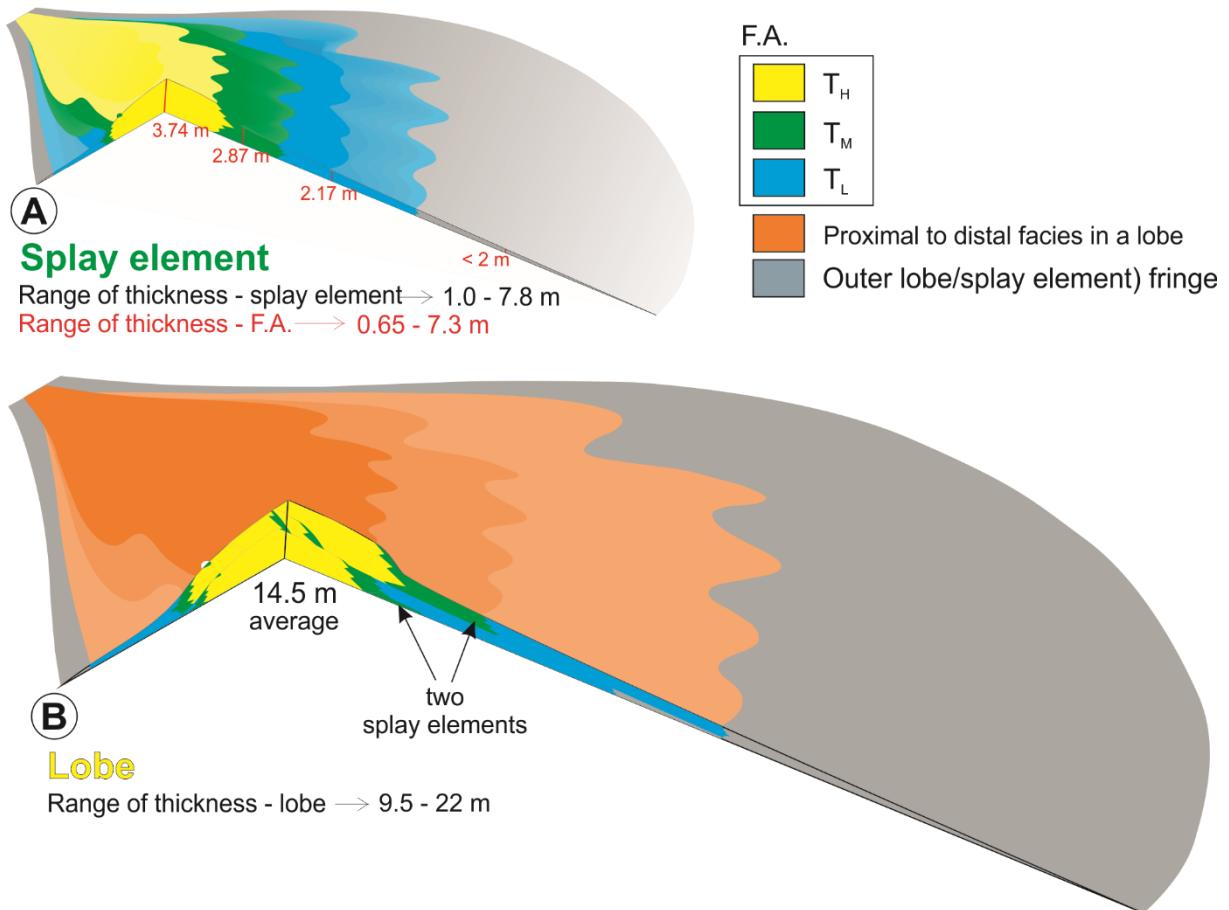
Fig. 17. Thickness variation of facies associations in splay element and lobe. (A) Average thicknesses for the three groups of facies associations (TH, TM and TL) within the splay element. (B) Lobe formed by groups of facies associations (i.e. splay elements), resulting in larger thicknesses.

In log 19, for example, facies associations with medium net-to-gross, mainly T_M-2, dominate the thickening-upwards succession, and low net-to-gross facies associations (T_L) the thinning-upwards succession of a 40 metre-thick lobe complex (Fig. 18).

The realization that facies associations are linked to splay elements is especially useful in the interpretation of the proximal and medial regions, since it is practically impossible to determine if there is more than one splay element in such thin distal successions (which incidentally also contain few beds to recognize cycles). Therefore, the succession similarities in distal portions become tough the division of facies association.

Fig. 18. Bed thickness analysis in log 19, with splay elements compared with facies associations (FA). Horizontal yellow lines represent the boundaries between lobes.

Relevance and field recognition of interlobes

Prélat *et al*. (2009) described the interlobes according to the hierarchical elements they separate: from the higher to the lower order, interlobe complex, interlobe and interlobe elements. According to Prélat *et al*. (2009), the interlobe element comprises of 2 cm of siltstone or less; interlobe is a thin-bedded siltstone, 0.2 to 2 m thick; and interlobe complex formed by at least 50 cm-thick claystone.

According to Grundvåg *et al*. (2014), there is very little difference in thickness between the interlobes separating lobe and lobe complex. In the Eocene Central Basin of Spitsbergen, the thickness of an interlobe unit separating lobes is about 7 m, while the interlobe unit separating interlobe complexes vary between 10 and 25 m. In both cases, the interlobe deposits comprise hemipelagic sediments from the basin.

Neither the criteria established by Prélat *et al*. (2009) nor by Grundvåg *et al*. (2014) are applicable to the Cingöz Formation, except maybe for the interlobe element (or intersplay here), characterized by a mudstone up to about 10 cm thick (Fig. 19). As seen in the literature, the interlobes (separating two lobes) in the Cingöz Formation are composed of thin-bedded turbidites (N:G <0.60 or T_L facies association), with thicknesses that can reach about 5 m, containing mudstone and siltstone of about 10 cm thick, but some thicker sandstones it is not rare.
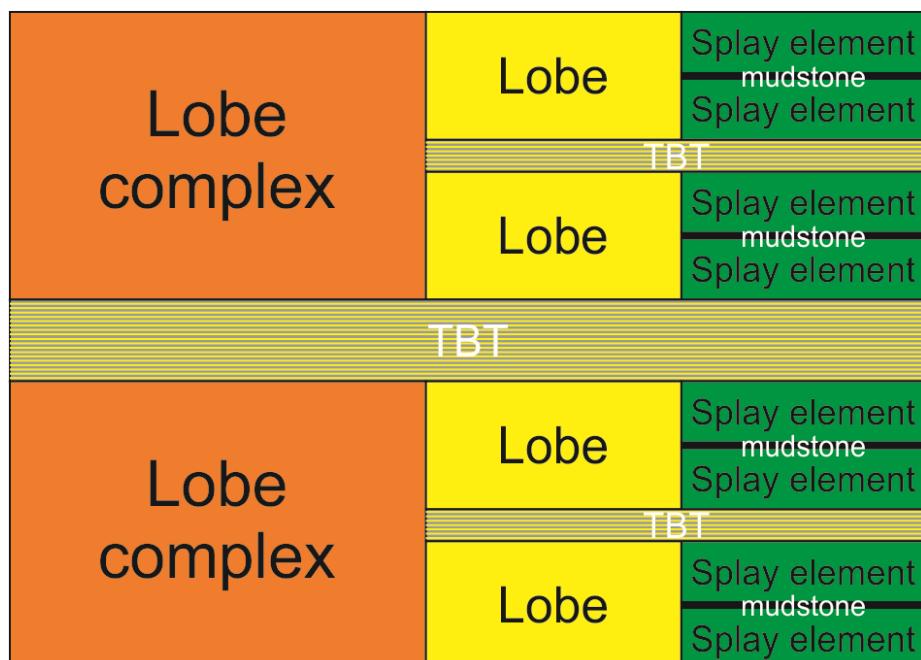
Fig. 19. Representation of the hierarchical position of thick TBTs and the mudstone (siltstone or shale) in the Cingöz Formation.

According to the Prélat *et al.* (2009) and Grundvåg *et al.* (2014), the interlobe complex contains hemipelagic deposits, suggesting that a lobe complex is deposited between periods of low sedimentation in that portion of the basin. Thick mudstone beds (up to 60 cm thick) occur in the basin, but they are interpreted as a deposit of turbidity currents, or turbidite mud from the flow, not as hemipelagic muds. Nowhere in the study area were metres of hemipelagic mudstone observed. Therefore, either it is not hemipelagic deposits that separate interlobe complexes in the Cingöz Formation, or thick hemipelagic deposits occur in this unit, but were not observed in the study area. Chances are that thick hemipelagic muds in the area would have been observed, had they existed.

Thick TBTs (> 5 m) in the Cingöz Formation were interpreted as interlobe complexes. They may even include hemipelagic mud interbedded with the TBTs. If these TBTs were interlobes (not interlobe complexes), one would expect them to separate only lobe levels (Fig. 19). However, all thick TBTs in the study area separate cycles that comprise of more than one scale, indicating at least two hierarchical lower levels.

The differences found in the Cingöz Formation in relation to other systems from the literature might be due to different types of system and tectonic setting of the basin, which will influence sedimentation rate, flow efficiency and other factors that control thickness and grain size. Nonetheless, the integration between the hierarchical scales and facies associations is essential to understanding of lobe architecture.

Stacking patterns

As seen previously, bed trends may indicate both the stacking pattern of a single hierarchical level and also lobe growth, the latter being one of the most discussed topics in the literature on lobes. Lobe progradation has been recognized by many authors (Mutti & Normark, 1991; Anderton, 1995; Lien *et al.*, 2003; Hodgson, *et al.*, 2006; Pyles, 2007), but lobe initiation mechanism remains poorly understood, since deep-marine deposits are not dependent on sea-level to aggrade, what decreases the importance of progradation (Hiscott, 1981; Chen & Hiscott, 1999; Macdonald *et al.*, 2011), which means a strong contribution of autocyclic controls (*e.g.*, avulsion) to develop the lobes.

Allocyclic and autocyclic controls are responsible for the main factors that contribute to the architectural elements of lobes (Marini *et al.*, 2011). Assuming the similar

allocyclic conditions in the WF and EF, autocyclic conditions will prevail to explain the stacking pattern in the EF.

Progradation, aggradation and compensational stacking represent ways that a lobe evolves (Fig. 20), these mechanisms are mainly controlled by the degree of confinement, or basin topography, and the flow (Deptuck *et al.*, 2008; Marini *et al.*, 2011; Masalimova *et al.*, 2016). Topography is responsible for guiding the flow, driving it to lower portions of the basin with more accommodation space.
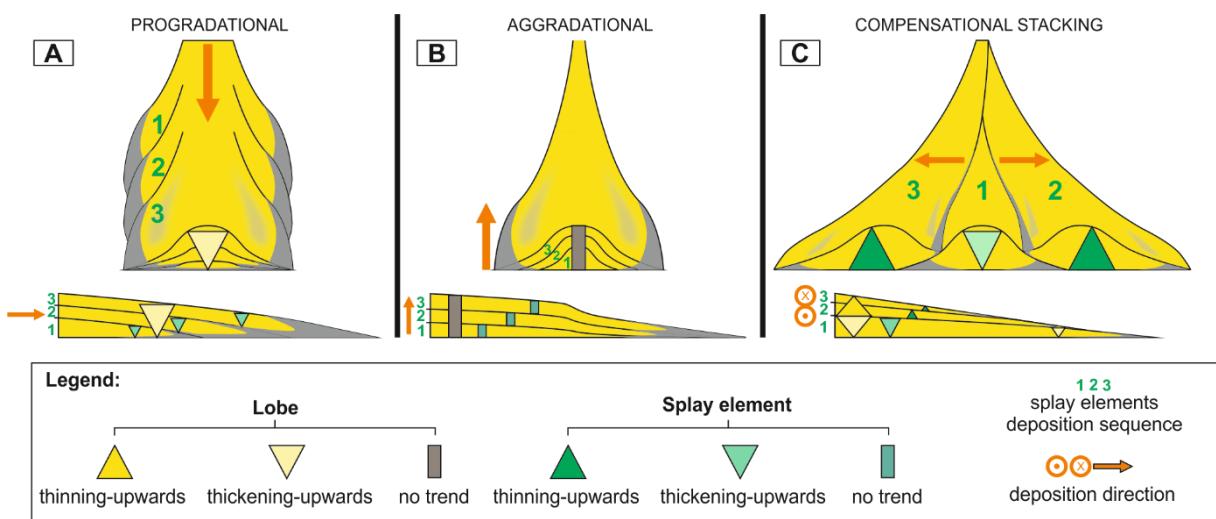
Fig. 20. Representation of how bed trends in lobes are developed for progradational (A), aggradational (B) and compensational stacking (C) successions. Progradation tends to show a thickening-upward trend due to the advance of splay elements downslope, while aggradation results in no trend along the axis (high N:G). Compensational stacking displays a variable trend, depending on the position analysed.

Depending on the degree of confinement, lobes show different stacking patterns (Macdonald *et al.*, 2011; Masalimova *et al.*, 2016). If the splay elements, for example, are stacked as a laterally or frontally continuous deposit, a thickening-upward succession is developed, resulting in progradation or compensational stacking (Macdonald *et al.*, 2011; Prélat & Hodgson, 2013; Zhang *et al.*, 2016). Aggradational sedimentation may display a range of depositional patterns, depending on the prevailing controls in the system (allocyclic and autocyclic). Aggradation may occur in disorganized shifts of the elements or lateral migration (compensational stacking), resulting in retrogradational or progradational patterns (Macdonald *et al.*, 2011). For that reason, it is hard to indicate the general pattern for aggradation, although, if only

the build-up of elements occurs, the tendency is to develop a no-trend pattern, creating laterally continuous beds (Fig. 20).

Figure 20C represents one of the models for compensational stacking, considering the lateral shift of splay elements. Although in the literature the common representation displays lateral stacking in one direction (Prélat & Hodgson, 2013; Zhang *et al.*, 2016), this study shows that, provided accommodation space is available and the topography helps, lobe (or splay element) shifts in multi-directions is more realistic.

Analysis of cycle trends in the EF (Fig. 10) showed decrease in symmetry of the cycles for lobe and splay element scales (dip section), or a tendency to "lose" the upper part of the cycles (*i.e.*, thinning-upwards succession). The proposed interpretation for this is shown in Figure 21.

The proposed interpretation of the stacking patterns in the Eastern Fan lobes shows a shift in splay elements (Fig. 21). The symmetric cycles observed in high N:G, or axial, parts of the splay element indicates equally representation of progradation and retrogradation. In the schematic example in Figure 21, each part of the cycle is represented by stacked beds forming a splay element. Cycle asymmetry will result from lateral shifts of the upper splay element, representing the retrogradational phase. These changes, from symmetric to asymmetric bed trends, suggest a compensational stacking of the elements.

A myriad of spatial changes is seen in lobe architecture, representing the diversity of lobe stacking. Here only the main interpretation of the compensational, or aggradational, stacking pattern in the Eastern Fan lobes is shown.

According to Hiscott (1981), a lateral migration in one direction would create a thickening-upward sequence (progradation). Nonetheless, Mutti & Sonnino (1981) advocated that only some areas display this pattern, showing a variability of cycles. Figure 21 suggest this complexity, depending on the size and amount of the elements.
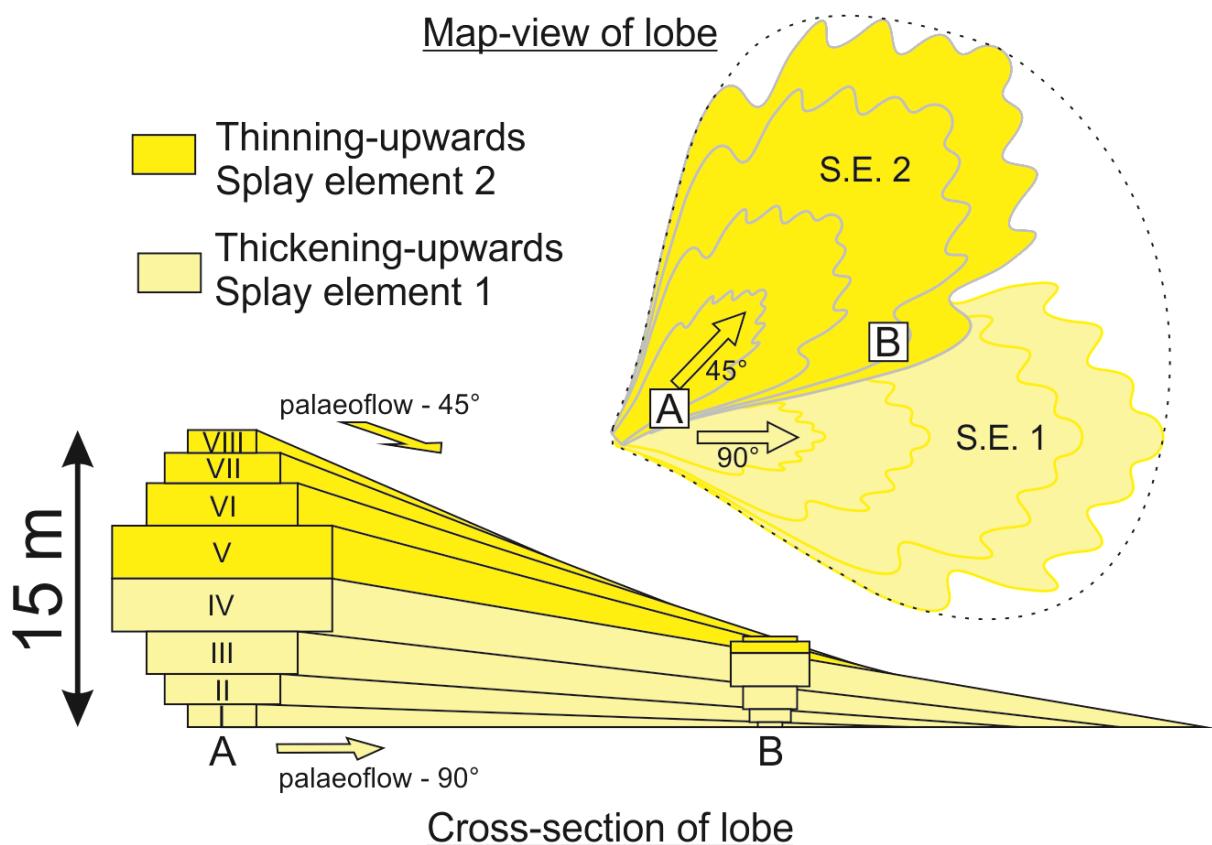
Fig. 21. Schematic drawing showing how the construction of splay elements result in the bed thickness trends identified in the Eastern Fan lobe cycles. Beds I to IV (stacked as a splay element) represent a thickening-upward succession in the proximal (A) and medial (B) portions of the lobe, while beds V to VIII represent the thinning-upward succession that forms a complete cycle. Differently from the symmetrical cycle in A, only beds V and VI occur in B, forming an asymmetric cycle. The map view (upper right) displays the compensational stacking of splay elements, reflected in the bed thickness trends of the lobe.

Many authors suggest a thickening-upwards succession as representative of confined settings (Macdonald *et al.*, 2011), independently of the position. The authors discussed the confinement degree in the Upper Carboniferous (Pennsylvanian) Ross Formation (Western Ireland), showing a relationship between the increase of erosion and the thickness of beds (or the increase of amalgamation due to the erosion) from bottom to top of lobes. These characteristics indicate a confinement, together with the thickening-upwards succession. Although, in EF results, the lack of both, a classical thickening-upward as the main succession and in the increase of erosion and the thickness of beds in lobe scale do not exclude a confined environment. The main palaeocurrent direction suggests a preferential pathway towards NE, also the

frontal confinement is evident in the EF onlap sections analysis. EF. Therefore, these characteristics are not enough to indicate a confinement degree in the study area, as a generally unconfined setting do not fit in the area.

Although, the discussion of confined and unconfined setting needs a geometry of the lobes approach, which will be discussed in the next section.

Thinning rate and lobe dimensions

The size and shape of lobes can be estimated from outcrop analysis using the thinning rate. The best exposure of the Cingöz Formation is located in eastern sector of the EF, where high, laterally continuous outcrops provide thickness and thinning rate data (Table 2) to reconstruct lobe dimensions.

Some key points were taken into consideration for the interpretation of data used in the reconstruction of architecture and evolution of lobes:

• Basin size and available space for lobe construction (fan surface area): considering location of the Channel 4 (Satur, 1999) as the best alternative for the feeder system, lobe dimensions cannot surpass 23 km in length and 15 km in width (Fig. 22). Despite the main EF feeder system is the Channel 1, Channel 4 is also possible, as it was interpreted as the last active channel, or younger (Satur, 1999);

• Palaeocurrent direction for the lobes, mainly measured in tool marks, indicate palaeocurrent to the NE or E. Therefore, the lobes are not oriented to the south;

• The main log correlation is along a strike section (N-S) in the eastern sector of the Eastern Fan. Therefore, estimate of lobe dimensions will take into account thickness and thinning rate on this area, and the lobe length (dimension along dip) will be extrapolated;

• Lobes with high N:G (>0.76) and/or high degree of amalgamation will be considered close to the axis, and hence size estimates will use this point as reference (Fig. 22);

• Size estimates for lobes with lower N:G and/or medium to low degree of amalgamation will be less accurate. Firstly, the facies association with the thickest deposit was measured to indicate the lobe position, and then the calculation of maximum thickness followed the same rules for high N:G deposits.
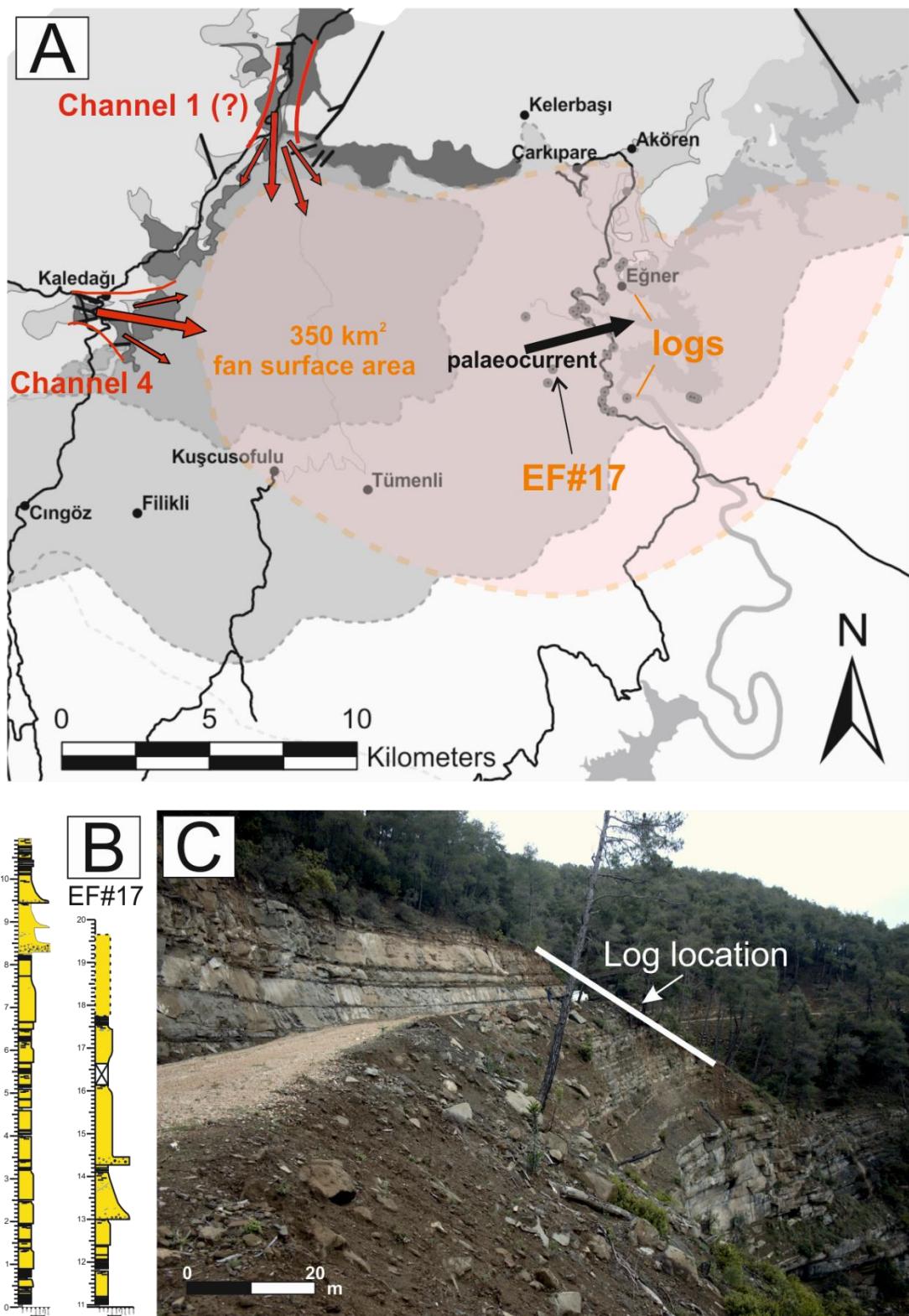
Fig. 22. Key parameters for estimation of lobe dimensions. (A) Lobe depositional area restricted to the eastern sector of the Eastern Fan. Channel 4 is indicated according to palaeocurrent directions. Black dots display the location of logs used for correlation and cross-section interpretation (N-S). Maximum lobe length is about 23 km and width about 15 km, forming a lobe area of approximately 350 km2 (in pink); (B-C) Log 17 (see location in A).

These guidelines were followed for each lobe analysis, in which the parameters considered for dimension estimates were the dominant palaeocurrent direction (longitudinal and transversal analyses), measured thickness, groups of facies association (splay elements), net-to-gross ratio, degree of amalgamation, fan surface area (<350 km^2) and log locations.

The majority of the sedimentary logs, where lobes were interpreted, represent a portion of the lobe with N:G greater than 76% and significant degree of amalgamation. Hence, measurements of lobe dimensions took into account the log section closest to the maximum thickness in all lobes, whereas no adjustment (estimate thickness) is necessary for the interpretation of the geometry of the lobes. Thinning rates in high N:G sites tend to be relatively small, and hence thickness does not change quickly in so short distances (<1 km) when it is compared with the medium N:G sites.

The lateral thinning rate (along strike) for the proximal region, in lobe scale, is about 4 m.km-1, while in the medial is 4.5 m.km^{-1}. Integrating this information with the maximum thickness of lobes scale in EF (about 22 m), lobe width is estimated to be between 3 and 10 km (Table 4).

Table 4. Estimated dimensions for lobes in the EF, considering the following parameters: lateral (Qs) and axial (Qd) thinning rates, length (L) and width (W) ratios, measured (M_{thk}) and estimated (E_{thk}) thicknesses. Estimated thickness based on M_{thk} and degree of amalgamation (reflected in N:G ratio).

Lobe complexes	Lobe unit	Relative N:G ratio	M_{thk} (m)	E_{thk} (m)	L (km)	Q_d (m.km^{-1})	W (km)	Q_s (m km^{-1})	L/W
LC-1	A	Low	11*	15	6	4	4	7	1.5
	B	Medium to high	>10*	15	6	4	4	7	1.5
LC-2	C	Low to medium	>9*	15	5	7	3	13*	1.7
	D	Medium	15*	22	5	7	3	13*	1.7
	E	Medium	>13*	15	5	5.7*	3	14*	1.7
LC-3	F	Medium	13*	15	8	2.4	7	4.4*	1.1
	G	Medium to high	18*	22	12	2.4	10	4.4	1.2
	H	Very high	19*	19	11	2.4	9	4.4	1.2
LC-4	I	Medium	10*	15	10	2	6	4*	1.7
	J	Low	>4*	15	10	2	6	4	1.7
	K	High	>13*	15	11	2	6	4	1.8
LC-5	L	High	16*	16	9	2.1*	7	4	1.3
	M	Medium	17*	22	12	2.4	10	4	1.2

*Direct measurement from sedimentary logs

The axial thinning rate (along dip) is less clear because the main section worked on is along strike, and hence only the thinning rate for the proximal region is given, about 2.4 m.km^{-1}. Based on that, the estimated length for the lobes ranges between 5 and 12 km. These results suggest a slightly radial-shaped lobe, as also indicated by the bed thickness analysis, with length/width (L/W) between 1.1 and 1.8 (Table 4).

Despite the assumption that lateral and axial thinning rate provide acceptable estimates for lobe dimensions, some data were calculated directly from measurements obtained in the correlation sections, while others were extrapolated or based on the similarities, and thus are interpretative (Table 4). The dimensions of lobes A and B were crudely estimated, since exposed sections in dip directions are rare. Estimates of lobe size took into account the stratigraphic position in relation to other lobes and the L/W ratio. The average rate was used, 2.4 m.km^{-1} for length and 4 m.km^{-1} for width.

The thickness of each lobe was measured directly from the logs in the correlation section, although in some of them only part of the lobe could be described. In this case, total thickness was estimated based on: 1) the N:G ratio, considering that the highest values are probably close to the maximum thickness; 2) the average thickness for the EF lobes (14.5 m); 3) the maximum thickness for the EF lobes (22 m). Hence lobe thicknesses vary between 9.5 and 22 m.

A comparison of lobe dimensions in the EF with the aspect ratio of confined and unconfined lobes indicates a change in lobe size and confinement settings during the evolution of the EF (Fig. 23). Prélat *et al.* (2010) and Fleming (2010) used width vs. maximum thickness to define the degree of confinement, distinguishing confined lobes, with aspect ratio of 100:1, from unconfined lobes (aspect ratio 1000:1).

Lobes A through E (belonging to the lobe complex 1 and 2) of the Eastern Fan plot close to the 100:1 line, suggesting a confined setting, according to the Prélat *et al.* (2010) interpretation. Lobes F through M (lobe complex 3, 4 and 5) display a more unconfined behaviour. Overall, according to Figure 23 and the results obtained, the lobes were developed in a semi-confined (basinal) setting.

The aspect ratio analysis showed consistent results of the EF lobes for the confinement degree, as the stacking pattern can indicate unconfined setting

(Macdonald *et al.*, 2011), but the palaeocurrent directions agree with the confined environment.

Marini *et al.* (2011) analysed the main relations between lobes and the degree of confinement. They highlighted that a shingled stacking pattern (continuous stacked), lobate shape and heterogeneous deposits is typical of a semi-confined setting. Moreover, they associated the semi-confined lobes with a compensational stacking. The same characteristics are seen in the EF lobes, suggesting strong topographic control (autocyclic).
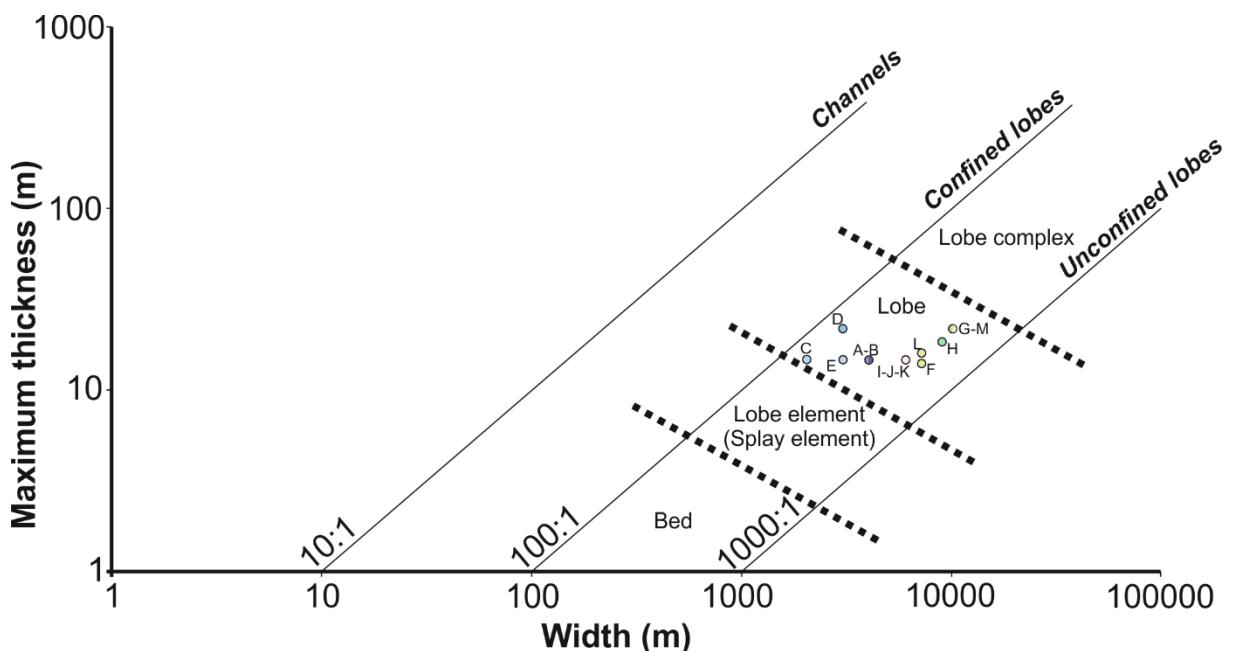
Fig. 23. Comparison between aspect ratios of confined and unconfined lobes, considering width versus maximum thickness for depositional elements of different systems. The A to M lobes are the EF studied area, which show distinct colours. Adapted from Prélat et al. (2010).

The analysis of lobe dimensions, integrated with spatial and stratigraphic distribution, allowed the interpretation of lobe evolution (Fig. 24). For this interpretation, horizontal distances between the sedimentary logs were maintained (Fig. 24A), and the maximum thickness of each lobe (Table 4) was considered the axis, with the width symmetrically distributed from it laterally (Fig. 24B). Figure 24C represents the reconstruction of lobe complexes that formed the Eastern Fan, based on the real vertical position of the axis (Figure 24B), complemented by the interpreted effect that topography left by the previous deposit.

Legend

- Reference locations
- Relevant dirt road
- Main paved roads
- Palaeocurrents
- Rivers
- Dam lakes
- Eastern Upper Fan
- Eastern Middle Fan
- Eastern Lower Fan
- Kaplankaya Fm.
- Karaisalı Fm.
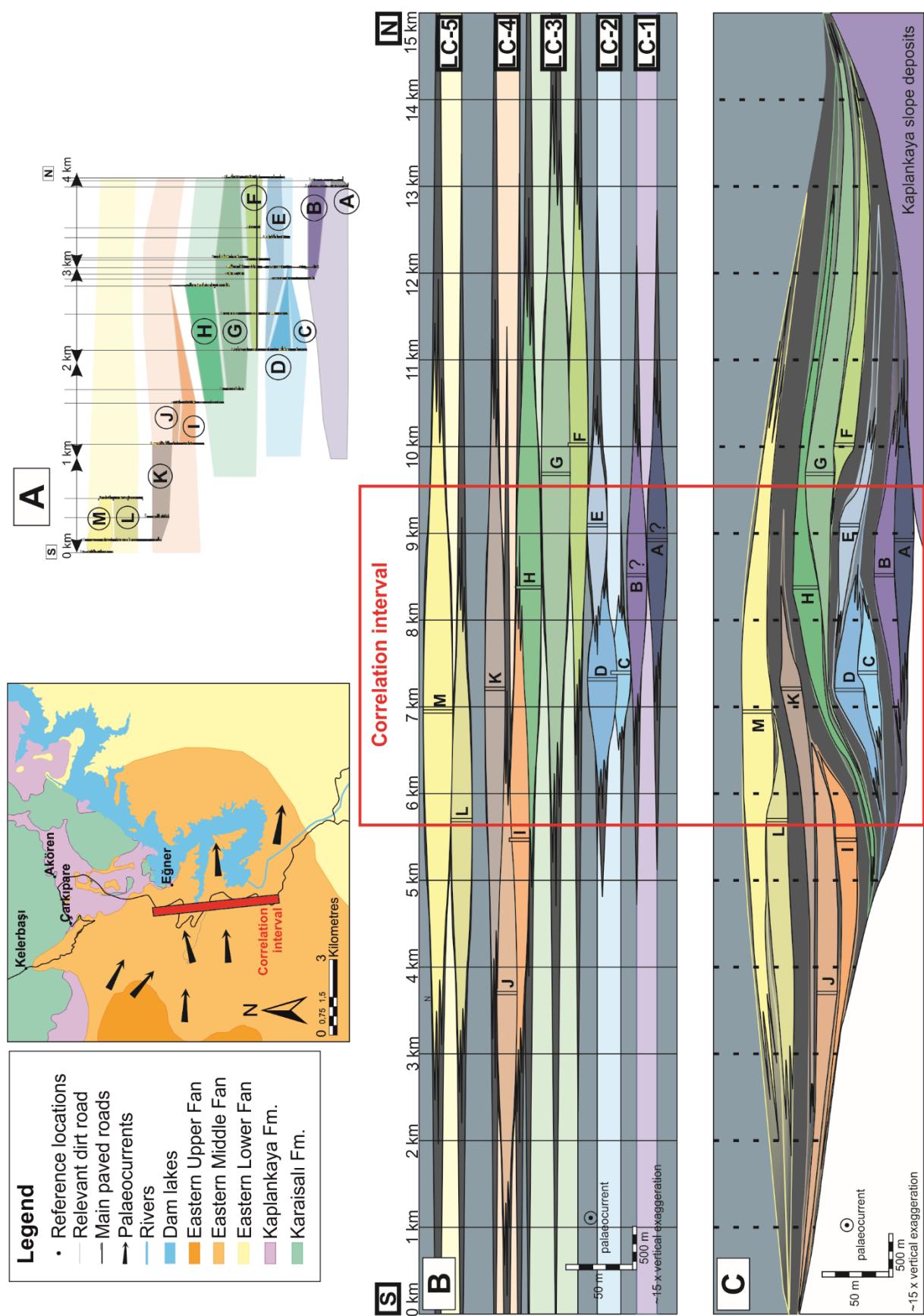
Fig. 24. Lobe architecture in the EF, interpreted from log correlation section. (A) log correlation section and interpreted lobes (A-M); (B) thickness and width for each lobe, keeping their positions along the correlation section. The lobes were grouped into five lobe complexes (LC-1 to 5); (C) schematic representation of lobe evolution, based on lobe dimensions, basin settings (size and palaeotopography) and position along correlation section. Correlation interval (measured in sedimentary logs) is shown in the red polygon.

The interpreted lobe evolution depicted in Figure 24 indicates slight confinement of the system, mainly at the base, and aggradation associated with compensational stacking. Since true thickness of each lobe is uncertain, when not measured, lobe length is not represented here, and the total volume of each lobe complex cannot be estimated. Therefore, progradational and retrogradational phases in the basin may be suggested only from the width interpretation. The lobe complexes in the Eastern Fan seem to have increased in size from base to top, representing a progradational phase.

Lobe Complex 1 (LC-1), formed by lobes A and B, is basal, since the logs that represent these lobes contain slope transition facies (siltstones and slumped facies). It is interpreted as mostly semi-confined. Overlying LC-1, LC-2, composed of lobes C, D and E, is also interpreted as "semi-confinement" due to its high thinning rate. LC-3 (with lobes F, G, H), deposited mainly in the northern portion of the basin, is the thickest and less confined complex. LC-4, formed by lobes I, J, K and deposited to the south, is also less-confined, but it was thinner and filled topographic lows created by the first three lobe complexes. Finally, LC-5, composed by lobes L and M, was deposited in a relatively unconfined setting. Lobe M probably extended from south to north.

Semi-confinement was probably a result of the proximity to slope deposits to the north and occurrence of previous turbidite deposits to the south, either from an earlier phase of the Eastern Fan, or even from the tongue-shaped deposits from the WF, mentioned by Satur (1999), produced by a confinement related to a high structural topography to the south and depositional slope to the north.

This interpretation on the degree of confinement is restricted to the eastern part of the EF, since uncertainties and the lack of relevant exposed sections in the central and western portions do not allow reliable interpretations.

The interpretation of lobe evolution in the EF shows an overall compensational stacking associated with aggradation of the system, as seen in the bed trend analysis. Estimation of length and width suggests slightly radial-shaped lobes in a semi-confined setting, or evolution from confined to unconfined. Compensational stacking is more common in unconfined than in confined lobes, due to the available space to grow and shift (Prélat *et al.*, 2010; Marini *et al.*, 2011). As seen in the study area, lobe shape reflects stacking pattern and vice versa. The slightly radial shape is probably due to frontal, rather than lateral (*e.g.*, slope) confinement, and it affected all lobes, depending on the main flow direction.

Modern analogue

Proximal lobes will receive sediments directly from the source, through canyons or short channels, whereas the outbuilding of distal lobes requires at least one large channel running across the basin floor to deliver sand in the deep basin (Bouma, 2000; Piper & Normark, 2001; Bouma, 2004). These feeder channels are very well observed in modern systems, especially in mud-rich systems, where channel-levee systems cut through the surrounding sediments (basinal fine-grained) towards lobe deposition. In sand-rich systems, the channels may run across the lobes ("distributary"), creating more lobes downdip, cutting through the previous lobes (coarse-grained) deposits.

Recognition of channels in ancient sand-rich systems is not straightforward. In the absence of a channel-levee system feeding the lobes, sediment delivery is carried out mainly by small secondary channels. As the lobes are built by several events, these channels commonly may be confused with sheets, especially when they are shallow and wide. Contrasting with the major channel in a channel-levee system, these secondary channels shift easily, due to the hierarchy of the lobe units that require continuous space availability, not allowing a long period of development (Chapin *et al.*, 1994; Gervais *et al.*, 2006; Etienne *et al.*, 2012).

In the EF lobes, some features may be associated with these secondary channels (Fig. 25).

Interpretation of geological features in 2D and 3D in outcrop studies may provide architectural models that can be used as reservoir analogues for subsurface interpretation, reducing the uncertainties in hydrocarbon production and development. Despite possible variations between the systems, comparative work is usually done on a basin or even architectural element scale. Detailed comparison of the internal architecture is more challenging due to the difficulty in subsurface interpretation on a sub seismic scale.
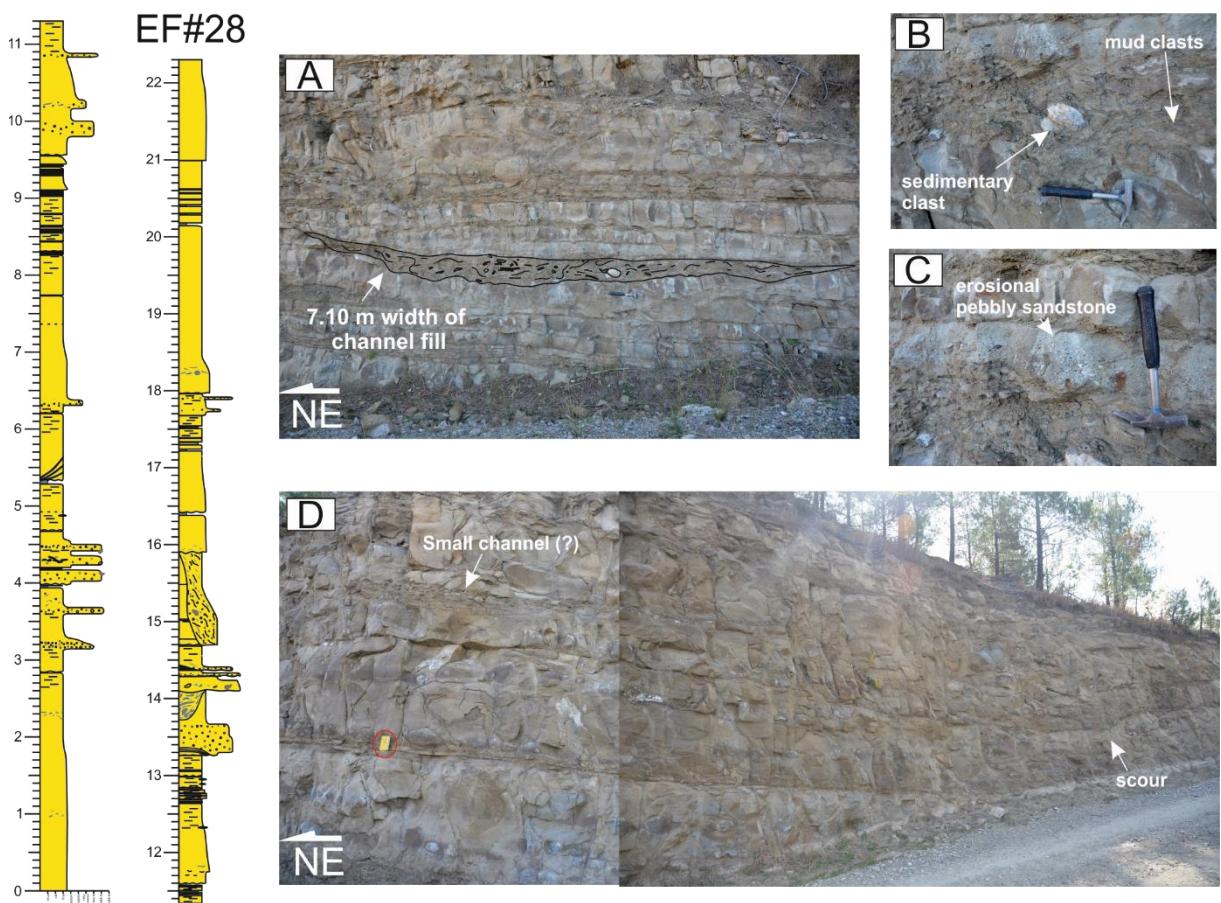
Fig. 25. Sedimentary log and representative photographs of an outcrop (log 28) in Kaledağ (inner Eastern Fan). (A) one small channel-fill deposit (detail of clasts in (B) interbedded with amalgamated sandstones. The topmost, channel-fill bed is pebbly at the base (C); (D) scour features and likely a channel in amalgamated sandstones. Notebook as scale (19 cm long).

Satur (1999) suggested subsurface analogues for the Cingöz Fm. (WF and EF) for each fan separated, mainly due to differences in the degree of confinement and feeder systems between the two fans. The WF was compared with the Crati Fan, in

the Corigliona Basin (Ionian Sea, Western Mediterranean), which is a small fan (70 m^2) with elongate lobes developed in an active margin. The EF was compared with fields in the North Sea: the Brae and T-Block fields were used as analogues for the gravel-rich feeder system, whereas the Miller field was proposed as analogue for the lobes.

Based on the analysis of lobe architecture and dimensions obtained in this study, the EF is comparable with the East Corsica lobes (Golo Fan), in the Corsican Trough, developed in a confined depression (but mainly frontal confinement) under a 900 m water depth. The drainage basin covers about 1100 km^2, with mountains elevated up to 2700 m, and shelf width ranging from 5 to 25 km (Deptuck *et al.*, 2008; Gervais *et al.*, 2006).

The Golo Fan lobes were separated into two distinct population, the Proximal Isolated Lobes (PILs) and Composite Mid-fan Lobes (CMLs), due to differences related to distance to the shelf break and dimensions, smaller in the PILs (Fig. 26). For comparative purposes, the Cingöz Eastern Fan was separated into two groups, based on dimensions and stratigraphic position of the lobes (Table 5). The overall characteristics of the two basins are similar. Both comprise systems with a sand-rich sediment source, developed in a relatively small basin. Confinement in the East Corsica system results from a topographic frontal barrier, similar to the EF, in which slope and previously accumulated deposits result in a slightly confined setting.

The dimensions are quite similar as well, despite uncertainties in lengths and widths in the Cingöz Fm. arisen from data limitation. Measurements in the EF point to lobes with intermediate dimensions between the PILs and the CMLs, what suggest that the thinning rates used to estimate lobe dimensions is realistic, taking into account the comparison between both systems.

Deptuck *et al.* (2008) calculated two different frontal thinning rates for the PILs, represented by the Pineto lobe, and CMLs, represented by C2 lobe. PILs showed average frontal thinning rate of 2.92 m.km^{-1}, whereas CMLs displayed 1.42 m.km^{-1}. Thinning rate in the Eastern Fan is 2.4 m.km^{-1}, an intermediate value even if only the proximal portion of the lobe is considered (Table 5). The maximum rate was 4.7 m.km^{-1} (Deptuck *et al.*, 2008), which approaches the value of 5.7 m.km^{-1} found in the present study.

Fig. 26. Bathymetric map showing East Corsican margin and location of the lobes system. Fi - Fium Alto lobe; Pi - Pineto lobe; NG - proximal North Golo lobe. From Deptuck et al. (2008).

Lateral thinning rates in the medial region are similar rates for both East Corsica and EF: 5 $m.km^{-1}$ for PILs and 5.8 $m.km^{-1}$ for CMLs, estimated 7 $m.km^{-1}$ for EF lower lobes and 4.5 $m.km^{-1}$ for EF upper lobes. In the proximal area, thinning rates for PILs, CMLs and EF lower lobes are similar (20, 15 and 14 $m.km^{-1}$, respectively), but much lower for EF upper lobes (4 $m.km^{-1}$). This is interpreted as reflecting the sub-radial shape of most of the upper lobes, given a relatively gentle lateral gradient. Thinning rates in the distal part cannot be compared due to the lack of data.

The comparison with East Corsica helps to understand the development of the EF, but it is important to highlight that the EF is part of the Cingöz Fm., the analysis was restricted to the eastern part of system. The results shown in the present work suggest that the evolution of the Cingöz Fm. encompassed several changes on the topographic relief created during lobe construction, what modified the degree of confinement degree during deposition.

Table 5. Comparison of lobe parameters between East Corsica (modern system) and Cingöz Eastern Fan (ancient system). East Corsica data from Deptuck *et al.* (2008).

	East Corsica		Cingöz Eastern Fan	
	Proximal isolated lobes (PILs)	**Composite mid-fan lobes (CMLs)**	**Lower lobes (LC-1, 2)**	**Upper lobes (LC-3, 4, 5)**
Age	Late Pleistocene		Middle Miocene	
Fan surface area	500 km^2		*>350 km^2	
Sediment source	Sand rich		Sand rich	
Basin floor topography	Confined (frontal)		Semi-confined (frontal and lateral confinement)	
Lobes	9	10	5	8
Length	7 km	15 – 36 km	5 – 6 km	8 – 12 km
Width	~1 – 4 km	~3 – 8 km	3 – 4 km	6 – 10 km
Individual lobe area	2 – 19 km^2	30 – 70 km^2	Not calculated	Not calculated
Max. thickness	9 – 20 m	25 – 40 m	15 – 22 m	15 – 22 m
Shape	elongate to semi-radial	lobate	elongate	elongate to semi-radial
L/W	<1 – 2	1.4 – 2.8	1.5 – 1.7 m	1.1 – 1.8 m
Average frontal thinning rate	**2.92 m.km^{-1}	**1.42 m.km^{-1}	**2.4 m.km^{-1}	**2.4 m.km^{-1}
Maximum frontal thinning rate	**4.7 m.km^{-1}	Not given	**5.7 m.km^{-1} (7 m.km-1 estimated)	2.4 m.km-1
Lateral thinning rate	Proximal 20 m.km^{-1} Medial 5 m.km^{-1} Distal 2.5 m.km^{-1}	15 m.km^{-1} **5.8 m.km^{-1} **2.0 m.km^{-1}	14 m.km^{-1} 7 m.km^{-1} -	4 m.km^{-1} 4.5 m.km^{-1} -

* Fan surface area based on the available space for lobe construction in the eastern part of EF, not on the entire EF surface area.

** Based on data from one lobe.

CONCLUSIONS

Four hierarchical levels were recognized for lobes. The basic element, representing sediments deposited in a single event, is the bed (maximum thickness of 1.9 m), the next level was named splay element (maximum thickness of 7.8 m), the splay elements stacked was called lobe, varying from 9.5 to 22 m thick, and finally the lobe complex (maximum thickness of 40 m). According to this study, the splay element is genetically related to a facies association, with the same average and maximum thicknesses, and hence the recognition of a facies association can be used to identify a splay element.

Bed-thickness trends and log correlation were valuable to explain lobe evolution and depositional architecture of the Eastern Fan (eastern sector). In high N:G ratios, the cycle trends in the study area show a pattern of symmetric, thickening- and thinning-upward successions, in both hierarchical levels (lobe and splay element). In medium N:G, the successions are dominantly thickening-then-thinning-upward, mainly with the thickening-upward portion of the cycle thicker than the thinning-upward one. This behaviour was interpreted as a compensational stacking pattern.

Analysis of lobe size and shape took into account the axial and lateral thinning rates obtained from log correlation. In lobe scale, the lateral thinning rate (along strike) for the proximal region is about 4 $m.km^{-1}$, while in the medial is 4.5 $m.km^{-1}$. The axial thinning rate (along dip) is less clear because the main correlation section is along strike, and hence only the thinning rate for the proximal region is given, about 2.4 $m.km^{-1}$. Hence, the estimated lobe width is between 3 and 10 km, while length ranges between 5 and 12 km, in a total of 13 lobes.

Interpretation and integration of the results allowed the understanding of how lobes are developed over time, in an overall compensational stacking associated with aggradation of the system. Estimation of length and width suggests the constructions of slightly radial-shaped lobes in a semi-confined setting, reflecting the evolution from confined to unconfined conditions.

Analysis of vertical bed trends showed that the overall tendency, controlled by stacked splay elements, in proximal environments (high N:G) is a symmetric

succession, becoming more asymmetric as the N:G ratio decreases distally. This distal asymmetry is interpreted as resulting from the shift of splay elements in distal parts, creating a progradational succession in a compensational stacking, depending on the evolution of the unit as a whole.

Lobe stacking patterns in the Eastern Fan were interpreted as aggradational, with some compensational stacking, due to semi-confined settings. Stratigraphically, lower lobes are more confined and smaller, bound by the slope to the north and ancient deposits to the south. Upper lobes were developed in an unconfined (or less confined) system, with preferred palaeocurrent direction towards NE, like all lobes in that region.

Overall, the EF of Cingöz Formation displays a great opportunity to study the architecture of lobes in detail providing a good source of hierarchy analysis and stacking patterns. This study can contribute to these schemes, with different views of the relationship between the hierarchy levels, which showed itself a good manner to compare different locations and maybe predict the thickness of the levels. The interpretations of stacking patterns showed here for confined or semi-confined basins will help future works to have a range of possible interpretations in this subject.

A comparison between the model for the lobes in the Cingöz Formation and a modern system (East Corsica lobes in the Golo Fan) shows some overall similarities with the Eastern Fan. Besides similarities regarding the fan and basin characteristics, measurements in the Eastern Fan point to lobes with intermediate dimensions and thinning rates between the Golo Fan lobes (Deptuck *et al*., 2008).

ACKNOWLEDGMENTS

REFERENCES

Aksu, A.E., Calon, T.J., Hall, J., Mansfield, S. and Yaşar, D. (2005) The Cilicia-Adana basin complex, Eastern Mediterranean: Neogene evolution of an active fore-arc basin in an obliquely convergent margin, *Marine Geology*, 221(1–4), pp. 121–159.

Anderton, R. (1995) Sequences, cycles and other nonsense: are submarine fan models any use in reservoir geology?, in Hartley A.J. and Prosser D.J. (eds.), *Characterisation of deep marine clastic systems: Geological Society Special Publication,* no. 94, p. 31–50.

Bayer da Silva, D., Cronin, B.T., Çelik, H. and Goldberg, K. (in press) Facies distribution in submarine frontal splays: an example from Cingoz Formation, Turkey.

Bouma, A.H. (2000) Coarse-grained and fine-grained turbidite systems as end member models: Applicability and dangers, *Marine and Petroleum Geology*, 17(2), pp. 137–143.

Bouma, A.H. (2004) Key controls on the characteristics of turbidite systems, *Geological Society, London, Special Publications*, 222(1), pp. 9–22.

Brinkmann, R. (1976) Geology of Turkey, pp. 158. *Elsevier Scientific Publishing Company*, Amsterdam, the Netherlands.

Burton-Ferguson, R., Aksu, A.E., Calon, T.J. and Hall, J. (2005) Seismic stratigraphy and structural evolution of the Adana Basin, eastern Mediterranean, *Marine Geology*, 221(1–4), pp. 189–222.

Chapin, M.A., Davies, P., Gibson, J.L. and Pettingill, H.S. (1994) Reservoir architecture of turbidite sheet sandstones in laterally extensive outcrops, Ross Formation, Western Ireland, in Weimer, P., Bouma, A.H. and Perkins, B.F. (eds.), *Submarine fans and turbidite systems: sequence stratigraphy, reservoir architecture, and production characteristics: Gulf Coast Section SEPM Foundation 15th Annual Research Conference Proceedings*, Houston, p. 53–68.

Chen, C. and Hiscott, R.N. (1999) Statistical analysis of turbidite cycles in submarine fan successions: tests for short-term persistence, *Journal of Sedimentary Research*, v. B69, p. 486–504.

Cipollari, P., Cosentino, D., Radeff, G., Schildgen, T.F., Faranda, C., Grossi, F., Gliozzi, E., Smedile, A., Gennari, R., Darbaş, G., Dudas, F.Ö., Gürbüz, K., Nazik, A. and Echtler, H. (2013) Easternmost Mediterranean evidence of the Zanclean flooding event and subsequent surface uplift: Adana Basin, southern Turkey, *Geological Society, London, Special Publications*, 372(1), pp. 473–494.

Cobain, S.L., Hodgson, D.M., Peakall, J. and Shiers, M.N. (2017) An integrated model of clastic injectites and basin floor lobe complexes: implications for stratigraphic trap plays, *Basin Research*, pp. 1–20.

Covault, J.A. and Romans, B.W. (2009) Growth patterns of deep-sea fans revisited: Turbidite-system morphology in confined basins, examples from the California Borderland, *Marine Geology. Elsevier B.V.*, 265(1–2), pp. 51–66.

Deptuck, M.E., Piper, D.J.W., Savoye, B. and Gervais, A. (2008) Dimensions and architecture of late Pleistocene submarine lobes off the northern margin of East Corsica, *Sedimentology*, 55(4), pp. 869–898.

Etienne, S., Mulder, T., Bez, M., Desaubliaux, G., Kwasniewski, A., Parize, O., Dujoncquoy, E. and Salles, T. (2012) Multiple scale characterization of sand-rich distal lobe deposit variability: Examples from the Annot Sandstones Formation, Eocene-Oligocene, SE France, *Sedimentary Geology*. Elsevier B.V., 273–274, pp. 1–18.

Fleming.A. (2010) *Stratigraphic architecture of lobe strata in a submarine fan setting, Point Loma Formtion, California*. MSc Dissertation. Colorado School of Mines, Colorado-USA 133 pp.

Gervais, A., Savoye, B., Mulder, T. and Gonthier, E. (2006) Sandy modern turbidite lobes: A new insight from high resolution seismic data, *Marine and Petroleum Geology*, 23(4), pp. 485–502.

Grundvåg, S.A., Johannessen, E.P., Helland-Hansen, W. and Plink-Björklund, P. (2014) Depositional architecture and evolution of progradationally stacked lobe

complexes in the Eocene Central Basin of Spitsbergen, *Sedimentology*, 61(2), pp. 535–569.

Gürbüz, K. (1993) *Identification and evolution of Miocene submarine fans in the Adana Basin, Turkey.* Unpublished PhD Thesis. University of Keele, Keele, 327 pp.

Gürbüz, K. (1999) Regional implications of structural and eustatic controls in the evolution of submarine fans; an example from the Miocene Adana Basin, southern Turkey, *Geological Magazine*, 136(3), pp. 311–319.

Gürbüz, K. and Kelling, G. (1993) Provenance of Miocene submarine fans in the northern Adana Basin, southern Turkey: A test of discriminant function analysis, *Geological Journal*, 28(3–4), pp. 277–293.

Haq, B.U., Hardenbol, J. and Vail, P. R. (1987) Chronology of Fluctuating Sea Levels Since the Triassic, *Science*, 235(4793), pp. 1156–1167.

Haq, B.U., Hardenbol, J. and Vail, P.R. (1988) Mesozoic and Cenozoic chronostratigraphy and cycles of sea-level change, in Wilgus, C.K., Hastins, B.S., Kendall, C.G., Posamentier, H.W., Ross, C.A. and Van Wagoner, J.C. (eds.), *Sea-Level Changes: An Integrated Approach.* C.K. Wilgus, B.S. Hastins, C.G.St.C. Kendall, H.W. Posamentier, C.A. Ross and J.C. Van Wagoner, SEPM Special Publication, p. 72-108.

Heller, P.L. and Dickinson, W.R. (1985) Submarine ramp facies model for delta-fed, sand-rich turbidite systems, *AAPG Bulletin*, 69: 960-975.

Hiscott, R.N. (1981) Deep-sea fan deposits in the Macigno Formation (middle upper Oligocene) of the Gordanna Valley,northern Apenines, Italy - Discussion, *Journal of Sedimentary Petrology*, 51:1015-10(3).

Hodgson, D.M., Flint, S.S., Hodgetts, D., Drinkwater, N.J., Johannessen, E.P. and Luthi, S.M. (2006) Stratigraphic Evolution of Fine-Grained Submarine Fan Systems, Tanqua Depocenter, Karoo Basin, South Africa, *Journal of Sedimentary Research*, 76(1), pp. 20–40.

Ilgar, A., Nemec, W., Hakyemez, A. and Karakuş, E. (2013) Messinian forced regressions in the Adana Basin: A near-coincidence of tectonic and eustatic forcing, *Turkish Journal of Earth Sciences*, 22(5), pp. 864–889.

Kane, I., Pontén, A., Vangdal, B., Eggenhuisen, J., Hodgson, D.M. and Spychala, Y.T. (2016) The stratigraphic record and processes of turbidity current transformation across deep-marine lobes, *Sedimentology*, p. 1236-1273.

Kelling, G., Gökçen, S.L., Floyd, P.A. and Gökçen, N. (1987) Neogene tectonics and plate convergence in the eastern Mediterranean : New data from southern Turkey, *Geology*, v. 15, p. 425–429.

Lien, T., Walker, R.G. and Martinsen, O.J. (2003) Turbidites in the Upper Carboniferous Ross Formation, western Ireland: reconstrucion of a channel and spillover system, *Sedimentology*, 50, pp. 113–148.

Macdonald, H. a., Peakall, J., Wignall, P.B. and Best, J. (2011) Sedimentation in deep-sea lobe-elements: implications for the origin of thickening-upward sequences, *Journal of the Geological Society*, 168(2), pp. 319–332.

Marini, M., Milli, S. and Moscatelli, M. (2011) Facies and architecture of the Lower Messinian turbidite lobe complexes from the Laga Basin (central Apennines, Italy), *Journal of Mediterranean Earth Sciences*, 3, pp. 45–72.

Marini, M., Milli, S., Ravnås, R. and Moscatelli, M. (2015) A comparative study of confined vs. semi-confined turbidite lobes from the Lower Messinian Laga Basin (Central Apennines, Italy): Implications for assessment of reservoir architecture, *Marine and Petroleum Geology*. Elsevier Ltd, 63, pp. 142–165.

Masalimova, L.U., Lowe, D.R., Sharman, G.R., King, P.R. and Arnot, M.J. (2016) Outcrop characterization of a submarine channel-lobe complex: The Lower Mount Messenger Formation, Taranaki Basin, New Zealand, *Marine and Petroleum Geology*. Elsevier Ltd, 71, pp. 360–390.

Milliman, J.D. and Syvitski, J.P.M. (1992) Geomorphic/Tectonic control of sediment discharge to the ccean: the importance of small mountainous rivers, *The Journal of Geology*, 100(5), pp. 525–544.

Mitchum, R.M., Vail, P.R. and Thompson, S. (1977) Seismic stratigraphy and global changes of sea level, part 2: the depositional sequence as a basic unit for stratigraphic analysis: section 2. Application of seismic reflection configuration to stratigraphic interpretation, *Seismic Stratigraphy: Applications to Hydrocarbon*

Exploration AAPG Memoir 26, pp. 53–62.

Murray, C.J., Lowe, D.R., Graham, S.A., Martinez, P.A., Zeng, J., Carroll, A.R., Cox, R., Hendrix, M., Heubeck, C., Miller, D., Moxon, I.W., Sobel, E., Wendebourg, J. and Williams, T. (1996) Statistical analysis of bed-thickness patterns in a turbidite section from the Great Valley Sequence, Cache Creek, Northern California, *Journal of Sedimentary Reseach*, pp. 900–908.

Mutti, E. (1977) Distinctive thin-bedded turbidite facies and related depositional environments in the Eocene Hecho Group (South-central Pyrenees, Spain), *Sedimentology*, 24, 107–131.

Mutti, E., Bernoulli, D., Lucchi, F. R. and Tinterri, R. (2009) Turbidites and turbidity currents from alpine "flysch" to the exploration of continental margins, *Sedimentology*, 56(1), pp. 267–318.

Mutti, E. and Normark, W.R. (1991) An integrated approach to the study of turbidite systems, in: Weimer, P., Link, M.L. (eds.), *Seismic Facies and Sedimentary Processes of Submarine Fans and Turbidite Systems*. Springer-Verlag, New York, pp. 75– 106.

Mutti, E. and Sonnino, M. (1981) Compensation cycles; a diagnostic feature of turbidite sandstone lobes, *International Association of Sedimentologists abstracts; 2nd European regional meeting.*, (October), pp. 120–123.

Nazik, A. and Gürbüz, K. (1992) Yöresi (Kb Adana) Alt-Orta Miyosen Yaşli Denizalt Yelpazelerinin Planktoni Foramini Biyostratigrafisi, *Türkiye Jeoloji Bülteni*, 32(February), pp. 67–80 (in Turkish).

Piper, D.J.W. and Normark, W.R. (2001) Sandy fans - from Amazon to Hueneme and beyond, *AAPG Bulletin, v. 85, no. 8* (August 2001), pp. 1407–1438.

Prather, B.E., Keller, F.B. and Chapin, M.A. (2000) Hierarchy of Deep-Water Architectural Elements With Reference to Seismic Resolution: Implications for Reservoir Prediction and Modeling, *Deep-Water Reservoirs of the World: 20th Annual*, pp. 817–835.

Prélat, A., Covault, J.A., Hodgson, D.M., Fildani, A. and Flint, S.S. (2010) Intrinsic controls on the range of volumes, morphologies, and dimensions of submarine lobes,

Sedimentary Geology. Elsevier B.V., 232(1–2), pp. 66–76.

Prélat, A. and Hodgson, D.M. (2013) The full range of turbidite bed thickness patterns in submarine lobes: controls and implications, *Journal of the Geological Society*, 170(1), pp. 209–214.

Prélat, A., Hodgson, D.M. and Flint, S.S. (2009) Evolution, architecture and hierarchy of distributary deep-water deposits: a high-resolution outcrop investigation from the Permian Karoo Basin, South Africa, *Sedimentology*, 56(7), pp. 2132–2154.

Pyles, D.R. (2007) Architectural elements in a ponded submarine fan, Carboniferous Ross Sandstone, western Ireland, in: Nilsen, T.H., Shew, R.D., Steffens, G.S. and Studlick, J.R.J. (eds.), *Atlas of Deep-water Outcrops. AAPG Studies in Geology*, 56, 19.

Radeff, G., Schildgen, T. F., Cosentino, D., Strecker, M. R., Cipollari, P., Darbaş, G. and Gürbüz, K. (2015) Sedimentary evidence for late Messinian uplift of the SE margin of the Central Anatolian Plateau: Adana Basin, southern Turkey, *Basin Research*, 29, pp. 488–514.

Robertson, A.H.F. (1998) Mesozoic-Tertiary tectonic evolution of the easternmost Mediterranean area: integration of marine and land evidence, *Proceedings of the Ocean Drilling Program, 160 Scientific Results*, 160.

Robertson, A.H.F. (2000) Mesozoic-Tertiary Tectonic-Sedimentary Evolution of a South Tethyan Oceanic Basin and its Margins in Southern Turkey, in Bozkurt, E., Winchester, J.A. and Piper, J.D. (eds.), *Tectonics and Magmatism in Turkey and the Surrounding Area. Geological Society, London, Special Publications*, 173, 97–138.

Saller, A., Werner, K., Sugiaman, F., Cebastiant, A., May, R., Glenn, D. and Barker, C. (2008) Characteristics of Pleistocene deep-water fan lobes and their application to an upper Miocene reservoir model, offshore East Kalimantan, Indonesia, *AAPG Bulletin*, 92(7), pp. 919–949.

Satur, N. (1999) *Internal architecture, facies distribution and reservoir modelling of the Cingöz deepwater clastic system in southern Turkey*. PhD Thesis. University of Aberdeen, Aberdeen, UK, 520 p.

Satur, N., Cronin, B.T., Hurst, A., Kelling, G. and Gürbüz, K. (2004) Down-channel

variations in stratal patterns within a conglomeratic, deepwater fan feeder system (Miocene, Adana Basin, Southern Turkey), in Lomas S. and Joseph, P. (eds.), *Confined turbidite systems: Geological Society (London) Special Publication* 222, p. 241–260.

Satur, N., Hurst, A., Kelling, G., Cronin, B.T. and Gürbüz, K. (2007) Controlling Factors on the Character of Feeder Systems to a Deep-water Fan, Cingöz Formation, Turkey, *Atlas of Deep-Water Outcrops, CD-ROM*, pp. 1–28.

Şengör, A.M.C., Gorür, N. and Saroğlu, F. (1985) Strike-Slip Faulting and Related Basin Formation in Zones of Tectonic Escape: Turkey as a Case Study, in: Biddle, K. and Christie-Blick, N., (eds.), *Strike-Slip Deformation, Basin Formation and Sedimentation, Special Publications, SEPM Society for Sedimentary Geology,* Tulsa, vol. 37, 227-264.

So, Y.S., Rhee, C.W., Choi, P.Y., Kee, W.S., Seo, J.Y. and Lee, E.J. (2013) Distal turbidite fan/lobe succession of The Late Paleozoic Taean Formation, Western Korea, *Geosciences Journal*, 17(1), pp. 9–25.

Sprague, A.R.G., Garfield, T.R., Goulding, F.J., Beaubouef, R.T., Sullivan, M.D., Rossen, C., Campion, K.M., Abreu, V., Schellpeper, M.E., Jensen, G.N., Jennette, D.C., Pirmez, C., Dixon, B.T., Ying, D., Ardill, J., Mohrig, D.C., Porter, M.L., Farrell, M.E. and Mellere, D. (2005) Integrated slope channel depositional models: the key to successful prediction of reservoir presence and quality in offshore West Africa, *CIPM, cuarto E-Exitep, Veracruz, Mexico,* 17, pp. 1–13.

Spychala, Y.T., Hodgson, D.M. and Lee, D.R. (2017) Autogenic controls on hybrid bed distribution in submarine lobe complexes, *Marine and Petroleum Geology*. Elsevier Ltd, 88, pp. 1078–1093.

Straub, K.M., Paola, C., Mohrig, D., Wolinsky, M. A. and George, T. (2009) Compensational Stacking of Channelized Sedimentary Deposits, *Journal of Sedimentary Research*, 79 (1981), pp. 673–688.

Ünlügenç, U.C. (1993) *Controls on Cenozoic sedimentation, Adana Basin, Southern Turkey*. PhD. Thesis. University of Keele, Keele, UK.

Williams, G.D., Ünlügenç, U.C., Kelling, G. and Demirkol, C. (1995) Tectonic

controls on stratigraphic evolution of the Adana Basin, Turkey, *Journal of the Geological Society*, 152, pp. 873–882.

Yetiş, C., Kelling, G., Gökçen, S.L. and Baroz, F. (1995) A revised stratigraphic framework for Late Cenozoic sequences in the northeastern Mediterranean region, *Geol Rundsch*, 84, pp. 794–812.

Zhang, J.J., Wu, S.H., Fan, T.E., Fan, H.J., Jiang, L., Chen, C., Wu, Q.Y. and Lin, P. (2016) Research on the architecture of submarine-fan lobes in the Niger Delta Basin, offshore West Africa, *Journal of Palaeogeography*. Elsevier Ltd, 5(3), pp. 185–204.

7.3. Artigo 3

Submetido à *Turkish Journal of Earth Science*

Evolution of sand-rich clastic submarine fans in a foreland basin (Adana Basin, Turkey)

DANIEL BAYER DA SILVA - Department of Stratigraphy, Federal University of Rio Grande do Sul, Av. Bento Gonçalves, 9500, CEP 91501-970, Porto Alegre, Brazil.

BRYAN T. CRONIN - Tullow Ghana Ltd, Plot 70, George Walker Bush Highway, North Dworzulu, Accra, Ghana

HASAN ÇELIK - Department of Geological Engineering, Engineering Faculty, Fırat University, 23119, Elazığ, Turkey.

KARIN GOLDBERG ˉ Department of Geological Engineering, Engineering Faculty, Fırat University, 23119, Elazığ, Turkey.

Assunto	**Fwd: TURKISH JOURNAL OF EARTH SCIENCES, YER-1808-23**
Remetente	Daniel Bayer <daniel.bayer.silva@gmail.com>
Para	<daniel.bayer@ufrgs.br>
Data	2018-08-26 12:22

CHASQUE WEBMAIL
Universidade Federal do Rio Grande do Sul

---------- Forwarded message ----------
From: <bmys-info@ulak.tubitak.gov.tr>
Date: qui, 23 de ago de 2018 às 21:54
Subject: TURKISH JOURNAL OF EARTH SCIENCES, YER-1808-23
To: <daniel.bayer.silva@gmail.com>

Dear DANIEL BAYER DA SILVA,

Your manuscript has been received and is currently being processed.

We thank you for your interest in our journal.

Yours sincerely,

Manuscript Title: Evolution of sand-rich clastic submarine fans in a foreland basin (Adana Basin, Turkey)
Manuscript Code Number: YER-1808-23

SEVAL ÖZGÜL
Journal Administrator

Note: For the manuscripts submitted via our online manuscript submission system, please use the following link:

http://online.journals.tubitak.gov.tr

--
Daniel Bayer da Silva
Geólogo/Geologist
Universidade Federal do Rio Grande do Sul (UFRGS)

Evolution of sand-rich clastic submarine fans in a foreland basin (Adana Basin, Turkey)

Daniel BAYER DA SILVA[1*], Bryan CRONIN[2], Hasan ÇELIK[3], Karin GOLDBERG[4]

[1] Department of Stratigraphy, Federal University of Rio Grande do Sul, Av. Bento Gonçalves, 9500, CEP 91501-970, Porto Alegre, Brazil.

[2] Tullow Ghana Ltd, Plot 70, George Walker Bush Highway, North Dworzulu, Accra, Ghana.

[3] Department of Geological Engineering, Engineering Faculty, Firat University, 23119, Elazığ, Turkey.

[4] Department of Geology, Kansas State University, 207 Thompson Hall, Manhattan, KS 66506, United States.

*Correspondence: daniel.bayer@ufrgs.br

Abstract: A complete longitudinal profile, from the continental shelf break to the basin floor, records a turbidite system in the northern sector of the Adana Basin, southern Turkey. Two coeval submarine fans, the Western and the Eastern Fans, comprise the Cingöz Formation. The Western Fan (WF) was feed by a single point source to the west, and the Eastern Fan (EF) was built by multiple fairways (four channels) to the north. The WF originated as a confined system with two depositional styles of frontal splay development: the tongue-shaped, elongate bodies, continuous for at least 15 km (1 km wide) and lobe-shaped, radial bodies, deposited on top of the tongues. The EF evolution is more complex, and the palaeocurrent patterns are critical to understanding the lobe evolution. A complete palaeocurrent analysis suggests that part of the EF was deposited onto the WF, meaning that the WF acted as a topographic high during the last phase of submarine fan construction, diverting the flow and depositing the EF lobes to the east. The new evidence contributes to the knowledge of the evolution in Cingöz Formation indicating the topography influence in this type of system.

Key words: submarine fan evolution, palaeocurrent, foreland basin, confined basin, sand-rich system, Cingöz Formation, Adana Basin

Introduction

Submarine fans are the most common sediment accumulators in deep-water (Mutti and Normark, 1987, 1991), reaching up to thousands of km^2 (Naini and Kolla, 1982;

Damuth et al, 1988; Curray et al., 2002 Loncke et al., 2006), but only in modern deep-water environments it is possible to observe the whole dimension and the surrounding areas, such as the source areas. Nevertheless, the recognition and the identification of the limits in these systems and their evolutive history is frequently challenger (Piper and Normark, 1983; Hodgson et al., 2006; Prélat et al., 2009). The evolution of a submarine fan (or turbidity systems) is dependent of a complex interplay of allocyclic and autocyclic controls, which creates a range of types, geometries, architectural elements (Richards and Bowman, 1998). These controls include the sea level fluctuations, regional tectonics and sediment supply characteristics.

In Cingöz Formation, northern sector of Adana Basin, southern Turkey (Figure 1) represents an excellent opportunity to study the whole system and interpret its development, including the source area, feeder system, continental shelf, slope and basin floor deposits. As the study area is a foreland basin, the tectonic represent an important play in the submarine fan development (Görür, 1992; Gürbüz, 1993; Williams et al., 1995). Authors as Gürbüz and Kelling (1993), Williams et al. (1995) and Satur (1999) worked on the basin and surrounding areas focused in the sediment supply, tectonic e the evolution. These authors recognized two coeval fans (Eastern Fan and Western Fan) and, according to Satur (1999), creating one large submarine fan system. The authors identified the limits, the interaction between both fans and part of the evolutionary history, based mainly on some seismic lines, one single well and palaeocurrent analysis, but new exposures described here represents a complementary data for new interpretations of the Cingöz Formation evolution. Interfingering of two or more fans are relatively common in modern fans such as the Rhône Neofan and Taranaki Basin (Bonnel et al., 2005; Masalimova et al., 2016), but the record in ancient environments are rare. The dimensions involved in submarine fans make an analysis difficult and the Cingöz Formation is a great opportunity to study this interaction.
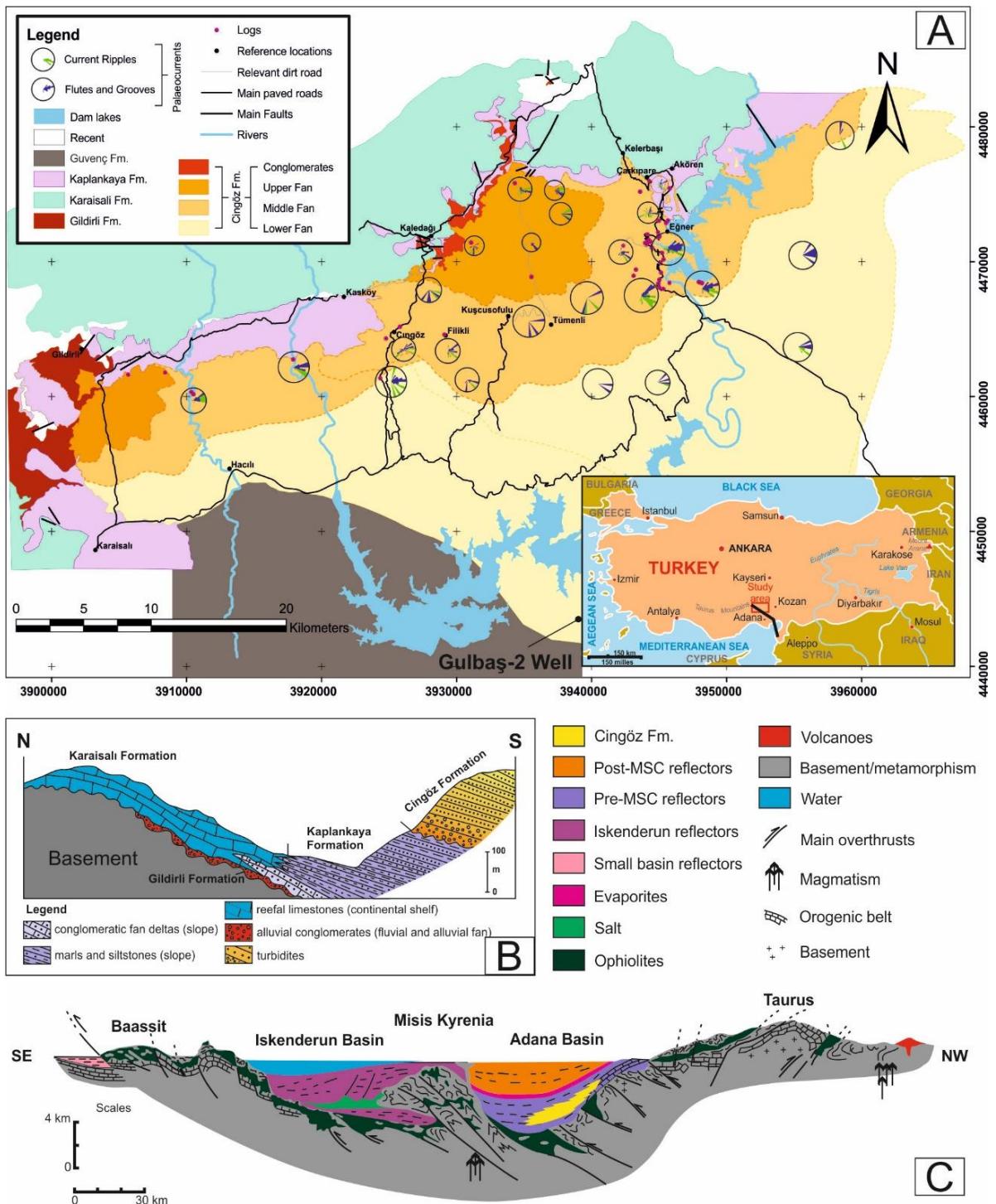
Figure 1. A) Geological map of the study area (after Gürbüz and Kelling, 1993), and the cross-section B) showing the relationship three main formations (redrawn after Gürbüz, 1993); C) Cross section (NW-SE) through the Tauride Mountains, with the Adana and the Iskenderun Basins and some relevant features highlighted. Adapted from Biju-Duval et al. (1978).

The palaeocurrent analysis is frequently used to clarify the origin and the direction of the flow, but the distinction and detail analysis of each indicator can give more than

the simple palaeocurrent direction, it can show the differences between the lower and upper part of the flow (e.g., turbidity current) the interaction with the topography and the deposition through time of the fan. The main indicators in turbidites are current ripple laminations (CRLs), flute casts and groove marks (clast imbrication for high-density turbidites). The CRLs provide an indicator of the flow in the upper part of the bed, representing the final phase of turbidity current deposition, while the sole marks indicate the flow direction when the flow passed onto the substrate (Allen, 1968; Allen, 1971). The significance of it can be seen, for example, when the flow interacts with the topography, diverting the flow and for consequence, the CRL will show a different direction in comparison with the sole marks. Moreover, the thin-bedded turbidites (TBTs) are deposit creating by relatively weak flows and the CRL are very common on it while in thick-bedded they are uncommon or hard to see due to the difficulties of exposures. That means you can have different palaeocurrent directions in CRL from TBTs and sole marks from thick-bedded. Overall, it is necessary to describe and measure the palaeocurrent indicators, because they can provide key evidence for the submarine fan evolution.

The purpose of this paper is to provide a new evolutionary interpretation of Cingoz Formation. The study is based on detailed description of new exposures and a comprehensive palaeocurrent analysis. In addition, the methodology used for the palaeocurrent analysis showed different views depending on the type of indicator and the bed thickness measured and how these can change the interpretation of the fan evolution. The interpretation of the evolution of Cingöz Formation can also be used to add knowledge of fan interaction in modern and ancient environments.

Geological Framework

The Adana Basin is situated on the southern Turkey, bounded to the N and NW by the Central Anatolian plateau, and to the S and SE by the Kyrenia and Misis Mountains (Kyrenia – Misis lineament) (Figure 2). It is the onshore part of Adana-Cilicia Basin (Brinkmann, 1976; Kelling et al., 1987), the Cilicia Basin being its offshore counterpart (Figure 2).
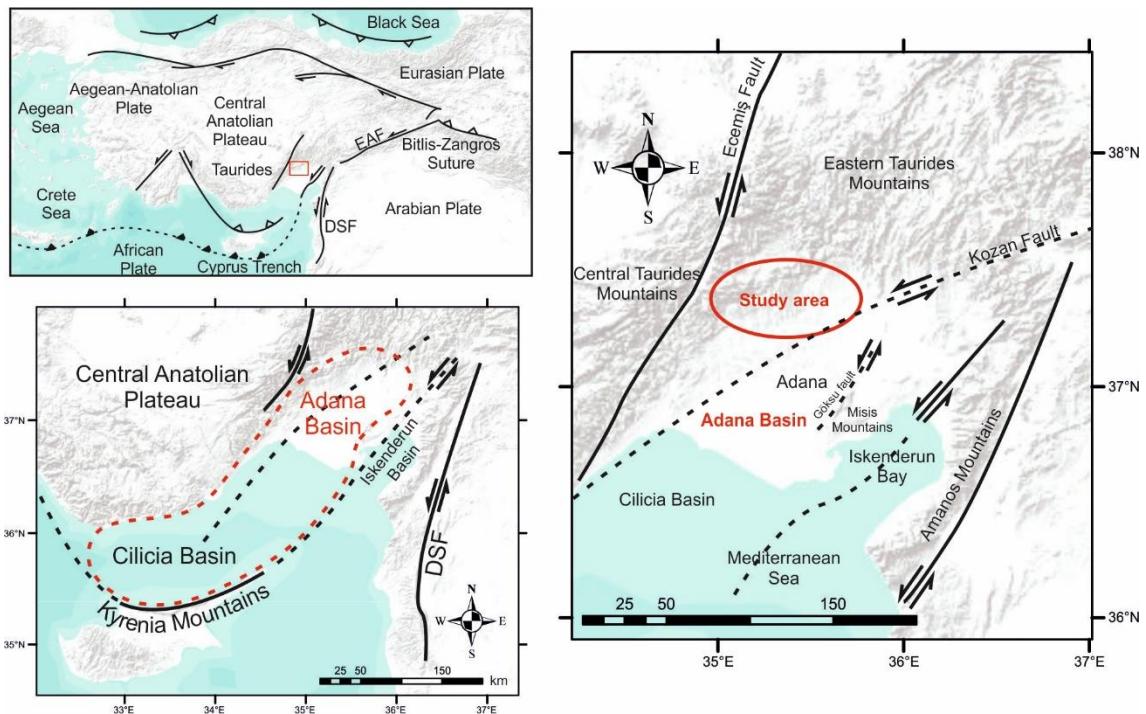
Figure 2. Tectonic map highlighting the Adana Basin and surroundings. In red dashed lines, the Adana-Cilicia Basin Complex. The study area (red circle) is located to the north of Adana and bounded to the north by the Central Tauride Mountains and to the south by the Kozan Fault. Adapted from Radeff et al. (2015).

Stratigraphy of Adana Basin

The Adana Basin stratigraphy was first proposed by Schmidt (1961). The sedimentary succession comprises up to 6 km of Miocene and Quaternary siliciclastic and carbonate deposits. The basement of the basin is composed of Palaeozoic rocks, including Devonian coralline limestones and sandstones, Permo-Carboniferous limestones, Mesozoic platformal carbonates and turbidites (Ilgar et al., 2013), together with an ophiolitic melange from the Tauride orogeny (Cipollari et al., 2013).

The Neogene fill in the Adana Basin is divided into three megasequences, based on the internal seismic character and boundary relationships (unconformities) (Williams et al. 1995), or into pre-transgressive, transgressive and regressive deposits (Yetiş et al., 1995; Satur, 1999) (Table).

According to Gürbüz (1993, 1999), the relative sea-level changes in the Adana Basin fit well with the global sea-level rise and fall scheme of Mitchum et al. (1977) and Haq et al. (1987, 1988) for the upper Palaeogene – Neogene (Satur, 1999). One lower-frequency transgressive-regressive cycle (approx. 15 my) comprises the entire

Neogene basin fill, with high frequencies representing the facies (Gürbüz, 1993, Ünlügenç, 1993, Satur, 1999).

Tertiary Formation	Environment (relative water depth)	Megasequence	Regressive/transgressive
Handere	Terrestrial/shallow-water	Megasequence 3	Regressive
Kuzgun			
Güvenç		Megasequence 2	Transgressive
Cingöz	Deep-water		
Kaplankaya			
Karaisalı	Shallow-water	Megasequence 1 (seismic basement)	Pre-transgressive
Gildirli	Terrestrial	Not resolved from seismic	
Karsanti			
Mesozoic	-		Basement

Table. Comparison of the stratigraphy based on megasequence (Williams et al., 1995) and regressive/transgressive cycles (Yetiş et al., 1995). From Satur (1999).

Based on biostratigraphic studies and sedimentary interpretations (Gürbüz, 1993, Nazik, 2004), a relative sea-level curve for the Adana Basin reveals a main transgression during the upper Burdigalian – Lower Langhian and a regression in the upper Serravallian (Figure 3). Three main formations were studied for this paper, the Karaisalı, Kaplankaya and Cingöz, with the main focus on the latter. A detailed description of each formation and the stratigraphy was performed by many authors (Schmidt, 1961; Yetiş, 1988; Ünlügenç et al., 1991; Gürbüz and Kelling, 1993; Yetiş et al. 1995; Radeff et al., 2015)

The Kaplankaya Formation comprising sandstones, siltstones, marlstones and sandy limestones (Burdigalian-Serravallian). This formation is interpreted as deposited mainly in continental slope environment (Figure 4), partially contemporaneous and topographically lateral and vertical to the Gildirli, Karaisalı and Cıngöz Formations (Gürbüz and Kelling, 1993).

The Karaisalı Formation (Figure 4) consists of reefal limestones (Görür, 1979; Nazik, 2004). The formation, with an age ranging from Burdigalian to Langhian, or possibly Serravallian (Görür, 1979), ranges from 20 – 350 m thick.
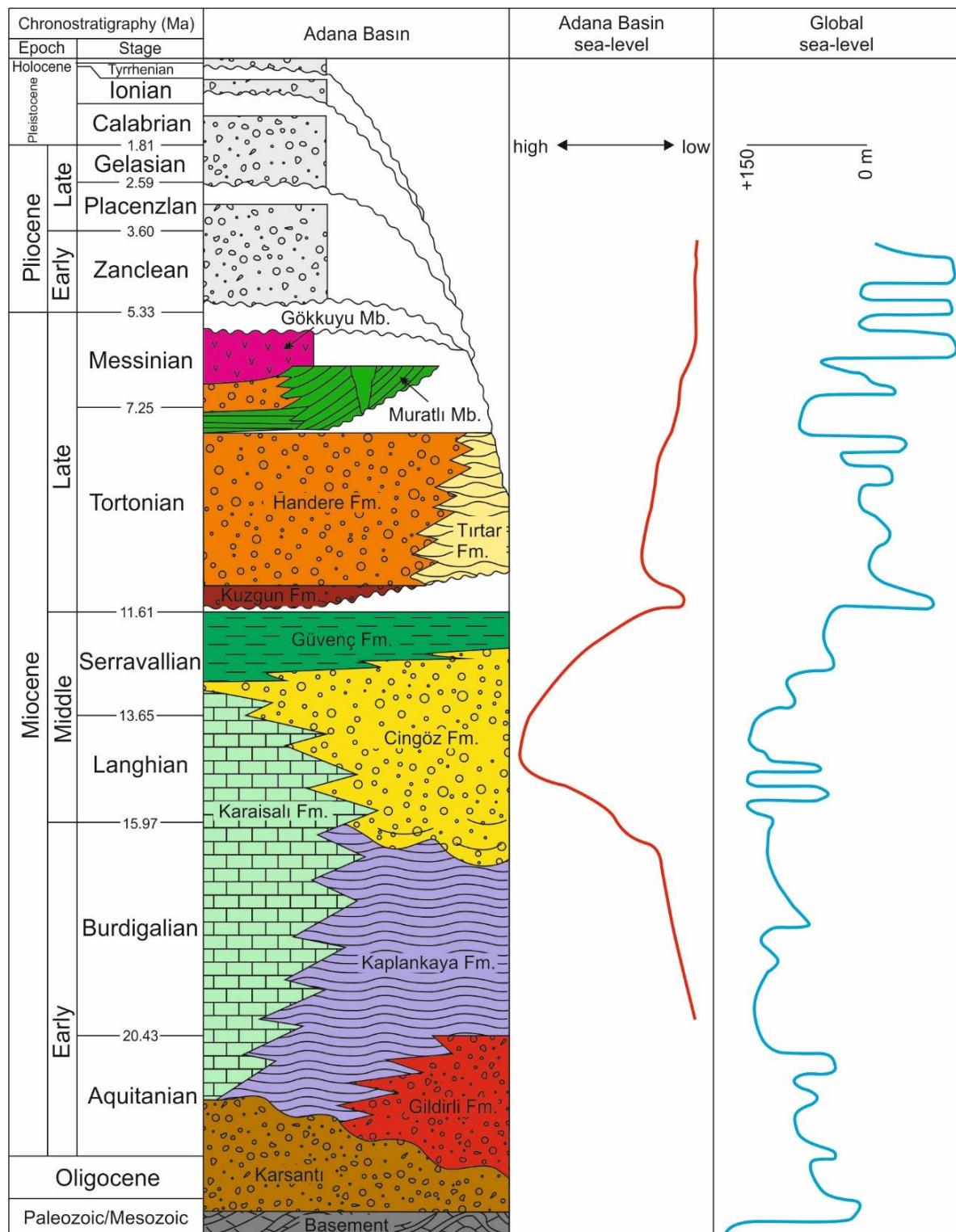
Figure 3. Stratigraphic chart of the Adana Basin with the sequence stratigraphic system tracts, and Adana Basin and Global sea-level curves. From Haq et al. (1987); Nazik and Gürbüz (1992); Gürbüz, (1993); Yetiş et al. (1995); Ilgar et al. (2013).

The Cingöz Formation (Figure 4) is composed of channelled, cobbly and pebbly sandstones to turbiditic tabular sandstones, also fine-grained sediments and MTDs

(Gürbüz and Kelling, 1993) deposited during the upper Burdigalian to Lower Serravallian (Nazik and Gürbüz, 1992). In the western part of the Cingöz Formation, a channels/canyon cut the Gildirli, Karaisalı and Kaplankaya Formations, creating the turbidite system (Görür, 1979; Yetiş and Demirkol, 1986; Yetiş, 1988; Gürbüz and Kelling, 1993; Williams et al. 1995; Satur, 1999). According to Gürbüz (1993), the Cingöz Formation deposits are 1000 – 3000 m thick and were deposited over 4 – 5 million years.
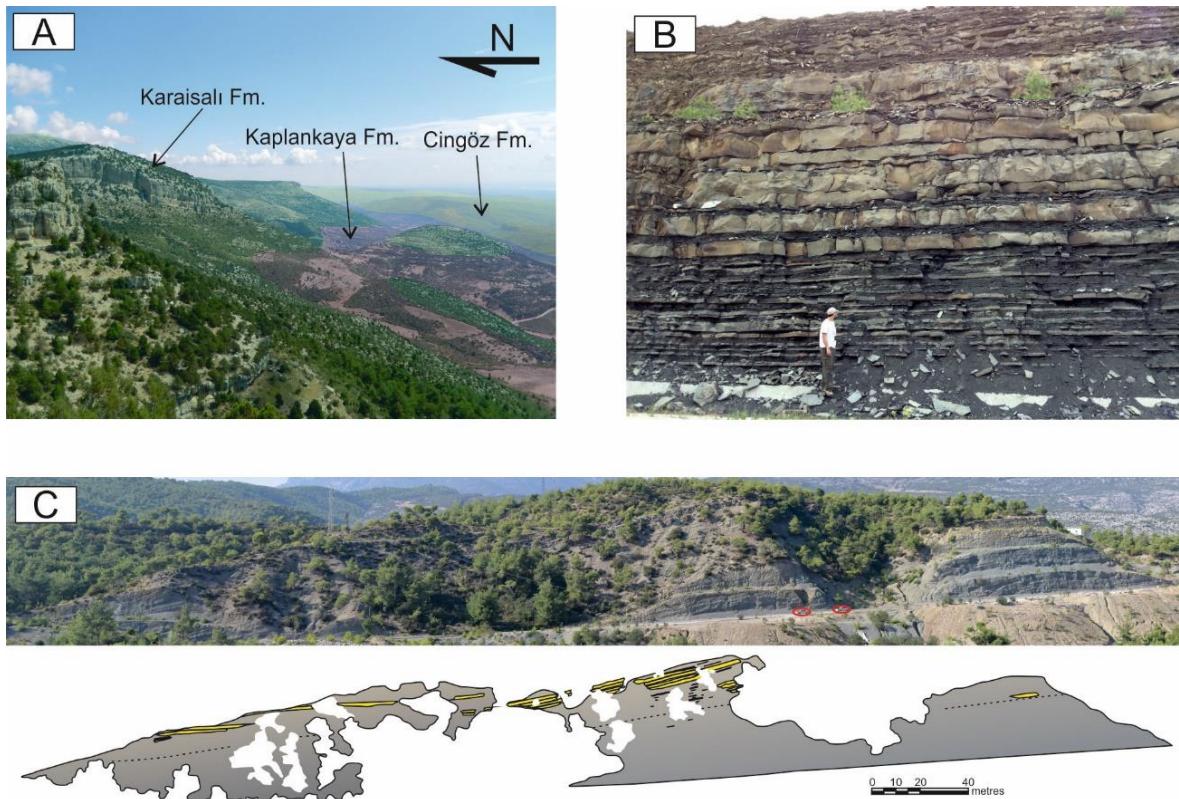

Figure 4. Overview of the three main formations focus of the present study: A) view from the top of Karaisalı Formation, dipping to the south towards the Kaplankaya and Cingöz Formations; B) thickening-upward succession of lobe sandstone from the Cingöz Formation; C) siltstone deposits from the Kaplankaya Formation.

The Cingöz Formation

Feeder systems

Previous studies interpreted this turbidite system as two coeval submarine fans fed by two distinct feeder systems (Satur, 1999): The Western Fan (WF) derived from a single point source to the west, whereas the Eastern Fan (EF) was built by multiple channels to the north (Gürbüz, 1993; Gürbüz and Kelling, 1993). The WF turbidity currents bypassed the contemporaneous carbonate shelf, delivering sediments predominantly to the east (080 – 110°). The present-day exposure allows us to

estimate that the channels were at least 9 km long, 3.5 – 4.0 km wide and approximately 360 m deep (Satur 1999). Based on the fan settings, Satur (1999) interpreted that, as the channel did erode into slope siltstones, confinement was due to palaeotopographic highs formed by reactivation of basement structures during deposition.

The thin-bedded sandstones along the southern margin of the feeder channel was interpreted as overbank deposits, based on the oblique palaeocurrents (090 – 185°) with regard to the main west-east channel palaeocurrents, and also the rapid change in the net-to-gross ratio (Fig. 5A). Another reason for considering them an overbank deposit is that they occur only in the southern margin due to the relatively high relief of the northern margin.

In contrast to the Western Fan, according to Satur et al., 2007, the Eastern Fan had at least four feeder channels, instead of one (Figure 5B-C). The main channel was named Channel 1, and the other three were interpreted as distributaries (Channels 2, 3 and 4). The western margin of Channel 1 is confined by carbonates from the continental shelf (Karaisalı Formation). The eastern margin is not exposed but field descriptions infer a channel width of at least 500 – 600 m (Satur et al., 2004). The major channel-fill lithotype is a clast-supported conglomerate and pebbly sandstones that provided a mean of palaeocurrent direction of 178° (Satur et al., 2007).

Three channels carried sediments to the Eastern Fan. Channels 2 and 3 were tributaries to Channel 1, and Channel 4 is younger (Satur et al., 2004). Channels 2 and 3 display similar facies to those described in the Channel 1 (Satur et al., 2007).

Channel 2 is located on the eastern margin of Channel 1 (Figure 5C) while the Channel 3 is on the western margin controlled by faults. Channel 4 is interpreted as the youngest one, cutting Channels 3 and 1 from west to east, with palaeocurrent direction of 090°. Like Channel 3, it seems to be controlled by faults. In the distal parts of Channel 4 it is possible to observe sandstones deposited in lobe sequences (Gürbüz, 1993).
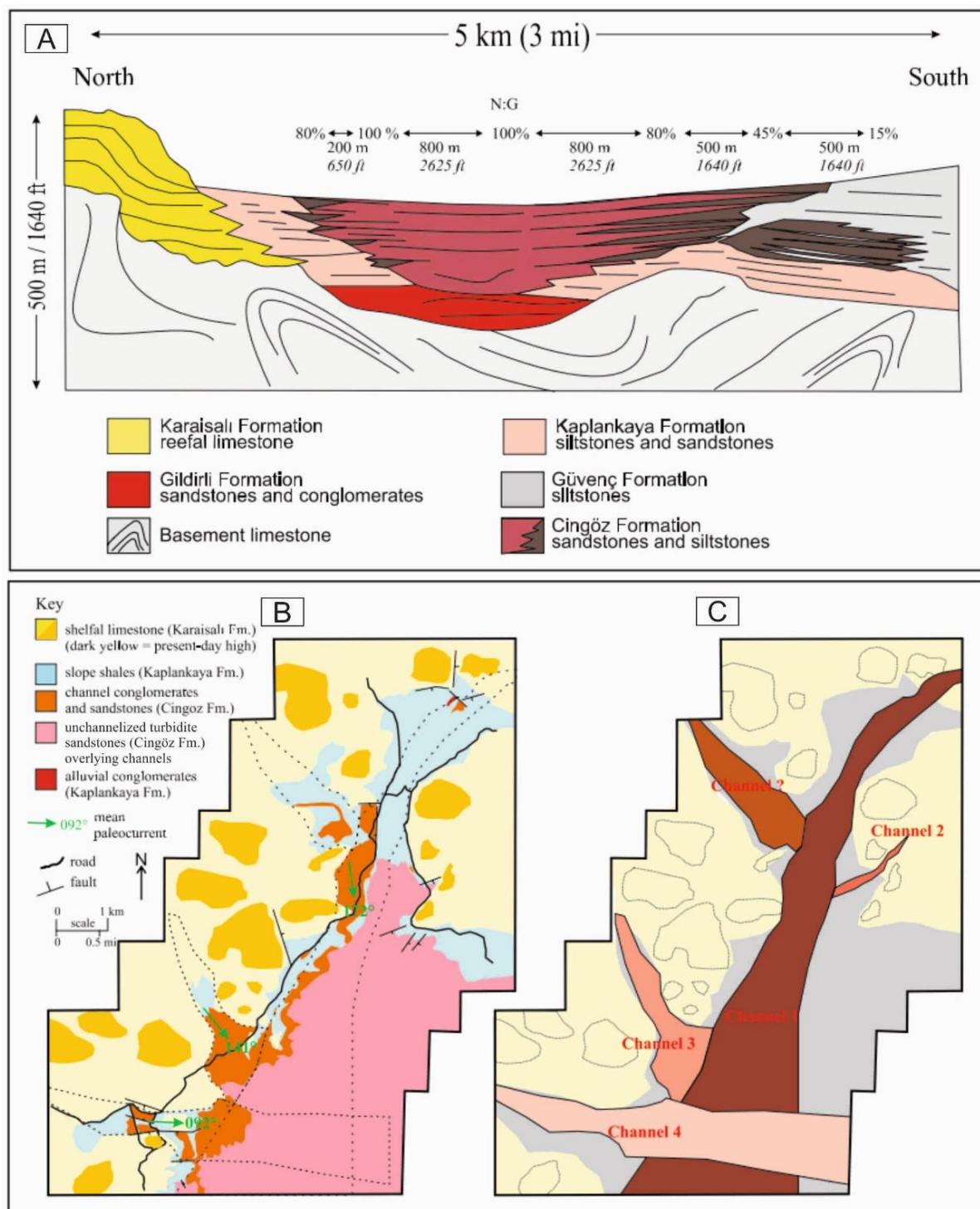
Figure 5. A) Interpreted cross-section of the channel in the Western Fan, eroding the Kaplankaya and Gildirli formations. The asymmetry observed in cross-section shows the N:G variation from the northern to southern margin, and distances in metres and in feet; B) Geological map (C) and feeder channels interpreted in the Eastern Fan. Palaeocurrent directions are mainly based on clast imbrication. From Satur et al. (2007).

Depositional systems

The WF is confined turbidite system (Şengör and Yilmaz, 1981; Satur, 1999; Satur et al., 2007). Satur (1999) distinguished two depositional styles of frontal splays: the tongue-shaped bodies (elongate) and lobe-shaped bodies (radial). Satur (1999) advocates that these tongues influenced the northeast palaeocurrents of the Eastern Fan deposits, instead to south.

The elongated bodies are separated vertically and laterally by 50 – 100 m thick thin-bedded sandstones (Figure 6). Each frontal splay is about 30 – 40 m thick for at least 15 km (1 km wide) (Satur et al., 2000, 2005, 2007), with mean palaeocurrent direction 74°. The lobes were deposited above the tongues, about 10 km downdip of the fairway head, and probably are stratigraphically equivalent to the upper part of the Western Fan (Satur 1999).

The Eastern Fan (approximately 750 km^2) was first described by Gürbüz and Kelling (1993) and Gürbüz (1993). These authors concluded that the EF is a low-efficiency (sand-rich) system with unchannelized lobes, sediment supply and relative sea-level fluctuations (Satur, 1999).
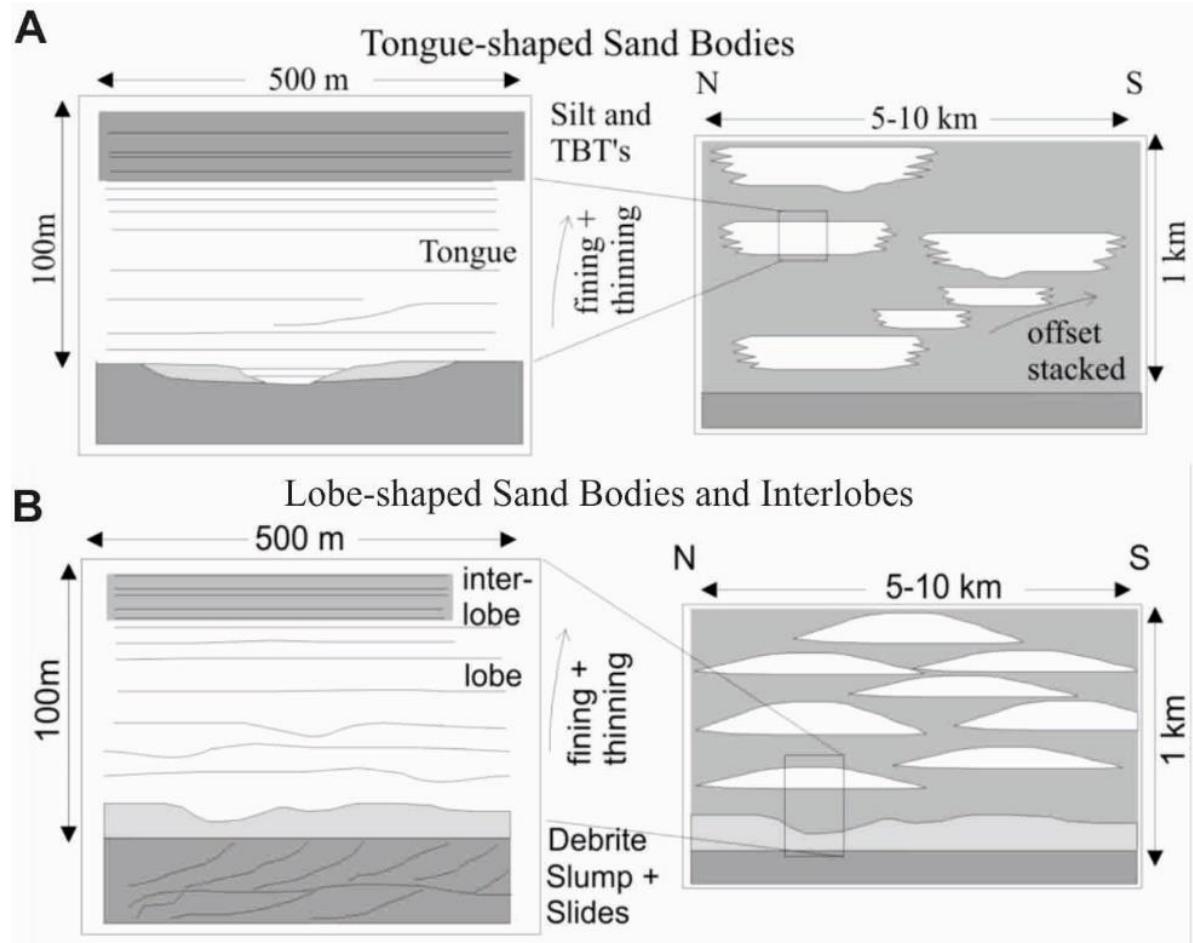
Figure 6. Comparison of stacking patterns, internal architecture and geometry between tongue- and lobe-shaped deposits. A) sheet sandstones with thickening- and thinning-upwards successions in vertical and offset stacking patterns of the tongues; B) the lobe-shaped bodies tend to deposit by compensational stacking, separated by siltstone "interlobes". From Satur (1999).

The Eastern Fan was divided into inner, middle and outer fan by Gürbüz and Kelling (1993). The inner fan consists of the feeder system and the "distributary channels", represented by strongly amalgamated, thick sandstone beds and rare thin-bedded sandstones. Gürbüz (1993) described unchannelized depositional lobes in the middle fan. In the outer fan, the thin-bedded turbidites are dominant (Figure 7).

Figure 7. A) Schematic vertical section based on the Gulbaş-2 Well showing alluvial deposits at the base (Gildirli Formation), overlain by channel and inner fan deposits (520 m), middle fan (155 m), outer-fan lobe (1200 m) deposits, capped by basin-plain sediments (~1000 m) from the Güvenç Formation. From Satur *et al.* (2007) based on Naz *et al.* (1991); B) Temporal and spatial development of the EF (Redrawn from Satur *et al.*, 2007); C) Interpreted seismic lines shot between 1986 and 1988 in the Adana Basin displaying the aggradational nature of reflectors of the megasequence 2 (Cingöz Formation). Adapted from Gürbüz (1999), after Ünlügenç (1993) and Williams *et al.* (1995).
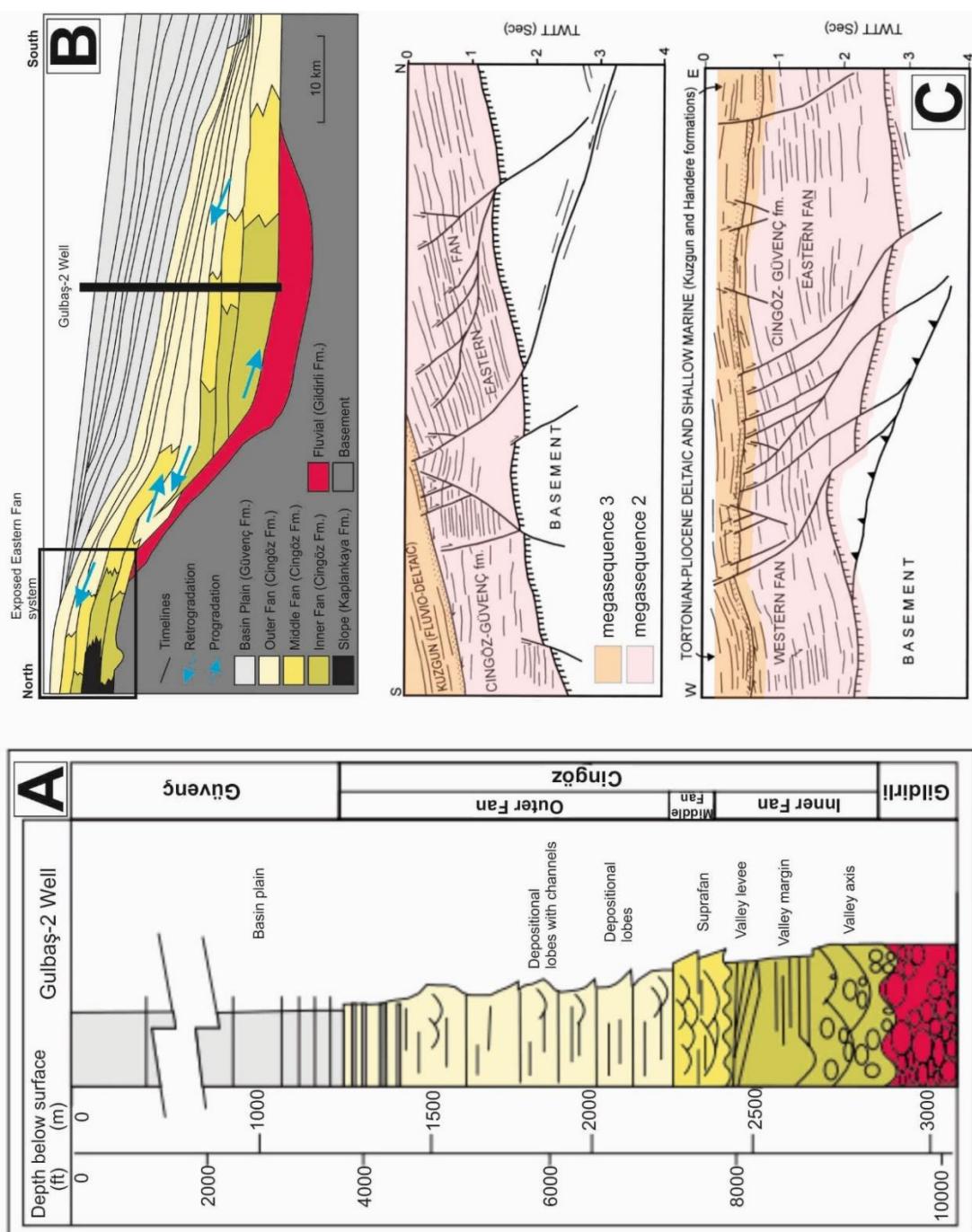
Relations between EF and WF

Gürbüz (1993) developed a generalized composite section for each of the fans (Figure 8). Both successions are broadly fining and thinning upward, with coarse, gravelly deposits at the base, representing the inner fan, succeeded by alternating sheet sandstone and mudstones, interpreted as lobe deposits that form the middle fan. The uppermost succession in both fans comprises very thin-bedded turbidites, deposited in the distal, outer fan (Figure 8).
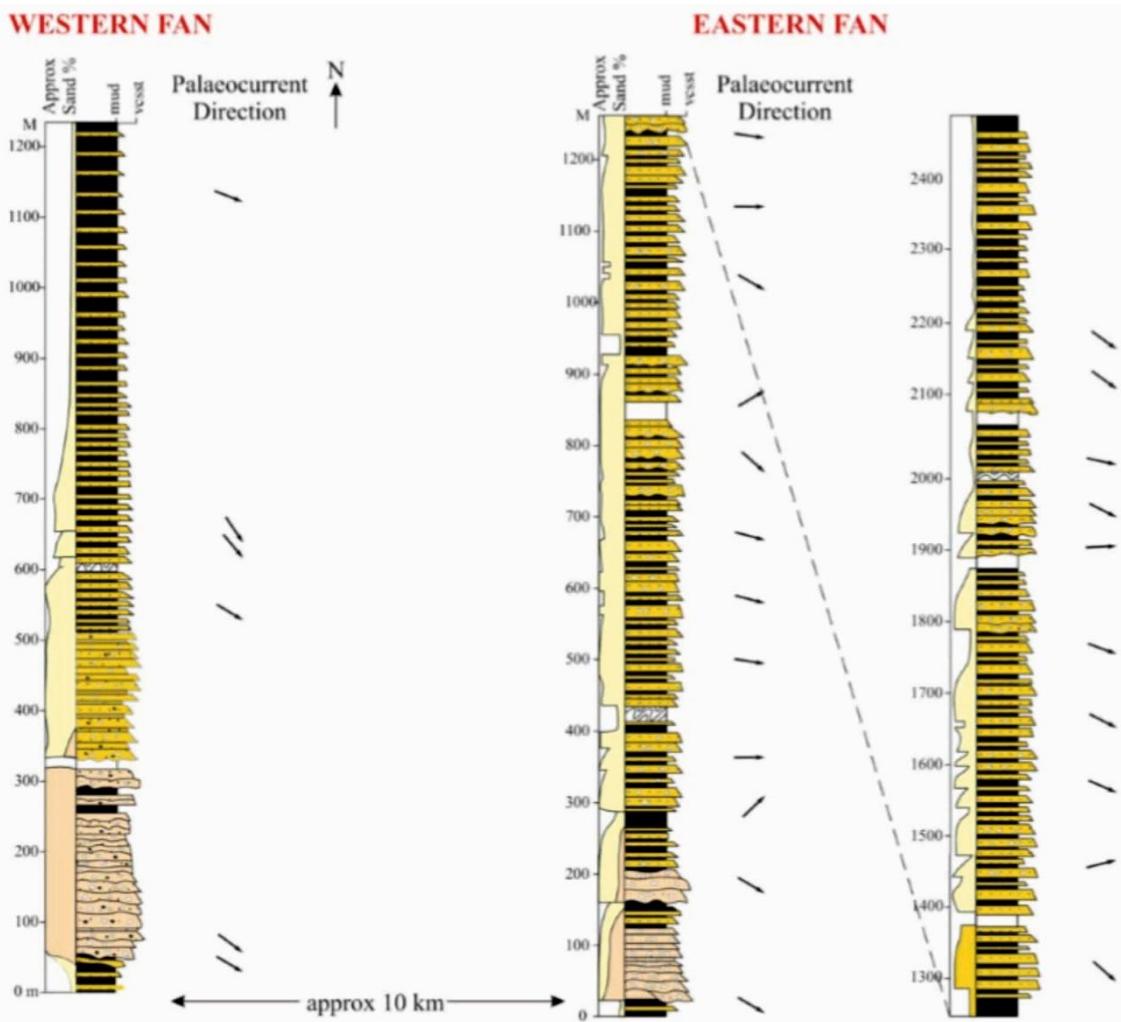

Figure 8. Generalized composite sections in the WF and EF. From Satur (1999) redrawn from Gürbüz (1999).

Some features are particular of each fan. An ichnological study of the Cingöz Formation (Demircan and Toker, 2003) revealed important differences between the two fans. The presence of *Cruziana* ichnofossil assemblage in the WF indicates an eutrophic environment in sublittoral zones with water depths of about 200 m, according to Frey and Pemberton (1984). In the EF, however, mixed and *Nereites*

ichnofossil assemblages point to a relatively oligotrophic environment in bathyal and abyssal zones (~500 to 5000 m of water depth) (Frey and Pemberton, 1984).

According to Gürbüz (1993) and Satur (1999), the WF interfingered with the EF at some point in time of the system evolution. Gürbüz (1993) suggested the interfingering in some time of the deposition because of the age based on biostratigraphy (planktonic foraminiferal and ostracods) of the entire system. Three measurements of palaeocurrent directions in one single location (Cingöz village) by Satur (1999) indicate palaeocurrent to the SW in the TBTs. Palaeocurrent directions measured in thick sandstones, however, indicate palaeocurrent towards NE, suggesting two opposing source directions.

Material and methods

The study was based on outcrop descriptions and palaeocurrent measurements along both submarine fans (WF and EF) in the Cingöz Formation. Field data included the detailed description of 42 outcrops in the area (purple circles in Figure 1) and construction of sedimentary logs 1:20 scale. These data were used for facies and stratigraphic analyses, in which the distinct lithofacies, facies associations, and bounding surfaces were identified.

The sedimentological description was also complemented by photomosaics in order to reconstruct the depositional architecture of the different stratigraphic intervals. These panels are intended to document: (i) the lateral and vertical facies relationships in detail within the depositional systems and (ii) vertical changes in sedimentation style, which may reflect the evolution of depositional systems.

Results

Palaeocurrent analysis

Palaeocurrent patterns are critical to understanding the evolution of a submarine fan. The study region is especially important because of its location where the two fans interact. The most common palaeocurrent indicators found are groove and flute casts following by current ripple laminations and rarely clast imbrication. Palaeocurrent measurements indicate a feeder system from the west (WF), and another one from the northwest (EF). Palaeocurrent analysis in the area shows different directions for current ripple laminations and flute casts: the first indicate palaeocurrent predominantly to SE, while flute casts point to a NE direction (Figure 9, 10 and 11). Each rosette represents the measurements in the surrounding area, rather than in a

specific location. Palaeocurrent analysis also investigated whether differences in palaeocurrent directions could be represented by bed thickness interpretations, and therefore the data was also separated in thin-bedded and thick-bedded sandstones (Figure 9 and 11).
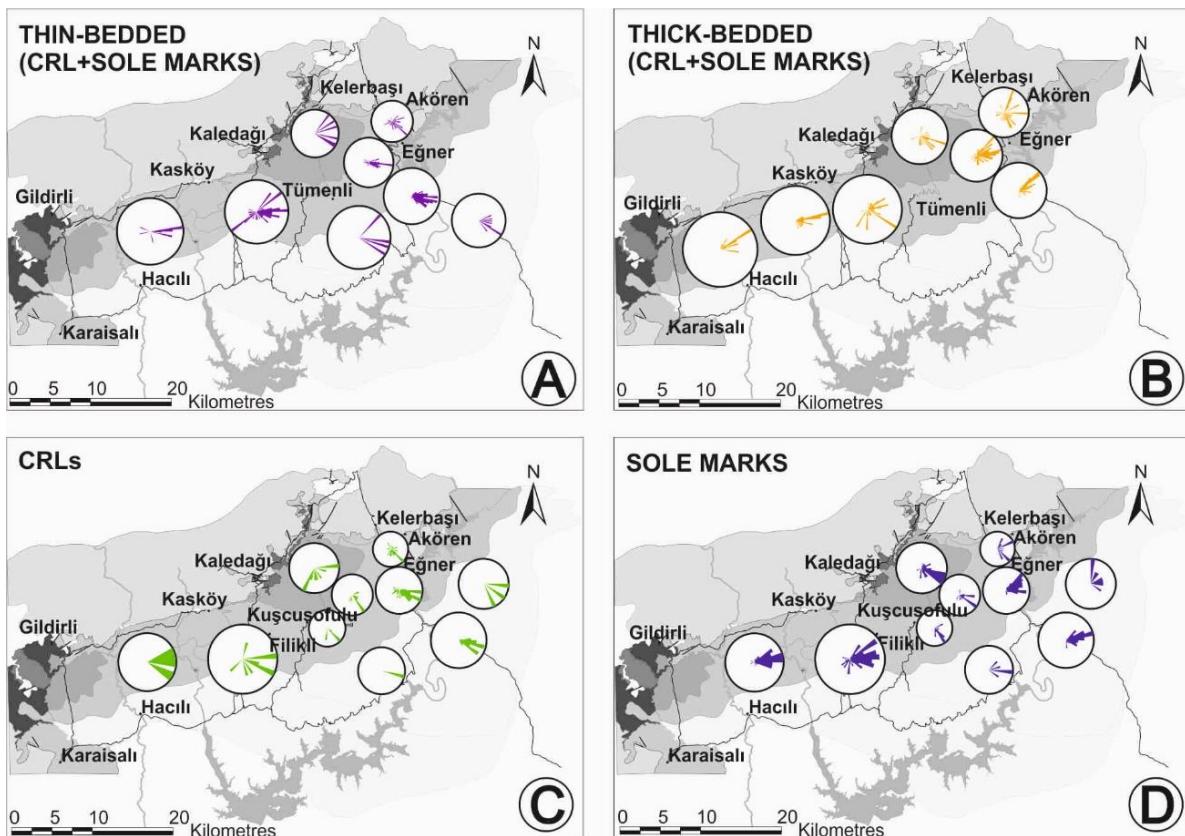

Figure 9. Palaeocurrent analysis in the Cingöz Formation. A-B) Palaeocurrent measurements in thin- and thick-bedded sandstones (CRLs = current ripple laminations); C) Palaeocurrent measurements in CRL only; D) Palaeocurrent measurements in sole marks only.

In the Western Fan, TBT deposits in the south are interpreted to be associated with a topographic high that confined the fan, resulting in a tendency of the upper part of the flow to deposit as overbank (Satur, 1999). This could be why the CRL display a SE palaeocurrent direction, as they are measured in mainly thin-bedded turbidites (Figure 9A-B).

In the Eastern Fan, the proximal area (inner fan) shows no difference between palaeocurrent directions measured in CRL and sole marks, both of which indicate palaeocurrent to SE. The differences are found in the eastern part of the system (Eastern Middle Fan) (Figure 9C-D).

The "interfingering" zone between the two fans displays an east direction in the Figure 10A (single blue circle in Cingöz village). In sole marks, however, the main direction is to the NE (Figure 10B), observed in the Western Fan and eastern part of the Eastern Fan. SE palaeocurrents are restricted to the central part of the system, including the entire Eastern Inner Fan and stretching southward towards the outer fan. Measurements in sole marks indicates palaeocurrent to the NE, comprising about 62 – 65% of measurements in the eastern sector only (Sanibey Dam and Aladağ-Imamoğlu road section), 10% more than the total measurements in sole marks for the entire system (about 56%) (Figure 11).
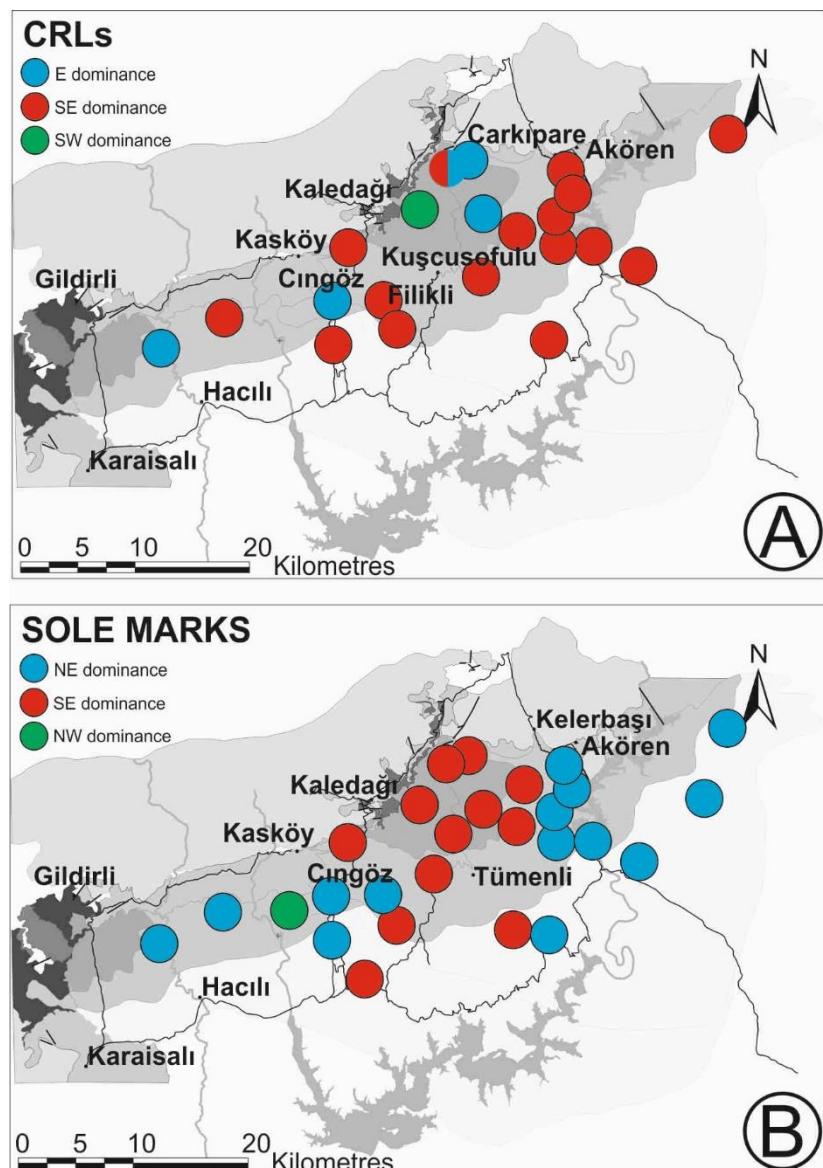

Figure 10. Palaeocurrent analysis in the Cingöz Formation. A) Distribution of dominant directions (quadrants) from CRLs; and B) Distribution of dominant directions (quadrants) from sole marks (blue = dominantly E, red = dominantly SE, and green = dominantly SW palaeocurrent directions).
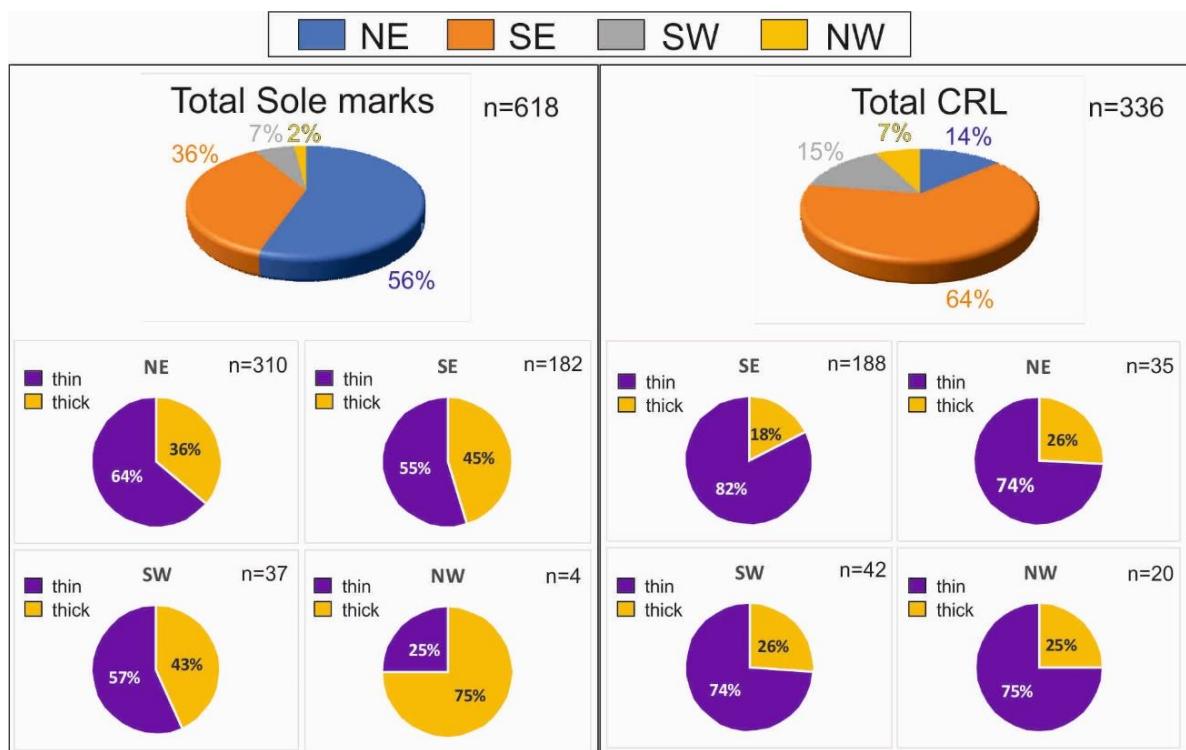
Figure 11. Pie charts depicting information on palaeocurrent directions and its patterns. The larger charts at the top represent the percentage of palaeocurrent measurements in four quadrants for all the Cingöz Formation. The smaller charts below display percentages for each quadrant measured in sole marks (on the left) and CRL (on the right), separated in thin or thick-bedded sandstones.

Figure 11 shows that the majority of palaeocurrent measurements, independent of the indicator, comes from thin-bedded sandstones. The suggested reason for that is because most of the palaeocurrent measurements was collected in thin-bedded, easier to identify than thick-bedded turbidites.

Discussion

Palaeocurrent interpretation

The analysis of the main palaeocurrent results shows that rarely in the study area were measurements recorded in both sole marks and CRLs in the same bed, in which case the two indicators usually agreed with each other. The main location of these beds (CRL and sole marks in the same bed) is the eastern sector of the EF, relatively close to the palaeo-slope, but only 15% of them has a difference greater than 90° between both indicators. For example, near Eğner town, located close to the palaeo-slope, where some of the measured palaeocurrent directions are opposite (SW/NW) to the main direction in the region (SE/NE) (Figure 9A, B, C).

These diverted directions in the eastern sector of the EF may result from two conditions. The first is related to the distance from the source (feeder system). As the flow moves farther away from the feeder system, flow partitioning may lead to increasing angle between measured indicators. For example, while the main flow body is following the topography that redirects the flow towards NE, the uppermost, fine-grained part of the flow could still move towards S-SE guided by Coriolis (for example), escaping over the topographic highs (Sinclair and Tomasso, 2002; Amy et al., 2007; Marini et al., 2015).

Another possibility is that the eastern part of the EF is actually the distal part of the WF, while the middle part of the WF was covered by the EF that flowed to the south. This possibility is plausible if the palaeocurrent measured in sole marks (Figure 10B), to the SE, are interpreted as the EF that covered the WF.

Overlapping/interfingering fans

Submarine fans can overlap or interfinger if the proximity, the topography duration of deposition allows. The Cingöz Formation, with two main feeder systems, is a good example of submarine fans that influence one another, based on palaeocurrent directions. Timing of these fans is also a crucial factor, since they will only interfingering or overlapping if developed at the same time. According to Gürbüz (1993), biostratigraphic data (Nazik and Gürbüz, 1992) indicate that WF and EF are of the same age, deposited during 4 or 5 My (Upper Burgalian – Serravallian), what would allow for their interaction. This means that sedimentation in the Western Fan stopped before it did in the Eastern Fan, probably in the Middle Serravalian, at the onset of the *Globorotalia Mayeri* biozone (Nazik and Gürbüz, 1992).

During field work, no evidence was found to indicate a barrier (*e.g.*, fault lineament) between the fans, and hence, according to the depositional ages, it is possible that the fans interfingering at least during some periods of their history.

The interfingering question can be explained by two regions where diverging palaeocurrents are found in the same location, possibly indicating the EF is at the top of the WF. The first location is a dirt road west of Cingöz vilage. The second and main location is in the Filikli/Nuhlu region, where two outcrops display abundant palaeocurrent indicators towards different directions (south and east-southeast) (Figure 12). In this location, it is very unlikely that the Western Fan produced palaeocurrents to the south. The east-southeast direction agrees with WF provenance.

The interpreted stratigraphic position of these two exposures, based on the satellite image, suggests that the last phase of the EF (?Serravallian?) was deposited onto the WF (Figure 12). If it is true, the potential implication is that the Western Fan could have acted as a topographic high during the last phase of submarine fan construction, diverting the flow and depositing the lobes in the east.

Evolution of the Cingöz Formation

The first geological map of the Adana Basin was prepared by Yetiş and Demirkol (1986), and the first detailed map of the Cingöz Formation, still in use nowadays, by Gürbüz (1993). This study will hopefully contribute with new data to improve the map (Figure 13).

The submarine fan subdivision used here followed the one from Gürbüz (1993), in which the inner fan comprises highly amalgamated sandstones, mostly associated with shallow, small channels. The middle fan, where the lobes are developed, is composed of alternating thick- and thin-bedded sandstone packages. The outer fan, dominated by TBT deposits, extend towards the fan margins, until the contact with basin floor deposits.
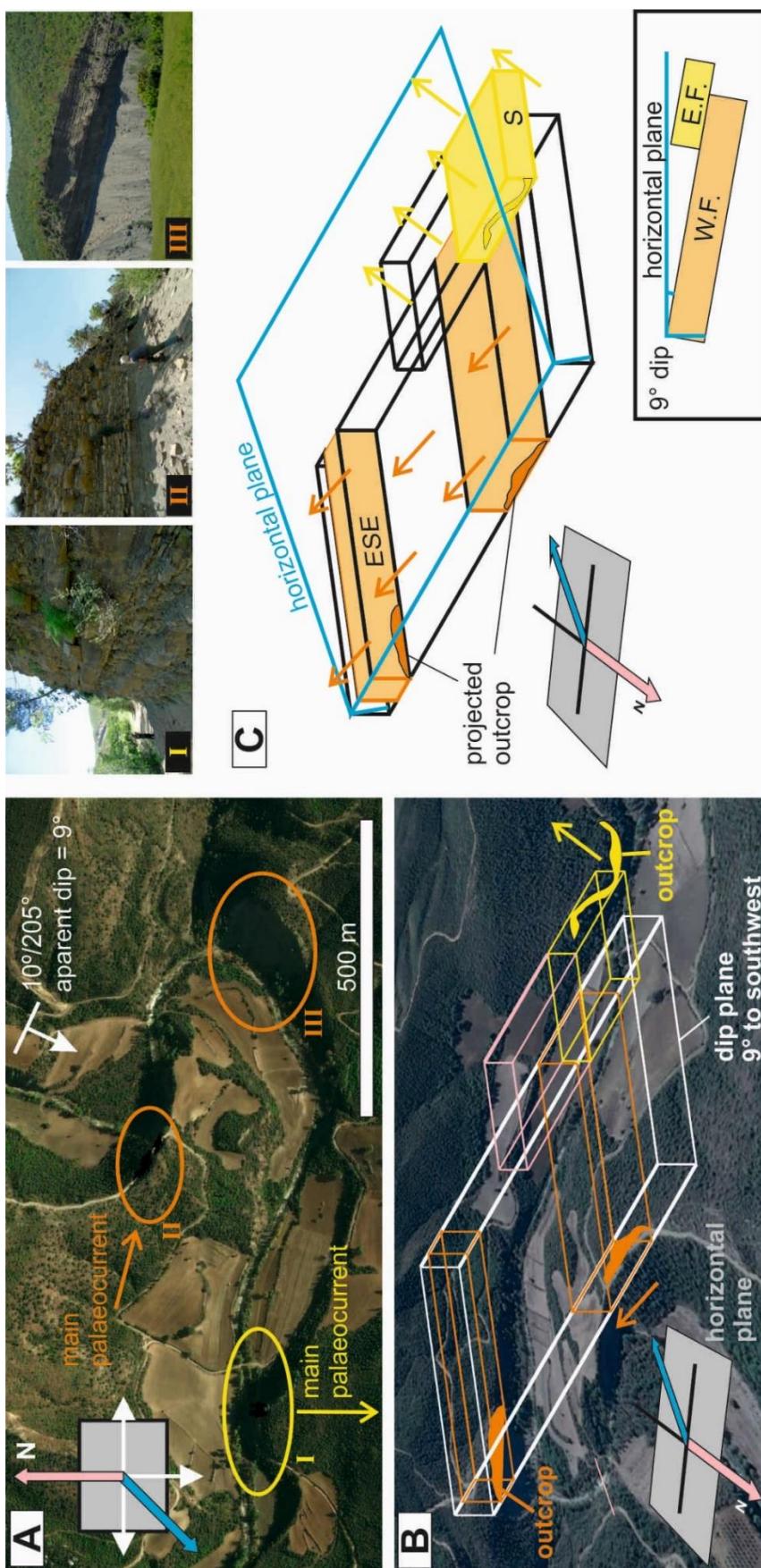
Figure 12. Schematic representation of the interpretation of stratigraphic relations between three outcrops in the zone of interaction between EF and WF, which display different palaeocurrent directions: A) a satellite plan view with outcrop locations, distances, palaeocurrent measurements and orientation, as well as photos of outcrops I, II and III; B) an oblique aerial view, with the outcrops highlighted in yellow and orange within the blocks that contain each succession (dipping 9° dip southwest); and C) the projected outcrops to show the stratigraphic position occupied by each succession, with palaeocurrent directions (orange for east-southeast trends and yellow for south trends). The plan view (in blue) highlights the dip of the blocks representing the Western Fan (orange) and Eastern Fan (yellow).

In addition to the valuable previous studies (Gürbüz, 1993; Satur, 1999) on the Cingöz Fm. evolution, the present study offers new information and interpretations to understanding the Cingöz Fm. history. The study of new outcrops shed light on the relationship between the fans, providing a large number of palaeocurrent measurements along the fans to better understand the final stages of evolution of the Cingöz Fm. Based on the data gathered in this study, integrated with literature compilation, the Figure 14 briefly summarizes the history of the Cingöz Fm. since its inception in the Upper Burdigalian. Depiction of the first stage (Figure 14A) used the data from Satur (1999) and Satur et al. (2007), the second stage (Figure 14B) likewise, augmented by data acquired from the sandstones in the WF (tongues), the onlap relationship and palaeocurrent measurements. The last stage (Figure 14C) displays the two alternative interpretations for the final stages: alternative 1 is based on palaeocurrent data that shows a south/southeast trend in the middle part of the system, interpreted as an EF source, while the east part of the EF represents the distal WF tongue that evolved to a lobe shape in a later stage; alternative 2 represents the interpretation that the deposits in the east part of EF were sourced in Channel 4 or surroundings, diverted by the tongue deposits from WF, allowing the fine sediments passed over it. Based on the lobes evolution interpretation of the Eastern Fan the alternative 2 seems to be the best to explain the development of EF lobes to the NE, due to the similarities of interpretation, which the building blocks of the lobes agree with the interpretation of a previous deposit to the south (possibly the WF) acting as a topographic high.
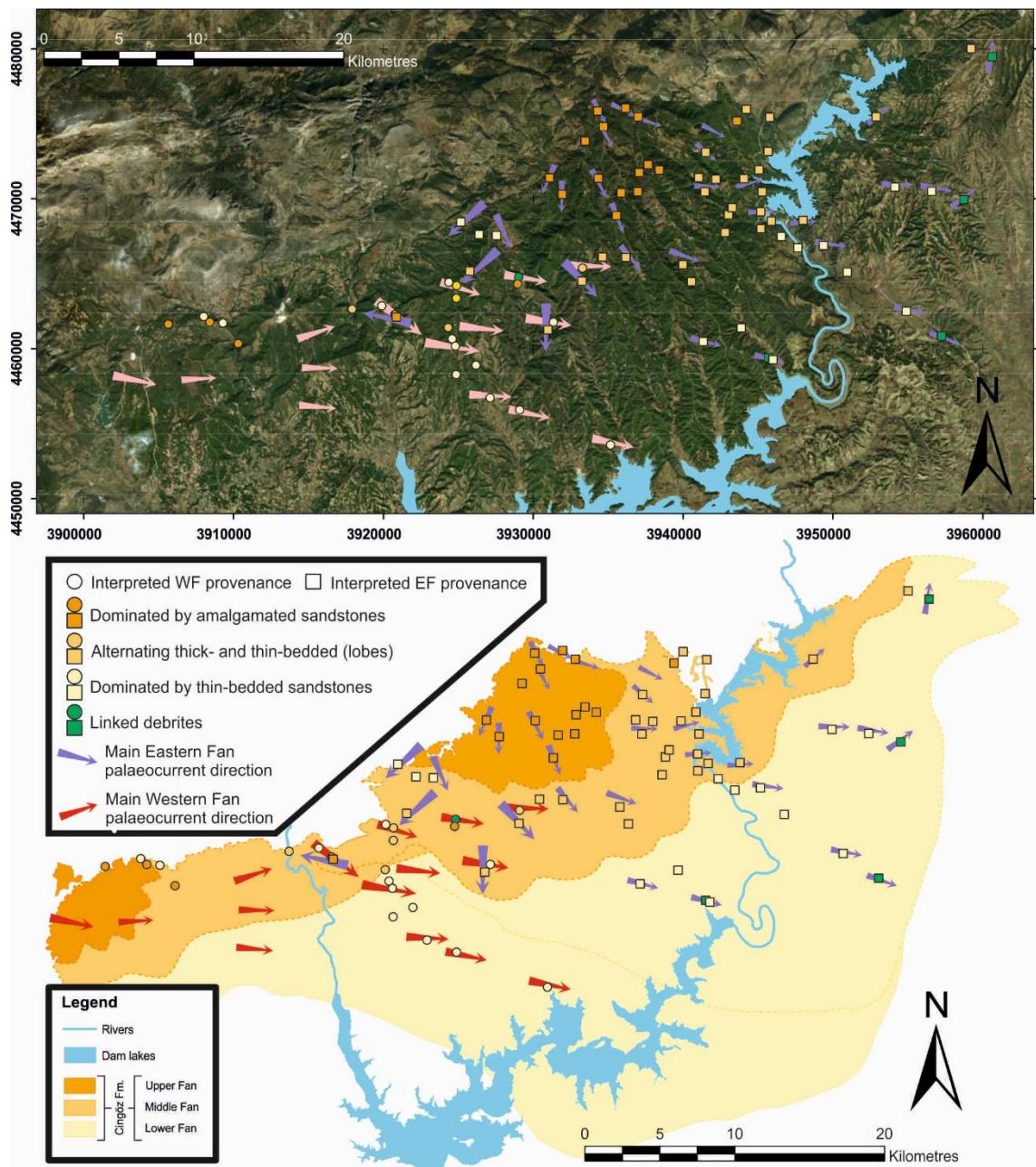
Figure 13. Compilation of the studied main locations to help in the interpretation of the geological map. The arrows represent palaeocurrent directions for each location (purple = input from the EF, red = input from the WF; squares = EF, circles = WF).
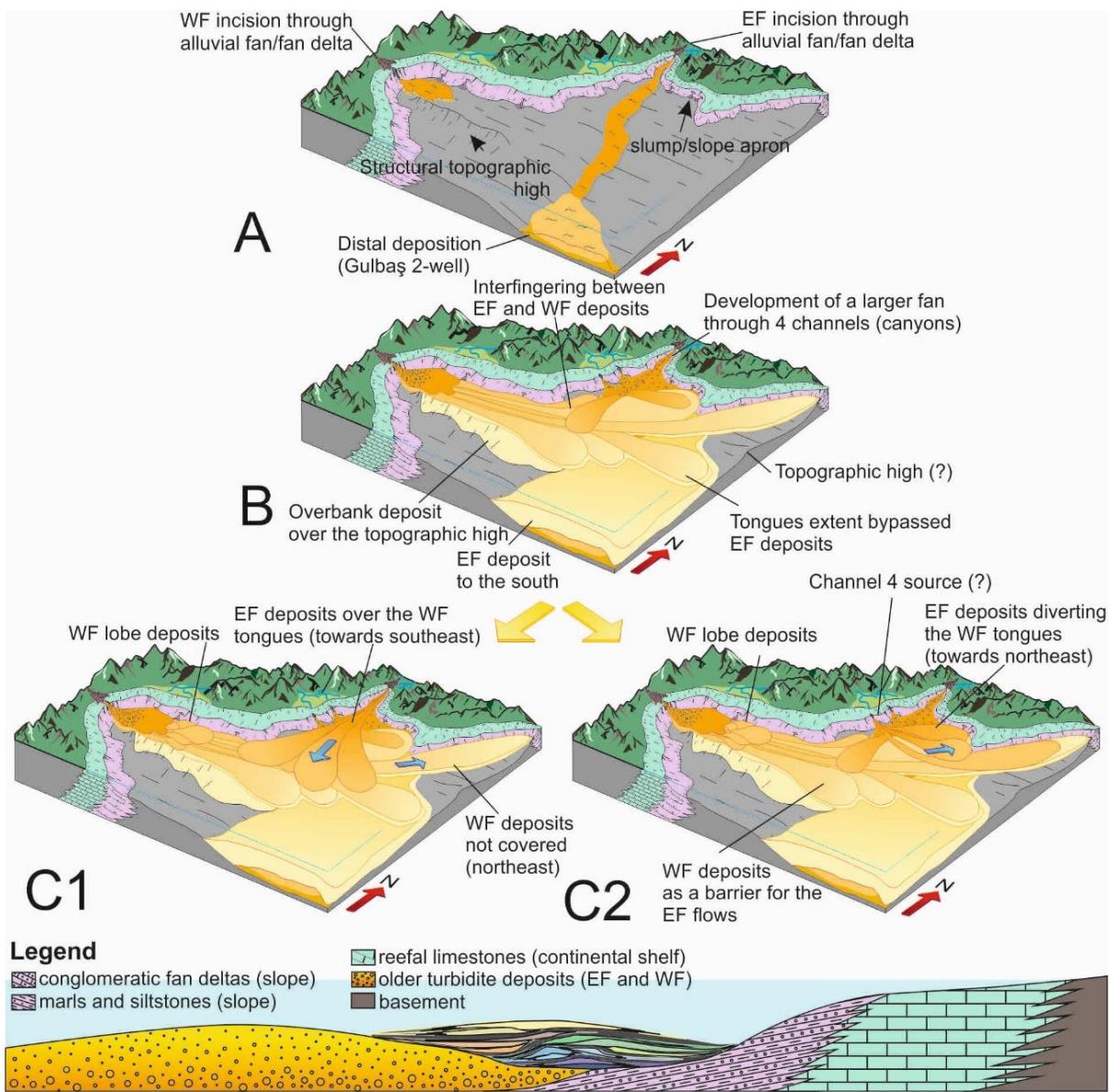
Figure 14. A) <u>Evolution of the Cingöz Fm. - Stage 1 (Upper Burdigallian): topography influences inception in both fans during early progradational succession</u>. Difference in water depth (shallower in the WF) allowed the coarse-grained EF to deliver sediments farther (towards south), following topographic lows. These sediments were sampled in the Gulbaş 2-well. The onset of incision and the relative confinement in WF was controlled by a structural topographic high. Adapted from Satur et al. (2007); B) <u>Evolution of the Cingöz Fm. - Stage 2 (Langhian-Serravallian): progradation of the entire system</u>. The Eastern Fan feeder system is complete, with four channels delivering sediments to the south mainly through Channel 1, but also to the E-NE through Channels 3 and 4. Deposition of the Western Fan tongues were probably guided by the basement extensional faulting along ENE – WSW, reaching the NE of the basin, where they interfingered with the EF deposits; C) <u>Evolution of the Cingöz Formation - Stage 3 (Serravallian): retrogradation and final stages.</u> The system

started to retrograde, when the lobes were deposited at the late stages of the WF (Satur et al., 2007). The EF is still active, following two alternative evolutionary paths: alternative C1 shows the EF depositing sediments towards south/southeast over the WF tongues (as interpreted near Cingöz/Filikli) mainly through Channel 1, whereas in alternative C2 sediments were delivered mainly through Channels 3 and 4 towards east/northeast, diverting from the tongues at the south, where only fine-grained sediments were allowed to pass by. Below the block diagrams, schematic interpretation of the lobe analysis of the Cingöz Formation evolution, showing the relationship between the 13 lobes deposited and interpreted as EF in semi-confined settings.

Conclusions

Palaeocurrent patterns are critical to understanding lobe evolution in a system like the Cingöz, where two fans interact. Two main palaeocurrent directions indicate the existence of a feeder system from the west and another one from northwest (WF and EF, respectively). A detailed analysis, however, shows different palaeoflow directions obtained from climbing ripple laminations (to SE) and flute casts (to NE), mainly for the EF, which points to a complex evolution over time.

Analysis of bed thickness suggests that thin-bedded sandstones tend to have a SE palaeocurrent direction. The best explanation for this in the Western Fan is the association with a topographic high that confined the fan, resulting in a tendency of the upper part of the flow to deposit as overbank (Satur, 1999). In the Eastern Fan, two alternatives explanations were considered: 1) being more distant from the source, flow partitioning may increase the angle between measured indicators and the fine-grained part of the flow that escapes over the topographic highs; 2) the eastern part of the EF is actually the distal part of the WF. This interpretation is different from what is suggested in the literature.

Outcrop analysis around Cingöz village suggests the EF (or at least the last phase of it) was deposited onto the WF. This means that the WF acted as a topographic high during the last phase of submarine fan construction, diverting the flow and depositing the EF lobes to the east.

Stratal terminations were used to determine lobe limits and understand the relation between lobes and slope. This analysis allowed the distinction between longitudinal and frontal upslope transport. Sandwich beds are more frequent in frontal upslope

transport, developing a thick debrite portion, as opposed to longitudinal upslope transport.

Acknowledgments

References

Allen, JRL (1968). Current ripples. North-Holland, Amsterdam, 433 pp.

Allen, JRL (1971). Instantaneous sediment deposition rates deduced from climbing-ripple cross-lamination. Journal of Geological Society of London, 127, 553–561.

Amy, LA, Kneller, BC and McCaffrey, WD (2007). Facies architecture of the Gres de Peira Cava, SE France: landward stacking patterns in ponded turbiditic basins, Journal of the Geological Society, 164(1), pp. 143–162.

Biju-Duval, B, Letouzey, J and Montadert, L (1978). Structure and evolution of the Mediterranean basins, Initial Reports of the Deep Sea Drilling Project, 42(1), pp. 951–984.

Bonnel, C, Dennielou, L, Droz, L, Mulder, T, and Berné, S (2005). Architecture and depositional pattern of the Rhône Neofan and recent gravity activity in the Gulf of Lions (western Mediterranean), Marine and Petroleum Geology, 22, 827-843.

Brinkmann, R (1976). Geology of Turkey, pp. 158. Elsevier Scientific Publishing Company, Amsterdam, the Netherlands.

Cipollari, P, Cosentino, D, Radeff, G, Schildgen, TF, Faranda, C, Grossi, F, Gliozzi, E, Smedile, A, Gennari, R, Darbaş, G, Dudas, FÖ, Gürbüz, K, Nazik, A and Echtler, H (2013). Easternmost Mediterranean evidence of the Zanclean flooding event and subsequent surface uplift: Adana Basin, southern Turkey,

Geological Society, London, Special Publications, 372(1), pp. 473–494.

Curray, JR., Emmel, FJ and Moore, DG (2002). The Bengal Fan: Morphology, geometry, stratigraphy, history and processes, Marine and Petroleum Geology, 19(10), pp. 1191–1223.

Damuth, JE, Flood, RD, Kowsmann, RO, Gorini, MA, Belderson, RH, Gorini, MA, (1988). Anatomy and growth- pattern of Amazon deep-sea fan revealed by long-range side-scan sonar (GLORIA) and high-resolution seismic studies. AAPG Bulletin 72, 885–911.

Dermican, H and Toker, V (2003). Trace fossils in the Western Fan of the Cingöz Formation in the northern Adana Basin (Southern Turkey), Fossils, 1862, pp. 15–32.

Frey, RW and Pemberton, SG (1984). Trace fossil facies models, in Walker, R. G. (eds.), Facies models, Geoscience Canada Reprint Series, p. 189-207.

Görür, N (1979). Karaisalı Kireçtaşı'nın (Miyosen) Sedimantolojisi, Türkiye Jeologi Kurumu Bülteni, 22, pp. 227–232.

Görür, N (1992). A tectonically controlled alluvial fan which developed into a marine fan-delta at a complex triple junction: Miocene Gildirli Formation of the Adana Basin, Turkey, Sedimentary Geology, 81(3–4), pp. 243–252.

Gürbüz, K (1993). Identification and evolution of Miocene submarine fans in the Adana Basin, Turkey. Unpublished PhD Thesis. University of Keele, Keele, 327 pp.

Gürbüz, K (1999). Regional implications of structural and eustatic controls in the evolution of submarine fans; an example from the Miocene Adana Basin, southern Turkey, Geological Magazine, 136(3), pp. 311–319.

Gürbüz, K and Kelling, G (1993). Provenance of Miocene submarine fans in the northern Adana Basin, southern Turkey: A test of discriminant function analysis, Geological Journal, 28(3–4), pp. 277–293.

Haq, BU, Hardenbol, J and Vail, PR (1987). Chronology of Fluctuating Sea Levels Since the Triassic, Science, 235(4793), pp. 1156–1167.

Haq, BU, Hardenbol, J and Vail, PR (1988). Mesozoic and Cenozoic chronostratigraphy and cycles of sea-level change, in Wilgus, CK, Hastins, BS, Kendall, CG, Posamentier, HW, Ross, CA and Van Wagoner, JC (eds.), Sea-Level Changes: An Integrated Approach. CK Wilgus, BS Hastins, CGStC Kendall, HW Posamentier, CA Ross and JC Van Wagoner, SEPM Special Publication, p. 72-108.

Hodgson, DM, Flint, SS, Hodgetts, D, Drinkwater, NJ, Johannessen, EP and Luthi, SM (2006). Stratigraphic Evolution of Fine-Grained Submarine Fan Systems, Tanqua Depocenter, Karoo Basin, South Africa, Journal of Sedimentary Research, 76(1), pp. 20–40.

Ilgar, A, Nemec, W, Hakyemez, A and Karakuş, E (2013). Messinian forced regressions in the Adana Basin: A near-coincidence of tectonic and eustatic forcing, Turkish Journal of Earth Sciences, 22(5), pp. 864–889.

Kelling, G, Gökçen, SL, Floyd, PA and Gökçen, N (1987). Neogene tectonics and plate convergence in the eastern Mediterranean : New data from southern Turkey, Geology, v. 15, p. 425–429.

Loncke, L, Gaullier, V, Mascle, J, Vendeville, B and Camera, L (2006). The Nile deep-sea fan: An example of interacting sedimentation, salt tectonics, and inherited subsalt paleotopographic features, Marine and Petroleum Geology, 23(3), pp. 297–315.

Marini, M, Milli, S, Ravnås, R and Moscatelli, M (2015). A comparative study of confined vs. semi-confined turbidite lobes from the Lower Messinian Laga Basin (Central Apennines, Italy): Implications for assessment of reservoir architecture, Marine and Petroleum Geology. Elsevier Ltd, 63, pp. 142–165.

Masalimova, LU, Lowe, DR, Sharman, GR, King, PR and Arnot, MJ (2016). Outcrop characterization of a submarine channel-lobe complex: The Lower Mount Messenger Formation, Taranaki Basin, New Zealand, Marine and Petroleum Geology. Elsevier Ltd, 71, pp. 360–390.

Mitchum, RM, Vail, PR and Thompson, S (1977). Seismic Stratigraphy and Global Changes of Sea Level, Part 2: The Depositional Sequence as a Basic Unit for Stratigraphic Analysis: Section 2. Application of Seismic Reflection Configuration to Stratigraphic Interpretation, Seismic Stratigraphy: Applications to Hydrocarbon Exploration AAPG Memoir 26, pp. 53–62.

Mutti, E and Normark, WR (1987). Comparing examples of modern and ancient turbidite systems: problems and concepts, in Leggett, JR and Zuffa, GG (eds.), Marine clastic sedimentology: concepts and case studies, London: G Graham and Trotman, pp. 1–37.

Mutti, E and Normark, WR, (1991). An integrated approach to the study of turbidite systems, in: Weimer, P, Link, ML (eds.), Seismic Facies and Sedimentary Processes of Submarine Fans and Turbidite Systems. Springer-Verlag, New York, pp. 75– 106.

Naini, BR and Kolla, V (1982). Acoustic character and thickness of sediments of the Indus Fan and the continental margin of western India, Marine Geology, 47(3–4), pp. 181–195.

Naz, H, Cuhadar, O and Yehiay, G (1991). Middle Miocene Cingöz deep-sea fan deposits of the Adana Basin, Southern Turkey, in Sungurlu, O. (eds.), Tectonics and hydrocarbon potential of Anatolia and surrounding regions, Ankara, Turkey.

Nazik, A (2004). Planktonic foraminiferal biostratigraphy of the Neogene sequence in the Adana Basin, Turkey, and its correlation with standard biozones, Geological Magazine, 141(3), pp. 379–387.

Nazik, A and Gürbüz, K (1992). Yöresi (Kb Adana) Alt-Orta Miyosen Yaşli Denizalt Yelpazelerinin Planktoni Foramini Biyostratigrafisi, Türkiye Jeoloji Bülteni, 32(February), pp. 67–80.

Piper, DJW and Normark, WR (1983). Turbidite deposition patterns and flow characteristics, Navy Submarine Fan, Californian Borderland, Sedimentology, 30(5), pp. 681–694.

Prélat, A, Hodgson, DM and Flint, SS (2009). Evolution, architecture and hierarchy of distributary deep-water deposits: a high-resolution outcrop investigation from the Permian Karoo Basin, South Africa, Sedimentology, 56(7), pp. 2132–2154.

Radeff, G, Schildgen, TF, Cosentino, D, Strecker, MR, Cipollari, P, Darbaş, G and Gürbüz, K (2015). Sedimentary evidence for late Messinian uplift of the SE margin of the Central Anatolian Plateau: Adana Basin, southern Turkey, Basin Research, 29, pp. 488–514.

Richards, M, Bowman, M and Reading, H (1998). Submarine-fan systems I: characterization and stratigraphic prediction, Marine and Petroleum Geology, 15(7), pp. 689–717.

Satur, N (1999). Internal architecture, facies distribution and reservoir modelling of the Cingöz deepwater clastic system in southern Turkey. PhD Thesis. University of Aberdeen, Aberdeen, UK, 520 p.

Satur, N, Cronin, BT, Hurst, A, Kelling, G and Gürbüz, K (2004). Down-channel variations in stratal patterns within a conglomeratic, deepwater fan feeder system (Miocene, Adana Basin, Southern Turkey), in Lomas S and Joseph, P (eds.), Confined turbidite systems: Geological Society (London) Special Publication 222, p. 241–260.

Satur, N, Hurst, A, Cronin, BT, Kelling, G and Gürbüz, K (2000). Sand body geometry

in a sand-rich deepwater clastic system, Miocene Cingöz Formation of southern Turkey, Marine and Petroleum Geology, pp. 128–141.

Satur, N, Hurst, A, Kelling, G, Cronin, BT and Gürbüz, K (2007). Controlling Factors on the Character of Feeder Systems to a Deep-water Fan, Cingöz Formation, Turkey, Atlas of Deep-Water Outcrops, CD-ROM, pp. 1–28.

Satur, N, Kelling, G, Cronin, BT, Hurst, A and Gürbüz, K (2005). Sedimentary architecture of a canyon-style fairway feeding a deep-water clastic system, the Miocene Cingöz Formation, southern Turkey: Significance for reservoir characterisation and modelling, Sedimentary Geology, 173(1–4), pp. 91–119.

Schmidt, G (1961). Stratigraphic nomenclature for the Adana region petroleum district VII. Petroleum Administration, Bulletin, v. 6, p. 47-63.

Şengör, AMC and Yılmaz, Y (1981). Tethyan evolution of Turkey: A plate tectonic approach, Tectonophysics, 75(3–4).

Sinclair, HD and Tomasso, M (2002). Depositional evolution of confined turbidite basins, Journal of Sedimentary Research, 72, 451–456.

Ünlügenç, UC (1993). Controls on Cenozoic sedimentation, Adana Basin, Southern Turkey. PhD. Thesis. University of Keele, Keele, UK.

Ünlügenç, UC, Kelling, G and Demirkol, C (1991). Aspects of basin evolution in the Neogene Adana Basin, SE Turkey, International Earth Scientific Congress on Aegean Regions, Proceedings, 1, 357–370.

Williams, GD, Ünlügenç, UC, Kelling, G and Demirkol, C (1995). Tectonic controls on stratigraphic evolution of the Adana Basin, Turkey, Journal of the Geological Society, 152, pp. 873–882.

Yetiş, C (1988). Reorganization of the Tertiary stratigraphy in the Adana Basin, Southern Turkey, Newsletters on Stratigraphy, 20(1), pp. 43–58.

Yetiş, C and Demirkol, C (1986). Adana baseni batı kesiminin detay jeoloji etüdü, MTA Enstitüsü, Derleme, 8037.

Yetiş, C, Kelling, G, Gökçen, SL and Baroz, F (1995). A revised stratigraphic framework for Late Cenozoic sequences in the northeastern Mediterranean region, Geol Rundsch, 84, pp. 794–812.

ANEXO I

Título da Dissertação/Tese:

"CARACTERIZAÇÃO ARQUITETURAL E DISTRIBUIÇÃO DE FÁCIES DE LOBOS TURBIDÍTICOS NO MIOCENO DA BACIA DE ADANA, TURQUIA"

Área de Concentração: Estratigrafia

Autor: **Daniel Bayer Da Silva**

Orientador: Prof. Dr. Eduardo Guimarães Barboza

Examinador: Prof. Dr. Juliano Kuchle

Data: 19/11/18

Conceito: A - excelente

PARECER:

Doutorando apresenta um volume excelente de dados e resultados relevantes. Domina a metodologia e possui conhecimento concreto, compatibilizando dados e interpretações.

Volume e apresentação muito bons e artigos submetidos de relevância.

Somente apresento como crítica a ausência de hipótese claramente nominada embora existente e a ausência de um capítulo de síntese integradora.

Parabéns ao doutorando.
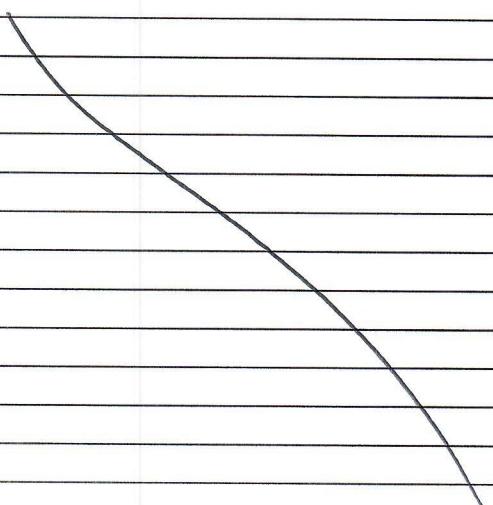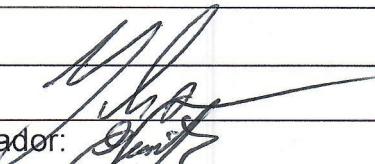
Assinatura: _____ Data: 29/11/18

Ciente do Orientador: _____

Ciente do Aluno: _____

ANEXO I

Título da Dissertação/Tese:

"CARACTERIZAÇÃO ARQUITETURAL E DISTRIBUIÇÃO DE FÁCIES DE LOBOS TURBIDÍTICOS NO MIOCENO DA BACIA DE ADANA, TURQUIA"

Área de Concentração: Estratigrafia

Autor: **Daniel Bayer Da Silva**

Orientador: Prof. Dr. Eduardo Guimarães Barboza

Examinador: Prof. Dr. Michael Holz

Data: 19/11/18

Conceito: B (BOM)

PARECER:

O trabalho contém um conjunto de dados muito grande, bem organizado em tabela de fácies e associações e perfis de correlação etc., mas há necessidade de re-interpretar algumas fácies e organizar melhor o texto todo, porque na forma atual é algo desconexo e não deixa claro o que era o objetivo fundamental da pesquisa. Esse problema decorre do fato do trabalho não conter uma hipótese de trabalho claramente formulada. A pergunta "qual é a Tese?" não é respondida no texto, e nem foi durante a defesa. Isso claramente denota falta de orientação. Um trabalho bem feito e amplo no conjunto de dados NÃO é uma tese de doutorado a não ser que esse conjunto de dados e os resultados obtidos corroborem (ou falsfiem) a hipótese de trabalho. Para que ninguém fez o(a) orientador(es) explicou isso ao doutorando. Contudo, como a parte técnica foi bem feita, é importante e cientificamente pertinente, aprovo o trabalho e parabenizo o doutorando pela dedicação e envolvimento com a temática, que é complexa e controverso.

Assinatura:

Ciente do Orientador:

Ciente do Aluno:

Data: 19 / 11 / 18

ANEXO I

Título da Dissertação/Tese:

"CARACTERIZAÇÃO ARQUITETURAL E DISTRIBUIÇÃO DE FÁCIES DE LOBOS TURBIDÍTICOS NO MIOCENO DA BACIA DE ADANA, TURQUIA"

Área de Concentração: Estratigrafia

Autor: **Daniel Bayer Da Silva**

Orientador: Prof. Dr. Eduardo Guimarães Barboza

Examinador: Dr. Adriano Rodrigues Viana

Data:

Conceito: B B

PARECER:

O candidato apresenta bom domínio técnico com uma boa apresentação oral que compensa o manuscrito que é confuso, com uma estrutura que antecipa resultados e não valoriza o esforço e o material coletado pelo candidato.

Assinatura: _____ Data: 19/01/2018

Ciente do Orientador: _____

Ciente do Aluno: _____